FACULTY OF
VETERINARY MEDICINE
accredited by EAEVE

Laboratory of Virology

Department of Virology, Parasitology and Immunology

Faculty of veterinary medicine

Ghent University

Genotyping of local feline immunodeficiency virus (FIV) isolates and characterization of FIV replication in peripheral blood mononuclear cells

Inge Roukaerts

Promotor: Prof. dr. Hans J Nauwynck

Dissertation submitted in fulfillment of the requirement for the degree of doctor in veterinary sciences (PhD), 2016

GHENT
UNIVERSITY

Nederlandstalige titel: Genotypering van lokale feliene immunodeficiëntie virus (FIV) isolaten en karakterisatie van FIV replicatie in feliene perifeer bloed mononucleaire cellen

Roukaerts I. (2016) Genotyping of local feline immunodeficiency virus (FIV) isolates and characterization of FIV replication in feline peripheral blood mononuclear

ISBN

This work was supported by the Agency for Innovation by Science and Technology in Flanders (IWT).

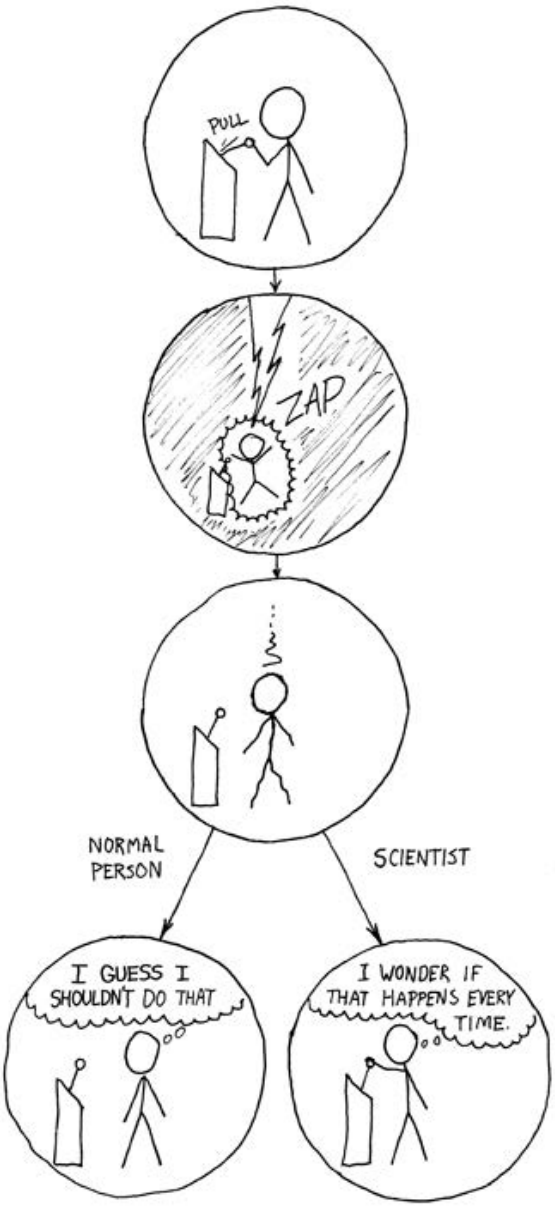
PULL
ZAP
NORMAL PERSON
SCIENTIST
I GUESS I SHOULDN'T DO THAT
I WONDER IF THAT HAPPENS EVERY TIME.

www.xkcd.com

Table of Contents

List of abbreviations

AP-1	activator protein 1
APOBEC3	apolipoprotein B mRNA editing enzyme, catalytic polypeptide-like 3
ARC	AIDS related complex
ATF	activating transcription factors
BEC	blood endothelial cells
bFGF	basic fibroblastic growth factor
BP	basepair
BST2	bone marrow stromal cell antigen 2
C/EBP	CCAAT-enhancer-binding proteins
CA	capsid
CCL	C-C motif chemokine ligand
CCR	C-C motif chemokine receptor
CD	cluster of differentiation
cDNA	complement deoxyribonucleic acid
CLEC-2	C-type lectin 2
CMJ	cortico-medullar junction
conA	concanavalin A
CREB	cAMP response element binding protein
CrFK	Crandell Rees feline kidney cells
cTEC	cortical thymic epithelial cells
CTL	cytotoxic $CD8^+$ T-lymphocytes
CXCL	C-X-C motif chemokine ligand
CXCR	C-X-C motif chemokine receptor
DNA	deoxyribonucleic acid
DU	deoxyuridine-phosphatase
ELISA	enzyme-linked immunosorbent assay
EMT	epithelial-mesenchymal transition
env	envelope gene
Env	envelope polyprotein
ER	endoplasmic reticulum
ESCRT	endosomal-sorting complexes required for transport
FBS	fetal bovine serum
FDC	follicular dendritic cell

FIV	feline immunodeficiency virus
FRC	fibroblastic reticular cell
FS	frame shift
gag	group specific antigen gene
Gag	group specific antigen polyprotein
GFox	GFP/Ox40 expressing CrFK cells
GM-CSF	granulocyte/macrophage colony stimulating factor
gp36	FIV transmembrane envelope glycoprotein
gp95	FIV surface envelope glycoprotein
HEK293	human embryonic kidney 293 cells
HEV	high endothelial venules
HIV	human immunodeficiency virus
HSC	hematopoietic stem cells
hTERT	human telomerase reverse transcriptase
IAP	integrin $\alpha 7^{+}$ pericytes
ICAM-1	intercellular adhesion molecule 1
IFN	interferon
IL	interleukin
IN	integrase
kDa	kilo dalton
LBP-1	lipopolysaccharide binding protein
LEC	lymphatic endothelial cells
LEDGF	lens epithelium derived growth factor
LPS	lipopolysaccharide
LTR	long terminal repeat
MA	matrix
MAb	monoclonal antibody
madCAM-1	mucosal addressin cell adhesion molecule 1
MALT	mucosa associated lymphoid tissue
MLV	murine leukemia virus
mRNA	messenger RNA
MSC	mesenchymal stem cells
mTEC	medullar thymic epithelial cells
NC	nucleocapsid

Nedd4-2	neural precursor cell expressed developmentally down-regulated protein 4
NF-1	nuclear factor 1
NF-κB	nuclear factor kappa-light-chain-enhancer of activated B cells
NK	natural killer cells
NLS	nuclear localization signal
NPC	nuclear pore complex
ORF	open reading frame
p.i.	post infection/inoculation
p24	FIV capsid protein
PA	polyadenylation
PBMC	peripheral blood mononuclear cells
PBS	phosphate buffered saline
PCR	polymerase chain reaction
PDGFR	platelet derived growth factor receptor
PECAM1	platelet/endothelial cell adhesion molecule 1
PGL	peripheral general lymphadenopathy
PIC	pre-integration complex
Pol	polymerase
pol	polymerase gene
PPT	polypurine tract
PR	protease protein
pro	retroviral protease gene
qPCR	quantitative real time polymerase chain reaction
RBC	red blood cell
rev	regulator of expression of virion gene
Rev	regulator of expression of virion proteins
RNA	ribonucleic acid
rPBS	Ca^{2+} and Mg^{2+} enriched phosphate buffered saline
RRE	rev responsive element
RT	reverse transcriptase
RT-PCR	reverse transcriptase polymerase chain reaction
RT-qPCR	reverse transcriptase quantitative polymerase chain reaction
SA	splice acceptor site
SAMHD1	SAM domain and HD domain-containing protein 1

SCZ	subcapsular zone
SD	splice donor site
SDF1	stromal derived factor 1
SIV	simian immunodeficiency virus
SMA	smooth muscle actin
SPF	specific pathogen free
SU	FIV surface envelope glycoprotein
SV40 T-Ag	simian vacuolating virus 40 large T antigen
TAE	Tris-acetate-EDTA
TCID50	50% tissue culture infectious dose
TCR	T-cell receptor
TF	transcription factor
TM	FIV transmembrane envelope glycoprotein
TNF	tumor necrosis factor
TNFR	tumor necrosis factor receptor
Treg	regulatory T-cells
TRIM5	tripartite motif-containing protein 5
Tsg101	tumor susceptibility gene 101 protein
V	variable loop
vif	viral infectivity factor gene
Vif	viral infectivity factor protein

Chapter 1

Introduction

1.1. Feline immunodeficiency virus (FIV)

1.1.1. Classification

Feline immunodeficiency virus (FIV) is a member of the family *Retroviridae*. Retroviruses are characterized by the presence of a viral transcriptase, and the integration of the viral genome into the host cell chromatin by a viral integrase. The name retrovirus refers to the reverse flow of information from the RNA genome to a DNA intermediate (provirus) during the viral life cycle. These viruses have 80-100 nm sized enveloped particles that contain a genome of 7-12 kb.

Historically, three groups of retroviruses were established; the oncoviruses, lentiviruses and spumaviruses. The oncoviruses include viruses that can easily immortalize or transform host cells. Lentiviruses have a slow onset of disease and are associated with neurological and immunosuppressive disease. Spumaviruses cause a distinct cytopathological effect and do not seem to cause clinical disease. The oncoviruses were further subclassified based on morphology into B-, C- and D-type particles (Vogt, 1997). Five types of retroviral particles can be distinguished as shown in Figure 1. First, A-type particles; nonenveloped cytoplasmatic particles with the appearance of a doughnut, represent the immature cores for B- and C-type particles. They are immature because their gag polyprotein is not proteolytically processed, and hence the typical condensed core of electrondense material is absent. The condensed core of mature particles is round or slightly angular in shape and lies centered (C-type) or eccentric (B-type) in the viral particle. D-type oncoviruses have a bar or rod shaped core. The fifth group are the lentiviruses that have a typical cone shaped core.

Following the latest report of the International Committee on Taxonomy of Viruses (ICTV), the family of the retroviruses is divided into two subfamilies; the former oncoviruses and lentiviruses are combined in the *Orthoretrovirinae*, while the *Spumaretrovirinae* remain separated. The viral particles of the *Orthoretrovirinae* carry two copies of linear, positive sense, single stranded RNA that is reverse transcribed during infection of a susceptible cell. *Spumaretrovirinae*, on the other hand, carry a double stranded DNA molecule as genome since reverse transcription takes place as a late step in the viral life cycle. The *Orthoretrovirinae* are further subdivided as defined by genetic evolutionary relatedness and complexity of the genome. This has led to the creation of six subgroups; alpha-, beta-, gamma-, delta-, and epsilon-retroviruses (the former oncoviruses), and lentiviruses (Table 1).

Together with its notorious cousin, the human immunodeficiency virus (HIV), FIV belongs to the genus lentivirus. Other retroviruses known to infect cats, are feline leukemia virus (FeLV) belonging to the genus Gammaretroviruses, and feline foamy virus (FFV) in the subfamily *Spumaretrovirinae*. FIV was first isolated in 1987 by Pedersen and colleagues, from FeLV negative cats that displayed an immunodeficiency syndrome similar to AIDS in humans (Pedersen *et al.*, 1987).

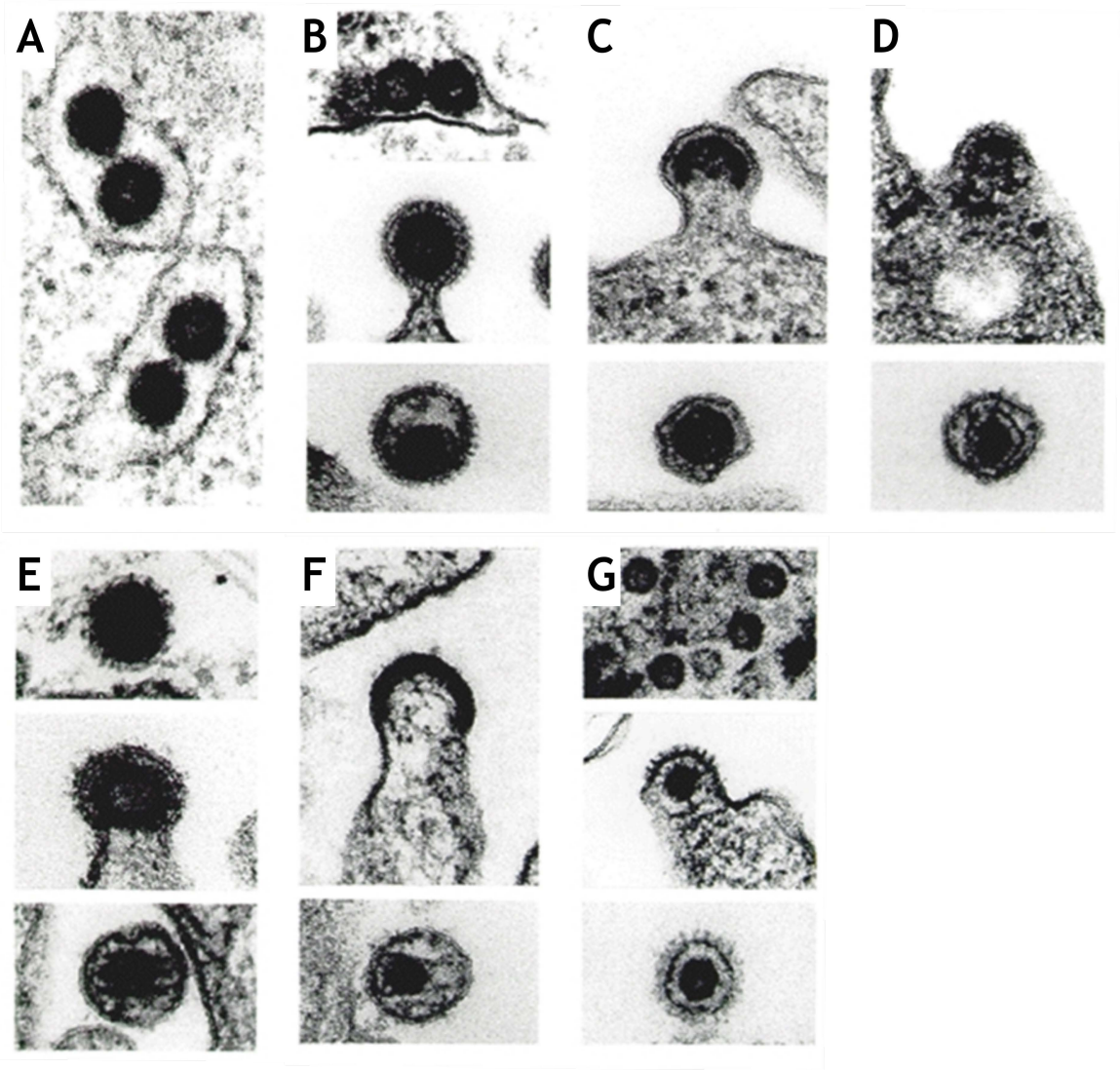

Figure 1: Electron micrographs of retroviral particles (courtesy of Gonda MA). (A) A-Type: intracisternal A particles in the endoplasmatic reticulum. (B) B-Type: Mouse mammary tumor virus (top, immature intracytopasmatic A-type particles; middle, budding particles; bottom, mature extracellular particle). (C) C-type with round core: Murine leukemia virus (top, budding; bottom, mature extracellular particles). (D) C-type with angular core: Avian leukosis virus (top, budding; bottom, mature extracellular particles). (E) D-type: Mason-Pfizer monkey virus (top, immature intracytopasmatic A-type particles; middle, budding particles; bottom, mature extracellular particle). (F) Lentivirus: Bovine immunodeficiency virus (top, budding; bottom, mature extracellular particles). (G) Spumavirus: Bovine syncytium virus (top, budding; bottom, mature extracellular particles). Adapted from (Vogt, 1997).

Table 1: Classification of the *Retroviridae* family based on the last report of the International Committee on Taxonomy of Viruses (ICTV).

Family	Subfamily	Genus	Species
Retroviridae			
	Orthoretrovirinae		
		Alpharetrovirus	Avian leukosis virus
		Betaretrovirus	Mouse mammary tumor virus
		Gammaretrovirus	Feline leukemia virus
		Deltaretrovirus	Bovine leukemia virus
		Epsilonretrovirus	Walleye dermal sarcoma virus
		Lentivirus	**Feline immunodeficiency virus**
			Human immunodeficiency virus
			Simian immunodeficiency virus
			Caprine arthritis and encephalitis virus
			Maedi-Visna virus
	Spumaretrovirinae		
		Spumavirus	Feline foamy virus

1.1.2. FIV genome

Members of the Retroviridae all share a similar genetic make-up, four large open reading frames (ORF). These ORF encode for structural and enzymatic proteins, important for the formation of new virus particles. Figure 2 represents the generalized retroviral DNA provirus and mRNA genome, and the FIV genome constellation. Starting from the 5' end, the first gene in the genome is the *group specific antigen* (*gag*) gene. This gene encodes the Gag polyprotein that encompasses the matrix protein (MA), capsid protein (CA) and nucleocapsid protein (NC). The *polymerase* (*pol*) gene is located next to the *gag* gene. This gene encodes for a polyprotein with several enzymatic functions. For FIV, the *pro* gene, encoding the viral protease, is part of the *pol* ORF. Hence, the FIV Pol polyprotein contains the protease (PR), reverse transriptase (RT), deoxyuridine-phosphatase (DU) and the integrase (IN). The fourth and last ORF contains the *envelope* (*env*) gene, that consists of two parts; the surface protein (SU) and the transmembrane protein (TM) (Talbott *et al.*, 1989). Depending on the subfamily and genus, retroviruses may contain additional ORF, positioned around the *env* gene, that encode for "accessory" proteins. Accessory proteins are involved in regulation of syntheses and processing of the virus, and combating host restriction factors. The FIV genome also codes three such viral accessory proteins; Vif (Felber *et al.*, 1989; Talbott *et al.*, 1989), OrfA (Talbott *et al.*, 1989) and Rev (Brown *et al.*, 1991; Kiyomasu *et al.*, 1991). The presence of these accessory proteins places the FIV genome in the group of complex retroviral genomes.

The Gag polyprotein and Gag-Pol chimeara are translated from a full length unspliced mRNA. The Gag-Pol polyprotein is translated after a ribosomal frameshift (FS) at the end of the *gag* gene, shifting the ribosome back one codon into the *pol* ORF (Morikawa & Bishop, 1992). The envelope protein is translated from a singly spliced mRNA molecule, after recombination of the primary splice donor site (SD) with the major splice acceptor site (SA).

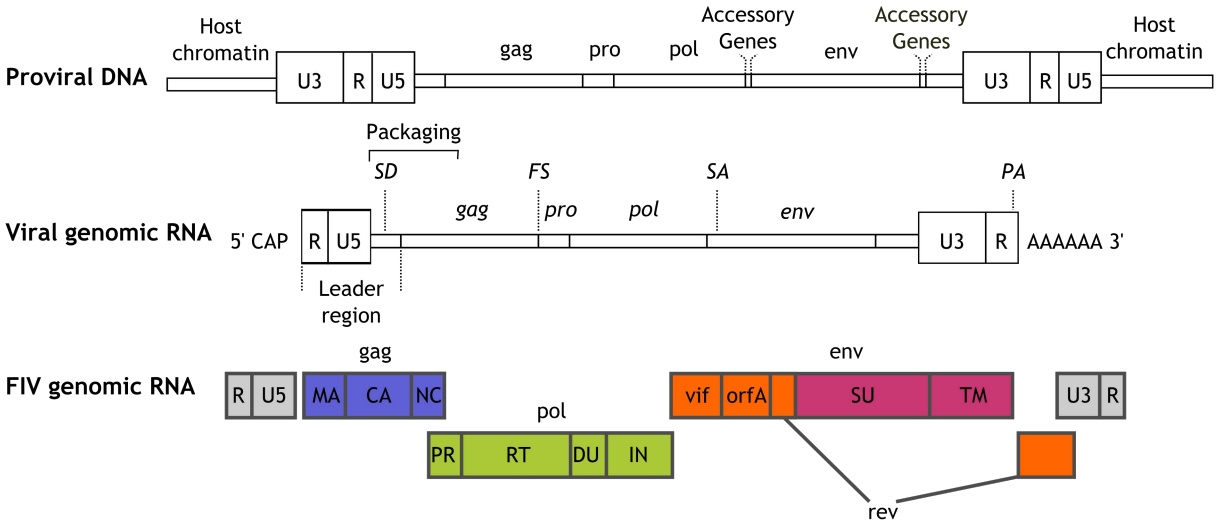

Figure 2: Genetic organization of the generalized retrovirus. The proviral DNA (top) that is inserted into the host cell chromatin, with long terminal repeats (LTRs) composed of U3, R and U5 elements at each end. The four major open reading frames *gag*, *pro*, *pol* and *env* are located at invariable positions in the retroviral genome. Accessory genes are located after the *pol* and/or *env* gene. The primary mRNA transcript is shown in the middle. The mRNA is capped at the 5' end and polyadenylated at the 3' end, with the R sequence encompassing the polyadenylation (PA) signal. The untranslated leader region contains the major splice donor (SD) site. The viral genome contains several splice acceptor sites (SA), with the most important one proximal to the env gene. The *pro* and *pol* genes are generally translated after a ribosomal frame shift (FS) in *gag*. The 5' end holds the encapsidation sequence that interacts with the *gag* gene product for genome packaging into the viral particle. In the FIV mRNA genome (bottom), *pro* is part of the *pol* open reading frame, in ORF-1 from *gag*. The *env* region contains several accessory genes, *vif*, *orf A*, and *rev*. The *rev* gene has two exons, one in front of and one after the *env* gene, with the second exon overlapping the 3' LTR region.

The genes in the DNA intermediate provirus are bracketed by the long terminal repeats (LTR) (Temin, 1981). These LTR are identical sequences that can be divided into three elements, and are created during reverse transcription. The unique region 3' (U3), derived from the sequence unique to the 3' end of the viral RNA. The repeat (R) is derived from a sequence repeated at both ends of the RNA, and U5 is derived from the sequence unique to the 5' end of the viral RNA. Transcription initiation motifs are located at the boundary between U3 and R, and the site of polyadenylation (PA) at the boundary between R and U5. The U3 contains most of the transcriptional control elements of the provirus, which include promoter and enhancer sequences, responsive

to cellular transcriptional activator proteins. The viral mRNA genome is packaged into virions via the encapsidation sequence that interacts with viral nucleocapsid proteins, located proximal to the 5' end. The mRNA molecules encoding the accessory proteins are all multiple spliced variants.

1.1.3. FIV subtyping

FIV is divided into five different clades (A to E), which vary in prevalence by geographic location (Yamamoto *et al.*, 2007). These clades are based on phylogenetic analyses of several variable regions (3 to 5) in the *env* gene. The intra-clade diversity at the nucleotide level in these variable regions range from 2.5 to 15%. A new clade arises when a sequence shows more than 20% genetic distance from other clades (Kakinuma *et al.*, 1995; Sodora *et al.*, 1994). While clade A strains are found worldwide, other clades indicate a separate evolution of FIV viruses in geographical isolated locations. For example, subtype E has only been found in South-America and subtype D is confined to Japan (Kakinuma *et al.*, 1995; Pecoraro *et al.*, 1996). Several reports have been made of *env* sequences clustering into new FIV clades, these were designated "F" (Duarte & Tavares, 2006; Hayward *et al.*, 2007; Weaver *et al.*, 2004) or "New Zealand-Unknown" (NZ-U) (Hayward *et al.*, 2007). A cat can be infected with multiple FIV strains. In places where multiple subtypes circulate, this can give rise to recombinant viruses. Recombination can occur either between gene regions giving rise to, for example, A/C subtypes; or within single gene regions, forming for instance A/B envelope protein chimaeras (Hayward & Rodrigo, 2008).

1.1.4. FIV gene products and virion architecture

The structure of the FIV virion is determined by the protein products of the *gag*, *pol*, and *env* gene. In addition, the virion contains several accessory proteins. First, the different FIV proteins will be discussed, in the order of their presence in the viral genome. Next, their interactions within the FIV virion will be presented.

1.1.4.1. Gag polyprotein

The Gag polyprotein is the product of the *gag* gene. The FIV Gag polyprotein comprises the major structural proteins, matrix, capsid, and nucleocapsid. Furthermore, it also contains a p2 protein, important for virion egress, as will be discussed later. Expression of the Gag polyprotein can induce the production of virus-like particles without the need for other viral proteins (Manrique *et al.*, 2001). The polyprotein is cleaved very late in virus assembly; hence important functions of the

different components (MA, CA and NC) are inevitably associated with the function of the full Gag polyprotein.

The Gag polyprotein is targeted to the plasma membrane by myristolyation and a stretch of basic residues in the **matrix (MA)** protein, common among retroviruses (Brown *et al.*, 2015; Elder *et al.*, 1993; Henderson *et al.*, 1983; Li *et al.*, 2013; Schultz & Oroszlan, 1983). The interaction with phospholipids of the cellular plasma membrane is essential for viral replication. It was recently shown that unlike other lentiviral matrix proteins, the FIV matrix protein is capable of dimerization, thus aiding the multimerization of the Gag polyprotein (Serrière *et al.*, 2013b), a function usually reserved for the capsid protein. Apart from interaction with the plasma membrane, the matrix protein is also important for proper incorporation of the viral envelope protein into the viral particle (Celma *et al.*, 2007).

The biggest portion of the Gag polyprotein is reserved for the **capsid (CA)** protein. The capsid protein is highly immunogenic and conserved among different FIV strains. It is therefore an important indicator for rapid diagnostic methods. The capsid protein induces multimerization of the gag polyprotein (Serrière *et al.*, 2013a) and constitutes the viral capsid that holds the viral genome and products of the pol gene. The capsid protein is capable of interaction with several cellular proteins. A first one is cyclophilin A (Lin & Emerman, 2006). The importance of this interaction remains enigmatic. However, it is suggested that the binding spot of cyclophilin A may also be used by tripartite motif 5 protein (TRIM5), a known cellular restriction factor for lentiviral infection (Dietrich *et al.*, 2011b; Waters *et al.*, 1996). Furthermore, HIV CA has been shown to interact with the cytoskeleton and cellular motors. This may be essential for transport of the viral capsid or pre-integration complex towards the nucleus.

The FIV **nucleocapsid (NC)** contains the packaging signal that binds the viral mRNA genome and incorporates it into the viral particle (Kemler *et al.*, 2002; Manrique *et al.*, 2004; Moscardini *et al.*, 2002). The “when and where” of this interaction remains unknown. However, Kemler and co-workers recently showed that the Gag polyprotein is able to shuttle between the cytoplasm and the nucleus, and that this shuttling is dependent on the NC (Kemler *et al.*, 2012). These results raise the possibility that Gag cycles to the nucleus to interact with the genomic FIV mRNA.

Apart from the above mentioned structural viral elements, the carboxyl end of the FIV Gag polyprotein contains the **p2** protein with a late domain (L-domain) required for efficient virion release from infected cells (Calistri *et al.*, 2009; Elder *et al.*, 1993;

Luttge *et al.*, 2008; Manrique *et al.*, 2004). L-domains are short proline rich motifs in viral genomes that have a function in the late phase of virus assembly (Demirov & Freed, 2004). The FIV p2 protein contains a conserved PSAP L-domain that is able to bind directly to Tsg101 (Luttge *et al.*, 2008), and is ubiquitinated by Nedd4-2 (Calistri *et al.*, 2009). Tsg101 is a subunit of the endosomal-sorting complexes required for transport (ESCRT)-I protein. Proteins of the ESCRT machinery drive membrane remodeling processes, which results in membranes bending and budding away from the cytoplasm. They depend on ubiqitination for some of their functions (Schuh & Audhya, 2014). The hijacking of the ESCRT machinery for viral release is a feature shared by many enveloped viruses (Votteler & Sundquist, 2013).

1.1.4.2. Pol polyprotein

The Pol polyprotein contains all FIV enzymes; protease, reverse transriptase, deoxyuridine-phosphatase, and integrase. As already mentioned in paragraph 1.1.2, the protease gene is part of the *pol* ORF in the FIV genome. Furthermore, the FIV genome contains an additional enzyme compared to primate lentiviruses, the deoxyuridine-phosphatase. The Pol polyprotein is translated after a ribosomal -1 frameshift from the *gag* ORF, creating a chimaeric Gag/Pol polyprotein (Morikawa & Bishop, 1992).

The viral **protease (PR)** is indispensible in the viral life cycle. When the Gag and Gag/Pol polyproteins assemble, the protease dimerizes and becomes active. After dimerization, the enzyme autocleaves, and cleaves the Gag and Gag/Pol polyproteins, hereby inducing virion maturation (Elder *et al.*, 1993). Cleavage of the Gag/Pol polyprotein activates the other enzymes carried within the virion.

The **reverse transcriptase (RT)** converts the viral mRNA genome to a double stranded DNA intermediate, and is key to retroviral replication. The enzyme has two enzymatic functions; an RNA-dependent DNA polymerase activity (North *et al.*, 1990) and an RNase H activity. The enzyme exists as a heterodimer with a full (66 kDa) and a truncated form (54 kDa) of the RT protein. The truncated form lacks the RNase H activity, and differs structurally from the full form (Elder *et al.*, 1992), but is indispensable for the function of the enzyme (Amacker *et al.*, 1995).

Like other non-primate lentiviruses, the FIV genome encodes for a **deoxyuridine-phosphatase (DU)**, an enzyme that degrades deoxyuridine triphosphate to prevent the misincorporation of uracil into the viral DNA intermediate (Elder *et al.*, 1992). FIV

viruses lacking DU can still infect cells, but show a higher mutation rate in cells that are not actively dividing (Lerner *et al.*, 1995).

After conversion of the viral RNA genome into dsDNA, the genome is integrated into the host cell chromatin by the viral **integrase (IN)**. The enzyme contains at least three active domains; one to bind and process the viral genome, a non specific DNA binding domain to interact with the host cell DNA, and a catalytic site to perform ligation between the viral and host DNA (Shibagaki *et al.*, 1997).

1.1.4.3. Envelope protein

FIV contains only one glycosylated envelope protein on the viral envelope. This envelope protein is composed of two parts, the **surface (SU)** protein and the transmembrane (TM) protein (Stephens *et al., 1991*; Verschoor *et al., 1993*), and exists as a trimer on the viral envelope. The transmembrane part is anchored to the viral envelope by interaction with the MA that lies just underneath the lipid bilayer. At the luminal side, SU is associated with TM but they are not covalently linked.

Figure 3 gives a prediction of the FIV envelope protein structure. The envelope contains eight regions that are prone to a high mutation rate, and are highly variable when compared between different strains; they are called the variable loops (V). Six of these regions can be found on SU (V1 to 6) and the other three on TM (V7 to 9) (Pancino *et al.*, 1993). Variable region four and five are speculated to be important for the initial binding to the cell surface, by interacting with CD134, the primary receptor of FIV (Elder *et al.*, 2010; Shimojima *et al.*, 2004). This interaction induces a conformational change that reveals the secondary receptor (CXCR4) binding epitope in the V3 region. After binding of the viral receptors, the fusion peptide located on TM can extend into the plasma membrane of the host cell and induce fusion with the viral envelope (Hosie *et al.*, 2009). This action releases the viral capsid into the cytoplasm of the host cell.

Figure 3 (next page): Predicted structure of the mature FIV envelope protein, cleaved into the surface (SU) and transmembrane part (TM). The two parts are non-covalently linked, and the mature Env proteins exist as timers on the virion surface. TM spans the viral envelope once. When comparing the genetic sequences of the env gene, SU contains 6 variable regions (V1 to 6), and TM contains 3 (V7 to 9). Every dot represents an amino acid, and the consensus glycosylation sites are indicated with forks. Adapted from (de Parseval *et al.*, 2006; Pancino *et al.*, 1993).

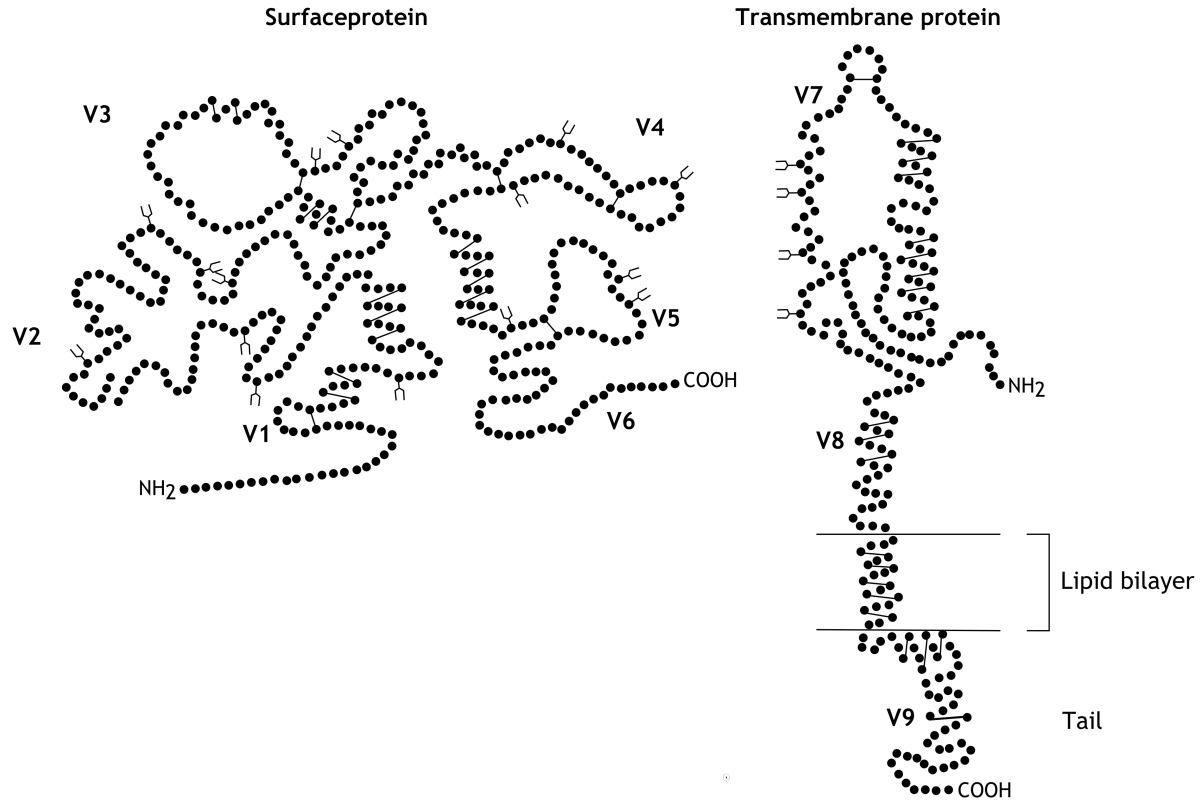

1.1.4.4. Accessory proteins

The FIV genome encodes several so called "accessory" proteins. These viral proteins are not per se involved in the structural make-up of the virion, but are important for virulence, infectivity and counteracting host restriction factors (Inoshima *et al.*, 1998a; Troyer *et al.*, 2013). The FIV genome contains three known accessory proteins, Rev, Vif and OrfA. Both the *vif* and *orfA* gene are located in front of the *env* gene. The *rev* gene, on the other hand, has two exons, one in front of *env*, and one after *env*, extending into the U3 region. All three proteins exert part of their function in the nucleus of the infected cell (Brown *et al.*, 1991; Chatterji *et al.*, 2000; Gemeniano *et al.*, 2004).

Rev or "**regulator of expression of virion proteins**" is responsible for transport of viral mRNA from the nucleus into the cytoplasm. This way, viral mRNA that is not fully spliced can leave the nucleus and code for the Gag, Gag-Pol and Env polyproteins, hence inducing productive replication (Kiyomasu *et al.*, 1991). The egress of unspliced viral RNA from the nucleus is also important for the incorporation of the full mRNA genome into newly formed viral particles. The Rev protein binds to the rev responsive element (RRE), a secondary RNA structure formed in the *env* gene (Brown *et al.*, 1991; Na *et al.*, 2010).

Vif, short for "**viral infectivity factor**" is found in all lentiviruses and counteracts the activity a cellular viral restriction factor; the apolipoprotein B mRNA editing enzyme, catalytic polypeptide-like 3 (APOBEC3) family. Vif can recruit an E3 ubiquitin ligase to APOBEC and label it for degradation by the proteasome (Gu *et al.*, 2016; Zielonka *et al.*, 2010). Vif is essential for cell-free infectivity (Tomonaga *et al.*, 1992), and productive infection of PBMC and monocyte-derived macrophages (Lockridge *et al.*, 1999). FIV mutants defective for Vif failed to replicate efficiently in cats (Inoshima *et al.*, 1998b). It has been described that Vif localized to the nucleus of FIV infected cells, but it's function here is unknown (Chatterji *et al.*, 2000).

Open reading frame A (**OrfA**) is a multifunctional protein present only in the FIV genome. FIV viruses lacking OrfA show no or a reduced replication efficiency in peripheral blood mononuclear cells (PBMC) *in vitro* and *in vivo* (Dean *et al.*, 1999; Na *et al.*, 2010; Pistello *et al.*, 2002; Tomonaga *et al.*, 1993a). The protein is important for viral particle formation and viral infectivity (Brunner & Pedersen, 1989). In the nucleus, OrfA can transactivate viral mRNA transcription through elements in the LTR (Chatterji *et al.*, 2002; de Parseval & Elder, 1999), and is able to induce a cell cycle arrest in the G2 phase (Gemeniano *et al.*, 2004). Furthermore, OrfA can downregulate cell surface expression of the primary FIV receptor, CD134, causing accumulation of the receptor in the Golgi apparatus (Hong *et al.*, 2010).

1.1.5. Virion architecture

FIV particles are characterized by a spherical phospholipid bilayer (envelope) and a cone shaped core, typical for lentiviruses. Figure 4 represents the FIV virion architecture. The FIV virions are approximately 90 to 120 nm in size. On the bilayer envelope the virus carries one glycosylated envelope protein that is important for host cell recognition. This envelope protein extends through the lipid envelope, and interacts with the viral matrix protein which anchors it to the virion. The cone shaped core is composed of the capsid protein, and contains the nucleocapsid protein that stabilizes two copies of the FIV mRNA genome. Besides these structural elements, the viral particle carries the viral enzymes important for virion maturation (PR), for integration of the DNA provirus into the cellular chromatin after infection (RT and IN), and for prevention of high mutation rate during reverse transcription (DU). It is still a matter of debate if the FIV virion contains all the accessory proteins (Vif, Rev and Orf A), important for virulence and inhibition of restriction factors in newly infected cells.

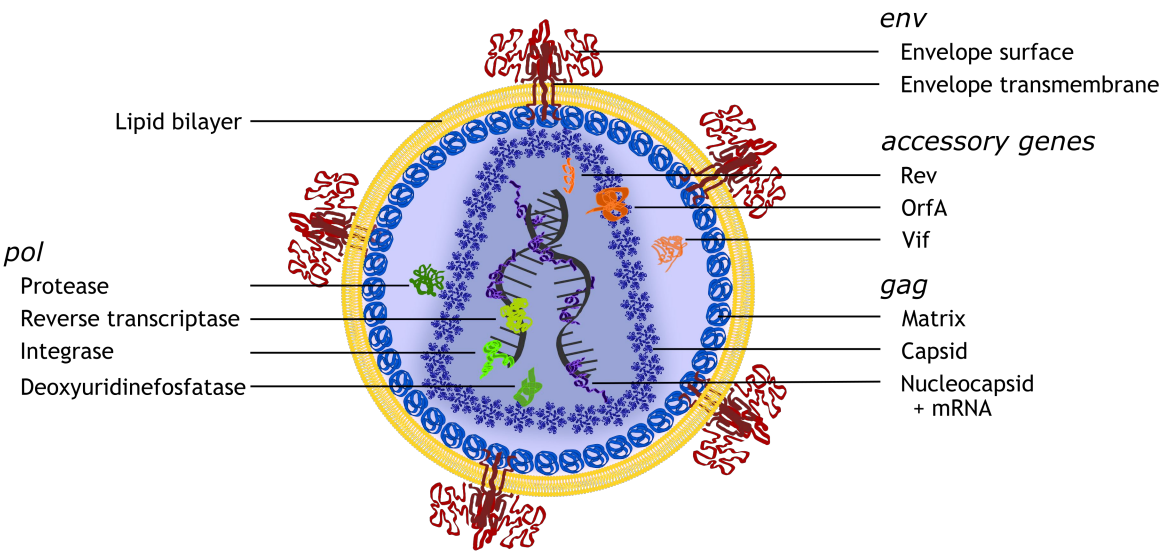

Figure 4: Feline immunodeficiency virus architecture. In red, the products of *env* ORF, the envelope protein that is expressed as a trimer on the lipid bilayer. In blue, products of the Gag polyprotein after proteolytic cleavage. The matrix protein lies just underneath the envelope and interacts with the envelope protein. The capsid protein is the major constituent of the viral core that contains two copies of the viral mRNA genome. The genome is stabilized by the nucleocapsid protein, and is associated with the reverse transcriptase, integrase and the deoxyuridinefosfatase. The viral protease is important for virion maturation after budding from the infected cell. In addition, the virion may also contain the accessory proteins OrfA, Vif and Rev.

1.1.6. Replication cycle

Retroviruses have a complex replication cycle (Fig. 5). The viral mRNA genome is first transcribed into a DNA intermediate that is subsequently integrated into the host cell chromatin, giving rise to the so called “provirus”. After creation of the provirus, the virus completely depends on the host cell transcription and translation machinery for the production of new viral genomes and proteins, and hence the formation of new FIV virions. The different steps are discussed in more detail in the following sections.

1.1.6.1. Entry

FIV enters the cell through the interaction between the envelope SU protein and two receptors. These receptors are: CD134, an activation marker of the tumor necrosis factor-receptor superfamily, and CXCR4, a CXC-chemokine receptor (Joshi *et al.*, 2005; Shimojima *et al.*, 2004). The interaction between SU and CD134 changes the conformation of SU and opens the cryptic CXCR4 binding loop. After binding with CXCR4, SU dissociates from the envelope TM protein, and the fusion peptide located on TM can now insert into the host cell plasma membrane (Hosie *et al.*, 2009). Next, the viral envelope and the host cell plasma membrane fuse, releasing the viral capsid into the cytoplasm. Today, there is still debate if fusion of the HIV viral and cellular membranes truly takes place at the plasma membrane and/or if the virus is endocytosed first (Melikyan, 2014). For FIV, on the other hand, no information exists.

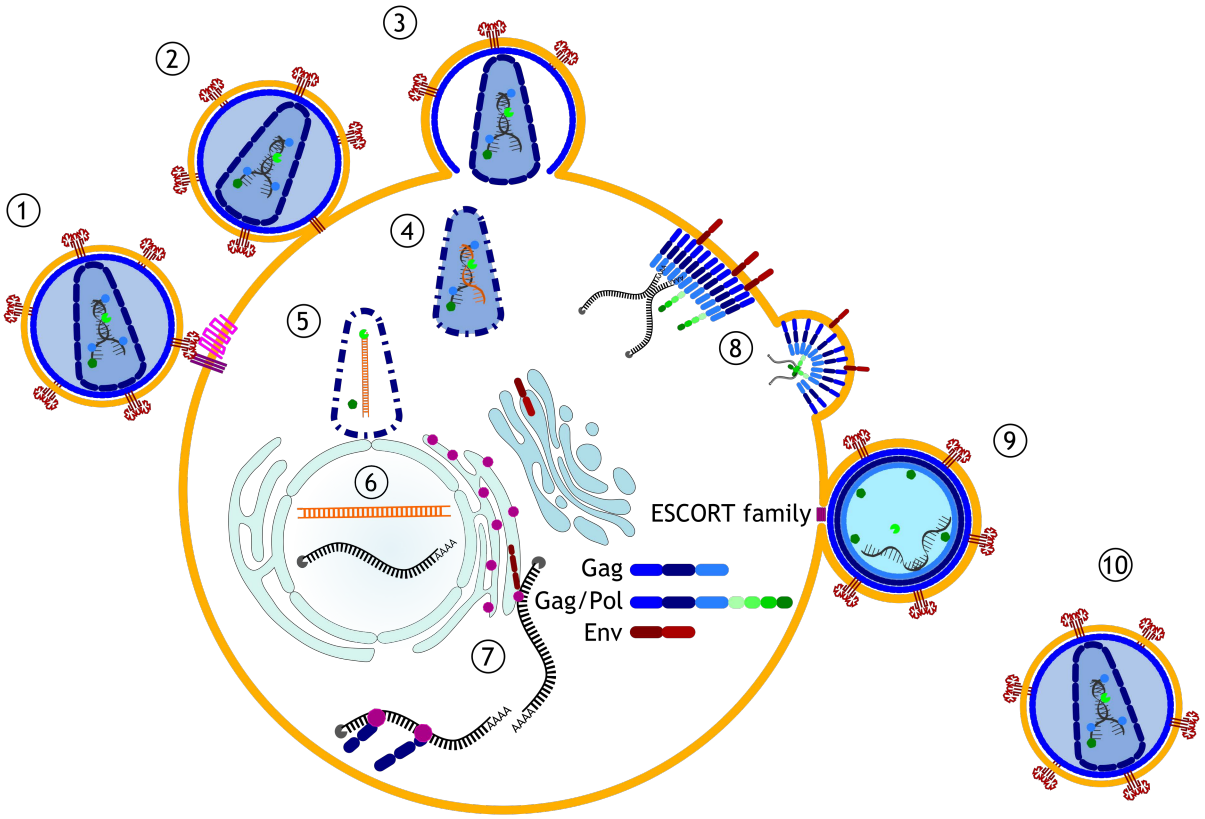

Figure 5: Steps in the FIV lifecycle. FIV enters the cell by sequential interaction between FIV SU and CD134 and CXCR4, respectively (1). Next SU is shed and the fusion peptide on TM inserts into the plasma membrane (2), causing fusion of the viral envelope and the cell membrane (3). The viral capsid is released into the cytoplasm and reverse transcription is initiated (4), converting the FIV mRNA genome into a dsDNA intermediate. The pre-integration complex docks at the nucleus (5) and viral dsDNA genome is transported across the nuclear pore. The viral IN inserts the viral genome into the host cell DNA (6). Now the cellular machinery is responsible for transcription and translation of the viral proteins (7). The Gag and Gag/Pol polyproteins assemble at the plasma membrane and recruit Env (8). After budding with help of the cellular ESCRT family (9), the virion matures by proteolytic cleavage of Gag, giving rise to the typical capsid core (10).

1.1.6.2. Uncoating and reverse transcription

The “when and where” of lentiviral particle uncoating remains a black box, and is also relevant in the debate about the manner of viral entry. In a first model, the viral capsid disassembles immediately after fusion. In another model, the viral capsid remains intact at least until reverse transcription is initiated, and gradually uncoats during transport towards the nucleus. The third model proposes that the capsid remains intact until it reaches the nuclear membrane, and uncoating takes place at the nuclear pore after completion of reverse transcription (Arhel, 2010). Recent studies on HIV favor the third model, in which premature uncoating is prevented to facilitate reverse transcription, and to permit passage to the nucleus without the activation of DNA sensing innate immune responses (Ambrose & Aiken, 2014).

As mentioned before, the mRNA viral genome has all the characteristics of a cellular mRNA molecule, with a 5' guanine cap and a polyadenylated 3' end. Like other polymerases, the FIV RT requires a primer for initiation of transcription. The 5' end of the viral genome is primed with a partially unwound cellular transfer RNA (tRNA) that is bound to the primer binding site (PBS) (Fig. 6A). From this primer, minus-strand DNA is synthesized until the 5' end of the genome is reached. This short fragment of DNA intermediate is called the minus-strand strong-stop DNA (-sssDNA). Due to the RNase H activity of the FIV RT the viral RNA in the RNA/-sssDNA duplex will be degenerated. Now the first strand transfer takes place, annealing the repeat (R) region in the -sssDNA to the 3' R sequence on the viral mRNA template (Fig. 6B). This event creates the LTR sequence, comprising the U3, R, and U5 region, respectively. The minus-strand synthesis now resumes, accompanied by RNase H digestion of the RNA template. Initiation of the plus-strand synthesis starts from two short polypurine tract (PPT) sequences, the 3' PPT and the central PPT, that are more or less resistant to RNase H degradation. At these places a RNA primer remains bound to the minus-strand DNA. The generation of the plus-strand is halted when a portion of the minus-strand primer tRNA is reverse-transcribed, this yields the plus-strand strong-stop DNA (+sssDNA). The remaining tRNA primer is removed by RNase H activity. A second strand transfer occurs, annealing the plus-strand and minus-strand PBS (Fig. 6C). Synthesis is completed with each DNA strand serving as a template for the other strand. Final elongation of the minus-strand displaces the portion of the minus-strand from which the plus strand was copied (5' LTR). Elongation of the +sssDNA stops at the central termination sequence, and leads to a discrete plus-strand displacement in the centre of the genome of the plus-strand initiates at the cPPT. The final product is a blunt-ended linear double stranded DNA molecule. Since the viral genome is provided in duplicate in the virion, strand transfer events can occur intramolecular or intermolecular. Existence of dual subtype viruses proves that the RT can even switch strands during elongation.

1.1.6.3. Genome integration

After reverse transcription, the pre-integration complex (PIC) needs to get access to the nucleus in order to integrate the viral genome into the host cell chromatin. Lentiviruses are capable of actively transporting their PIC across the nuclear pore complex (NPC) and can therefore infect non-dividing cells. The precise composition of the PIC is not known today. However, several viral and cellular proteins have been identified to be involved in successful integration (reviewed in (Matreyek & Engelman,

2013)). While both the viral integrase and matrix protein contain a nuclear localization signal (NLS), the viral capsid protein is now being viewed as an important factor for nuclear transport. It is speculated that CA interacts with cellular proteins for docking and transport across the NPC. It is therefore unlikely that uncoating of the viral capsid occurs passively, as already described before. After transport, the lentiviral integrase interacts with cellular nuclear factors that bind to active transcription units, and tethers the PIC to the chromatin. One of the most intensively studied is lens epithelium derived growth factor (LEDGF/p75) (Christ & Debyser, 2013; Kang *et al.*, 2006). The integration itself occurs in two catalytic steps. First the viral LTRs are processed by removing dinucleotides adjacent to a highly conserved "CA" dinucleotide from the 3' strand on both sides. This exposes a 3' hydroxyl group that is used to attack the target DNA during the second step, the joining reaction, in which the viral genome is inserted into the cellular DNA (Engelman *et al.*, 1991; Vink *et al.*, 1991). Nicks that remain in the DNA after the insertion are repaired by the cellular base excision repair pathway (Yoder *et al.*, 2011).

Figure 6 (next page): Steps in the retroviral reverse transcription process. (A) The first step in the process, creation of the minus-strand strong-stop DNA (-sssDNA). (B) The -sssDNA is then transferred for further synthesis of the minus-strand and creation of the +sssDNA. (C) Second transfer of the minus-strand DNA to dimerize with the PBS on the +sssDNA, and completion of the reverse transcription. The full description of the process can be found in the text. Black lines, RNA; Orange lines, minus-strand DNA; Red lines, plus-strand DNA.

A. Initiation of reverse transcription from PBS

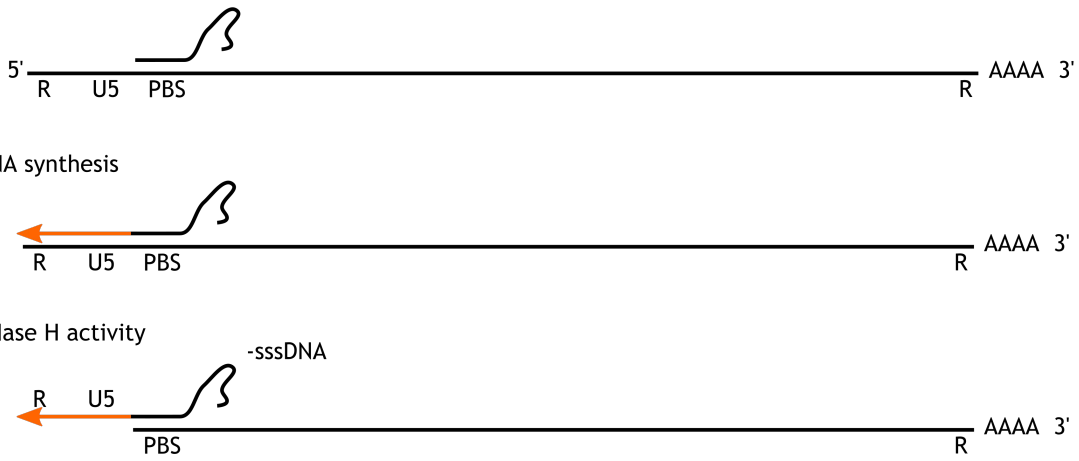

B. First strand transfer

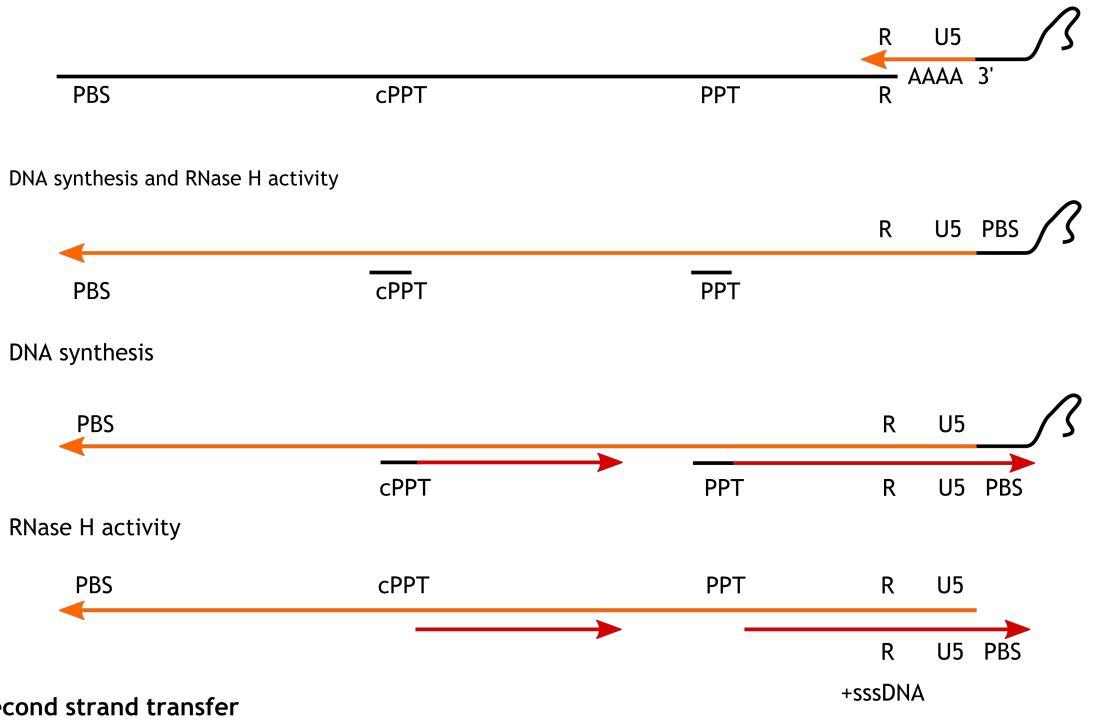

C. Second strand transfer

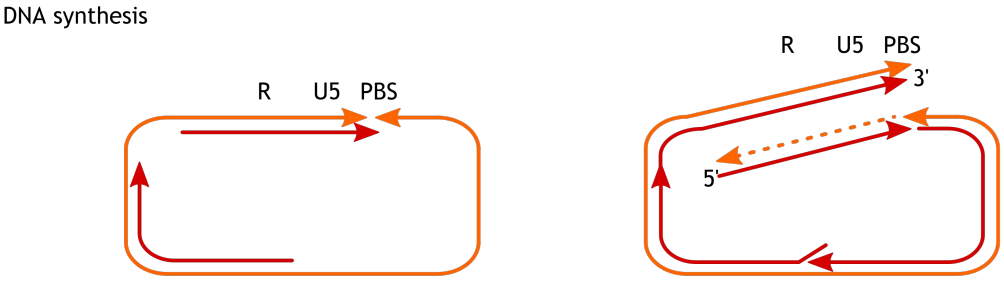

D. FIV DNA intermediate

1.1.6.4. Viral transcription and translation

After integration of its genome in the host cell chromatin, FIV uses the cellular machinery to replicate. The TATA-box is the core promoter element in the viral promoter and initiates basal transcription of the viral genome. Apart from the TATA-box, a number of regulatory control elements are located in the LTRs. Some of these sites are conserved between FIV isolates, like AP-4, AP-1 and ATF/CREB sites (Sparger *et al.*, 1992; Talbott *et al.*, 1989). Some viruses may also contain additional sites to bind transcription factors (TF) like NF-κB, NF-1, C/EBP and LBP-1 (Sparger *et al.*, 1992; Thompson *et al.*, 1994). These TF binding sites make the transcription of FIV sensitive to cellular activation signals. As already mentioned before, the FIV OrfA protein can transactivate viral mRNA transcription through elements in the LTR (Chatterji *et al.*, 2002; de Parseval & Elder, 1999).

Transcription of the FIV provirus generates a viral mRNA molecule that has all the features of a cellular mRNA molecule. The host cell nuclear transport system has a preference for fully spliced mRNA that no longer contains splice acceptor sites, which indicate intron structures. Like other lentiviruses, the FIV genome contains a major splice donor site proximal to the 5' LTR (Fig. 2). Downstream, multiple splice acceptor site can be found for creation of differently spliced viral mRNAs that code for different viral proteins (Tomonaga *et al.*, 1993b). The first mRNA to be exported is fully spliced and encodes the Rev protein. Rev is responsible for the efficient transport of unspliced (genomic, and encoding Gag and Pol) and singly spliced (for Env, Vif and OrfA) viral RNA, from the nucleus to the cytoplasm (Kiyomasu *et al.*, 1991).

Translation of viral proteins starts after transport of the (spliced) viral mRNA from the cellular nucleus. FIV uses the host cell machinery for translation. While Env is translated by ribosomes on the rough endoplasmic reticulum, the other proteins are translated by free ribosomes. The Gag and Gag/Pol polyprotein are both translated from a non-spliced mRNA. The Gag/Pol chimaeras are created after a ribosomal frameshift of -1 codon on a slippery region at the 3' end of the gag gene. This frameshift occurs in approximately 5% of the translational events.

1.1.6.5. Assembly and budding

FIV is an enveloped virus and obtains its bilipid layer from the budding site before entering the extracellular space. Lentiviruses assemble at the plasma membrane in lymphocytes, but they may also use an (membrane connected) intracellular compartment like multi vesicular bodies in macrophages (Benaroch *et al.*, 2010; Joshi

et al., 2009; Ono & Freed, 2004). The Gag polyprotein seems to be choreographer of the assembly and budding of retroviruses. A lot of the functions that were described for the Gag polyprotein under heading 1.1.3.1 come into action here. The matrix protein interacts with particular lipids in the membranes (Ono *et al.*, 2004; Waters *et al.*, 1996) and assures anchoring to the lipid membrane via a myristyl moiety. The spatial lattice of the multimeric MA allows for interaction with the cytoplasmic tail of the Env protein (Affranchino & González, 2014; Celma *et al.*, 2007; Manrique *et al.*, 2001). Between the Gag polyproteins, some chimaeric Gag/Pol polyproteins are inserted, ensuring the incorporation of the viral enzymes into the viral particle. The NC and MA protein interact with the genomic viral mRNA (Kemler *et al.*, 2002). However the "when and where" of this interaction is not known yet. Budding of the virion is driven by members of the cellular ESCRT machinery through interaction with the p2 protein located in the C-terminal part of Gag (Calistri *et al.*, 2009; Luttge *et al.*, 2008). The cellular proteins drive the membrane remodeling and the constriction of the cellular membrane to result in a free FIV virion.

1.1.6.6. Maturation

During or shortly after budding, the FIV particle matures by cleavage of the Gag/Pol and Gag polyproteins into their separate components. The maturation event starts by dimerisation of the PR subunits in the Gag/Pol protein. The dimerisation of PR creates active enzymatic site, and the functional protease is released by autoproteolysis (Kräusslich, 1991; Laco *et al.*, 1997). Although the precise timing of the proteolytic event is not known, it is essential for the formation of infectious particles (Kräusslich, 1991). The cleavage releases the structural elements MA, CA and NC, of which CA will create the typical conical core, and creates the separate viral enzymes PR, IN, RT and DU.

1.1.7. Pathogenesis

FIV is transmitted through biting incidents between cats. Territorial behavior puts male free roaming cats at a higher risk for contraction of FIV compared to female cats (Tompkins *et al.*, 2008). Virus or FIV infected cells present in the saliva enter the bite wound and eventually get drained to the lymph nodes. FIV infects a range of immune cell lineages; T- and B-lymphocytes, and cells of the myeloid lineage, including monocytes, macrophages and astrocytes (Brown *et al.*, 1991; English *et al.*, 1993; Lerner *et al.*, 1995). It is unclear if infiltrating immune cells at the entry wound can become infected before draining to the lymph nodes.

The clinical acute phase starts 4-8 weeks p.i., and peaks at 8-12 weeks. The cat may present some flu-like symptoms, mild anorexia, and neutropenia which may last from days to several weeks, and a generalized lymphadenopathy that can last up to 9 months (Pedersen *et al.*, 1989). During this acute phase, the immune system successfully counteracts the viral replication, and viral titers in the blood become almost undetectable (Fig. 7). After an initial decline in CD4+ T-cell numbers due to FIV replication and bystander apoptosis, there is a partial restoration once antibodies and cytotoxic T-cells control the infection. There is a steep decrease in the number of infected CD4+ T-cells, but a shift of infection to macrophages. Unfortunately, the infection is not cleared and the disease course enters an asymptomatic phase which can last for years, depending on the age of the cat, pathogenicity of the infecting FIV strain, and exposure to secondary infections (Lerner *et al.*, 1995). Some cells that were infected early during infection may become latently infected, with the viral genome incorporated in the cellular chromatin, but no productive viral replication. Latently infected cells may become activated, which can induce FIV replication (McDonnel *et al.*, 2012). Recent information showed that ongoing viral replication occurs in the lymph nodes, while this is hampered in blood circulating cells (Eckstrand *et al.*, 2016). This means that the FIV infection is persistent as well. The ongoing low-level FIV replication during the asymptomatic phase over time induces a dysregulation of the immune system and a decline in the CD4+ T-cell count. Over the course of time, this results in a peripheral general lymphadenopathy (PGL) and development of the AIDS related complex (ARC). Cats develop leukopenia due to declining T-cell numbers an may develop other leukocyte depletions as well (Shelton *et al.*, 1990). Cats present weight loss and some chronic infections, usually in the mouth, airways and eyes (Lerner *et al.*, 1995; Pedersen *et al.*, 1989). Within 18 months the cat will develop full blown feline AIDS, that is characterized by a rise in the FIV plasma viral load, further CD4+ T-cell decline (Fig. 7), and failure to generate an immune response against secondary and opportunistic infections. Some cats may develop neurological symptoms related with FIV infection in the brain (Phillips *et al.*, 1994; Prospéro-García *et al.*, 1994), or blood neoplasms (Beatty *et al.*, 1998; Steigerwald *et al.*, 1999). Up till now, no antiretroviral therapy is available, and cats are treated symptomatically for concomitant infections. Most cats succumb to severe anorexia due to a chronic stomatitis and gingivitis, and failure to clear secondary infections.

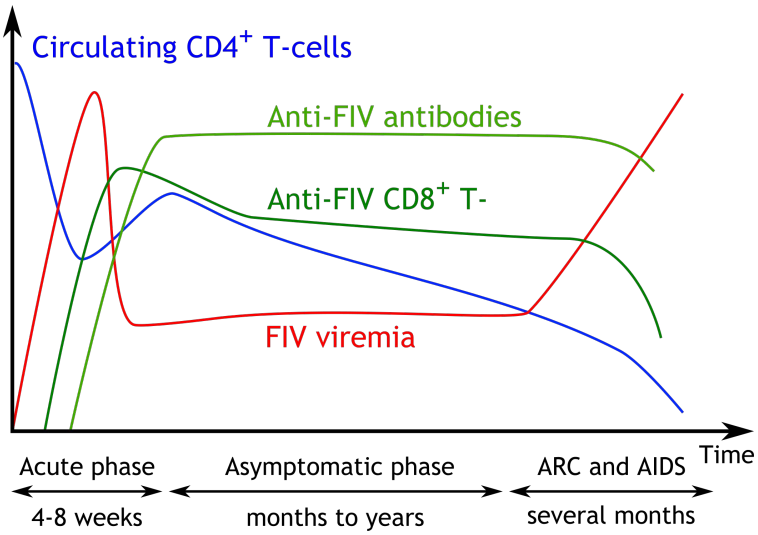

Figure 7: FIV disease course. Adapted from (Lecollinet & Richardson, 2008).

1.1.7.1. Pathogenesis of lentiviruses in other mammalian hosts

The genus lentivirus contains eight viruses that can infect only their specific mammalian host, and persist through life. All viruses in this group are transmitted through contact with one or more body fluids from infected individuals. The main targets of lentiviruses are monocytes/macrophages and lymphocytes, both important cells of the immune system. Pathogenesis caused by lentiviruses can be divided into roughly two groups. The first group contains the small ruminant lentiviruses, caprine arthritis and encephalitis virus (CAEV) and maedi-visna virus (MVV), that mainly infect goat and sheep respectively, but can also cross between these species. These animals represent with symptoms of chronic inflammation in specific tissues. Another member of the first group is equine infectious anemia virus (EIAV), that infects all members of the *Equidae* family; horses, ponies, donkeys, mules, and zebras. EIAV causes recurrent episodes of diseases with high fever, anemia and wasting symptoms as the most important signs. The members of this first group of lentiviruses only infect macrophages and not lymphocytes.

The second group contains the immunodeficiency viruses infecting humans (HIV-1 and HIV-2), non-human primates (SIV), felines (FIV), and bovines (BIV). These viruses infect both monocytes/macrophages and lymphocytes. They cause a severe dysregulation of the immune system, leading to an acquired immunodeficiency. Non-human primates and bovines have adapted to infection with their respective lentiviruses, and infection causes no or little disease. Also in felines, FIV only causes disease among domestic cats. Wild cats have their own FIV strains, and infected individuals show no signs of disease. The human viruses, HIV-1 and HIV-2, are believed to originate from SIV infecting chimpanzees and sooty mangabey

respectively, in relatively recent events. While causing no disease in their natural host, crossing of the species barrier allowed these viruses to be pathogenic in their new host. Since HIV is new virus in humans, we are poorly adapted to fight and restrict the disease caused by these viruses.

Table 2: Overview of pathogenesis of lentiviruses in different mammalian hosts.

Virus	Host	Transmission	Cell tropism		Pathogenesis	
			mono-cytes	lympho-cytes	progression	symptoms
CAEV	goat/sheep	milk	+	-	slow (strain differences)	arthritis, pneumonia, mastitis, encephalitis
MVV	sheep/goat	milk	+	-	Fast (strain differences)	encephalitis, chronic pneumonia
EIAV	equines	biting insects, body fluid contact	+	-	Recurrent episodes	high fever, anemia, wasting
HIV 1	human	body fluid contact	+	+	quick	drop in T-cell numbers, immune-deficiency, central nervous system disease
HIV 2	human	body fluid contact	+	+	slow	
FIV	felines	saliva	+	+	slow	
SIV	non-human primates	body fluid contact	+	+	non-pathogenic/slow	
BIV	bovines	body fluid contact	+	+	non-pathogenic/slow	

FIV is often proposed as a natural occurring small animal research model for HIV because of many similarities in pathogenesis. As described above, FIV infection causes a short acute phase, followed by a long asymptomatic phase that progresses into a terminal phase characterized by immunologic decompensation, increase in plasma viral load, and clinical symptoms of immunodeficiency with opportunistic infections. All these phases of disease are also evident in HIV infected humans. Lymphoid tissue alterations are similar with those found in HIV infected humans and neurological manifestations are also evident. HIV and FIV share the general retroviral genome make-up, containing the large open reading frames *gag*, *pro*, *pol* and *env*. However, FIV lacks *vpr*, *vpu*, and *nef* accessory genes that are present in HIV. The accessory genes *vif* and *rev* are shared, but FIV has an additional ORF called *orfA*. Another difference is the broader cellular tropism of FIV. Unlike HIV, FIV is able to infect B-lymphocytes (Shimojima *et al.*, 2004). Thus although the general pathogenesis and clinical manifestations seem similar for both viruses, underlying mechanism might be different due to important differences in cell tropism and genetic make-up.

1.1.8. Immune response

During the acute phase of FIV infection a vigorous immune response is generated leading to a steep decline in viral plasma load. The next section will discuss the innate restriction factors against retroviruses, and the response by the adaptive immune system against FIV in particular.

1.1.8.1. Cellular restriction factors

Mammalian cells have an innate defense against retroviruses that act on various steps of the virus replication cycle (Fig.8). Upon entry, the viral capsid can be bound by tripartite motif-containing protein 5 (TRIM5). **TRIM5** is an ubiquitin ligase that can target the capsid protein for degradation by the proteasome. Binding of TRIM5 to the viral capsid accelerates the uncoating of the viral capsid, hindering reverse transcription and integration of the viral genome. However, due to a truncation in feline TRIM5, there is no restriction in felids against FIV (McEwan *et al.*, 2009).

Upon reverse transcription of the RNA molecule harboring the viral genome, the single stranded DNA intermediate can be attacked by members of the apolipoprotein B mRNA editing enzyme, catalytic polypeptide-like 3 (APOBEC3) family. These cellular proteins are incorporated into the virion, and exert their activity in the next replication round. **APOBEC3** is a cytidine deaminase that catalyzes the deamination of cytidine (C) to uridine (U) in the single stranded DNA substrate. This C to U substitution can cause extensive and inactivating levels of FIV genome hypermutation. Different members of the feline APOBEC3 proteins are active against the different feline retroviruses (Münk *et al.*, 2008).

In non-cycling cells like dendritic cells, monocytes and macrophages, SAM domain and HD domain-containing protein 1 (**SAMHD1**) is starving the viral reverse transcriptase from nucleotides. Hydrolyzation of the intracellular deoxynucleoside triphosphates (dNTPs) by SAMHD1 lowers their concentrations below those required for the synthesis of the viral DNA by reverse transcriptase (Laguette *et al.*, 2011; Lahouassa *et al.*, 2012). Furthermore, SAMHD1 has an RNAse function that may degrade viral RNA (Ryoo *et al.*, 2014). According to Gramberg and colleagues, SAMHD1 may also be active against FIV (Gramberg *et al.*, 2013).

While all restriction factors described above work on elements early in the viral life cycle, **tetherin**, also known as bone marrow stromal cell antigen 2 (BST2), plays a role at the very end of the replication process. Tetherin is a plasma membrane protein,

and expression is upregulated following an interferon (IFN) signal. It inhibits spread of newly formed viral particles by tethering them to the plasma membrane of infected cells post budding or release (Neil *et al.*, 2008). It remains unclear is feline tetherin if also effective against FIV spread (Dietrich *et al.*, 2011a).

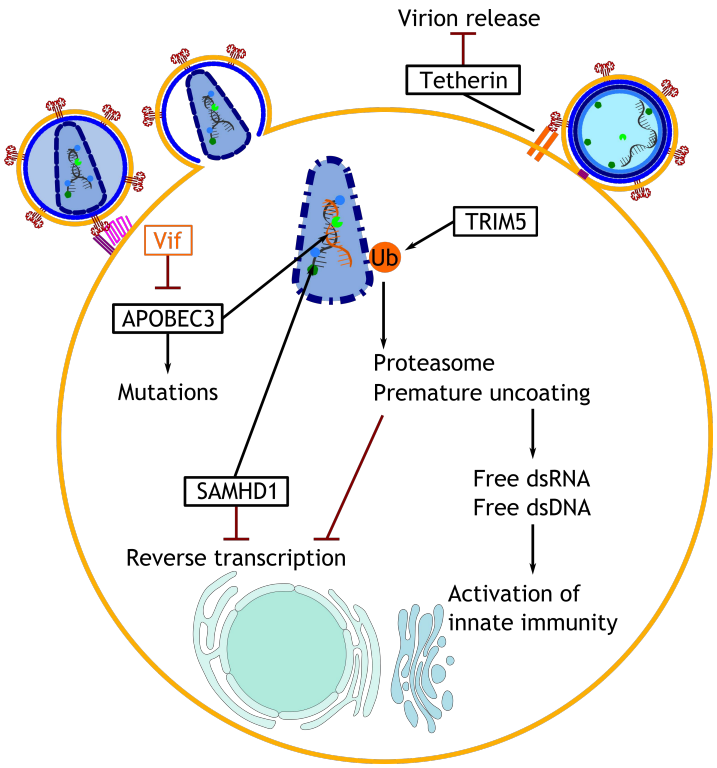

Figure 8: Schematic representation of cellular restriction factors against FIV infection and countermeasures of FIV. Upon release of the viral capsid in the cell, TRIM5 ubiquitin (Ub) ligases can target the FIV capsid protein for degradation by the proteasome. APOBEC3 is incorporated into virion during replication and executes its function when reverse transcription is initiated. It attacks the cytidines in the DNA intermediate introducing extensive mutations of the viral genome. FIV Vif can recruit ubiquitin ligases to APOBEC, targeting the protein for degradation. SAMHD1 lowers the amount of available nucleotides inside the cell, hindering reverse transcription. Furthermore, it has an RNAse function that can attack the viral RNA genome. When FIV is able to infect and replicate, virus release can still be inhibited by expression of the cellular protein tetherin, which can anchor newly produced virions to the plasma membrane.

1.1.8.2. Adaptive immune response

Seroconversion occurs 1 to 6 weeks after infection, depending on several factors like initial viral load, route of inoculation, virus strain, and host-dependent factors (Burkhard *et al.*, 2001; Calzolari *et al.*, 1995; Grant *et al.*, 2009; Podell *et al.*, 1997). The first antibodies are generated against structural elements of the FIV virion, the Env protein and viral core (MA, CA, and NC) proteins. Later, antibodies against the reverse transcriptase can be detected as well. Potentially neutralizing antibodies arise after 5 to 6 weeks (Tozzini *et al.*, 1993). Antibody titers are maintained throughout the infection. A hypergammaglobulinemia comprising antibodies against non-FIV

antigens can be detected in FIV infected cats due to non-specific stimulation of B-cells (Pedersen *et al.*, 2001).

CD8$^+$ T-cells can inhibit FIV replication by non-cytolytic and cytolytic activity. CD8$^+$ T-cells produce unknown soluble factor(s) in the acute phase of FIV infection (within 1 week of p.i.) that inhibit post-integration steps of the viral lifecycle (Flynn *et al.*, 1999; Flynn *et al.*, 2002; Hohdatsu *et al.*, 1998). FIV specific cytotoxtic CD8$^+$ T-lymphocytes (CTL) can be detected 4 to 6 weeks p.i. (Bucci *et al.*, 1998; Zielonka *et al.*, 2010) and remain present during the FIV disease course. Shimojima and co-workers also reported an increase in a specific subset of CD8$^+$ cells and phenotypic changes of these cells post-FIV-infection (Shimojima *et al.*, 1998; Shimojima *et al.*, 2003). Natural killer (NK) cells, on the other hand, are defective in killing FIV infected cells (Hanlon *et al.*, 1993; Zaccaro *et al.*, 1995).

1.1.9. Immune evasion and dysregulation

To establish a lifelong infection, retroviruses have developed several immune evasive mechanisms. Information about FIV immune evasion is limited, but strategies known to be employed by FIV will be discussed in more detail below. Because FIV infects cells of the immune system, a profound immune dysregulation develops as the disease progresses. The most important processes leading to the final stage of acquired immunodeficiency will also be reviewed.

1.1.9.1. FIV immune evasion

FIV replication can spread to a larger cellular machinery using formation of **syncytia**. Interaction between cell surface expressed Env and the FIV receptors on an interacting cell can induce fusion of the cellular membranes (Pedersen *et al.*, 1987).

The retroviral RNA genome can mutate quickly under impulse of replication restraining factors, like the mounted immune response or antiretroviral therapy, leading to **escape mutants**. Like HIV, the FIV *env* gene allows large sequence variation in the hypervariable regions as described in 1.1.4.3. This sequence variation leads to the emergence of different FIV clades with little cross-protection (Westman *et al.*, 2016), allowing for infection with multiple FIV viruses, and making it difficult to generate effective vaccines (Carpenter *et al.*, 1998). FIV Env even allows the generation of quasispecies with reduced need for primary receptor binding (Hartmann *et al.*, 2012).

Most lentiviruses contain a number of accessory proteins important for virulence, infectivity, and immune evasion. FIV contains 3 known accessory proteins, Rev, Vif and OrfA (discussed in detail sub 1.1.4.4.). The latter two contain immune evasive properties. FIV **Vif**, like Vif of human and primates immunodeficiency viruses, has an anti-APOBEC3 function. Vif can recruit an E3 ubiquitin ligase to APOBEC and label it for degradation by the proteasome (Gu 2016). The lower cellular concentrations of APOBEC reduce the likelihood that APOBEC is incorporated in the virion, and will be able to execute its function in the next replication round. **OrfA** is unique for FIV, and has functions overlapping those of accessory proteins that are known for other lentiviruses. For instance, OrfA downregulates CD134 (FIV primary receptor) expression on the cell surface, similar to Nef for HIV. Sündstrom and colleagues reported that expression of OrfA downregulated the expression of genes important for the ubiquitination-proteasome system, thereby possibly hindering destruction of viral proteins (Sundstrom *et al.*, 2008). The relevance of these findings, however, are yet to be proven.

1.1.9.2. FIV induced immune dysregulation

Early after the discovery of FIV it was noticed that immune cells of FIV infected cats showed a reduced ability to proliferate in response to primary and memory antigens, and mitogenic agents (Bishop *et al.*, 1992a; b; Torten *et al.*, 1991). Furthermore, FIV positive cats have an unremitting polyclonal hypergammaglobulinemia (Pedersen *et al.*, 2001), and an increase in phenotypically activated $CD8^+$ T-cells (Shimojima *et al.*, 1998; Shimojima *et al.*, 2003) and regulatory T-cells (Treg) (Vahlenkamp *et al.*, 2004b). Therefore, it can be stated that FIV infection induces a dysregulation of the immune system. The dysregulation is characterized by: (1) a reduced activity of innate immunity, (2) immunologic anergy and apoptosis, and (3) an inappropriate activation of certain immune cells.

Several mechanisms have been proposed to contribute to the observed immune dysregulation. First, FIV infected cats show a distorted cytokine balance. FIV infected cats show a constitutive increase of IL10, IFNγ and TNFα, but decreased IL2 and IL12 levels in the lymph nodes. In response to challenge of the immune system with a secondary agent, these cats fail to mount an adequate immune response, with depressed IL2, IL6, IL12 and IFNγ levels compared to control cats (Dean *et al.*, 2006; Levy *et al.*, 1998). Inversion of the IL10/IL12 balance may suppress Th1 cells to generate a cell-mediated immune response. Second, Treg cells are activated early in

FIV infection, as a direct effect of FIV infection in these cells (Mexas *et al.*, 2008; Miller *et al.*, 2013). FIV preferentially replicates in Treg cells due to high CXCR4 expression, and elevated activation of the proviral LTR (Joshi *et al.*, 2005). Treg cells of FIV infected cats inhibit IL2 production and proliferation of $CD4^+$ T-cells, hence inducing immunologic anergy (Meng *et al.*, 2014) and induce anergy in $CD8^+$ cells (Fogle *et al.*, 2010). In addition, chronic stimulation of immune cells with FIV antigens can lead to the upregulation of B7 and CTLA-4 on T-cells. B7 is the counterpart of both CD28 and CLTA-4, while CD28 enhances T-cell survival, the elevated expression of CTLA-4 induces apoptosis. The upregulation of B7 and CTLA-4 correlates with spontaneous T-cell apoptosis in lymph nodes of FIV infected cats (Tompkins *et al.*, 2002; Vahlenkamp *et al.*, 2004a). The massive apoptosis of immune cells may account for the destruction of the lymph node structure in advanced stages of FIV infection (Matsumura *et al.*, 1994; Rideout *et al.*, 1992) and the steady decline of $CD4^+$ T-cell numbers. These phenomena over time increase the observed immune dysfunction, leading to the acquired immunodeficiency of FIV infected cats.

Keeping FIV negative cats indoors is the only preventive measure owners can take. A lot of FIV research has focused on the development of a FIV vaccine, with development of a commercial dual subtype vaccine as a result. The vaccine, called Fel-O-Vax FIV® (Boehringer Ingelheim), contains inactivated cells infected with a Japanese FIV subtype D strain (Shizuoka) and an American FIV subtype A strain (Petaluma). However, vaccination against FIV is not recommended in Europe (Hosie *et al.*, 2009). Safety concerns have been raised since there are several reports of vaccine-mediated enhancement of disease (Lecollinet & Richardson, 2008). Furthermore, cross-protection against European isolates is still under discussion (Dunham *et al.*, 2006). In Australia and New Zealand the vaccine is in use, recently an Australian study assed the protective rate of the vaccine in the field using 139 vaccinated cats and 301 un-vaccinated controls. They registered 5 vaccine-breakthroughs, as well as two infection cases in vaccinated cats with missing follow-up vaccinations. There was no difference in FIV prevalence between the vaccinated and un-vaccinated group of cats, raising doubts about the efficacy of the Fel-O-Vax vaccine in the field (Westman *et al.*, 2016).

1.1.10. FIV disease prevention and control

FIV infected cats usually do not develop severe symptoms until 4-6 year after infection. Cats presenting with chronic gingivostomatitis, chronic rhinitis, weight loss, lymphadenopathy, immune-mediated glomerulonephritis, unusual or severe parasitic

skin disease, or blood tumors should alert the clinician to the possibility of FIV infection. FIV infection can be checked with a commercial point-of-care SNAP test. Several test are on the market, and some are available as a combo test for both feline retroviruses; FIV and FeLV. In an FIV SNAP test, a drop of blood is applied to chromatographic paper that contains FIV antigen. If the cat has antibodies against FIV, the test will return a positive result. It is advised to confirm positive SNAP test results in low-risk groups by western blot (Hosie *et al.*, 2009).

FIV-infected cats are usually not treated as long as no symptoms are present. Owners are advised to keep seropositive cats indoors to avoid spread of FIV and contraction of other diseases. Male cats should be neutered to avoid fighting when held in a multi-cat household. Regular health checks are advised to allow early intervention for developing problems. In case of sickness longer or more aggressive treatment than usual may be needed. Supportive treatment can be given when chronic problems like gingivostomatitis develop (Hosie *et al.*, 2009). Specific anti-FIV drugs do not exist, and antiviral therapy against FIV is not generally used in veterinary practice. However, some clinical trials have been performed with antiretroviral drugs developed against HIV. One of the first nucleoside analogue reverse transcriptase inhibitors that was developed against HIV, 3'-azido-2',3'-dideoxythymidine (AZT, Zidovudine) has been used successful in inhibiting FIV replication and improving immunological and clinical status of FIV-infected cats (Arai *et al.*, 2002; Hartmann *et al.*, 1992). Caution is needed when using this drug, since development of resistance has been reported, and AZT my cause non-regenerative anemia (Medeiros *et al.*, 2016; Zhu *et al.*, 1996). Other anti-HIV drugs, like Tenofovir and Plerixafor have been tested and seemed effective against FIV but no recommendations for use have been made (Hartmann *et al.*, 2012; Taffin *et al.*, 2015; Vahlenkamp *et al.*, 1995).

1.2. Lymphoid tissues

The role of lymphoid tissues in the FIV and HIV pathogenesis is a hot topic in current lentiviral research. In this doctoral thesis there is also a focus on the influence of these tissues on FIV replication. Therefore, the following sections will give a short overview of the normal physiological organization and function of the primary (hematopoiesis and development of immune cells) and secondary lymphoid organs (orchestration of the immune system), and the changes in these organs induced by FIV infection.

1.2.1. Primary lymphoid organs

1.2.1.1. Bone marrow

There are two types of bone marrow, the red and the yellow bone marrow. The red bone marrow is the major site of hematopoiesis, while the yellow bone marrow is fatty with little to no hematopoiesis. Hematopoietic stem cells (HSC) in the red bone marrow provide lymphoid and myeloid progenitor cells, based on the demand of the body (Fig. 9). The progenitors are supported by a network of reticular stromal cells that produce extracellular matrix components, cytokines, growth factors and hormones to stimulate mitosis and early differentiation of HSC. The yellow bone marrow lost the hematopoietic function but still contains multipotent mesenchymal stem cells that can differentiate into hematopoietic supportive stromal cells, fibroblasts, myoblasts, adipocytes, chondrocytes and osteocytes.

In the bone marrow, mononuclear cells and megakaryocytes can become FIV infected, and produce FIV provirus carrying progeny cells. Tissue abnormalities seen in the bone marrow of FIV infected cats are lymphoid follicular hyperplasia, increase in number of granulocyte and monocyte precursor cells (immaturity), and excess of eosinophils (Beebe *et al.*, 1992; Huisman *et al.*, 2004; Shelton *et al.*, 1990).

1.2.1.2. Thymus

The thymus is responsible for further differentiation and selection of non-self T-cells and natural killer (NK) cells that arrive in the thymus from the bone marrow (Rossi *et al.*, 2005). The thymus has 4 major zones that have a specific cellular composition and chemokine profile that aid in the selection process; the subcapsular zone (SCZ), the cortex, the cortico-medullar junction (CMJ) and the medulla (Fig. 9) (Bunting *et al.*, 2011). T-cells that do not survive the selection undergo apoptosis and are removed by residential macrophages. Single positive naive mature T-cells leave the thymus via blood vessels in the medulla.

FIV infection strikes hard in the thymus, with almost complete depletion of thymocytes in the cortex and concomitant involution of the cortex. The medulla, on the contrary, shows an increase in the number of cells due to follicular hyperplasia, and even the formation of germinal centers. The heavy FIV infection in the thymus leads to the influx of activated immune cells leading to thymitis (Huisman *et al.*, 2004; Woo *et al.*, 1997).

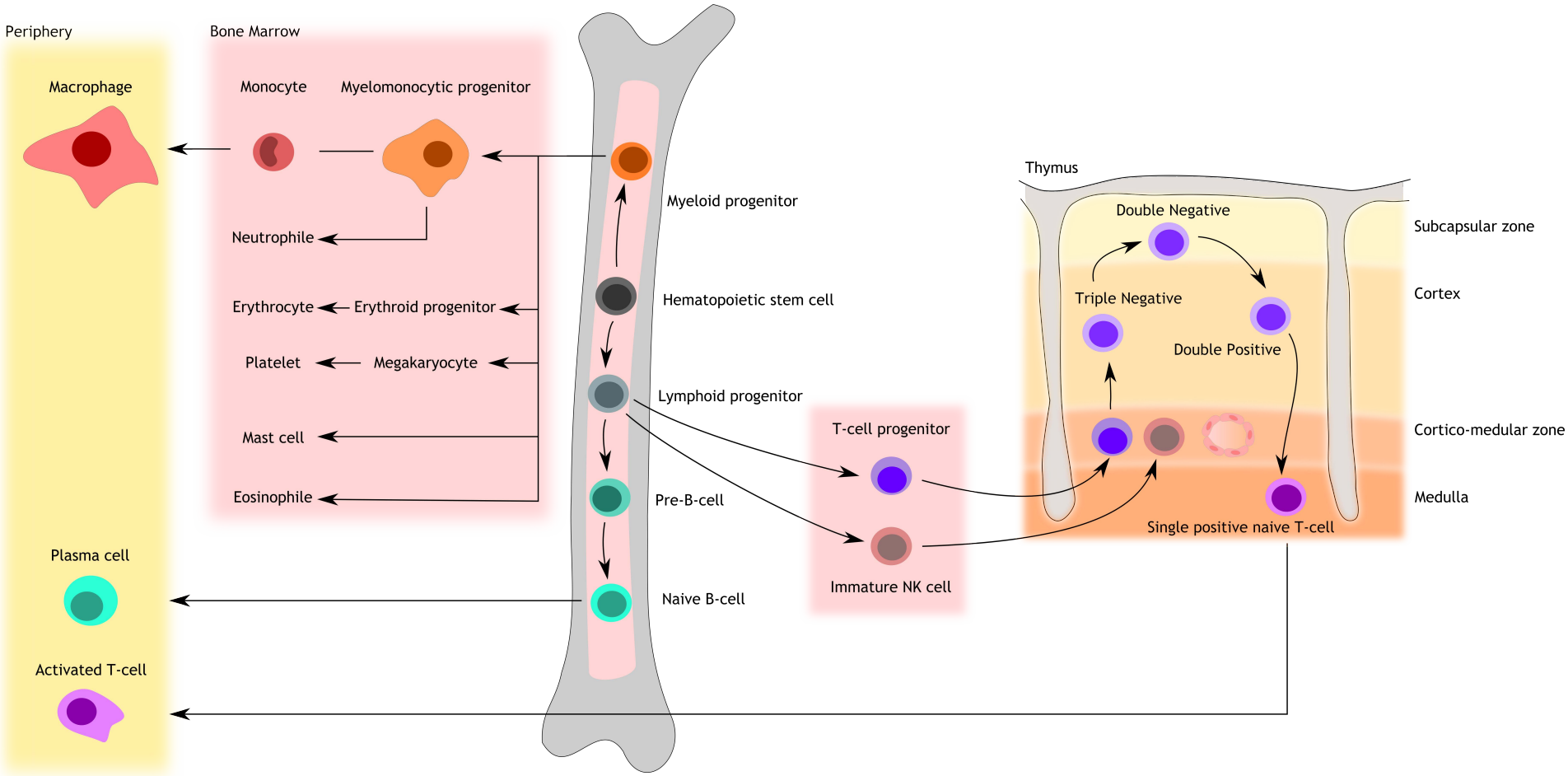

Figure 9: Schematic overview of immune cell development in the primary lymphoid organs. In adult animals red bone marrow is mainly located in flat bones and heads of long bones, at other sites the bone marrow is converted to hematopoietic silent yellow bone marrow. Hematopoietic stem cells (HSC) differentiate into two large lineages; the myeloid and the lymphoid lineage. The myeloid lineage gives rise to monocytes, to leukocytes important for innate immunity: neutrophils, eosinophils and mast cells, but also to red blood cells and platelets. The lymphoid progenitor gives rise to mature naïve B-lymphocytes, natural killer cells (NK-cells) and T-cell precursors. The NK-cells and T-cells finish their differentiation in the thymus (on the right). Triple negative progenitor T-cells (no T-cell receptor (TCR), CD4 or CD8 expression) travel through the thymus and differentiate into double positive (TCR, CD4 and CD8 expression) cells. On their way to the medulla, double positive T-cells become positively selected if they recognize self-MHC molecules and commit to the CD4 or CD8 lineage, generating single positive T-cells. In the medulla self-tolerance is ascertained by negatively selecting cells that react to self-antigens.

1.2.2. Secondary lymphoid organs

The secondary lymphoid organs are organized in a way to increase the likelihood that a naïve lymphocyte will interact with their specific antigen. Some antigens may diffuse freely into these organs while others are carried from the periphery and are presented by professional antigen presenting cells. Stimulation of the naive lymphocytes by antigens will induce activation and clonal expansion of these cells, and lead to an adaptive immune response against the source of the recognized antigen. Overall, the secondary lymphoid organs have an analogous structure. In a network of reticular cells and fibers, primary lymphoid follicles that mainly contain recirculating naive B-cells are surrounded by extranodular lymphoid tissue constituted of recirculating naïve T-cells and macrophages. Upon antigen recognition, the primary lymphoid nodule may evolve into a germinal centre that contains lymphoblasts involved in the immune response.

1.2.2.1. Lymph nodes

Lymph nodes (Fig. 10a) are bean-like structures that are located at sites of converging lymphatic vessels that drain a specific tissue or area. The afferent lymphatic vessels carry fluid and antigen-carrying cells from the periphery into the lymph nodes. The lymphatic vessels end in lymphatic sinuses in the parenchyma of the lymph node and are lined by endothelio-like reticular cells. This lining is discontinuous and is connected to the lymph node reticular network. Naive lymphocytes enter the lymph node via blood vessels that end in high endothelial venules (HEV) (Girard & Springer, 1995). Segregation of the T-and B-cell zones and the attraction of naive cells to the lymph nodes depends on a delicate interchange of signaling between immune cells and factors produced by different subtypes of stromal reticular cells. B-cells migrate to the cortex, where they concentrate into follicles populated by follicular dentritic cells of mesenchymal origin (Aguzzi *et al.*, 2014; Cupedo *et al.*, 2004). Activation of B-cells in the follicle will lead to the development of germinal centers with intense proliferation and differentiation of B-cells into plasma cells that produce antibodies. T-cells are concentrated within a vast network of fibroblastic reticular cells in the paracortex (Brown & Turley, 2015; Cyster, 2000; Seibert *et al.*, 1995). In the medulla a mixture of B-cells, T-cells and antigen presenting cells (APC) can be found. The medulla contains numerous lymphatic sinuses that lead cells out of the lymph nodes to the efferent lymphatic vessels.

In the acute phase of FIV infection, lymph nodes are hyperplastic, and cells are attracted via the high endothelial venules, which show increased accumulation of lymphocytes in pockets located around these venules. There is an increase in number and size of follicles and germinal centra, which can be aberrant in shape. The paracortex also has an increase in the number of lymphocytes, lymphoblasts and macrophages (Bach *et al.*, 1994; Huisman *et al.*, 2004). In the AIDS phase, lymph nodes may show involution or may even be depleted of cells (Rideout *et al.*, 1992).

1.2.2.2. Spleen

The spleen is a giant sieve for dying red blood cells, blood borne pathogens and large antigens. The red pulp mainly contains red blood cells and antigens, while the lymphoid cells are concentrated in the white pulp (Fig. 10b). Arterial blood arrives into cords in the red pulp, channel-like structures consisting of reticular fibers produced by reticular cells, that are populated with macrophages and plasma cells. From these cords, the blood is passed into venous sinuses, which are lined with endothelial cells, a discontinuous basement membrane and lopsided reticular fibers. This specialized endothelial lining determines the efflux of RBC from the spleen and retains aging RBC (Mebius & Kraal, 2005). The white pulp, on the other hand, located around arterioles, is a dense lymphoid tissue that lodges B- and T-lymphocytes into specific compartments. T-cells are concentrated around the periarteriolar lymphoid sheats, while B-cells reside in follicles. In cats and ruminants, the lymphatic tissue (white pulp) is less abundant compared to dogs and pigs, and occurs mainly as B-cell follicles (Landsverk & Press). The marginal zone separates the red and white pulp, and contains specialized macrophages, non-circulating marginal zone B-cells important for responses against polysaccharide antigens, and some T-cells.

Abnormalities seen in the spleen of FIV infected cats are similar to those observed in the lymph nodes. There is an increase in the number and size of the follicles in the white pulp, an increase in the number of lymphocytes and macrophages in the marginal zone, and myeloid metaplasia of the red pulp (Bach *et al.*, 1994; Huisman *et al.*, 2004).

1.2.2.3. MALT

A lot of pathogens enter the body at the mucosa of the gastrointestinal and respiratory tract. The epithelial lining of these systems contains specialized epithelial cells called microfold (M-) cells (Fig 10c). The M-cells overlay a central follicle of B-cells surrounded by T-cells and dendritic cells. M-cells take up antigens by pinocytoses and

transport them to the sub-epithelial tissues where they encounter dendritic cells that process the antigen for presentation to the lymphocytes.

FIV infected cells can be found in high numbers in the Peyer's patches and lamina propria of the gut. MALT tissues, show an increase of the number and size of the lymphoid follicles, similar to the lymph nodes and spleen (Huisman *et al.*, 2004).

Figure 10 (next page): Overview of the structure of the secondary lymphoid organs. (a) Organization of the lymph nodes. B-cells concentrate in the primary lymphoid follicle and plasma cells are found in germinal centers. In the paracortex, T-cells are concentrated, while the medullar chords contain a mixture of B-cells, T-cells and macrophages. (b) Transection of the spleen. The red pulp mainly contains red blood cells, macrophages and plasma cells. Around the central arteriole, in the periarteriolar sheets, most T-cells can be found. B-cells gather in follicles, that may contain germinal centers. Together the periarteriolar sheets and the B-cell zones form the white pulp. Between the red and white pulp lies the marginal zone that contains macrophages and specialized B-cells. (c) Organization of mucosa associated lymphoid tissue. In the epithelial layer specialized M-cells overlay a dome of T-cells. These T-cells surround a central follicle with B-cells that may contain a germinal centre with plasma cells. Location of the B-cells, T-cells and plasma cells in these tissues are colour coded in the drawings; white for B-cells, yellow for plasma cells and blue for T-cells. Figure based on illustrations in Janeway's Immunobiology 8th edition.

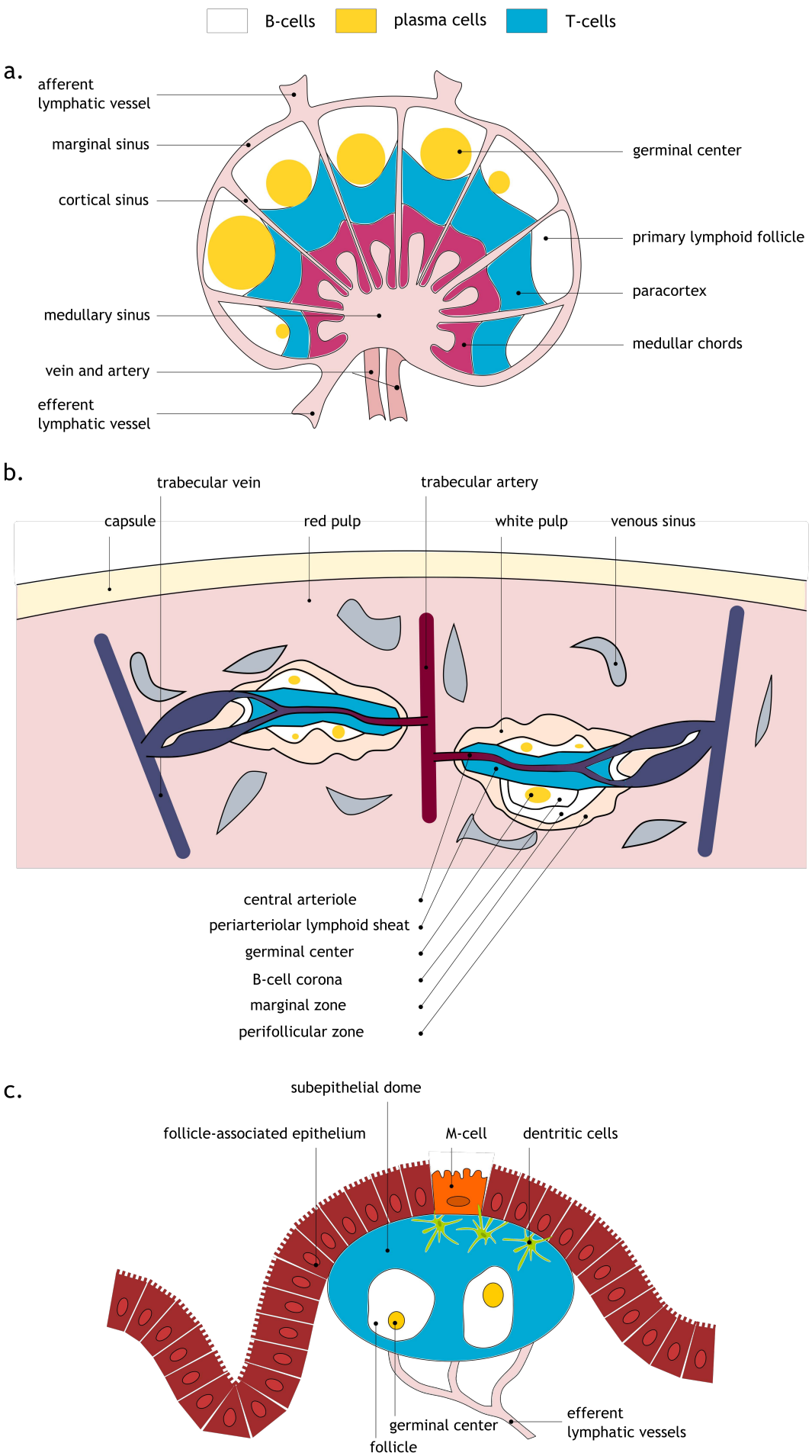
B-cells
plasma cells
T-cells
a.
afferent lymphatic vessel
marginal sinus
cortical sinus
medullary sinus
vein and artery
efferent lymphatic vessel
germinal center
primary lymphoid follicle
paracortex
medullar chords
b.
trabecular vein
trabecular artery
capsule
red pulp
white pulp
venous sinus
central arteriole
periarteriolar lymphoid sheat
germinal center
B-cell corona
marginal zone
perifollicular zone
c.
subepithelial dome
follicle-associated epithelium
M-cell
dentritic cells
germinal center
follicle
efferent lymphatic vessels

References

Affranchino, J. L. & González, S. A. (2014). Understanding the process of envelope glycoprotein incorporation into virions in simian and feline immunodeficiency viruses. *Viruses* **6**, 264-283.

Aguzzi, A., Kranich, J. & Krautler, N. J. (2014). Follicular dendritic cells: origin, phenotype, and function in health and disease. *Trends Immunol* **35**, 105-113.

Amacker, M., Hottiger, M. & Hübscher, U. (1995). Feline immunodeficiency virus reverse transcriptase: expression, functional characterization, and reconstitution of the 66- and 51-kilodalton subunits. *J Virol* **69**, 6273-6279.

Ambrose, Z. & Aiken, C. (2014). HIV-1 uncoating: connection to nuclear entry and regulation by host proteins. *Virology* **454-455**, 371-379.

Arai, M., Earl, D. D. & Yamamoto, J. K. (2002). Is AZT/3TC therapy effective against FIV infection or immunopathogenesis? *Vet Immunol Immunopathol* **85**, 189-204.

Arhel, N. (2010). Revisiting HIV-1 uncoating. *Retrovirology* **7**, 96.

Bach, J. M., Hurtrel, M., Chakrabarti, L., Ganiere, J. P., Montagnier, L. & Hurtrel, B. (1994). Early stages of feline immunodeficiency virus infection in lymph nodes and spleen. *AIDS Res Hum Retroviruses* **10**, 1731-1738.

Beatty, J. A., Lawrence, C. E., Callanan, J. J., Grant, C. K., Gault, E. A., Neil, J. C. & Jarrett, O. (1998). Feline immunodeficiency virus (FIV)-associated lymphoma: a potential role for immune dysfunction in tumourigenesis. *Vet Immunol Immunopathol* **65**, 309-322.

Beebe, A. M., Gluckstern, T. G., George, J., Pedersen, N. C. & Dandekar, S. (1992). Detection of feline immunodeficiency virus infection in bone marrow of cats. *Vet Immunol Immunopathol* **35**, 37-49.

Benaroch, P., Billard, E., Gaudin, R., Schindler, M. & Jouve, M. (2010). HIV-1 assembly in macrophages. *Retrovirology* **7**, 29.

Bishop, S. A., Williams, N. A., Gruffydd-Jones, T. J., Harbour, D. A. & Stokes, C. R. (1992a). An early defect in primary and secondary T cell responses in asymptomatic cats during acute feline immunodeficiency virus (FIV) infection. *Clin Exp Immunol* **90**, 491-496.

Bishop, S. A., Williams, N. A., Gruffydd-Jones, T. J., Harbour, D. A. & Stokes, C. R. (1992b). Impaired T-cell priming and proliferation in cats infected with feline immunodeficiency virus. *AIDS* **6**, 287-293.

Brown, F. D. & Turley, S. J. (2015). Fibroblastic reticular cells: organization and regulation of the T lymphocyte life cycle. *J Immunol* **194**, 1389-1394.

Brown, L. A., Cox, C., Baptiste, J., Summers, H., Button, R., Bahlow, K., Spurrier, V., Kyser, J., Luttge, B. G., Kuo, L., Freed, E. O. & Summers, M. F. (2015). NMR structure of the myristylated feline immunodeficiency virus matrix protein. *Viruses* **7**, 2210-2229.

Brown, W. C., Bissey, L., Logan, K. S., Pedersen, N. C., Elder, J. H. & Collisson, E. W. (1991). Feline immunodeficiency virus infects both CD4+ and CD8+ T lymphocytes. *J Virol* **65**, 3359-3364.

Brunner, D. & Pedersen, N. C. (1989). Infection of peritoneal macrophages in vitro and in vivo with feline immunodeficiency virus. *J Virol* **63**, 5483-5488.

Bucci, J. G., English, R. V., Jordan, H. L., Childers, T. A., Tompkins, M. B. & Tompkins, W. A. (1998). Mucosally transmitted feline immunodeficiency virus induces a CD8+ antiviral response that correlates with reduction of cell-associated virus. *J Infect Dis* **177**, 18-25.

Bunting, M. D., Comerford, I. & McColl, S. R. (2011). Finding their niche: chemokines directing cell migration in the thymus. *Immunol Cell Biol* **89**, 185-196.

Burkhard, M. J., Mathiason, C. K., Bowdre, T. & Hoover, E. A. (2001). Feline immunodeficiency virus Gag- and Env-specific immune responses after vaginal versus intravenous infection. *AIDS Res Hum Retroviruses* **17**, 1767-1778.

Calistri, A., Del Vecchio, C., Salata, C., Celestino, M., Celegato, M., Göttlinger, H., Palù, G. & Parolin, C. (2009). Role of the feline immunodeficiency virus L-domain in the presence or absence of Gag processing: involvement of ubiquitin and Nedd4-2s ligase in viral egress. *J Cell Physiol* **218**, 175-182.

Calzolari, M., Young, E., Cox, D., Davis, D. & Lutz, H. (1995). Serological diagnosis of feline immunodeficiency virus infection using recombinant transmembrane glycoprotein. *Vet Immunol Immunopathol* **46**, 83-92.

Carpenter, M. A., Brown, E. W., MacDonald, D. W. & O'Brien S, J. (1998). Phylogeographic patterns of feline immunodeficiency virus genetic diversity in the domestic cat. *Virology* **251**, 234-243.

Celma, C. C., Paladino, M. G., González, S. A. & Affranchino, J. L. (2007). Importance of the short cytoplasmic domain of the feline immunodeficiency virus transmembrane glycoprotein for fusion activity and envelope glycoprotein incorporation into virions. *Virology* **366**, 405-414.

Chatterji, U., de Parseval, A. & Elder, J. H. (2002). Feline immunodeficiency virus OrfA is distinct from other lentivirus transactivators. *J Virol* **76**, 9624-9634.

Chatterji, U., Grant, C. K. & Elder, J. H. (2000). Feline immunodeficiency virus Vif localizes to the nucleus. *J Virol* **74**, 2533-2540.

Christ, F. & Debyser, Z. (2013). The LEDGF/p75 integrase interaction, a novel target for anti-HIV therapy. *Virology* **435**, 102-109.

Cupedo, T., Lund, F. E., Ngo, V. N., Randall, T. D., Jansen, W., Greuter, M. J., de Waal-Malefyt, R., Kraal, G., Cyster, J. G. & Mebius, R. E. (2004). Initiation of cellular organization in lymph nodes is regulated by non-B cell-derived signals and is not dependent on CXC chemokine ligand 13. *J Immunol* **173**, 4889-4896.

Cyster, J. G. (2000). Leukocyte migration: scent of the T zone. *Curr Biol* **10**, R30-33.

de Parseval, A. & Elder, J. H. (1999). Demonstration that orf2 encodes the feline immunodeficiency virus transactivating (Tat) protein and characterization of a unique gene product with partial rev activity. *J Virol* **73**, 608-617.

de Parseval, A., Grant, C. K., Sastry, K. J. & Elder, J. H. (2006). Sequential CD134-CXCR4 interactions in feline immunodeficiency virus (FIV): soluble CD134 activates FIV Env for CXCR4-dependent entry and reveals a cryptic neutralization epitope. *J Virol* **80**, 3088-3091.

Dean, G. A., Himathongkham, S. & Sparger, E. E. (1999). Differential cell tropism of feline immunodeficiency virus molecular clones in vivo. *J Virol* **73**, 2596-2603.

Dean, G. A., LaVoy, A., Yearley, J. & Stanton, C. (2006). Cytokine modulation of the innate immune response in feline immunodeficiency virus-infected cats. *J Infect Dis* **193**, 1520-1527.

Demirov, D. G. & Freed, E. O. (2004). Retrovirus budding. *Virus Res* **106**, 87-102.

Dietrich, I., Hosie, M. J. & Willett, B. J. (2011a). The role of BST2/tetherin in feline retrovirus infection. *Vet Immunol Immunopathol* **143**, 255-264.

Dietrich, I., McEwan, W. A., Hosie, M. J. & Willett, B. J. (2011b). Restriction of the felid lentiviruses by a synthetic feline TRIM5-CypA fusion. *Vet Immunol Immunopathol* **143**, 235-242.

Duarte, A. & Tavares, L. (2006). Phylogenetic analysis of Portuguese Feline Immunodeficiency Virus sequences reveals high genetic diversity. *Vet Microbiol* **114**, 25-33.

Dunham, S. P., Bruce, J., MacKay, S., Golder, M., Jarrett, O. & Neil, J. C. (2006). Limited efficacy of an inactivated feline immunodeficiency virus vaccine. *Vet Rec* **158**, 561-562.

Eckstrand, C. D., Hillman, C., Smith, A. L., Sparger, E. E. & Murphy, B. G. (2016). Viral Reservoirs in Lymph Nodes of FIV-Infected Progressor and Long-Term Non-Progressor Cats during the Asymptomatic Phase. *PLoS One* **11**, e0146285.

Elder, J. H., Lerner, D. L., Hasselkus-Light, C. S., Fontenot, D. J., Hunter, E., Luciw, P. A., Montelaro, R. C. & Phillips, T. R. (1992). Distinct subsets of retroviruses encode dUTPase. *J Virol* **66**, 1791-1794.

Elder, J. H., Lin, Y. C., Fink, E. & Grant, C. K. (2010). Feline immunodeficiency virus (FIV) as a model for study of lentivirus infections: parallels with HIV. *Curr HIV Res* **8**, 73-80.

Elder, J. H., Schnolzer, M., Hasselkus-Light, C. S., Henson, M., Lerner, D. A., Phillips, T. R., Wagaman, P. C. & Kent, S. B. (1993). Identification of proteolytic processing sites within the Gag and Pol polyproteins of feline immunodeficiency virus. *J Virol* **67**, 1869-1876.

Engelman, A., Mizuuchi, K. & Craigie, R. (1991). HIV-1 DNA integration: mechanism of viral DNA cleavage and DNA strand transfer. *Cell* **67**, 1211-1221.

English, R. V., Johnson, C. M., Gebhard, D. H. & Tompkins, M. B. (1993). In vivo lymphocyte tropism of feline immunodeficiency virus. *J Virol* **67**, 5175-5186.

Felber, B. K., Hadzopoulou-Cladaras, M., Cladaras, C., Copeland, T. & Pavlakis, G. N. (1989). rev protein of human immunodeficiency virus type 1 affects the stability and transport of the viral mRNA. *Proc Natl Acad Sci U S A* **86**, 1495-1499.

Flynn, J. N., Cannon, C. A., Sloan, D., Neil, J. C. & Jarrett, O. (1999). Suppression of feline immunodeficiency virus replication in vitro by a soluble factor secreted by CD8+ T lymphocytes. *Immunology* **96**, 220-229.

Flynn, J. N., Dunham, S., Mueller, A., Cannon, C. & Jarrett, O. (2002). Involvement of cytolytic and non-cytolytic T cells in the control of feline immunodeficiency virus infection. *Vet Immunol Immunopathol* **85**, 159-170.

Fogle, J. E., Mexas, A. M., Tompkins, W. A. & Tompkins, M. B. (2010). CD4(+)CD25(+) T regulatory cells inhibit CD8(+) IFN-gamma production during acute and chronic FIV infection utilizing a membrane TGF-beta-dependent mechanism. *AIDS Res Hum Retroviruses* **26**, 201-216.

Gemeniano, M. C., Sawai, E. T. & Sparger, E. E. (2004). Feline immunodeficiency virus Orf-A localizes to the nucleus and induces cell cycle arrest. *Virology* **325**, 167-174.

Girard, J. P. & Springer, T. A. (1995). High endothelial venules (HEVs): specialized endothelium for lymphocyte migration. *Immunol Today* **16**, 449-457.

Gramberg, T., Kahle, T., Bloch, N., Wittmann, S., Müllers, E., Daddacha, W., Hofmann, H., Kim, B., Lindemann, D. & Landau, N. R. (2013). Restriction of diverse retroviruses by SAMHD1. *Retrovirology* **10**, 26.

Grant, C. K., Fink, E. A., Sundstrom, M., Torbett, B. E. & Elder, J. H. (2009). Improved health and survival of FIV-infected cats is associated with the presence of autoantibodies to the primary receptor, CD134. *Proc Natl Acad Sci U S A* **106**, 19980-19985.

Gu, Q., Zhang, Z., Ortiz, L. C., Franco, A. C., Häussinger, D. & Münk, C. (2016). FIV Vif N-Terminal Residues Selectively Counteract Feline APOBEC3s. *J Virol.*

Hanlon, M. A., Marr, J. M., Hayes, K. A., Mathes, L. E., Stromberg, P. C., Ringler, S., Krakowka, S. & Lafrado, L. J. (1993). Loss of neutrophil and natural killer cell function following feline immunodeficiency virus infection. *Viral Immunol* **6**, 119-124.

Hartmann, K., Donath, A., Beer, B., Egberink, H. F., Horzinek, M. C., Lutz, H., Hoffmann-Fezer, G., Thum, I. & Thefeld, S. (1992). Use of two virustatica (AZT, PMEA) in the treatment of FIV and of FeLV seropositive cats with clinical symptoms. *Vet Immunol Immunopathol* **35**, 167-175.

Hartmann, K., Stengel, C., Klein, D., Egberink, H. & Balzarini, J. (2012). Efficacy and adverse effects of the antiviral compound plerixafor in feline immunodeficiency virus-infected cats. *J Vet Intern Med* **26**, 483-490.

Hayward, J. J. & Rodrigo, A. G. (2008). Recombination in feline immunodeficiency virus from feral and companion domestic cats. *Virol J* **5**, 76.

Hayward, J. J., Taylor, J. & Rodrigo, A. G. (2007). Phylogenetic analysis of feline immunodeficiency virus in feral and companion domestic cats of New Zealand. *J Virol* **81**, 2999-3004.

Henderson, L. E., Krutzsch, H. C. & Oroszlan, S. (1983). Myristyl amino-terminal acylation of murine retrovirus proteins: an unusual post-translational proteins modification. *Proc Natl Acad Sci U S A* **80**, 339-343.

Hohdatsu, T., Okubo, M. & Koyama, H. (1998). Feline CD8+ T cell non-cytolytic anti-feline immunodeficiency virus activity mediated by a soluble factor(s). *J Gen Virol* **79 (Pt 11)**, 2729-2735.

Hong, Y., Fink, E., Hu, Q. Y., Kiosses, W. B. & Elder, J. H. (2010). OrfA downregulates feline immunodeficiency virus primary receptor CD134 on the host cell surface and is important in viral infection. *J Virol* **84**, 7225-7232.

Hosie, M. J., Addie, D., Belak, S., Boucraut-Baralon, C., Egberink, H., Frymus, T., Gruffydd-Jones, T., Hartmann, K., Lloret, A., Lutz, H., Marsilio, F., Pennisi, M. G., Radford, A. D., Thiry, E., Truyen, U. & Horzinek, M. C. (2009). FELINE IMMUNODEFICIENCY ABCD guidelines on prevention and management. *Journal of Feline Medicine and Surgery* **11**, 575-584.

Huisman, W., Schrauwen, E. J., Pas, S. D., Karlas, J. A., Rimmelzwaan, G. F. & Osterhaus, A. D. (2004). Antibodies specific for hypervariable regions 3 to 5 of the feline immunodeficiency virus envelope glycoprotein are not solely responsible for vaccine-induced acceleration of challenge infection in cats. *J Gen Virol* **85**, 1833-1841.

Inoshima, Y., Miyazawa, T. & Mikami, T. (1998a). In vivo functions of the auxiliary genes and regulatory elements of feline immunodeficiency virus. *Vet Microbiol* **60**, 141-153.

Inoshima, Y., Miyazawa, T. & Mikami, T. (1998b). The roles of vif and ORF-A genes and AP-1 binding site in in vivo replication of feline immunodeficiency virus. *Arch Virol* **143**, 789-795.

Joshi, A., Ablan, S. D., Soheilian, F., Nagashima, K. & Freed, E. O. (2009). Evidence that productive human immunodeficiency virus type 1 assembly can occur in an intracellular compartment. *J Virol* **83**, 5375-5387.

Joshi, A., Garg, H., Tompkins, M. B. & Tompkins, W. A. (2005). Preferential feline immunodeficiency virus (FIV) infection of CD4+ CD25+ T-regulatory cells correlates both with surface expression of CXCR4 and activation of FIV long terminal repeat binding cellular transcriptional factors. *J Virol* **79**, 4965-4976.

Kakinuma, S., Motokawa, K., Hohdatsu, T., Yamamoto, J. K., Koyama, H. & Hashimoto, H. (1995). Nucleotide sequence of feline immunodeficiency virus: classification of Japanese isolates into two subtypes which are distinct from non-Japanese subtypes. *J Virol* **69**, 3639-3646.

Kang, Y., Moressi, C. J., Scheetz, T. E., Xie, L., Tran, D. T., Casavant, T. L., Ak, P., Benham, C. J., Davidson, B. L. & McCray, P. B. (2006). Integration site choice of a feline immunodeficiency virus vector. *J Virol* **80**, 8820-8823.

Kemler, I., Barraza, R. & Poeschla, E. M. (2002). Mapping the encapsidation determinants of feline immunodeficiency virus. *J Virol* **76**, 11889-11903.

Kemler, I., Saenz, D. & Poeschla, E. (2012). Feline immunodeficiency virus Gag is a nuclear shuttling protein. *J Virol* **86**, 8402-8411.

Kiyomasu, T., Miyazawa, T., Furuya, T., Shibata, R., Sakai, H., Sakuragi, J., Fukasawa, M., Maki, N., Hasegawa, A. & Mikami, T. (1991). Identification of feline immunodeficiency virus rev gene activity. *J Virol* **65**, 4539-4542.

Kräusslich, H. G. (1991). Human immunodeficiency virus proteinase dimer as component of the viral polyprotein prevents particle assembly and viral infectivity. *Proc Natl Acad Sci U S A* **88**, 3213-3217.

Laco, G. S., Fitzgerald, M. C., Morris, G. M., Olson, A. J., Kent, S. B. & Elder, J. H. (1997). Molecular analysis of the feline immunodeficiency virus protease: generation of a novel form of the protease by autoproteolysis and construction of cleavage-resistant proteases. *J Virol* **71**, 5505-5511.

Laguette, N., Sobhian, B., Casartelli, N., Ringeard, M., Chable-Bessia, C., Ségéral, E., Yatim, A., Emiliani, S., Schwartz, O. & Benkirane, M. (2011). SAMHD1 is the dendritic- and myeloid-cell-specific HIV-1 restriction factor counteracted by Vpx. *Nature* **474**, 654-657.

Lahouassa, H., Daddacha, W., Hofmann, H., Ayinde, D., Logue, E. C., Dragin, L., Bloch, N., Maudet, C., Bertrand, M., Gramberg, T., Pancino, G., Priet, S., Canard, B., Laguette, N., Benkirane, M., Transy, C., Landau, N. R., Kim, B. & Margottin-Goguet, F. (2012). SAMHD1 restricts the replication of human immunodeficiency virus type 1 by depleting the intracellular pool of deoxynucleoside triphosphates. *Nat Immunol* **13**, 223-228.

Landsverk, T. & Press, C. Chapter 8 Immune system. In *Textbook of Veterinary Histology*.

Lecollinet, S. & Richardson, J. (2008). Vaccination against the feline immunodeficiency virus: the road not taken. *Comp Immunol Microbiol Infect Dis* **31**, 167-190.

Lerner, D. L., Wagaman, P. C., Phillips, T. R., Prospero-Garcia, O., Henriksen, S. J., Fox, H. S., Bloom, F. E. & Elder, J. H. (1995). Increased mutation frequency of feline immunodeficiency virus lacking functional deoxyuridine-triphosphatase. *Proc Natl Acad Sci U S A* **92**, 7480-7484.

Levy, J. K., Ritchey, J. W., Rottman, J. B., Davidson, M. G., Liang, Y. H., Jordan, H. L., Tompkins, W. A. & Tompkins, M. B. (1998). Elevated interleukin-10-to-interleukin-12 ratio in feline immunodeficiency virus-infected cats predicts loss of type 1 immunity to Toxoplasma gondii. *J Infect Dis* **178**, 503-511.

Li, F., Jin, J., Herrmann, C. & Mothes, W. (2013). Basic residues in the matrix domain and multimerization target murine leukemia virus Gag to the virological synapse. *J Virol* **87**, 7113-7126.

Lin, T. Y. & Emerman, M. (2006). Cyclophilin A interacts with diverse lentiviral capsids. *Retrovirology* **3**, 70.

Lockridge, K. M., Himathongkham, S., Sawai, E. T., Chienand, M. & Sparger, E. E. (1999). The feline immunodeficiency virus vif gene is required for productive infection of feline peripheral blood mononuclear cells and monocyte-derived macrophages. *Virology* **261**, 25-30.

Luttge, B. G., Shehu-Xhilaga, M., Demirov, D. G., Adamson, C. S., Soheilian, F., Nagashima, K., Stephen, A. G., Fisher, R. J. & Freed, E. O. (2008). Molecular characterization of feline immunodeficiency virus budding. *J Virol* **82**, 2106-2119.

Manrique, M. L., Celma, C. C., González, S. A. & Affranchino, J. L. (2001). Mutational analysis of the feline immunodeficiency virus matrix protein. *Virus Res* **76**, 103-113.

Manrique, M. L., Rauddi, M. L., González, S. A. & Affranchino, J. L. (2004). Functional domains in the feline immunodeficiency virus nucleocapsid protein. *Virology* **327**, 83-92.

Matreyek, K. A. & Engelman, A. (2013). Viral and cellular requirements for the nuclear entry of retroviral preintegration nucleoprotein complexes. *Viruses* **5**, 2483-2511.

Matsumura, S., Ishida, T., Washizu, T. & Tomoda, I. (1994). Histopathology and viral antigen distribution in lymph nodes of cats naturally infected with feline immunodeficiency virus. *J Vet Med Sci* **56**, 523-528.

McDonnel, S. J., Sparger, E. E., Luciw, P. A. & Murphy, B. G. (2012). Pharmacologic reactivation of latent feline immunodeficiency virus ex vivo in peripheral CD4+ T-lymphocytes. *Virus Res* **170**, 174-179.

McEwan, W. A., Schaller, T., Ylinen, L. M., Hosie, M. J., Towers, G. J. & Willett, B. J. (2009). Truncation of TRIM5 in the Feliformia explains the absence of retroviral restriction in cells of the domestic cat. *J Virol* **83**, 8270-8275.

Mebius, R. E. & Kraal, G. (2005). Structure and function of the spleen. *Nat Rev Immunol* **5**, 606-616.

Medeiros, S. e. O., Abreu, C. M., Delvecchio, R., Ribeiro, A. P., Vasconcelos, Z., Brindeiro, R. e. M. & Tanuri, A. (2016). Follow-up on long-term antiretroviral therapy for cats infected with feline immunodeficiency virus. *J Feline Med Surg* **18**, 264-272.

Melikyan, G. B. (2014). HIV entry: a game of hide-and-fuse? *Curr Opin Virol* **4**, 1-7.

Meng, L., Tompkins, M., Miller, M. & Fogle, J. (2014). Lentivirus-activated T regulatory cells suppress T helper cell interleukin-2 production by inhibiting nuclear factor of activated T cells 2 binding to the interleukin-2 promoter. *AIDS Res Hum Retroviruses* **30**, 58-66.

Mexas, A. M., Fogle, J. E., Tompkins, W. A. & Tompkins, M. B. (2008). CD4+CD25+ regulatory T cells are infected and activated during acute FIV infection. *Vet Immunol Immunopathol* **126**, 263-272.

Miller, M. M., Fogle, J. E. & Tompkins, M. B. (2013). Infection with feline immunodeficiency virus directly activates CD4+ CD25+ T regulatory cells. *J Virol* **87**, 9373-9378.

Morikawa, S. & Bishop, D. H. (1992). Identification and analysis of the gag-pol ribosomal frameshift site of feline immunodeficiency virus. *Virology* **186**, 389-397.

Moscardini, M., Pistello, M., Bendinelli, M., Ficheux, D., Miller, J. T., Gabus, C., Le Grice, S. F., Surewicz, W. K. & Darlix, J. L. (2002). Functional interactions of nucleocapsid protein of feline immunodeficiency virus and cellular prion protein with the viral RNA. *J Mol Biol* **318**, 149-159.

Münk, C., Beck, T., Zielonka, J., Hotz-Wagenblatt, A., Chareza, S., Battenberg, M., Thielebein, J., Cichutek, K., Bravo, I. G., O'Brien, S. J., Löchelt, M. & Yuhki, N. (2008). Functions, structure, and read-through alternative splicing of feline APOBEC3 genes. *Genome Biol* **9**, R48.

Na, H., Huisman, W., Ellestad, K. K., Phillips, T. R. & Power, C. (2010). Domain- and nucleotide-specific Rev response element regulation of feline immunodeficiency virus production. *Virology* **404**, 246-260.

Neil, S. J., Zang, T. & Bieniasz, P. D. (2008). Tetherin inhibits retrovirus release and is antagonized by HIV-1 Vpu. *Nature* **451**, 425-430.

North, T. W., Cronn, R. C., Remington, K. M., Tandberg, R. T. & Judd, R. C. (1990). Characterization of reverse transcriptase from feline immunodeficiency virus. *J Biol Chem* **265**, 5121-5128.

Ono, A., Ablan, S. D., Lockett, S. J., Nagashima, K. & Freed, E. O. (2004). Phosphatidylinositol (4,5) bisphosphate regulates HIV-1 Gag targeting to the plasma membrane. *Proc Natl Acad Sci U S A* **101**, 14889-14894.

Ono, A. & Freed, E. O. (2004). Cell-type-dependent targeting of human immunodeficiency virus type 1 assembly to the plasma membrane and the multivesicular body. *J Virol* **78**, 1552-1563.

Pancino, G., Fossati, I., Chappey, C., Castelot, S., Hurtrel, B., Moraillon, A., Klatzmann, D. & Sonigo, P. (1993). Structure and variations of feline immunodeficiency virus envelope glycoproteins. *Virology* **192**, 659-662.

Pecoraro, M. R., Tomonaga, K., Miyazawa, T., Kawaguchi, Y., Sugita, S., Tohya, Y., Kai, C., Etcheverrigaray, M. E. & Mikami, T. (1996). Genetic diversity of Argentine isolates of feline immunodeficiency virus. *J Gen Virol* **77 (Pt 9)**, 2031-2035.

Pedersen, N. C., Ho, E. W., Brown, M. L. & Yamamoto, J. K. (1987). Isolation of a T-lymphotropic virus from domestic cats with an immunodeficiency-like syndrome. *Science* **235**, 790-793.

Pedersen, N. C., Leutenegger, C. M., Woo, J. & Higgins, J. (2001). Virulence differences between two field isolates of feline immunodeficiency virus (FIV-APetaluma and FIV-CPGammar) in young adult specific pathogen free cats. *Vet Immunol Immunopathol* **79**, 53-67.

Pedersen, N. C., Yamamoto, J. K., Ishida, T. & Hansen, H. (1989). Feline immunodeficiency virus infection. *Vet Immunol Immunopathol* **21**, 111-129.

Phillips, T. R., Prospero-Garcia, O., Puaoi, D. L., Lerner, D. L., Fox, H. S., Olmsted, R. A., Bloom, F. E., Henriksen, S. J. & Elder, J. H. (1994). Neurological abnormalities associated with feline immunodeficiency virus infection. *J Gen Virol* **75 (Pt 5)**, 979-987.

Pistello, M., Moscardini, M., Mazzetti, P., Bonci, F., Zaccaro, L., Isola, P., Freer, G., Specter, S., Matteucci, D. & Bendinelli, M. (2002). Development of feline immunodeficiency virus ORF-A (tat) mutants: in vitro and in vivo characterization. *Virology* **298**, 84-95.

Podell, M., Hayes, K., Oglesbee, M. & Mathes, L. (1997). Progressive encephalopathy associated with CD4/CD8 inversion in adult FIV-infected cats. *J Acquir Immune Defic Syndr Hum Retrovirol* **15**, 332-340.

Prospéro-García, O., Herold, N., Phillips, T. R., Elder, J. H., Bloom, F. E. & Henriksen, S. J. (1994). Sleep patterns are disturbed in cats infected with feline immunodeficiency virus. *Proc Natl Acad Sci U S A* **91**, 12947-12951.

Rideout, B. A., Lowensteine, L. J., Hutson, C. A., Moore, P. F. & Pedersen, N. C. (1992). Characterization of morphologic changes and lymphocyte subset distribution in lymph nodes from cats with naturally acquired feline immunodeficiency virus infection. *Vet Pathol* **29**, 391-399.

Rossi, F. M., Corbel, S. Y., Merzaban, J. S., Carlow, D. A., Gossens, K., Duenas, J., So, L., Yi, L. & Ziltener, H. J. (2005). Recruitment of adult thymic progenitors is regulated by P-selectin and its ligand PSGL-1. *Nat Immunol* **6**, 626-634.

Ryoo, J., Choi, J., Oh, C., Kim, S., Seo, M., Kim, S. Y., Seo, D., Kim, J., White, T. E., Brandariz-Nuñez, A., Diaz-Griffero, F., Yun, C. H., Hollenbaugh, J. A., Kim, B., Baek, D. & Ahn, K. (2014). The ribonuclease activity of SAMHD1 is required for HIV-1 restriction. *Nat Med* **20**, 936-941.

Schuh, A. L. & Audhya, A. (2014). The ESCRT machinery: from the plasma membrane to endosomes and back again. *Crit Rev Biochem Mol Biol* **49**, 242-261.

Schultz, A. M. & Oroszlan, S. (1983). In vivo modification of retroviral gag gene-encoded polyproteins by myristic acid. *J Virol* **46**, 355-361.

Seibert, S. A., Howell, C. Y., Hughes, M. K. & Hughes, A. L. (1995). Natural selection on the gag, pol, and env genes of human immunodeficiency virus 1 (HIV-1). *Mol Biol Evol* **12**, 803-813.

Serrière, J., Fenel, D., Schoehn, G., Gouet, P. & Guillon, C. (2013a). Biophysical characterization of the feline immunodeficiency virus p24 capsid protein conformation and in vitro capsid assembly. *PLoS One* **8**, e56424.

Serrière, J., Robert, X., Perez, M., Gouet, P. & Guillon, C. (2013b). Biophysical characterization and crystal structure of the Feline Immunodeficiency Virus p15 matrix protein. *Retrovirology* **10**, 64.

Shelton, G. H., Linenberger, M. L., Grant, C. K. & Abkowitz, J. L. (1990). Hematologic manifestations of feline immunodeficiency virus infection. *Blood* **76**, 1104-1109.

Shibagaki, Y., Holmes, M. L., Appa, R. S. & Chow, S. A. (1997). Characterization of feline immunodeficiency virus integrase and analysis of functional domains. *Virology* **230**, 1-10.

Shimojima, M., Miyazawa, T., Ikeda, Y., McMonagle, E. L., Haining, H., Akashi, H., Takeuchi, Y., Hosie, M. J. & Willett, B. J. (2004). Use of CD134 as a primary receptor by the feline immunodeficiency virus. *Science* **303**, 1192-1195.

Shimojima, M., Miyazawa, T., Kohmoto, M., Ikeda, Y., Nishimura, Y., Maeda, K., Tohya, Y. & Mikami, T. (1998). Expansion of CD8alpha+beta- cells in cats infected with feline immunodeficiency virus. *J Gen Virol* **79 (Pt 1)**, 91-94.

Shimojima, M., Nishimura, Y., Miyazawa, T., Tohya, Y. & Akashi, H. (2003). Phenotypic changes in CD8+ peripheral blood lymphocytes in cats infected with feline immunodeficiency virus. *Microbes Infect* **5**, 1171-1176.

Sodora, D. L., Shpaer, E. G., Kitchell, B. E., Dow, S. W., Hoover, E. A. & Mullins, J. I. (1994). Identification of three feline immunodeficiency virus (FIV) env gene subtypes and comparison of the FIV and human immunodeficiency virus type 1 evolutionary patterns. *J Virol* **68**, 2230-2238.

Sparger, E. E., Shacklett, B. L., Renshaw-Gegg, L., Barry, P. A., Pedersen, N. C., Elder, J. H. & Luciw, P. A. (1992). Regulation of gene expression directed by the long terminal repeat of the feline immunodeficiency virus. *Virology* **187**, 165-177.

Steigerwald, E. S., Sarter, M., March, P. & Podell, M. (1999). Effects of feline immunodeficiency virus on cognition and behavioral function in cats. *J Acquir Immune Defic Syndr Hum Retrovirol* **20**, 411-419.

Stephens, E. B., Monck, E., Reppas, K. & Butfiloski, E. J. (1991). Processing of the glycoprotein of feline immunodeficiency virus: effect of inhibitors of glycosylation. *J Virol* **65**, 1114-1123.

Sundstrom, M., Chatterji, U., Schaffer, L., de Rozières, S. & Elder, J. H. (2008). Feline immunodeficiency virus OrfA alters gene expression of splicing factors and proteasome-ubiquitination proteins. *Virology* **371**, 394-404.

Taffin, E., Paepe, D., Goris, N., Auwerx, J., Debille, M., Neyts, J., Van de Maele, I. & Daminet, S. (2015). Antiviral treatment of feline immunodeficiency virus-infected cats with (R)-9-(2-phosphonylmethoxypropyl)-2,6-diaminopurine. *J Feline Med Surg* **17**, 79-86.

Talbott, R. L., Sparger, E. E., Lovelace, K. M., Fitch, W. M., Pedersen, N. C., Luciw, P. A. & Elder, J. H. (1989). Nucleotide sequence and genomic organization of feline immunodeficiency virus. *Proc Natl Acad Sci U S A* **86**, 5743-5747.

Temin, H. M. (1981). Structure, variation and synthesis of retrovirus long terminal repeat. *Cell* **27**, 1-3.

Thompson, F. J., Elder, J. & Neil, J. C. (1994). Cis- and trans-regulation of feline immunodeficiency virus: identification of functional binding sites in the long terminal repeat. *J Gen Virol* **75 (Pt 3)**, 545-554.

Tomonaga, K., Miyazawa, T., Sakuragi, J., Mori, T., Adachi, A. & Mikami, T. (1993a). The feline immunodeficiency virus ORF-A gene facilitates efficient viral replication in established T-cell lines and peripheral blood lymphocytes. *J Virol* **67**, 5889-5895.

Tomonaga, K., Norimine, J., Shin, Y. S., Fukasawa, M., Miyazawa, T., Adachi, A., Toyosaki, T., Kawaguchi, Y., Kai, C. & Mikami, T. (1992). Identification of a feline immunodeficiency virus gene which is essential for cell-free virus infectivity. *J Virol* **66**, 6181-6185.

Tomonaga, K., Shin, Y. S., Fukasawa, M., Miyazawa, T., Adachi, A. & Mikami, T. (1993b). Feline immunodeficiency virus gene expression: analysis of the RNA splicing pattern and the monocistronic rev mRNA. *J Gen Virol* **74 (Pt 11)**, 2409-2417.

Tompkins, M. B., Bull, M. E., Dow, J. L., Ball, J. M., Collisson, E. W., Winslow, B. J., Phadke, A. P., Vahlenkamp, T. W. & Tompkins, W. A. (2002). Feline immunodeficiency virus infection is characterized by B7+CTLA4+ T cell apoptosis. *J Infect Dis* **185**, 1077-1093.

Tompkins, T. A., Hagen, K. E., Wallace, T. D. & Fillion-Forte, V. (2008). Safety evaluation of two bacterial strains used in Asian probiotic products. *Can J Microbiol* **54**, 391-400.

Torten, M., Franchini, M., Barlough, J. E., George, J. W., Mozes, E., Lutz, H. & Pedersen, N. C. (1991). Progressive immune dysfunction in cats experimentally infected with feline immunodeficiency virus. *J Virol* **65**, 2225-2230.

Tozzini, F., Matteucci, D., Bandecchi, P., Baldinotti, F., Siebelink, K., Osterhaus, A. & Bendinelli, M. (1993). Neutralizing antibodies in cats infected with feline immunodeficiency virus. *J Clin Microbiol* **31**, 1626-1629.

Troyer, R. M., Thompson, J., Elder, J. H. & VandeWoude, S. (2013). Accessory genes confer a high replication rate to virulent feline immunodeficiency virus. *J Virol* **87**, 7940-7951.

Vahlenkamp, T. W., Bull, M. E., Dow, J. L., Collisson, E. W., Winslow, B. J., Phadke, A. P., Tompkins, W. A. & Tompkins, M. B. (2004a). B7+CTLA4+ T cells engage in T-T cell interactions that mediate apoptosis: a model for lentivirus-induced T cell depletion. *Vet Immunol Immunopathol* **98**, 203-214.

Vahlenkamp, T. W., De Ronde, A., Balzarini, J., Naesens, L., De Clercq, E., van Eijk, M. J., Horzinek, M. C. & Egberink, H. F. (1995). (R)-9-(2-phosphonylmethoxypropyl)-2,6-diaminopurine is a potent inhibitor of feline immunodeficiency virus infection. *Antimicrob Agents Chemother* **39**, 746-749.

Vahlenkamp, T. W., Tompkins, M. B. & Tompkins, W. A. (2004b). Feline immunodeficiency virus infection phenotypically and functionally activates immunosuppressive CD4+CD25+ T regulatory cells. *J Immunol* **172**, 4752-4761.

Verschoor, E. J., Hulskotte, E. G., Ederveen, J., Koolen, M. J., Horzinek, M. C. & Rottier, P. J. (1993). Post-translational processing of the feline immunodeficiency virus envelope precursor protein. *Virology* **193**, 433-438.

Vink, C., Yeheskiely, E., van der Marel, G. A., van Boom, J. H. & Plasterk, R. H. (1991). Site-specific hydrolysis and alcoholysis of human immunodeficiency virus DNA termini mediated by the viral integrase protein. *Nucleic Acids Res* **19**, 6691-6698.

Vogt, V. M. (1997). Retroviral virions and genomes. In *Retroviruses*, 1st edn. Edited by J. M. Coffin, S. H. Hughes & H. E. Varmus. Cold Spring Harbor (NY): Cold Spring Harbor Laboratory Press.

Votteler, J. & Sundquist, W. I. (2013). Virus budding and the ESCRT pathway. *Cell Host Microbe* **14**, 232-241.

Waters, A. K., De Parseval, A. P., Lerner, D. L., Neil, J. C., Thompson, F. J. & Elder, J. H. (1996). Influence of ORF2 on host cell tropism of feline immunodeficiency virus. *Virology* **215**, 10-16.

Weaver, E. A., Collisson, E. W., Slater, M. & Zhu, G. (2004). Phylogenetic analyses of Texas isolates indicate an evolving subtype of the clade B feline immunodeficiency viruses. *J Virol* **78**, 2158-2163.

Westman, M. E., Malik, R., Hall, E., Harris, M. & Norris, J. M. (2016). The protective rate of the feline immunodeficiency virus vaccine: An Australian field study. *Vaccine* **34**, 4752-4758.

Woo, J. C., Dean, G. A., Pedersen, N. C. & Moore, P. F. (1997). Immunopathologic changes in the thymus during the acute stage of experimentally induced feline immunodeficiency virus infection in juvenile cats. *J Virol* **71**, 8632-8641.

Yamamoto, J. K., Pu, R., Sato, E. & Hohdatsu, T. (2007). Feline immunodeficiency virus pathogenesis and development of a dual-subtype feline-immunodeficiency-virus vaccine. *AIDS* **21**, 547-563.

Yoder, K. E., Espeseth, A., Wang, X. H., Fang, Q., Russo, M. T., Lloyd, R. S., Hazuda, D., Sobol, R. W. & Fishel, R. (2011). The base excision repair pathway is required for efficient lentivirus integration. *PLoS One* **6**, e17862.

Zaccaro, L., Falcone, M. L., Silva, S., Bigalli, L., Cecchettini, A., Giorgi, F., Malvaldi, G. & Bendinelli, M. (1995). Defective natural killer cell cytotoxic activity in feline immunodeficiency virus-infected cats. *AIDS Res Hum Retroviruses* **11**, 747-752.

Zhu, Y. Q., Remington, K. M. & North, T. W. (1996). Mutants of feline immunodeficiency virus resistant to 2',3'-dideoxy-2',3'-didehydrothymidine. *Antimicrob Agents Chemother* **40**, 1983-1987.

Zielonka, J., Marino, D., Hofmann, H., Yuhki, N., Löchelt, M. & Münk, C. (2010). Vif of feline immunodeficiency virus from domestic cats protects against APOBEC3 restriction factors from many felids. *J Virol* **84**, 7312-7324.

Chapter 2

Aims

Feline immunodeficiency virus (FIV) is a major cat pathogen with seroprevalences of up to 30% in urban areas (Yamamoto et al., 2007). It was discovered a few years after the human immunodeficiency virus (HIV) in cats that presented symptoms similar to seropositive humans with AIDS (Pedersen et al., 1989).

FIV strains are classified into several genetically distinct clades. When starting the current FIV research in Belgium, no up-to-date information existed on strains circulating in the Benelux. In **Chapter 3** FIV field strains collected from naturally FIV infected cats living in Belgium and The Netherlands were genotyped. Insights into genotypes occurring in the Benelux will allow us to select a relevant FIV strain for further work.

Once FIV is contracted, it establishes a lifelong infection in its host and causes a severe immunodeficiency that eventually leads to death. The FIV envelope protein (Env) and Gag protein are major stimulators of the anti-FIV response. Although infected cats develop a strong antiviral response, FIV is not cleared. This implies that FIV successfully escapes from detection by the immune system. **Chapter 4** aims at investigating the expression of FIV Env and Gag, and the availability of different epitopes on these viral proteins during replication. The well characterized American FIV subtype A strain “FIV-PPR”, was chosen for all further experiments because of the close resemblance with the FIV field strains in Belgium and The Netherlands. Knowledge about the timing of expression of viral proteins, their trafficking in the cell and availability of epitopes on these proteins when exposed to the extracellular milieu will broaden our view on the immune-evasive strategies employed by FIV.

Another aspect of the FIV pathogenesis is the absence of FIV replication in blood leukocytes while the disease is asymptomatic but nonetheless progressing. The hunt for so called “replication reservoirs” has been ongoing for many years. Recently, it was shown that FIV replication is active in lymphoid tissues during the asymptomatic phase. **Chapter 5a** focuses on the isolation, characterization and immortalization of feline mesenchymal cells from primary lymphoid tissues (bone marrow and thymus) and secondary lymphoid tissues (lymph nodes and spleen). These cells create the network essential for proper function of the lymphoid organs. In **Chapter 5b** the influence of these lymphoid organ-derived mesenchymal cells on FIV replication in peripheral blood mononuclear cells (PBMC) and PBMC sensitivity for FIV infection was examined.

Chapter 3

Phylogenetic analysis of feline immunodeficiency virus strains from naturally infected cats in Belgium and The Netherlands

Adapted from:

Roukaerts ID, Theuns S, Taffin ER, Daminet S, and Nauwynck HJ, 2015. Virus Research 196, 30-36.

Abstract

Feline immunodeficiency virus (FIV) is a major pathogen in feline populations worldwide, with seroprevalences up to 26%. Virus strains circulating in domestic cats are subdivided into different phylogenetic clades (A to E), based on the genetic diversity of the V3-V4 region of the *env* gene. In this report, a phylogenetic analysis of the V3-V4 *env* region, and a variable region in the *gag* gene was made for 36 FIV strains isolated in Belgium and The Netherlands. All newly generated *gag* sequences clustered together with previously known clade A FIV viruses, confirming the dominance of clade A viruses in Northern Europe. The same was true for the obtained *env* sequences, with only one sample of an unknown *env* subtype. Overall, the genetic diversity of FIV strains sequenced in this report was low. This indicates a relatively recent introduction of FIV in Belgium and The Netherlands. However, the sample with an unknown *env* subtype indicates that new introductions of FIV from unknown origin do occur and this will likely increase genetic variability in time.

3.1. Introduction

Feline immunodeficiency virus (FIV) is a common pathogen in cat populations worldwide. The virus is mainly spread by biting, especially during fights between tomcats (Natoli *et al.*, 2005; Yamamoto *et al.*, 1989). It causes a dysfunction of the immune system, in part by directly targeting cells of the immune system, leading to a persistent infection (Tompkins & Tompkins, 2008). After a long asymptomatic phase, infection with FIV can cause an AIDS-like disease, characterized by a depletion of CD4+ T-cells, increase in plasma viral load and severe immune suppression. Clinical signs are usually not directly caused by the FIV infection, but are the result of secondary infections or immune hyper-stimulation.

FIV is divided into five different clades (A to E), which vary in prevalence by geographic location (Yamamoto *et al.*, 2007). These clades are based on phylogenetic analyses of variable regions 3 to 5 in the *env* gene. The intra-clade diversity in these regions range from 2.5 to 15% at the nucleotide level. A new clade arises when a sequence shows more than 20% genetic distance from other clades (Kakinuma *et al.*, 1995; Sodora *et al.*, 1994). While clade A strains are found worldwide, other clades indicate a separate evolution of these viruses in geographical isolated locations. For instance, subtype E has only been found in South-America and subtype D in Japan (Kakinuma *et al.*, 1995; Pecoraro *et al.*, 1996). Several reports have been made of *env* sequences clustering into new FIV clades, these were designated “F”(Duarte & Tavares, 2006; Hayward *et al.*, 2007; Weaver, 2010) or “New Zealand-Unknown” (NZ-U) (Hayward *et al.*, 2007). A cat can be infected by multiple FIV strains. In places where multiple subtypes circulate, this can give rise to recombinant viruses. Recombination can occur either between gene regions, giving rise to, for example, A/C subtypes or within single gene regions, forming for instance A/B envelope chimaeras (Hayward and Rodrigo 2008).

Routine vaccination with the dual clade (A & D) vaccine (Fel-O-Vax, Boehringer Ingelheim) is not recommended in Europe. Safety concerns have been raised since there are several reports of vaccine-mediated enhancement of disease (Lecollinet & Richardson, 2008). This enhancement might be related to humoral factors (Siebelink *et al.*, 1995) and/or by inducing memory cells that are rapidly activated upon FIV infection. These activated lymphocytes are an ideal target for FIV (de Parseval *et al.*, 2004; Gramaglia *et al.*, 1998; Joshi *et al.*, 2005). Furthermore, it is important to

mention that cross-protection against European isolates is under discussion (Dunham *et al.*, 2006).

Clades A and B are reported to circulate in Western Europe (Samman *et al.*, 2011; Steinrigl *et al.*, 2010; Yamamoto *et al.*, 2007), but data from Belgium are lacking. Serological surveys in Belgium have shown an FIV prevalence of 11% in urban stray cats (Dorny *et al.*, 2002) and 14% in healthy cats of six years and older (Paepe *et al.*, 2013). However, virus was not isolated and phylogenetic analyses were not performed. In the present study, *env* and *gag* sequences derived from 36 naturally infected cats living in Flanders and The Netherlands were phylogenetically analyzed.

3.2. Materials and methods

3.2.1. Samples

Samples were obtained from naturally infected cats living in Belgium (n=26) and The Netherlands (n=10). Cats were presented to the Clinic for Small Companion Animals of Ghent University. All cats were privately owned and owners provided a signed consent. Blood samples were taken by jugular venipuncture. Genomic DNA was isolated from 50µl heparin-treated blood with the Quick-gDNA™ Blood Microprep kit (Zymo Research).

3.2.2. PCR and sequencing

Sequences for variable regions in *gag* and *env* (V3-V4) were amplified, using primers FIV-960F and FIV-1709R for *gag*, and primers FIV-7224F and FIV-8000R for *env* (Iwata & Holloway, 2008; Steinrigl & Klein, 2003). All primer sequences can be found in Table 1. PCR was performed using Herculase II Fusion DNA polymerase (Aligent Technologies) in a 50 µl reaction mix containing 0.25 µM of the forward and reverse primer, 0.5 µl template DNA, 1 mM dNTPs, 0.5 µl polymerase and 2.5 mM MgCl2. The PCR product was visualized on a 1% agarose gel, excised and purified with the NucleoSpin® Gel and PCR Clean-up kit (Machery-Nagel GmbH & Co. KG, Düren). Sequencing was performed by GATC Biotech (Constance, Germany) with both forward and reverse primers on an ABI 3730XL Sanger sequencing platform. When sequencing failed, the fragment was cloned into a commercial vector (pCR®-Blunt) with the Zero Blunt PCR cloning kit (InvitrogenTM, life technologies) following manufacturer's instructions and sequenced from the M13 reverse primer.

Table 1: Location and 5' to 3' sequence of primers used for sequencing the variable *gag* fragment and the V3-V4 region of the env gene (Iwata & Holloway, 2008; Steinrigl & Klein, 2003).

Gene	Location	Forward primer	Reverse primer
gag	960-1709	TCA GAT GGG ATT AGA CAC	CTT CTG CCA AGA GTT GC
env	7224-8000	GTA CAG ACC CAT TAC AAA	CTG CCA CTG GGT TAT ACC

3.2.3. Phylogenetic analysis

Sequences were analyzed and corrected with the 4Peaks software (Mekentosj). The fragments for *gag* and the V3-V4 *env* fragment were aligned together with reference strains in the MEGA 6.06 software package (Tamura *et al.*, 2013), using the ClustalW algorithm. Names and GenBank accession numbers of the used reference strains can be found in Supplementary Table 1. All further phylogenetic analyses were made in MEGA 6.06. To determine the parameter model for genetic distance calculation at the nucleotide level, a model test was performed in MEGA. Hence, genetic distances were calculated with the Tamura 3-parameter model for nucleotide sequences with a gamma distribution with 5 rate categories. Maximum likelihood trees were constructed starting from an initial neighbor-joining tree, using bootstrap analysis based on 1000 resamplings.

3.2.4. GenBank accession numbers

Nucleotide sequences were uploaded in GenBank and accession numbers for *gag* and *env* sequences can be found in Table 2.

3.2.5. Recombination analysis

Bootscan analysis for recombination events was performed in the SimPlot 3.5.1 program (Lole *et al.*, 1999). Reference sequences for the different FIV clades in the analysis were M25381 (Petaluma, clade A), U11820 (USIL2489_7B, clade B), AF474246 (BM3070, clade C), AY679785/D37811 (Shizuoka, clade D) (Steinrigl *et al.*, 2010). The Kimura 2-parameter model was used as a distance model, the window was reduced to 140 bp and stepsize was 20bp.

3.3. Results

3.3.1. Sample details

All cats enclosed in the study were naturally infected with FIV. Samples were collected from across Belgium, dominantly from the Flanders region, with only one cat in the Walloon region. The samples from The Netherlands were more distributed across the whole country (Figure 1). Ages at the moment of sample collection ranged from 2 to 15 years old, with a median age of 8 years. The majority of samples (90%) originated from male cats (Table 2). The infected cats were at different stages of infection, but all cats had clinical signs, covering a broad spectrum from mild, with fever, anorexia, stomatitis, and gingivitis, to severe malignancies (e.g. blood neoplasms).

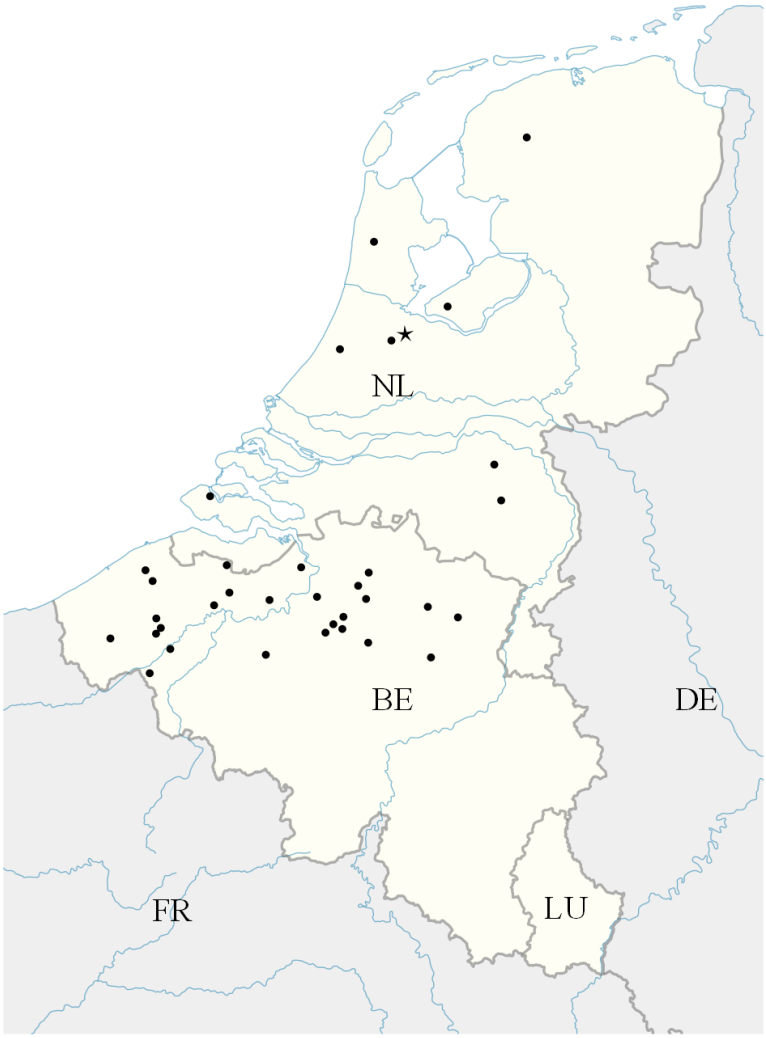

Figure 1: Geographic distribution of samples collected in Belgium and The Netherlands. The sample (NLUTkuvi) that formed a separate branch in the env neighbor-joining tree (Figure 3) is indicated with a star.

Table 2: Sample identification, origin, age and subtype assignment. All samples were named following Bachmann (Bachmann *et al.*, 1997), the first two letters indicate the home country, followed by two letter indicating the province, the next four letters are based on the cat's name and town. *Gag* and env genbank accession numbers are indicated for samples that generated new unique FIV sequences.

Identification	Location	Age	sex	Clade *gag*	Clade *env*	Accession number	
						gag	*env*
BEWVdooo	Oostkamp	8	M	A	A	KM880118	KM880108
BEWVkhde	Deerlijk	6	M	A	A	KM880119	
BEWVflpo	Poelkapelle	5	M	A	A		
BEWVprpi	Pittem	8	M	A	A		
BEWVslin	Ingelmunster	12	M	A	A		
BEWVvisa	Sint-Andries	8	M	A	A		
BEOVbaoo	Oostakker	4	M	A	A		KM880105
BEOVboze	Zele	12	M	A	A		
BEOVmame	Melsele	3	M	A	A		
BEOVmido	Drongen	10	M	A	A		
BEOVvias	Assenede	2	M	A	A		KM880106
BEOVzwni	Ninove	4	M	A	A		
BEANchgr	Grobbendonk	8	M	A	A		
BEANcuhe	Heist-op-den-berg	6	M	A	A		
BEANslbe	Bevel	11	M	A	A	KM880116	
BEANzwbo	Boom	2	M	A	A		
BEVBcahe	Hever	3	F	A	A		
BEVBfika	Kampenhout	7	F	A	A		
BEVBozke	Kessel-lo	15	M	A	A		KM880107
BEVBshvi	Vilvoorde	8	M	A	A	KM880121	KM880109
BEVBziel	Elewijt	15	M	A	A		
BEANfrme	Meulebeke	3	M	A	A		
BEHEramo	Moeskroen	10	M	A	A	KM880120	
BELIflzo	Zonhoven	12	M	A	A		
BELIomst	Sint-Truiden	4	M	A	A		
BELIpopa	Paal	12	M	A	A		
NLFLsnal	Almere	8	M	A	A		KM880113
NLFRfrgr	Grou	8	M	A	A		KM880114
NLNBbrhe	Helmond	8	M	A	A		
NLNBtahe	Helmond	13	F	A	A		
NLNHpial	Alkmaar	8	M	A	A		KM880115
NLNHzwud	Uden	8	M	A	A		
NLUTkuvi	Vinkeveen	8	M	A	Unknown	KM880117	KM880110
NLUTpimi	Mijdrecht	8	M	A	A		KM880112
NLZEkowa	Walcheren	8	F	A	A		KM880111
NLZHrole	Leiden	8	M	A	A		

3.3.2. Phylogenetic analysis of *gag* sequences

Sequences were aligned with FIV strains that represented clades A to E, additionally *gag* sequences from other EU countries were included as well. The 36 *gag* fragments sequenced in the present study clustered together with clade A reference strains (Figure 2). Only 4 *gag* fragments had an unique sequence, and represented 11% of the total sample size. They originated from geographically distinct parts of Belgium and The Netherlands. Two samples, BEWVkhde and BEHEramo, formed a cluster together with the French isolate Wo (Pancino *et al.*, 1993). All other 32 samples had an identical *gag* sequence, and clustered together with the San Diego isolate FIV PPR (Phillips *et al.*, 1990). These samples are represented in GenBank by the sample BEVBshvi. The mean genetic distance within these unique isolates was 4.3 ± 1%, which was close to the 4.4 ± 1.5% divergence seen within clade A reference sequences.

3.3.3. Phylogenetic analysis of *env* sequences

With 11 new unique sequences, the *env* gene showed more genetic diversity than *gag*. From these 11 sequences, 6 came from The Netherlands and 5 from Flanders, this made 60% of the samples of the Netherland unique, while the samples from Flanders generated only 19% unique sequences. The other samples (n=25) that were analyzed, had an *env* sequence that was identical to FIV PPR. All new samples clustered together within clade A, except for NLUTkuvi (Figure 3). This sample from Utrecht, The Netherlands, formed a separate cluster with a significant bootstrap value together with DESLc08. The latter strain was first reported by Steinrigl and colleagues, and originated from a cat that was infected with FIV in Sri Lanka.

Bootscan analysis of the *gag-env* concatenated sequences showed no recombination between different subtypes. Furthermore, none of the reference sequences for clades A to D formed a parental strain for *env* fragment of DESLc08, while the *gag* fragment was suggested to share a common ancestor with clade A viruses (Steinrigl *et al.*, 2010). Hence, a bootscan analysis was performed on NLUTkuvi with reference strains for clade A (Petaluma), B (USIL2489_7B), C (BM3070), D (Fukuoka), and DESLC08 as potential parent sequences (Figure 4). The analysis revealed DESLc08 as the parental sequence for most of the *env* fragment of NLUTkuvi. The *gag* fragment, on the other hand, resembled the clade A reference sequence. This is no surprise, as NLUTkuvi clustered within clade A in the *gag* phylogenetic tree.

Figure 2: Unrooted maximum likelihood tree for *gag* sequences constructed under the Tamura 3-parameter model and tested by a 1000 bootstrap iterations. Belgian sequences are indicated with black triangles, while samples from the Netherlands are indicated with an open triangle. The 36 samples generated 4 unique sequences (BEWVkhde, BEWVdooo, BEHEramo, BEANslbe), while all other sequences clustered together with the San Diego isolate FIV PPR. Bootstrap values above 70 % are indicated at significant nodes. The origin of reference sequences are mentioned when not apparent from the sequence name.

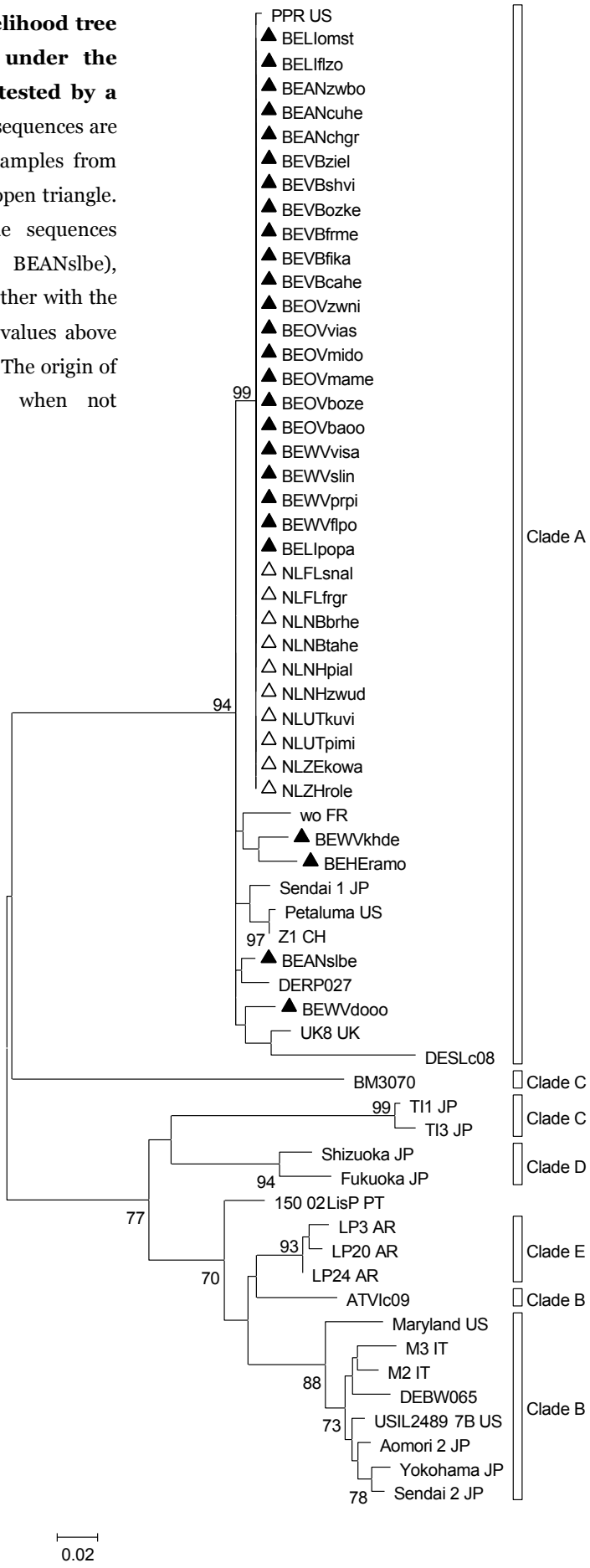

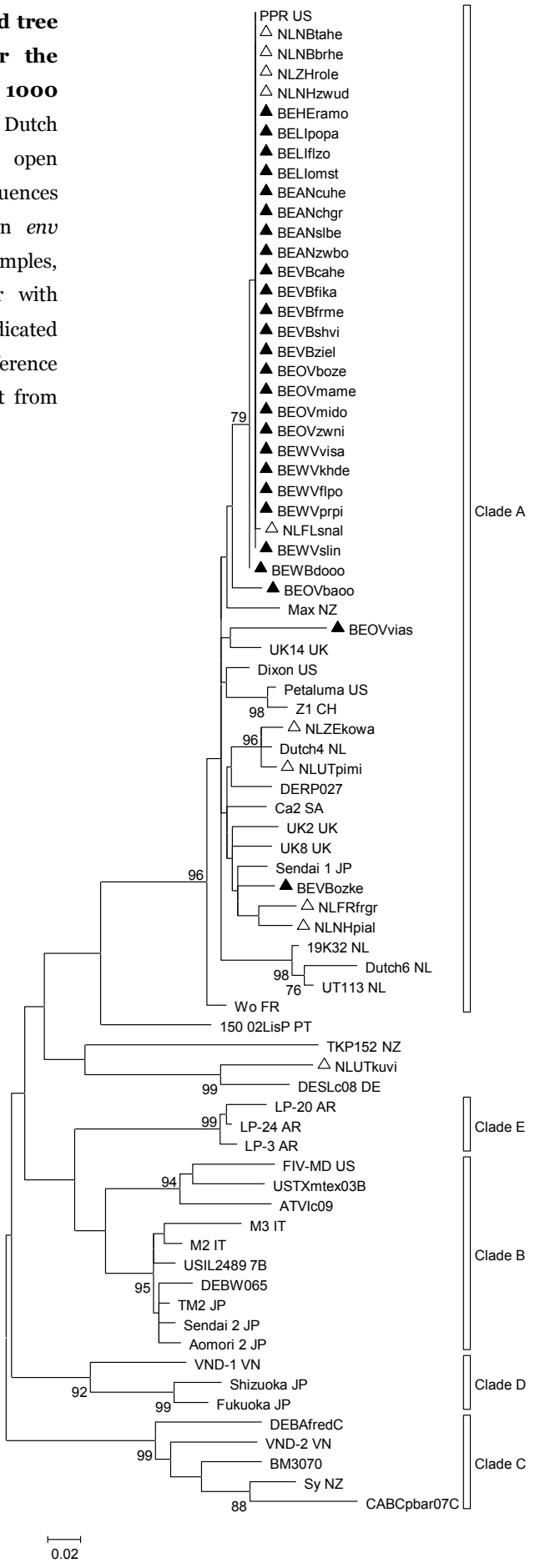

Figure 3: Unrooted maximum likelihood tree for *env* sequences constructed under the Tamura 3-parameter model tested by a 1000 bootstrap iterations. Belgian and Dutch sequences are indicated with black and open triangles respectively. Only 10 new *env* sequences were discovered, all other samples had an *env* sequence identical to FIV PPR. One of the samples, NLUTkuvi, formed a new cluster together with DESLc08. Bootstrap values above 70 % are indicated at significant nodes. The origin of reference sequences are mentioned when not apparent from the sequence name.

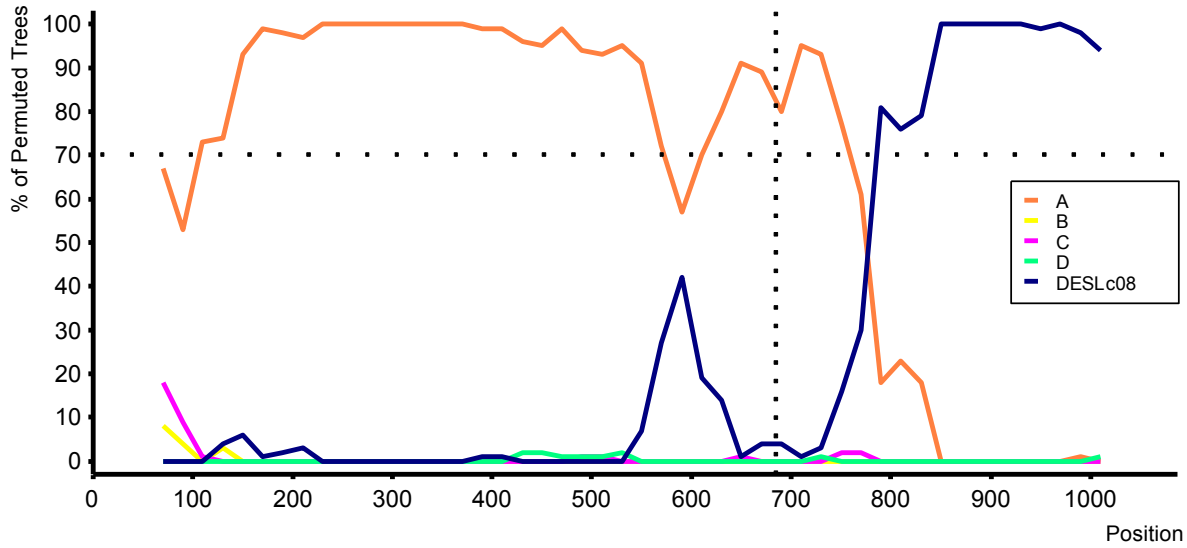

hvg

Figure 4: Bootscan analysis performed with Simplot 3.5.1. The concatenated *gag-env* sequence of NLUTkuvi was tested against reference sequences of FIV subtypes A (orange), B (yellow), C (pink), and D (green) and against the German sample DESLc08 (Blue). The vertical dotted line indicates the transition from the *gag* to *env* fragment. The 70% bootstrap level is marked by the horizontal dotted line.

Genetic distances between the *env* sequence of the newly formed cluster with NLUTkuvi and DESLc08 and the established clades A to E were calculated, and are shown in Table 3. Distances to these clades always exceeded 20%, therefore NLUTkuvi and DESLc08 could be considered a new *env* subtype. The distance between DESLc08 and NLUTkuvi on the other hand was 9.5 ± 2.2%, representing an intra-clade variance (Sodora *et al.*, 1994). The mean genetic distance between the generated clade A *env* fragments was 6.6 ± 2.4%, comparable to 7.9 ± 2.6 % between the clade A reference sequences. Two samples, NLZEkowa and NLUTpimi, formed a significant cluster with the older Dutch isolate Dutch4 (Rigby *et al.*, 1993). NLFRfrgr and NLNHpial, two samples coming from the north of The Netherland, formed a bootstrap significant cluster together. Apart from BEWVdooo, none of the samples with a unique *gag* sequence presented an unique *env* sequence.

Table 3: Mean genetic distance (± standard deviation) between the *env* fragments of samples NLUTkuvi, DESLc08 and BEVBshvi and the different FIV clades A to E based on the reference strains used for building the *env* phylogenetic tree.

	Clade				
Sample	**A**	**B**	**C**	**D**	**E**
DESLc08	27.6 ± 2.6 %	30.3 ± 3.5 %	34.3 ± 2.8 %	27.2 ± 2.0 %	29.6 ± 3.3 %
NLUTkuvi	25.3 ± 2.8 %	35.8 ± 2.1 %	35.5 ± 3.2 %	30.1 ± 4.7 %	37.1 ± 4.0 %
BEVBshvi	5.8 ± 2.3 %	24.3 ± 4.3 %	27.2 ± 2.8 %	25.1 ± 1 %	24.6 ± 1.2 %

3.4. Discussion

Consistent with previous reports, the majority of the FIV infected samples were derived from male cats (Hayward *et al.*, 2007; Hosie *et al.*, 1989; Reggeti & Bienzle, 2004). Territorial male behavior leads to a higher fighting incidence and, consequently, an increased risk for FIV infection (Natoli *et al.*, 2005). The *gag* sequences from samples collected in Belgium and The Netherlands showed a low genetic diversity, although these cats lived in geographically distinct locations. Only 14% of the samples generated a new unique *gag* sequence. Two Belgian samples, BEWVkhde and BEWVramo, clustered together with the French isolate Wo (Pancino *et al.*, 1993). Although the branch did not have a significant bootstrap value, these samples did come from cats that live close to the French border. It is likely that cats living in that area cross the border more frequently, either as a stray or by movement upon purchase.

The newly described sequences for the *env* gene showed a larger variation, with a total of 33% unique sequences. Surprisingly most of these unique sequences came from samples collected in The Netherlands, even though the sample size from that country was smaller. Chances of finding new sequences should increase with larger sample sizes, but this was not the case. A possible explanation for this bigger sequence variation, could be the presence of more physical borders in The Netherlands when compared to Belgium. The Netherlands are more compartmentalized by large rivers, lakes and the sea than Belgium, blocking free movement across these natural obstacles for stray and feral cats. These constrains on virus spread could lead to a more local evolution of virus strains. On two occasions, on the other hand, two strains that were not geographically related, did share a significant branch. In one of these cases, the significant branch was an older Dutch strain, Dutch4, originating from Amsterdam. It could be speculated, that there is a larger overall sequence variability in The Netherlands compared to Belgium, with occasional spread of local strains by movement of households. In contrast with other European countries (Duarte & Tavares, 2006; Samman *et al.*, 2011; Steinrigl *et al.*, 2010), FIV samples from Belgium and The Netherlands, show a low genetic diversity. All samples, besides one were subtyped as clade A FIV strains, confirming the observation made by Steinrigl et al., that genetic diversity is higher in Southern European countries (Austria, Italy and Portugal), compared with a more uniform variation found in Germany. The lower

variability, and the presence of clade A viruses only, may indicate a more recent introduction of FIV in the Northern European countries.

One of the *env* sequences, NLUTkuvi, did not show any relationship to previously identified clades, either by phylogenetic tree building or bootscan analysis for recombination. The sequence clustered together with the German strain DESLc08, originating from a cat that was infected with an unknown subtype in Sri Lanka (Steinrigl *et al.*, 2010). The genetic distance to known FIV subtypes indicates that these sequences might belong to a new *env* subtype. The *gag* fragment of NLUTkuvi belonged to the clade A FIV viruses. Therefore, it could be speculated that NLUTkuvi is a recombinant between clade A and the unknown clade to which DESLc08 belongs. Another explanation is that co-infection with both subtype A and the unkown subtype occurred in this cat and that the generated *gag* and *env* sequences are derived from separate viruses. Sequencing of the *gag* gene showed unambiguous results when repeated (data not shown), making co-infection a less likely conclusion.

Unlike *gag*, *env* is under pressure from the humoral immune response (Seibert *et al.*, 1995), causing positive selection of escape mutants. This leads to a large sequence variability, especially in the variable loops. The FIV clade system is based on a highly variable region in the *env* gene, V3-V4. Several reports show that intragenic and intergenic recombination occurs in the different FIV genes, making it difficult to classify these strains in the clade system, as it is only based on *env* sequences (Bachmann *et al.*, 1997; Carpenter *et al.*, 1998; Hayward & Rodrigo, 2008; Kann *et al.*, 2007; Reggeti & Bienzle, 2004). In this report, the current clade system is also not well supported by significant bootstrap values in phylogenetic trees for *gag* and *env*, especially for clade B. To date, there is some evidence that the *env* subtyping predicts pathogenicity and disease progression. Several authors have suggested that clade C FIV viruses are more pathogenic than clade A viruses (de Rozìeres *et al.*, 2008; Pedersen *et al.*, 2001), and for clade B viruses the opposite was proposed (Bachmann *et al.*, 1997). However, classification to a FIV clade does not seem to predict good cross-protection in vaccination studies (Dunham *et al.*, 2006). Therefore, it might be interesting to integrate other genetic regions into the current FIV clade system to improve correlations between virus subtyping and virus virulence, disease progression and cross-protection upon vaccination. Recently, it was shown that the genes *vif* and *orfA* are important determinants of replication rate in vitro, partly by interaction of Vif with the cellular protein APOBEC (Troyer *et al.*, 2013). While *env* variability is an

important strategy of FIV to deceive the immune system, other proteins can play a major role in immune evasion and pathogenicity of a virus strain as well. Incorporation of these genes in phylogenetic analyses, and classification based on amino acid level may provide a better prediction on pathogenicity.

In conclusion, a low genetic variability was seen for the FIV *gag* and V3-V4 *env* sequences from Belgium and The Netherlands. This is in accordance with a more uniform variability of FIV as already reported for Northern Europe. We reported one V3-V4 *env* sequence that did not match with any of the previously known FIV subtypes, but showed a large similarity to a strain that was first detected in a cat that was infected in Sri Lanka. As more FIV sequences from different regions become available, more new subtypes seem to emerge. Therefore, it would be interesting to generate more full genome FIV sequences or to look into additional regions in the genome to ameliorate classification of different FIV strains. This can help to improve correlations between virus subtyping and virus virulence, disease progression and cross-protection upon vaccination.

3.5. Supplementary data

Supplementary Table 4: FIV references for *gag* and *env* sequences used in the alignments for phylogenetic analysis and neighbor-joining tree building.

Clade A	***Gag***	***Env***
19K32		M73965
Ca2		DQ873714
DERP027	GQ339817	GQ339804
Dixon		L00608
Dutch4		X69498
Dutch6		X69499
Max		GQ357642
Petaluma	M25381	M25381
PPR	M36968	M36968
Sendai 1	D37820	D37813
UK14		X69497
UK2		X69494
UK8	GU055218	X69496
UT113		X60725
wo	L06311	L06311
Z1	X57002	X57002
Clade B	***Gag***	***Env***
Aomori 2	D37824	D37817
ATVIc09	GQ339806	GQ339803
DEBW065	GQ339837	GQ339805
FIV-MD		AF452126
M2	Y13866	X69501
M3	Y13867	X69502
Maryland	AF361320	
Sendai 2	D37821	D37814
TM2		M59418
USIL24897B	U11820	U11820
USTXmtex03B		U02422
Yokohama	D37819	

Clade C	***Gag***	***Env***
BM3070	AF474246	AF474246
CABCpbaro7c		U02397
DEBAfredC		U57020
Sy		GQ357641
TI1	AB027298	
TI3	AB027300	
VND-2		AB083503
Clade D	***Gag***	***Env***
Fukuoka	D37822	D37815
Shizuoka	D37818	D37811
VND-1		AB083502
Clade E	***Gag***	***Env***
LP3	AB027302	D84496
LP20	AB027303	D84498
LP24	LP7304	D84500
Clade F	***Gag***	***Env***
150 02LisP	DQ0722542	DQ072566
Unassigned	***Gag***	***Env***
DESLc08	GQ339807	GQ339802
TKP152		GQ357640

Acknowledgements

We thank Ytse Noppe and Bieke Weyn for their excellent technical support. IDMR was supported by the Agency for Innovation by Science and Technology in Flanders (IWT-Vlaanderen).

References

Bachmann, M. H., Mathiason-Dubard, C., Learn, G. H., Rodrigo, A. G., Sodora, D. L., Mazzetti, P., Hoover, E. A. & Mullins, J. I. (1997). Genetic diversity of feline immunodeficiency virus: dual infection, recombination, and distinct evolutionary rates among envelope sequence clades. *J Virol* **71**, 4241-4253.

Carpenter, M. A., Brown, E. W., MacDonald, D. W. & O'Brien S, J. (1998). Phylogeographic patterns of feline immunodeficiency virus genetic diversity in the domestic cat. *Virology* **251**, 234-243.

de Parseval, A., Chatterji, U., Sun, P. & Elder, J. H. (2004). Feline immunodeficiency virus targets activated CD4+ T cells by using CD134 as a binding receptor. *Proc Natl Acad Sci U S A* **101**, 13044-13049.

de Rozìeres, S., Thompson, J., Sundstrom, M., Gruber, J., Stump, D. S., de Parseval, A. P., VandeWoude, S. & Elder, J. H. (2008). Replication properties of clade A/C chimeric feline immunodeficiency viruses and evaluation of infection kinetics in the domestic cat. *J Virol* **82**, 7953-7963.

Dorny, P., Speybroeck, N., Verstraete, S., Baeke, M., De Becker, A., Berkvens, D. & Vercruysse, J. (2002). Serological survey of Toxoplasma gondii, feline immunodeficiency virus and feline leukaemia virus in urban stray cats in Belgium. *Vet Rec* **151**, 626-629.

Duarte, A. & Tavares, L. (2006). Phylogenetic analysis of Portuguese Feline Immunodeficiency Virus sequences reveals high genetic diversity. *Vet Microbiol* **114**, 25-33.

Dunham, S. P., Bruce, J., MacKay, S., Golder, M., Jarrett, O. & Neil, J. C. (2006). Limited efficacy of an inactivated feline immunodeficiency virus vaccine. *Vet Rec* **158**, 561-562.

Gramaglia, I., Weinberg, A. D., Lemon, M. & Croft, M. (1998). Ox-40 ligand: a potent costimulatory molecule for sustaining primary CD4 T cell responses. *J Immunol* **161**, 6510-6517.

Hayward, J. J. & Rodrigo, A. G. (2008). Recombination in feline immunodeficiency virus from feral and companion domestic cats. *Virol J* **5**, 76.

Hayward, J. J., Taylor, J. & Rodrigo, A. G. (2007). Phylogenetic analysis of feline immunodeficiency virus in feral and companion domestic cats of New Zealand. *J Virol* **81**, 2999-3004.

Hosie, M. J., Robertson, C. & Jarrett, O. (1989). Prevalence of feline leukaemia virus and antibodies to feline immunodeficiency virus in cats in the United Kingdom. *Vet Rec* **125**, 293-297.

Iwata, D. & Holloway, S. A. (2008). Molecular subtyping of feline immunodeficiency virus from cats in Melbourne. *Aust Vet J* **86**, 385-389.

Joshi, A., Garg, H., Tompkins, M. B. & Tompkins, W. A. (2005). Preferential feline immunodeficiency virus (FIV) infection of CD4+ CD25+ T-regulatory cells correlates both with surface expression of CXCR4 and activation of FIV long terminal repeat binding cellular transcriptional factors. *J Virol* **79**, 4965-4976.

Kakinuma, S., Motokawa, K., Hohdatsu, T., Yamamoto, J. K., Koyama, H. & Hashimoto, H. (1995). Nucleotide sequence of feline immunodeficiency virus: classification of Japanese isolates into two subtypes which are distinct from non-Japanese subtypes. *J Virol* **69**, 3639-3646.

Kann, R., Seddon, J., Kyaw-Tanner, M. & Meers, J. (2007). Co-infection with different subtypes of feline immunodeficiency virus can complicate subtype assignment by phylogenetic analysis. *Arch Virol* **152**, 1187-1193.

Lecollinet, S. & Richardson, J. (2008). Vaccination against the feline immunodeficiency virus: the road not taken. *Comp Immunol Microbiol Infect Dis* **31**, 167-190.

Lole, K. S., Bollinger, R. C., Paranjape, R. S., Gadkari, D., Kulkarni, S. S., Novak, N. G., Ingersoll, R., Sheppard, H. W. & Ray, S. C. (1999). Full-length human immunodeficiency virus type 1 genomes from subtype C-infected seroconverters in India, with evidence of intersubtype recombination. *J Virol* **73**, 152-160.

Natoli, E., Say, L., Cafazzo, S., Bonanni, R., Schmid, M. & Pontier, D. (2005). Bold attitude makes male urban feral domestic cats more vulnerable to Feline Immunodeficiency Virus. *Neurosci Biobehav Rev* **29**, 151-157.

Paepe, D., Verjans, G., Duchateau, L., Piron, K., Ghys, L. & Daminet, S. (2013). Routine health screening: findings in apparently healthy middle-aged and old cats. *J Feline Med Surg* **15**, 8-19.

Pancino, G., Fossati, I., Chappey, C., Castelot, S., Hurtrel, B., Moraillon, A., Klatzmann, D. & Sonigo, P. (1993). Structure and variations of feline immunodeficiency virus envelope glycoproteins. *Virology* **192**, 659-662.

Pecoraro, M. R., Tomonaga, K., Miyazawa, T., Kawaguchi, Y., Sugita, S., Tohya, Y., Kai, C., Etcheverrigaray, M. E. & Mikami, T. (1996). Genetic diversity of Argentine isolates of feline immunodeficiency virus. *J Gen Virol* **77 (Pt 9)**, 2031-2035.

Pedersen, N. C., Leutenegger, C. M., Woo, J. & Higgins, J. (2001). Virulence differences between two field isolates of feline immunodeficiency virus (FIV-APetaluma and FIV-CPGammar) in young adult specific pathogen free cats. *Vet Immunol Immunopathol* **79**, 53-67.

Phillips, T. R., Talbott, R. L., Lamont, C., Muir, S., Lovelace, K. & Elder, J. H. (1990). Comparison of two host cell range variants of feline immunodeficiency virus. *J Virol* **64**, 4605-4613.

Reggeti, F. & Bienzle, D. (2004). Feline immunodeficiency virus subtypes A, B and C and intersubtype recombinants in Ontario, Canada. *J Gen Virol* **85**, 1843-1852.

Rigby, M. A., Holmes, E. C., Pistello, M., Mackay, A., Brown, A. J. & Neil, J. C. (1993). Evolution of structural proteins of feline immunodeficiency virus: molecular epidemiology and evidence of selection for change. *J Gen Virol* **74 (Pt 3)**, 425-436.

Samman, A., McMonagle, E. L., Logan, N., Willett, B. J., Biek, R. & Hosie, M. J. (2011). Phylogenetic characterisation of naturally occurring feline immunodeficiency virus in the United Kingdom. *Vet Microbiol* **150**, 239-247.

Seibert, S. A., Howell, C. Y., Hughes, M. K. & Hughes, A. L. (1995). Natural selection on the gag, pol, and env genes of human immunodeficiency virus 1 (HIV-1). *Mol Biol Evol* **12**, 803-813.

Siebelink, K. H., Tijhaar, E., Huisman, R. C., Huisman, W., de Ronde, A., Darby, I. H., Francis, M. J., Rimmelzwaan, G. F. & Osterhaus, A. D. (1995). Enhancement of feline immunodeficiency virus infection after immunization with envelope glycoprotein subunit vaccines. *J Virol* **69**, 3704-3711.

Sodora, D. L., Shpaer, E. G., Kitchell, B. E., Dow, S. W., Hoover, E. A. & Mullins, J. I. (1994). Identification of three feline immunodeficiency virus (FIV) env gene subtypes and comparison of the FIV and human immunodeficiency virus type 1 evolutionary patterns. *J Virol* **68**, 2230-2238.

Steinrigl, A., Ertl, R., Langbein, I. & Klein, D. (2010). Phylogenetic analysis suggests independent introduction of feline immunodeficiency virus clades A and B to Central Europe and identifies diverse variants of clade B. *Vet Immunol Immunopathol* **134**, 82-89.

Steinrigl, A. & Klein, D. (2003). Phylogenetic analysis of feline immunodeficiency virus in Central Europe: a prerequisite for vaccination and molecular diagnostics. *J Gen Virol* **84**, 1301-1307.

Tamura, K., Stecher, G., Peterson, D., Filipski, A. & Kumar, S. (2013). MEGA6: Molecular Evolutionary Genetics Analysis version 6.0. *Mol Biol Evol* **30**, 2725-2729.

Tompkins, M. B. & Tompkins, W. A. (2008). Lentivirus-induced immune dysregulation. *Vet Immunol Immunopathol* **123**, 45-55.

Troyer, R. M., Thompson, J., Elder, J. H. & VandeWoude, S. (2013). Accessory genes confer a high replication rate to virulent feline immunodeficiency virus. *J Virol* **87**, 7940-7951.

Weaver, E. A. (2010). A detailed phylogenetic analysis of FIV in the United States. *PLoS One* **5**, e12004.

Yamamoto, J. K., Hansen, H., Ho, E. W., Morishita, T. Y., Okuda, T., Sawa, T. R., Nakamura, R. M. & Pedersen, N. C. (1989). Epidemiologic and clinical aspects of feline immunodeficiency virus infection in cats from the continental United States and Canada and possible mode of transmission. *J Am Vet Med Assoc* **194**, 213-220.

Yamamoto, J. K., Pu, R., Sato, E. & Hohdatsu, T. (2007). Feline immunodeficiency virus pathogenesis and development of a dual-subtype feline-immunodeficiency-virus vaccine. *AIDS* **21**, 547-563.

Chapter 4

Differences in expression pattern and conformational changes of Env and Gag proteins in FIV-infected feline PBMC compared to infected and transfected feline model cell lines

Adapted from:

Roukaerts ID, Grant CK, Theuns S, Christiaens I, Acar DD, Van Bockstael S, Desmarets LM, and Nauwynck HJ, 2016. Virus Research, accepted.

Abstract

Env and Gag are key components of the FIV virion that are targeted to the plasma membrane for virion assembly. They are both important stimulators and targets of anti-FIV immunity. To investigate the expression pattern and conformational changes of Gag and Env during FIV infection of feline PBMC (the natural FIV host cells) and GFox, and after FIV transfection of CrFK, FIV Env and Gag specific MAbs were used. A kinetic follow up of Gag and Env expression showed a polarization of both Gag and Env expression to specific sites at the plasma membrane of PBMC. In infected GFox and PBMC, Env showed antigenic changes during processing and trafficking which were not seen in transfected CrFK. Interestingly, mature trimeric Env expressed on the plasma membrane of CrFK and GFox was antigenically different from mature Env on PBMC. Epitopes available on intracellular immature Env of PBMC were masked on plasma membrane expressed Env. In conclusion, mature trimeric cell surface expressed Env is antigenically distinct from intracellular monomeric Env in PBMC and may mask cells from the feline humoral immunity; it is restricted to a small area on the plasma membrane and co-localizes with a large moiety of Gag, which may represent a preferred FIV budding site, or initiation of virological synapses with direct cell-to-cell virus transmission.

4.1. Introduction

Feline immunodeficiency virus (FIV) is a member of the *Retroviridae* and belongs to the genus *lentivirus*. It is mainly transmitted through biting incidents between cats (Natoli et al., 2005). The virus has a broad cell tropism, since it replicates in cells of the monocyte/macrophage lineage, and in T- and B-lymphocytes (Beebe et al., 1994; Brown et al., 1991; Brunner and Pedersen, 1989; Dow et al., 1999; English et al., 1993). The effective immune-evasive properties of FIV allow the virus to cause a lifelong infection. After a long asymptomatic incubation phase, FIV infection can cause an AIDS-like disease, which is characterized by a depletion of $CD4^+$ T-cells, an increase in plasma viral load, and severe immune suppression (Hartmann, 2012; Pedersen et al., 1989; Tompkins and Tompkins, 2008).

Lentiviruses are enveloped viruses that have only one heavily glycosylated envelope protein in their viral membrane. FIV Env is translated in the rough endoplasmic reticulum (ER) as a 150 kDa glycosylated polyprotein. After cleavage of the leader sequence, the protein is transported from the ER to the Golgi apparatus, where the protein is further processed and cleaved by furin into a surface protein (SU) of 95 kDa and a transmembrane protein (TM) of 36 kDa (Stephens et al., 1991; Verschoor et al., 1993). The envelope surface and transmembrane part remain associated but are non-covalently linked. Mature Env protein is transported towards the cell surface of infected cells and is finally incorporated into the FIV particle as a trimer. Sequence alignments showed that the viral envelope protein contains 8 hypervariable regions (V1-V9), of which 5 (V1-V6) can be found on SU and 3 on TM (V7-V9) (Pancino et al., 1993). For infection, the surface protein sequentially interacts with the CD134 primary virus receptor and the secondary virus entry port, CXCR4 (de Parseval et al., 2004; Richardson et al., 1999; Shimojima et al., 2004; Willett et al., 1997). Conformation changes in SU result in the exposure of the extracellular portion of the TM protein that contains a hydrophobic fusion peptide, responsible for fusion between the viral envelope and the plasma membrane of the host cell (de Parseval et al., 2006; Garg et al., 2004). Subsequently, the virus core containing the viral genome is released into the host cell cytoplasm.

Another important FIV structural protein is the Gag polyprotein, which contains the matrix (MA), capsid (CA) and nucleocapsid (NC) protein. After translation, the Gag polyprotein associates with the plasma membrane through a group of basic residues and by myristolyation of the MA part (Brown et al., 2015; Elder et al., 1993; Manrique

et al., 2001). The capsid protein ensures polymerization of the Gag polyprotein, which is required for particle formation (Serrière et al., 2013). Incorporation of the FIV RNA genome is mediated by the nucleocapsid that contains a packaging signal (Kemler et al., 2002; Moscardini et al., 2002). Only after budding, the Gag polyprotein is cleaved by the viral protease, giving rise to the mature virion core components: the MA underneath the envelope, the typical lentiviral cone shaped CA, and the NC that stabilizes the viral genome.

FIV protein expression and conformational changes during viral replication have not been extensively studied in feline leukocytes, the natural host cells. Most information on FIV behaviour is derived from experiments with the adherent endothelial-like Crandell Rees feline kidney cell line (CrFK) transfected with an infectious clone of FIV, or GFox cells, which are CrFK cells that stably express the FIV receptor CD134, and hence can be infected with FIV (de Parseval et al., 2004). Because important differences may exist in the behaviour of viruses in these research cell lines in comparison with feline blood mononucleair cells, the information gathered from infection models in cell lines should be taken with caution. In the present study, we wanted to investigate if there are differences in expression pattern and conformational changes of FIV proteins Env and Gag between infected PBMC and infected/transfected cell lines.

4.2. Materials and methods

4.2.1. Cells

CrFK cells were grown in MEM (Gibco) supplemented with 5% fetal bovine serum (FBS), 2 % lactalbumine, 100 U/ml penicillin, 0.1 mg/ml streptomycin. GFox cells were a kind gift from Dr. J.H. Elder (The Scripps Research Institute). GFox were cultured in DMEM medium (Gibco) supplemented with 10% FBS, 100 U/ml penicillin, 0.1 mg/ml streptomycin, 1% non-essential amino acids (100 x), and 2 mM sodium pyruvate. Peripheral blood mononuclear cells (PBMC) were collected from fresh blood obtained by venipuncture of the jugular vein of SPF cats (approved by the local ethical committee EC2015/79). PBMC were purified by density centrifugation of the blood over Ficoll Paque (GE Healthcare). Cells were kept in RPMI (Gibco), 10% FBS, 100 U/ml penicillin, 0.1 mg/ml streptomycin, 1% non-essential amino acids (100 x), and 2 mM sodium pyruvate. Following isolation and culture plastic adherence of monocytes for 24 h, suspension cells were stimulated for 3 days with 2.5 μg/ml concanavalin A

(Sigma), hereafter 100 U/ml interleukin 2 (IL2) (Roche) was added for the duration of the culture.

4.2.2. Virus

FIV-PPR was obtained from Dr. J.H. Elder through the AIDS Reagent Program, Division of AIDS, NIAID, NIH (Phillips et al., 1990). Virus was grown and titrated by end-point dilution in GFox cells.

4.2.3. Infection and transfection

IL2-stimulated PBMC were inoculated with FIV-PPR by spinoculation. Cells were washed and resuspended at a concentration of 500,000 cells/ml in virus inoculum containing 1000 TCID50/ml. Cells were centrifuged in a 6-well plate at 1200 xg for 90 minutes at 32°C. Next, plates were incubated an additional half hour at 37°C and 5% CO_2. For FIV-PPR infection in GFox, cells were seeded at 150,000 cells/ml in a 24-well plate on glass inserts. The next day, cells were inoculated with 200 µl virus suspension at 1000 TCID50/ml for 1 h. CrFK cells were transfected with the FIV-PPR infectious molecular clone. Briefly, CrFK cells were seeded in antibiotic-free medium at 150,000 cells/ml in a 24-well plate on a glass coverslip. The next day, each well was transfected with 0.25 µg plasmid DNA pre-complexed with 0.25 µl PlusReagent® (Invitrogen) using 1.5 µl Lipofectamin-LTX® (Invitrogen). Cells were incubated with this transfection mix in MEM for 4 h; subsequently the medium was replaced with complete CrFK medium without antibiotics.

4.2.4. Antibodies

Mouse monoclonal antibodies against FIV were provided by Custom Monoclonals Intl. Corp. (Sacramento, US). Two different antibodies against the FIV Gag polyprotein were used, PAK3-2 and P24CR1. The antibody PAK3-2C1 recognizes both the Gag polyprotein and the processed capsid protein and was designated αCA-gag, while P24CR1 only recognizes the processed FIV capsid protein and was designated αCA-mature throughout the paper. The anti-FIV SU MAbs used in this paper target, amino- to carboy-terminal order, the V2 region (SU2-6, SU2-8, SU2-11 and SU1-12), the V3 region (SU1-30, SU2-5, SU1-10 and SU1-7), and the V4 region (SU2-3). For clarity, the SU MAbs are named after the epitope they target, for instance the antibody SU2-6 which targets the V2-1 epitope is called αV2-1, as further illustrated in Figure 1.

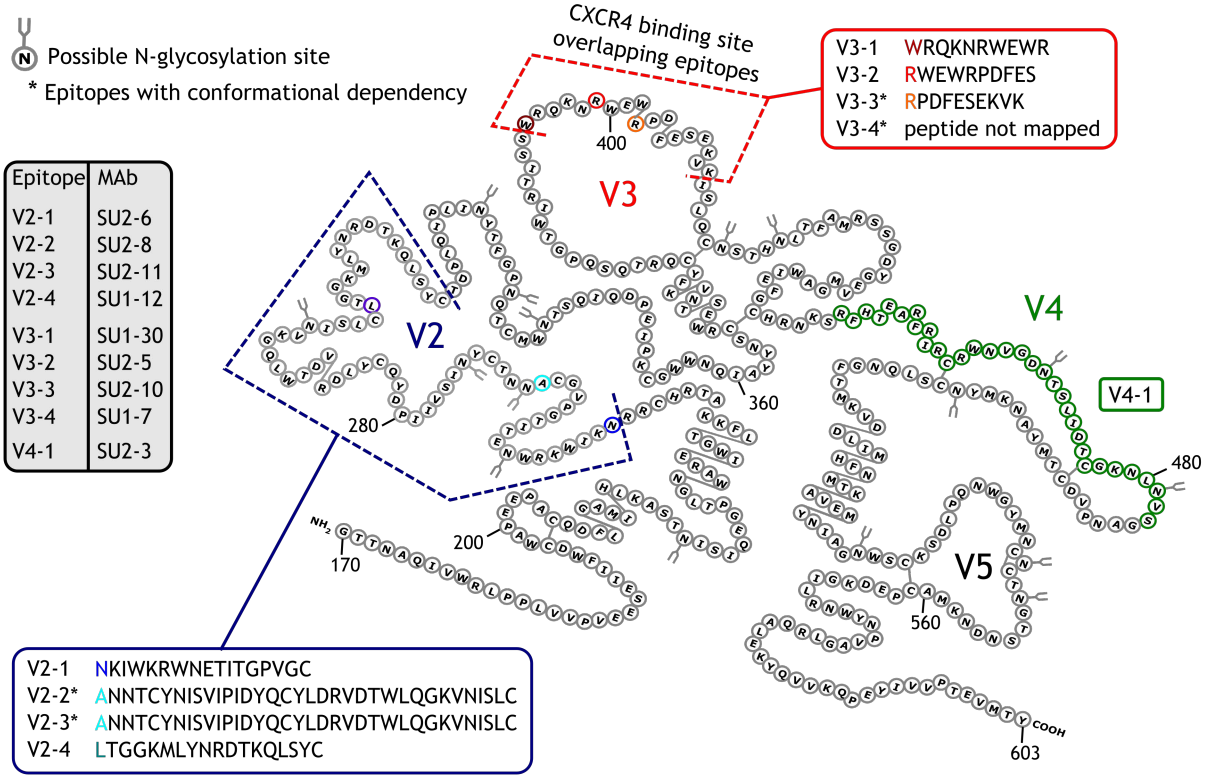

Figure 1: Diagram of the FIV-PPR SU protein with indication of the SU MAb epitopes. The V2 loop (blue) contains linear epitopes, V2-1 and V2-4, as well as conformational epitopes, V2-2 and V2-3. The V3 (red) contains the CXCR4 binding region. V3-1, V3-2 and V3-3 are linear epitopes with the latter being exposed only after SU-receptor interaction, while V3-4 is conformational. The V4 loop (green) contains only one linear epitope, V4-1.

4.2.5. Immunocytochemistry

Plasma membrane staining was performed at 4°C or after fixation with 1 % paraformaldehyde in PBS for 5 minutes at room temperature. For intracellular staining, the fixed cells were permeabilized with cold acetone/water 80% v/v for 5 minutes at -20°C. Suspension cells were spun onto silicon coated microscopic slides prior to permeabilization. Cells were incubated with 20 µg/ml anti-FIV antibody or an isotype-matched control antibody in cold DMEM at 4°C or PBS containing 10% normal goat serum at 37°C for 1h. Primary antibodies were visible with a complementing fluorescently conjugated secondary antibody and nuclei with Hoechst33342 (ThermoFisher). Coverslips were mounted on microscopic slides with glycerin/PBS containing 2.5% 1,4-diazabicyclo(2,2,2)octane (Janssens). Samples were analyzed by confocal laser scanning microscopy (Leica TSC SPE system with Leica DM2500 CQS microcope). Pictures were taken with the Leica LAS X interface. Subsequent processing of the pictures was performed with ImageJ software (NIH).

4.2.6. Western blot for FIV proteins

Cellular lysates were prepared from FIV transfected CrFK cells and infected GFox and PBMC by lysis in buffer containing 50mM TRIS-HCl, 150 mM NaCl, 1% Nonidet P-40, 0.1% SDS, 5mM EDTA, and protease inhibitor cocktail (Roche) in water. Samples were diluted in loading buffer containing β-mercaptoethanol, boiled for 5 minutes and loaded on a 10% acrylamide (Biorad) gel. After electrophoresis, proteins were blotted on a PVDF-membrane (GE Healthcare). Remaining protein binding sites were blocked in a 5% milk solution in PBS containing 0.1% TWEEN-20 (Sigma) overnight. FIV protein detection was performed by overnight incubation with αV3-1 (SU1-30) and αCA-gag (PAK3-2C1). After washing, blots were incubated with goat-anti-mouse-HRP (Sigma) secondary antibodies for 1 h at room temperature. Viral proteins were detected with Amersham ECL Prime western blotting detection reagent (GE Healthcare) on a ChemiDoc MP System (Biorad).

4.3. Results

4.3.1. Expression kinetics of the FIV structural proteins Env and Gag in PBMC, GFox and CrFK

To get more insights into the FIV viral protein processing and trafficking during the replication cycle, the FIV structural proteins Gag and Env were stained at several time points (0, 3, 6, 9, 12, 18, 24 and 48 h) post inoculation (p.i.) or transfection. The results are summarized in Table 1. FIV virion formation by the different cells was confirmed by titration by end-point dilution of the cell culture medium that was collected prior to the staining experiments at 48 h p.i. (data not shown).

After 12 h p.i., the first infected PBMC were detected by positive cytoplasmic Gag (stained with αCA-gag) and Env (stained with αV3-1) expression. Starting at 24 h p.i., 28 ± 6% of the FIV^+ cells showed an accumulation of Gag polyprotein in specific areas at the plasma membrane, as is shown in Figure 2a-2b. The amount of FIV^+ cells showing this accumulation of Gag polyprotein remained around 30% during the following time points, and was also observed at later time points (7 days p.i.). At 36 h p.i., the accumulating Gag was accompanied by cell surface expression of FIV Env. The Env protein expressed on the cell surface of the infected PBMC was not distributed evenly, but concentrated in one or several clusters on the plasma membrane (Fig. 3a). These patches of envelope proteins showed a 100% co-localization with the accumulations of Gag polyprotein (Fig. 4a). The first giant cells, containing multiple

nuclei, were also detected 36 h p.i., confirming the appearance of Env on the plasma membrane and interaction between the Env and the FIV receptors on susceptible cells (Fig. 4b). Mature FIV capsid protein (stained with αCA-mature) was observed from 36 h p.i.. Unlike its precursor, the Gag polyprotein, mature capsid protein was not found cytoplasmically, but only in protrusions connected to the plasma membrane (Fig. 2c).

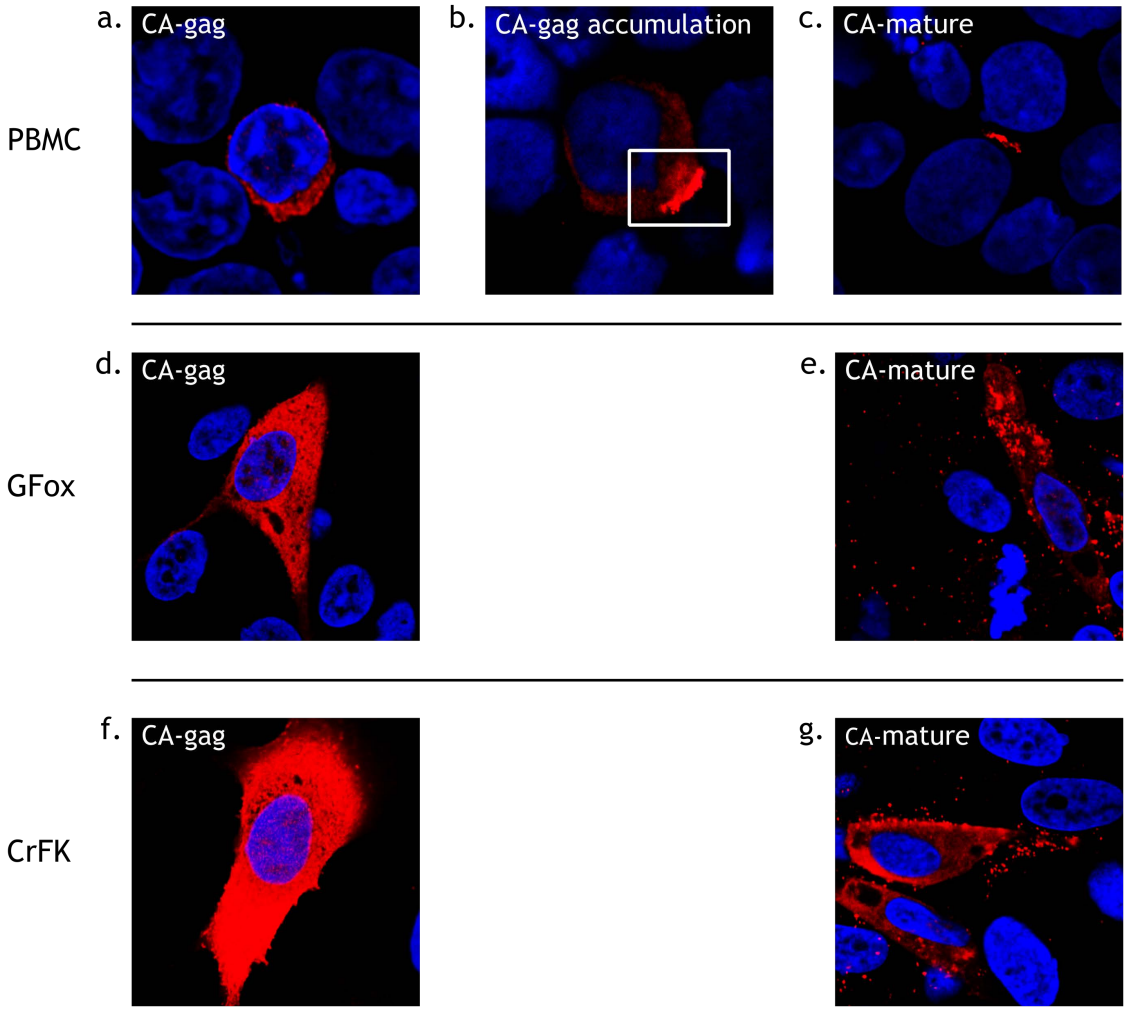

Figure 2: Expression of FIV Gag polyprotein and mature capsid protein in FIV infected PBMC, infected GFox and transfected CrFK. (a) Expression of Gag polyprotein in infected PBMC. (b) Accumulation of Gag polyprotein in infected PBMC (white box), starting 24 h p.i. and seen in 30% of FIV infected PBMC for the remainder of the culture. (c) Expression of mature capsid protein in infected PBMC, visible after 36 h p.i.. (d) Expression of Gag polyprotein in infected GFox. (e) Expression of mature capsid protein in infected GFox. (f) Expression of Gag polyprotein in transfected CrFK. (g) Expression of mature capsid protein in transfected CrFK.

In GFox cells, the first intracellular FIV Gag polyprotein and Env expression was visualized at 24 h p.i.. Although cell surface expression of Env was not yet detected, the presence of syncytia indicated that Env was already expressed on the plasma membrane. Failure to detect Env by staining could be due to a low amount of protein on the plasma membrane. At later time points (36 h and 48 h p.i.) Env was clearly

detected on the cell surface of infected GFox cells. Unlike the infected PBMC, plasma membrane expressed Env was distributed evenly on the cell surface (Fig. 3b). Also, no accumulation of Gag polyprotein at the plasma membrane of FIV infected GFox was noticed at any given time point (Fig. 2d). In contrast with infected PBMC, mature capsid protein (stained with αCA-mature) was present in the cytoplasm of FIV infected GFox, as can be seen in Figure 2e.

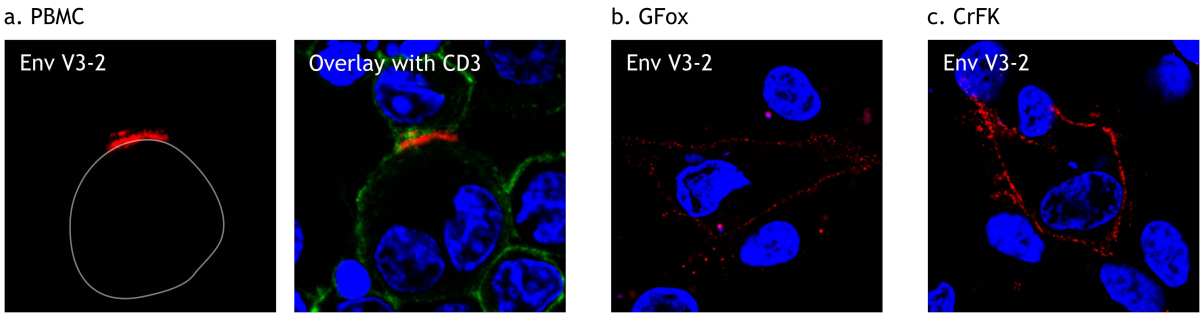

Figure 3: Cell surface expression of FIV Env SU on (a) FIV infected PBMC, (b) infected GFox and (c) transfected CrFK. Plasma membrane expression of the FIV envelope protein stained with αV3-2 (Env SU V3 region) on paraformaldehyde fixed cells.

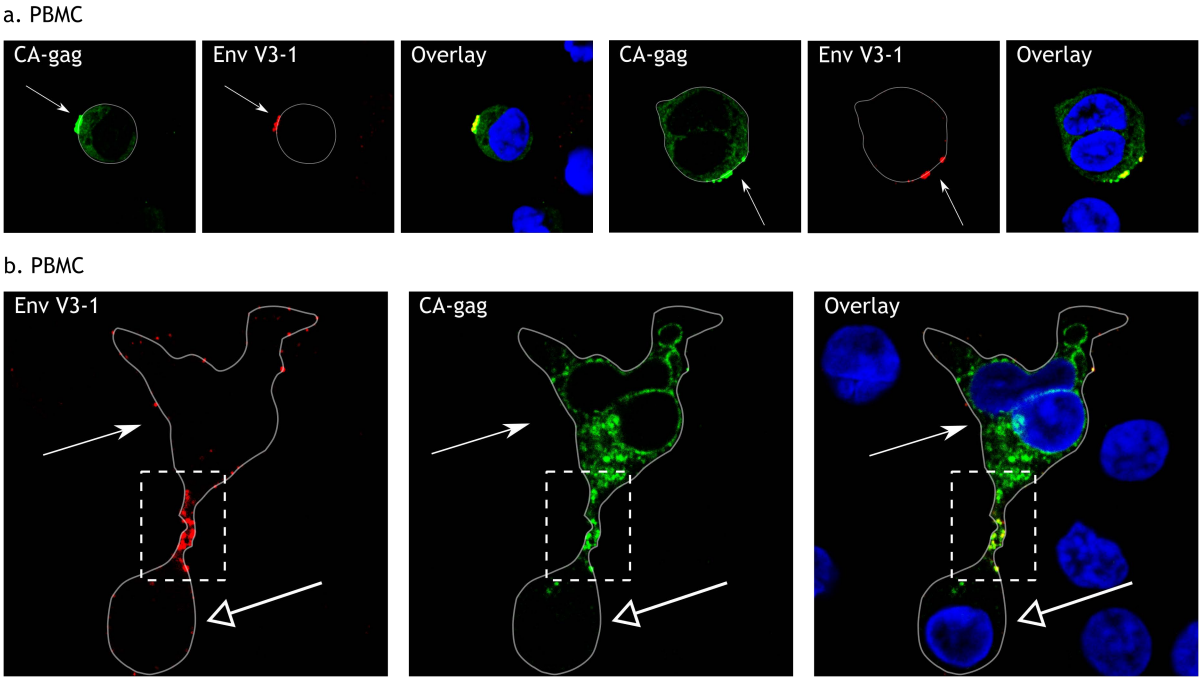

Figure 4: Co-localization of cell surface expressed FIV Env and accumulations of the FIV Gag polyprotein in infected PBMC. (a) Co-localization between FIV Gag polyprotein accumulations (stained with αCA-gag in green) and cell surface expressed Env protein (stained with αV3-1 in red), 48 h p.i.. (b) FIV infected syncytia (full arrow) interacting with non-infected cell (hollow arrow). Concentration of Env and Gag proteins can be seen at the contact site (box).

In CrFK transfected with the FIV infectious clone, cytoplasmic expression of Env and Gag was noticeably faster, starting at 6 h post transfection. Three hours later (9 h post transfection), Env was also detected on the cell surface of CrFK. Figure 3c shows that

similar to the infected GFox cells, Env expression was uniformly scattered across the plasma membrane. Also like the infected GFox cells, there was no accumulation of the Gag polyprotein at the plasma membrane, while mature capsid protein was detected in the cytoplasm of FIV protein expressing CrFK cells (Fig. 2f-2g).

Table 1: Summary of the kinetics of FIV Env and Gag expression in FIV infected PBMC, infected GFox and transfected CrFK.

Time	Infected PBMC			Infected GFOx			Transfected CrFK		
	Gag	Env in*	Env out**	Gag	Env in*	Env out**	Gag	Env in*	Env out**
3h	-	-	-	-	-	-	-	-	-
6 h	-	-	-	-	-	-	+	+	-
9 h	-	-	-	-	-	-	+	+	+
12 h	+	+	-	-	-	-	+	+	+
18 h	+	+	-	-	-	-	+	+	+
24 h	+(1)	+	-	+	+	-(4)	+	+	+
36 h	+(2)	+	+(3)	+	+	+	+	+	+
48 h	+	+	+(3)	+	+	+	+	+	+

*Env in: in the cytoplasm, **Env out: on the plasma membrane, 1 Gag accumulation, 2 mature capsid, 3 localized, 4 syncytia present

The expression and processing of the Gag polyprotein and Env protein in the different cell types was also analyzed by western blot. In all cell types, the mature capsid protein (a cleavage product of Gag) with a molecular weight of 24 kDa can be clearly seen (Fig. 5a). The band at 51 kDa represents the uncleaved Gag polyprotein. The larger band at approximately 150 kDa, lane 1 (CrFK cells), represents the Gag-Pol chimera protein. Also in lane 1, the cellular lysate of transfected CrFK cells shows more cleavage forms of the Gag protein (Lin et al., 2006) compared to infected GFox and PBMC in lanes 2 and 3 respectively. Cellular lysate of transfected CrFK cells (Fig. 5b, lane 1) showed two prominent bands for FIV Env protein at 130 kDa and 100 kDa. The upper band reflects the Env precursor without the leader sequence of approximately 20 kDa (Verschoor et al., 1993). The lower band is the SU part (gp95) of the cleaved FIV Env protein. Cell lysates from infected GFox and PBMC initially showed only one band at 130 kDa, in lanes 2 and 3 respectively. Longer exposure times (Fig. 5b, lanes 4-6) revealed a very faint band at around 100 kDa in cellular lysate of PBMC. The Env staining results already indicated a much higher FIV protein translation in transfected CrFK compared to infected GFox and PBMC. The lower percentage of infected cells in PBMC compared to GFox cells is reflected in a lower staining intensity on the blot, which was confirmed by calculation after correction based on the tubulin staining intensity on the blot.

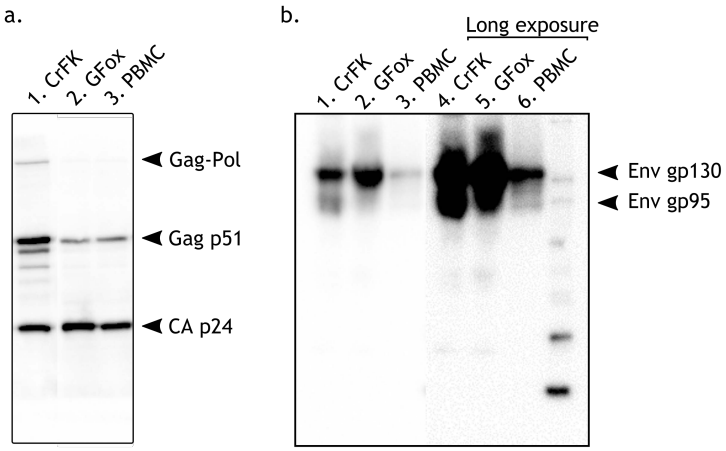

Figure 5: Western blot for FIV Gag and cleavage products, and FIV Env SU on cellular lysates of FIV infected PBMC, infected GFox and transfected CrFK. (a) Western blot for FIV Gag protein on cellular lysates from transfected CrFK (lane 1), infected GFox (lane 2), and infected PBMC (lane 3). (b) Western blot for FIV Env protein on cellular lysates from transfected CrFK (lane 1), infected GFox (lane 2), and infected PBMC (lane 3). Lanes 4-6 are long exposure pictures of lanes 1-3 respectively.

4.3.2. FIV envelope protein expression in CrFK, GFox and feline PBMC

Expression of FIV envelope protein was assessed in more detail at the moment cell surface expression of Env was detectable in all cells used, 48 h p.i. or post transfection. By using antibodies that recognize epitopes on different variable loops of SU, trafficking and concomitant processing of Env was followed. Epitopes recognized by the anti-SU antibodies have previously been mapped (de Parseval et al., 2006; Elder et al., 2010; Hu et al., 2014; Sundstrom et al., 2008), and a diagram of the FIV SU protein with indication of SU MAb epitopes is pictured in Figure 1. Staining for FIV SU protein was performed both for intracellular expression on permeabilized cells, and for cell surface expression on live cells at 4°C and on fixed cells.

4.3.2.1. Epitope availability on cytoplasmically expressed FIV Env

Clear differences were seen in epitope availability of intracellular FIV Env expressed in infected PBMC or GFOx compared to transfected CrFK cells (Table 2). The FIV Env V2-loop epitopes (Fig. 6a) behaved similarly and were detected only in close proximity but not co-localizing with the Golgi apparatus. This may possibly represent transport vesicles that are leaving the Golgi complex. The single exception was the behaviour of V2-1. In infected PBMC this epitope was clearly better detected by staining compared to the other V2 epitopes, and in transfected CrFK αV2-1 (antibody SU2-6) which targets the amino-terminal linear epitope gave a very intense staining, making it difficult to distinguish cytoplasmic compartments. Cellular localization of the Env staining was confirmed by double staining with calnexin and 58K Golgi protein; representative pictures are given in Figure 7.

The V3 region contains three linear epitopes; V3-1, V3-2 and V3-3, of which the latter is exposed only after interaction between SU and CXCR4 (Grant CK, unpublished results). We were not able to map the αV3-4 (antibody SU1-7) binding peptide, because it is most likely a conformational epitope. Visualization of the linear epitopes V3-1 and V3-2 was similar in infected PBMC and GFOx, and transfected CrFK (Fig.6b). These V3 epitopes induced a strong Env staining, and clearly marked Env expression in the ER. The epitopes V3-3 and V3-4 delivered a distinct staining pattern compared to V3-1 and V3-2 in FIV infected PBMC and GFox, but not in transfected CrFK. In GFox, the V3-3 and V3-4 epitope were mainly detected in the Golgi apparatus but not in the ER. In PBMC, V3-3 and V3-4 were only seen at sites of cell contact as a discrete line. The V4 epitope (Fig. 6c) on Env was detected in transfected CrFK, at a lower level in infected PBMC, but never in GFox cells. Extracellular particles were found in infected GFox cell cultures stained against V4-1 .

4.3.2.2. Cell surface accessibility of specific epitopes on FIV Env

Cell surface expression of mature trimeric Env protein reveals large differences in availability of individual SU epitopes with all three cell types examined (Table 2). Expression of FIV SU was detected on living CrFK and GFox at 4°C with αV2-1, αV3-1, αV3-2, αV3-3, αV3-4, but not with αV2-2, αV2-3 and αV2-4. On CrFK, fixation of the cells led to detection of Env with αV2-4 as well, suggesting that fixation induced a change in the Env protein within the V2, thereby allowing the V2-4 epitope to be recognized. Detection of Env with the V4 epitope (V4-1) was only possible on CrFK cells. In sharp contrast with CrFK cells or GFox cells, all the FIV SU specific MAbs were negative against Env on live PBMC at 4°C. If PBMC were gently fixed (0.4 % paraformaldehyde), then the V3 epitopes V3-1 and V3-2 became available and were recognized by MAbs αV3-1, αV3-2.

Table 2: FIV Env SU epitope recognition by anti-SU MAbs in FIV infected PBMC, infected GFox and transfected CRFK. Plasma membrane and cytoplasmic staining was performed 48 h after transfection or infection. Monoclonal antibodies against different epitopes in the variable loops on the FIV SU protein are ranked from the N- to the C-terminal end.

MAb	Epitope	Amino-acid region of epitope	Recognition of FIV-PPR SU											
			Infected PBMC				Infected GFox				Transfected CrFK			
			ER	Golgi	Vesicles	Cell surface	ER	Golgi	Vesicles	Cell surface	ER	Golgi	Vesicles	Cell surface
SU2-6	V2-1	251 – 268	-	-	++	-	-	-	+	++*	+++	++	++	+++*
SU2-8	V2-2	*conformational epitope*	-	-	+	+ *(extracellular)*	-	-	+	-	+	+	+	-
SU2-11	V2-3	*conformational epitope*	-	-	+	-	-	-	+	-	+	+	+	-
SU1-12	V2-4	303 – 320	-	-	+	-	-	-	+	-	+	+	+	+
SU1-30	V3-1	392 – 402	+	+	+	+	++	+	+	++*	+++	++	++	+++*
SU2-5	V3-2	399 – 408	+	+	+	+	++	+	+	++*	+++	++	++	+++*
SU2-10	V3-3	403 – 410	-	-	-	+ *(cell contacts)*	-	+	+	++*	+++	++	++	+++*
SU1-7	V3-4	*conformational epitope*	-	-	-	+ *(cell contacts)*	-	+	+	++*	+++	++	++	+++*
SU2-3	V4-1	451 – 483	-	-	+	-	-	-	-	-	+	++	+++	+++*

* staining also possible on live cells at 4°C

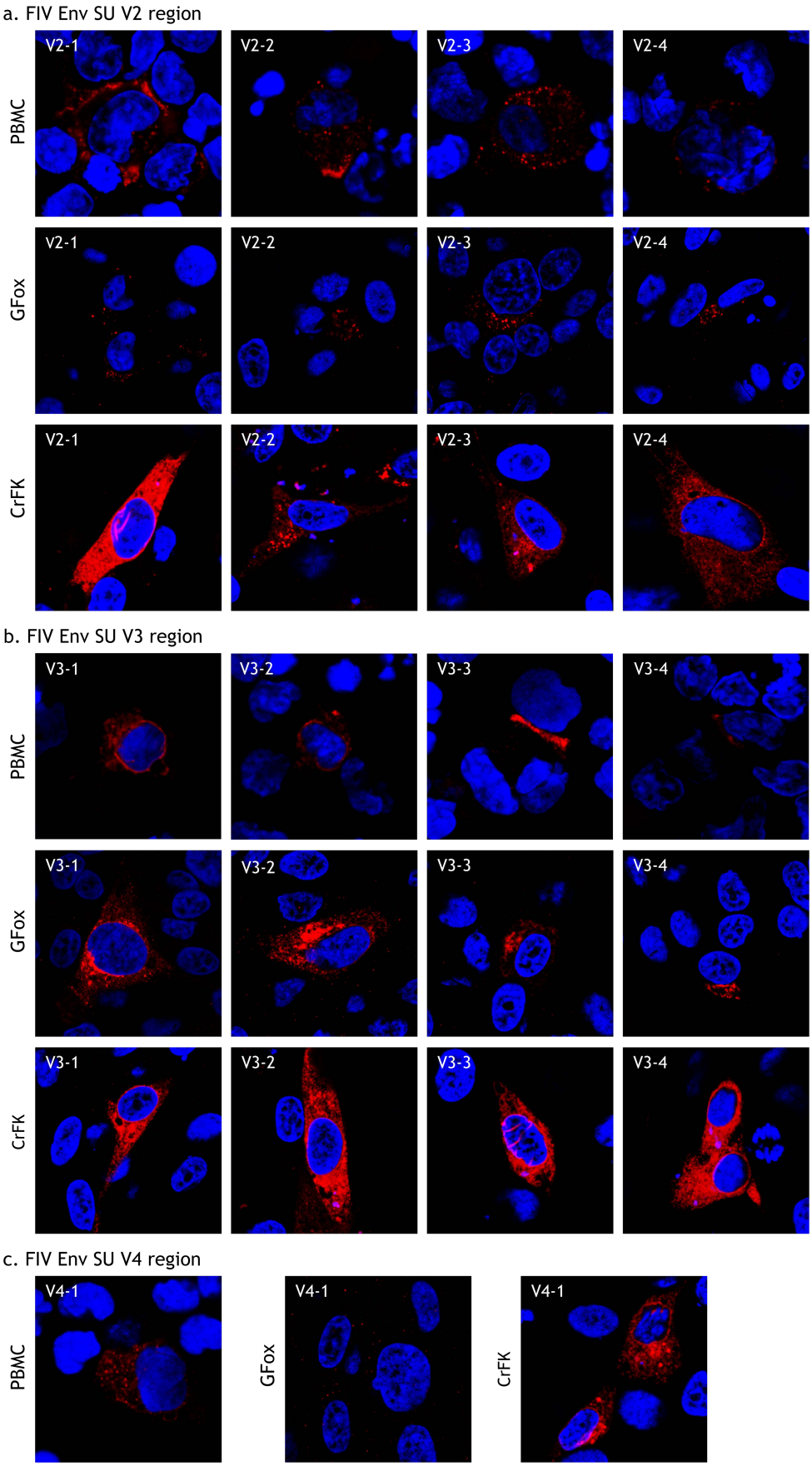

Figure 6: Cytoplasmic FIV Env SU epitope availability in infected PBMC, infected GFox and transfected CrFK. (a) Epitopes V2-1 to V2-4 on the FIV Env SU V2 region. (b) Epitopes V3-1 to V3-4 on the FIV Env SU V3 region. (c) Epitope V4-1 on the FIV Env SU V4 region.

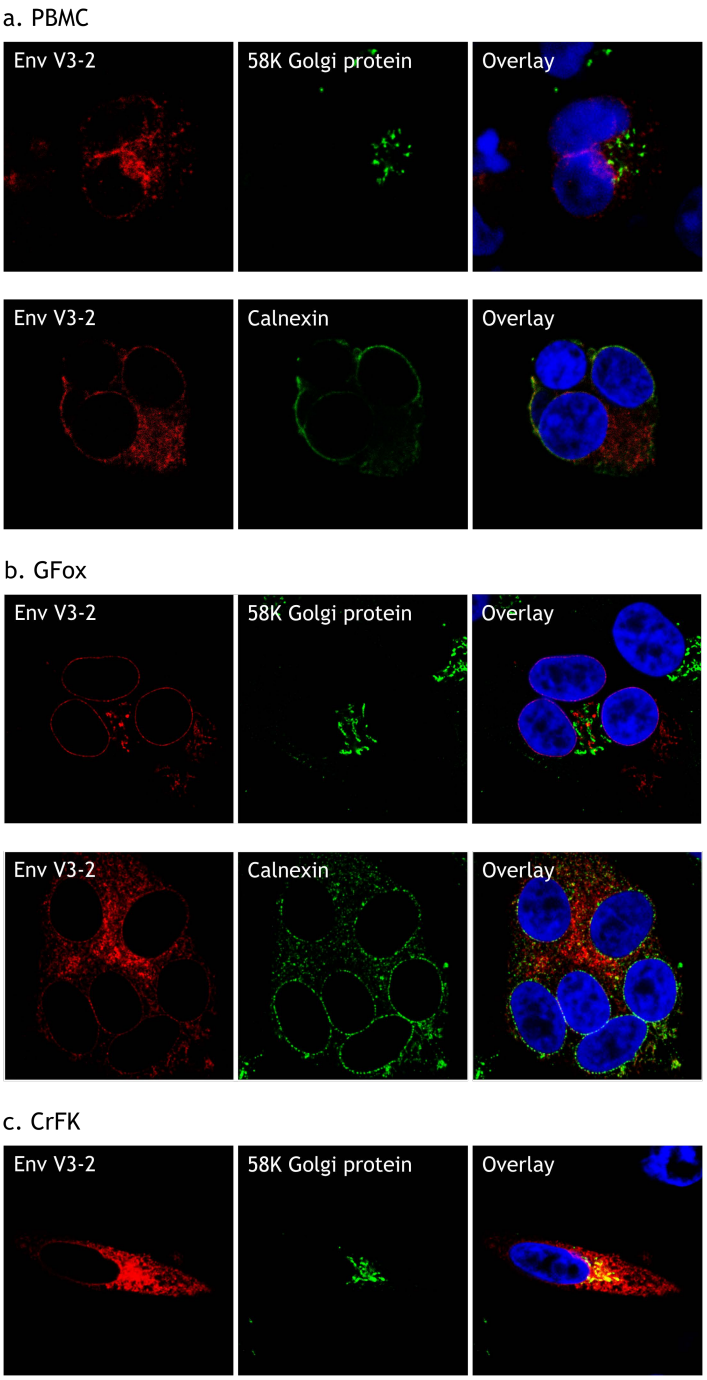

Figure 7: Double staining of FIV Env and markers for the Golgi apparatus and the ER. FIV Env is stained with αV3-2, and the ER and Golgi are marked by antibodies against calnexin and 58K Golgi protein, respectively. (a) infected PBMC, (b) infected GFox, and (c) transfected CrFK

4.4. Discussion

Kinetic follow-up of FIV Gag and Env expression during the FIV life cycle allowed us to study the "when and where" of FIV protein expression in different cell types. The early onset of viral protein translation in transfected CrFK is no surprise, since the transfected proviral DNA does not need to be transcribed and integrated into the host chromatin before transcription and translation can occur, as is the case for the viral mRNA genome in the infection environment.

During the FIV expression kinetics experiments we noted a high concentration of both Gag and Env proteins at focal points in the plasma membrane of infected PBMC. After translation, Gag protein is targeted towards the plasma membrane by myristoylation involving a patch of basic residues (Manrique et al., 2001; Manrique et al., 2004). Recently, Brown and colleagues showed that depletion of PI(4,5)P2, a lipid that serves as a docking site for proteins, from the plasma membrane of FIV-infected CRFK cells inhibited production of FIV particles (Brown et al., 2015). Furthermore, the FIV Env protein has been shown to be palmitoylated, a protein modification that can target proteins to lipid rafts. Our results indicate that on PBMC FIV Env expression is targeted to specific sites at the plasma membrane. Taken together, these results are indicative that FIV proteins are targeted to specific microdomains in the plasma membrane of infected PBMC. We hypothesize that this polarization may indicate active cell sites preferred for virus budding, and/or be the prerequisite for the formation of virological synapses, similar to viral egress of HIV and murine leukemia virus (Fais et al., 1995; Jolly et al., 2004; Jolly et al., 2011; Owens et al., 1991). Unlike murine leukemia virus, FIV was not able to induce polarized expression of its viral proteins at cell contacts in CrFK or GFox, which are unpolarized cells. It is therefore reasonable that FIV, similar to HIV, can hijack the natural polarization of activated PBMC for its egress (Jolly et al., 2011; Miranda et al., 2002). Further research is needed to further elucidate these processes associated with FIV spread between PBMC.

Processed Gag protein (mature capsid protein) was detected inside the cytoplasm of transfected CrFK and infected GFox, while only the Gag polyprotein could be detected in the cytoplasm of feline PBMC. Western blot also showed more cleavage variants of Gag in the CrFK cellular lysate compared to GFox and PBMC. Cleavage of the Gag polyprotein is believed to occur upon virion budding, and correct timing is essential to the production of infectious virus particles. Manrique and co-workers (2001) also showed that the Gag polyprotein is sensitive to cleavage by cellular proteases, which might also be the case in CrFK and GFox (Manrique et al., 2001). Possibly, a premature cleavage of the Gag polyprotein occurs in CrFK and GFox due to premature dimerization of the viral protease as a result of a higher viral protein production.

Clear differences were seen in epitope availability of intracellular FIV Env expressed in transfected CrFK cells compared to infected GFOx or PBMC. Except for V2-4, antibody targeting of the V2 epitopes is highly dependent on correct N-linked glycosylation

(data not shown). In the Golgi complex the N-linked sugars on Env are further processed and the Env precursor is cleaved into the SU and TM part. These processing events may possibly induce important changes in the SU molecule, with increased accessibility of the V2 epitopes as a consequence. Aberrant Env folding may explain the availability of V2 epitopes in the ER under transfection conditions, and why brefeldin A treatment was able to induce V2 epitope availability in the ER of FIV infected cells (data not shown). The epitopes V3-3 and V3-4 delivered a distinct staining pattern compared to V3-1 and V3-2 in infected GFox and PBMC, but not in CrFK. All the V3 epitopes studied span the CXCR4 binding site that is located in a cryptic loop which is opened after interaction with the primary receptor CD134 (de Parseval et al., 2006). SU binding to the FIV receptors induces a series of conformational changes, which eventual lead to dissociation between SU and TM (Garg et al., 2004). Since the V3-3 epitope is exposed only after FIV receptor binding (Grant CK, unpublished results), it is possible that enough SU molecules in a post-receptor interaction conformation are trapped in between cells to result in detection, as they would otherwise be discarded in the extracellular milieu. The same might be true for V3-4, which is most likely also a conformational epitope. Premature interaction between the SU molecule and FIV receptors in the Golgi complex may explain the accessibility of these epitopes in the Golgi complex of infected GFox. In PBMC, Env protein expression might be too low to detect the V3-3 and V3-4 epitopes in the Golgi apparatus. While the CD134 side of the FIV Env-CD134 binding is elucidated (de Parseval et al., 2005; Willett et al., 2006), the sites on FIV SU responsible for CD134 binding are not. Failure to detected the V4-1 epitope in $CD134^{high}$ GFox cells, and to a lower degree in $CD134^{low}$ PBMC, might be caused by interaction between V4-1 and CD134, blocking MAb binding. The V4 epitope was detected after processing in infected PBMC, but never in GFox cells. Detection of the V4 loop was not hampered by glycosylations, and is also not sensitive to ER stress induced (mis)folding like the V2 loop (data not shown).

Env proteins on the cell surface of infected cells and on the virion are important targets for anti-viral immunity. Epitope availability and distribution of cell surface expressed Env trimers was similar between CrFK and GFox, with exception of the V2-1 and V4-1 epitope. In contrast, the Env protein expressed on the cell surface of live PBMC could not be detected at all. Our results might indicate that the FIV Env trimers expressed on the plasma membrane of PBMC, like mature HIV Env, adopts a “closed” conformation, hiding the receptor binding site on V3 (Wyatt et al., 1998). The epitopes

on V2 may be protected V4 epitopes conformation occlusion and/or by glycosylation. It has been demonstrated that uncleaved Env precursor and monomeric Env proteins are present on the plasma membrane of infected cells (Celma et al., 2007; Dey et al., 2008). Compared to normal trimeric Env, these aberrant proteins might not be able to conceal certain epitopes from antibody binding. Since Env production and expression seems more controlled in PBMC, the low amount of unprocessed gp130 and/or monomeric Env on the plasma membrane cells might not be detectable by staining.

Our staining results of FIV Env on the plasma membrane of PBMC show that the epitopes that are preferentially targeted by sera of naturally FIV infected cats are not accessible for antibody binding on the cell surface expressed mature trimeric Env complexes (CK Grant,unpublished results; Bendinelli et al., 1995). This is in line with work by Richardson and coworkers who suggested that most linear B-cell epitopes are poorly exposed on functional trimeric FIV Env, and therefore do not contribute to virus neutralization (Richardson et al., 1996). Work on HIV proposed that most of the anti-Env response is directed against the unprocessed Env protein and/or against disassembled Env, that is released as cellular or viral debris (Parren et al., 1997). In light of these results it is probable that FIV Env expressed on infected cells or present on newly formed viral particles will not be recognized by the immune system, allowing them to escape from the humoral response so effectively mounted against them.

In summary, our results show important differences between Env and Gag expression, processing and targeting between the natural host cells of FIV, the feline PBMC, and feline adherent cell lines infected or transfected with FIV that are often used. Env and Gag proteins seem to be transported towards specific sites at the plasma membrane of infected PBMC only, but further research is needed to establish if these events lead to synapses between cells and subsequently direct virus transmission from one cell to another. Epitopes on Env crucial for virus infectivity were carefully shielded from antibody recognition on PBMC, although these regions are immunodominant in sera from FIV infected cats.

Acknowledgements

We thank Dr. J.H. Elder (The Scripps Research Institute) for providing the GFox cells, FIV SU preparations and for allowing the usage of the FIV-PPR SU diagram. We thank Ytse Noppe for her outstanding technical support. IDMR was supported by the Agency for the Promotion of Innovation through Science and Technology in Flanders (IWT-

Vlaanderen). ST was supported by a post-doctoral fellowship from IWT-Vlaanderen. SVB was supported by the Special Research Fund of Ghent University.

References

Baldinotti, F., Matteucci, D., Mazzetti, P., Giannelli, C., Bandecchi, P., Tozzini, F. & Bendinelli, M. (1994). Serum neutralization of feline immunodeficiency virus is markedly dependent on passage history of the virus and host system. *J Virol* **68**, 4572-4579.

Beczkowski, P. M., Techakriengkrai, N., Logan, N., McMonagle, E., Litster, A., Willett, B. J. & Hosie, M. J. (2014). Emergence of CD134 cysteine-rich domain 2 (CRD2)-independent strains of feline immunodeficiency virus (FIV) is associated with disease progression in naturally infected cats. *Retrovirology* **11**, 95.

Beebe, A. M., Dua, N., Faith, T. G., Moore, P. F., Pedersen, N. C. & Dandekar, S. (1994). Primary stage of feline immunodeficiency virus infection: viral dissemination and cellular targets. *J Virol* **68**, 3080-3091.

Bendinelli, M., Pistello, M., Lombardi, S., Poli, A., Garzelli, C., Matteucci, D., Ceccherini-Nelli, L., Malvaldi, G. & Tozzini, F. (1995). Feline immunodeficiency virus: an interesting model for AIDS studies and an important cat pathogen. *Clin Microbiol Rev* **8**, 87-112.

Brown, L. A., Cox, C., Baptiste, J., Summers, H., Button, R., Bahlow, K., Spurrier, V., Kyser, J., Luttge, B. G., Kuo, L., Freed, E. O. & Summers, M. F. (2015). NMR structure of the myristylated feline immunodeficiency virus matrix protein. *Viruses* **7**, 2210-2229.

Brown, W. C., Bissey, L., Logan, K. S., Pedersen, N. C., Elder, J. H. & Collisson, E. W. (1991). Feline immunodeficiency virus infects both CD4+ and CD8+ T lymphocytes. *J Virol* **65**, 3359-3364.

Brunner, D. & Pedersen, N. C. (1989). Infection of peritoneal macrophages in vitro and in vivo with feline immunodeficiency virus. *J Virol* **63**, 5483-5488.

Burkhard, M. J., Mathiason, C. K., Bowdre, T. & Hoover, E. A. (2001). Feline immunodeficiency virus Gag- and Env-specific immune responses after vaginal versus intravenous infection. *AIDS Res Hum Retroviruses* **17**, 1767-1778.

Calzolari, M., Young, E., Cox, D., Davis, D. & Lutz, H. (1995). Serological diagnosis of feline immunodeficiency virus infection using recombinant transmembrane glycoprotein. *Vet Immunol Immunopathol* **46**, 83-92.

Celma, C. C., Paladino, M. G., González, S. A. & Affranchino, J. L. (2007). Importance of the short cytoplasmic domain of the feline immunodeficiency virus transmembrane glycoprotein for fusion activity and envelope glycoprotein incorporation into virions. *Virology* **366**, 405-414.

de Parseval, A., Chatterji, U., Morris, G., Sun, P., Olson, A. J. & Elder, J. H. (2005). Structural mapping of CD134 residues critical for interaction with feline immunodeficiency virus. *Nat Struct Mol Biol* **12**, 60-66.

de Parseval, A., Chatterji, U., Sun, P. & Elder, J. H. (2004). Feline immunodeficiency virus targets activated CD4+ T cells by using CD134 as a binding receptor. *Proc Natl Acad Sci U S A* **101**, 13044-13049.

de Parseval, A., Grant, C. K., Sastry, K. J. & Elder, J. H. (2006). Sequential CD134-CXCR4 interactions in feline immunodeficiency virus (FIV): soluble CD134 activates FIV Env for CXCR4-dependent entry and reveals a cryptic neutralization epitope. *J Virol* **80**, 3088-3091.

Dey, A. K., David, K. B., Ray, N., Ketas, T. J., Klasse, P. J., Doms, R. W. & Moore, J. P. (2008). N-terminal substitutions in HIV-1 gp41 reduce the expression of non-trimeric envelope glycoproteins on the virus. *Virology* **372**, 187-200.

Dow, S. W., Mathiason, C. K. & Hoover, E. A. (1999). In vivo monocyte tropism of pathogenic feline immunodeficiency viruses. *J Virol* **73**, 6852-6861.

Egberink, H. F., Keldermans, C. E., Koolen, M. J. & Horzinek, M. C. (1992). Humoral immune response to feline immunodeficiency virus in cats with experimentally induced and naturally acquired infections. *Am J Vet Res* **53**, 1133-1138.

Elder, J. H., Lin, Y. C., Fink, E. & Grant, C. K. (2010). Feline immunodeficiency virus (FIV) as a model for study of lentivirus infections: parallels with HIV. *Curr HIV Res* **8**, 73-80.

Elder, J. H., Schnolzer, M., Hasselkus-Light, C. S., Henson, M., Lerner, D. A., Phillips, T. R., Wagaman, P. C. & Kent, S. B. (1993). Identification of proteolytic processing sites within the Gag and Pol polyproteins of feline immunodeficiency virus. *J Virol* **67**, 1869-1876.

English, R. V., Johnson, C. M., Gebhard, D. H. & Tompkins, M. B. (1993). In vivo lymphocyte tropism of feline immunodeficiency virus. *J Virol* **67**, 5175-5186.

Fais, S., Capobianchi, M. R., Abbate, I., Castilletti, C., Gentile, M., Cordiali Fei, P., Ameglio, F. & Dianzani, F. (1995). Unidirectional budding of HIV-1 at the site of cell-to-cell contact is associated with co-polarization of intercellular adhesion molecules and HIV-1 viral matrix protein. *AIDS* **9**, 329-335.

Garg, H., Fuller, F. J. & Tompkins, W. A. (2004). Mechanism of feline immunodeficiency virus envelope glycoprotein-mediated fusion. *Virology* **321**, 274-286.

Grant, C. K., Fink, E. A., Sundstrom, M., Torbett, B. E. & Elder, J. H. (2009). Improved health and survival of FIV-infected cats is associated with the presence of autoantibodies to the primary receptor, CD134. *Proc Natl Acad Sci U S A* **106**, 19980-19985.

Hartmann, K. (2012). Clinical aspects of feline retroviruses: a review. *Viruses* **4**, 2684-2710.

Hosie, M. J. & Jarrett, O. (1990). Serological responses of cats to feline immunodeficiency virus. *AIDS* **4**, 215-220.

Hu, Q. Y., Fink, E., Grant, C. K. & Elder, J. H. (2014). Selective interaction of heparin with the variable region 3 within surface glycoprotein of laboratory-adapted feline immunodeficiency virus. *PLoS One* **9**, e115252.

Hu, Q. Y., Fink, E., Hong, Y., Wang, C., Grant, C. K. & Elder, J. H. (2010). Fine definition of the CXCR4-binding region on the V3 loop of feline immunodeficiency virus surface glycoprotein. *PLoS One* **5**, e10689.

Jolly, C., Kashefi, K., Hollinshead, M. & Sattentau, Q. J. (2004). HIV-1 cell to cell transfer across an Env-induced, actin-dependent synapse. *J Exp Med* **199**, 283-293.

Jolly, C., Welsch, S., Michor, S. & Sattentau, Q. J. (2011). The regulated secretory pathway in CD4(+) T cells contributes to human immunodeficiency virus type-1 cell-to-cell spread at the virological synapse. *PLoS Pathog* **7**, e1002226.

Kemler, I., Barraza, R. & Poeschla, E. M. (2002). Mapping the encapsidation determinants of feline immunodeficiency virus. *J Virol* **76**, 11889-11903.

Lin, Y. C., Brik, A., de Parseval, A., Tam, K., Torbett, B. E., Wong, C. H. & Elder, J. H. (2006). Altered gag polyprotein cleavage specificity of feline immunodeficiency virus/human immunodeficiency virus mutant proteases as demonstrated in a cell-based expression system. *J Virol* **80**, 7832-7843.

Manrique, M. L., Celma, C. C., González, S. A. & Affranchino, J. L. (2001). Mutational analysis of the feline immunodeficiency virus matrix protein. *Virus Res* **76**, 103-113.

Manrique, M. L., González, S. A. & Affranchino, J. L. (2004). Functional relationship between the matrix proteins of feline and simian immunodeficiency viruses. *Virology* **329**, 157-167.

Moscardini, M., Pistello, M., Bendinelli, M., Ficheux, D., Miller, J. T., Gabus, C., Le Grice, S. F., Surewicz, W. K. & Darlix, J. L. (2002). Functional interactions of nucleocapsid protein of feline immunodeficiency virus and cellular prion protein with the viral RNA. *J Mol Biol* **318**, 149-159.

Natoli, E., Say, L., Cafazzo, S., Bonanni, R., Schmid, M. & Pontier, D. (2005). Bold attitude makes male urban feral domestic cats more vulnerable to Feline Immunodeficiency Virus. *Neurosci Biobehav Rev* **29**, 151-157.

O'Connor, T. P., Tanguay, S., Steinman, R., Smith, R., Barr, M. C., Yamamoto, J. K., Pedersen, N. C., Andersen, P. R. & Tonelli, Q. J. (1989). Development and evaluation of immunoassay for detection of antibodies to the feline T-lymphotropic lentivirus (feline immunodeficiency virus). *J Clin Microbiol* **27**, 474-479.

Owens, R. J., Dubay, J. W., Hunter, E. & Compans, R. W. (1991). Human immunodeficiency virus envelope protein determines the site of virus release in polarized epithelial cells. *Proc Natl Acad Sci U S A* **88**, 3987-3991.

Pancino, G., Chappey, C., Saurin, W. & Sonigo, P. (1993a). B epitopes and selection pressures in feline immunodeficiency virus envelope glycoproteins. *J Virol* **67**, 664-672.

Pancino, G., Fossati, I., Chappey, C., Castelot, S., Hurtrel, B., Moraillon, A., Klatzmann, D. & Sonigo, P. (1993b). Structure and variations of feline immunodeficiency virus envelope glycoproteins. *Virology* **192**, 659-662.

Parren, P. W., Burton, D. R. & Sattentau, Q. J. (1997). HIV-1 antibody--debris or virion? *Nat Med* **3**, 366-367.

Pedersen, N. C., Yamamoto, J. K., Ishida, T. & Hansen, H. (1989). Feline immunodeficiency virus infection. *Vet Immunol Immunopathol* **21**, 111-129.

Phillips, T. R., Talbott, R. L., Lamont, C., Muir, S., Lovelace, K. & Elder, J. H. (1990). Comparison of two host cell range variants of feline immunodeficiency virus. *J Virol* **64**, 4605-4613.

Richardson, J., Fossati, I., Moraillon, A., Castelot, S., Sonigo, P. & Pancino, G. (1996). Neutralization sensitivity and accessibility of continuous B cell epitopes of the feline immunodeficiency virus envelope. *J Gen Virol* **77 (Pt 4)**, 759-771.

Richardson, J., Pancino, G., Merat, R., Leste-Lasserre, T., Moraillon, A., Schneider-Mergener, J., Alizon, M., Sonigo, P. & Heveker, N. (1999). Shared usage of the chemokine receptor CXCR4 by primary and laboratory-adapted strains of feline immunodeficiency virus. *J Virol* **73**, 3661-3671.

Rimmelzwaan, G. F., Siebelink, K. H., Broos, H., Drost, G. A., Weijer, K., van Herwijnen, R. & Osterhaus, A. D. (1994). gag- and env-specific serum antibodies in cats after natural and experimental infection with feline immunodeficiency virus. *Vet Microbiol* **39**, 153-165.

Serrière, J., Fenel, D., Schoehn, G., Gouet, P. & Guillon, C. (2013). Biophysical characterization of the feline immunodeficiency virus p24 capsid protein conformation and in vitro capsid assembly. *PLoS One* **8**, e56424.

Shimojima, M., Miyazawa, T., Ikeda, Y., McMonagle, E. L., Haining, H., Akashi, H., Takeuchi, Y., Hosie, M. J. & Willett, B. J. (2004). Use of CD134 as a primary receptor by the feline immunodeficiency virus. *Science* **303**, 1192-1195.

Sparger, E. E., Shacklett, B. L., Renshaw-Gegg, L., Barry, P. A., Pedersen, N. C., Elder, J. H. & Luciw, P. A. (1992). Regulation of gene expression directed by the long terminal repeat of the feline immunodeficiency virus. *Virology* **187**, 165-177.

Stephens, E. B., Monck, E., Reppas, K. & Butfiloski, E. J. (1991). Processing of the glycoprotein of feline immunodeficiency virus: effect of inhibitors of glycosylation. *J Virol* **65**, 1114-1123.

Sundstrom, M., White, R. L., de Parseval, A., Sastry, K. J., Morris, G., Grant, C. K. & Elder, J. H. (2008). Mapping of the CXCR4 binding site within variable region 3 of the feline immunodeficiency virus surface glycoprotein. *J Virol* **82**, 9134-9142.

Thompson, F. J., Elder, J. & Neil, J. C. (1994). Cis- and trans-regulation of feline immunodeficiency virus: identification of functional binding sites in the long terminal repeat. *J Gen Virol* **75 (Pt 3)**, 545-554.

Tompkins, M. B. & Tompkins, W. A. (2008). Lentivirus-induced immune dysregulation. *Vet Immunol Immunopathol* **123**, 45-55.

Verschoor, E. J., Hulskotte, E. G., Ederveen, J., Koolen, M. J., Horzinek, M. C. & Rottier, P. J. (1993). Post-translational processing of the feline immunodeficiency virus envelope precursor protein. *Virology* **193**, 433-438.

Willett, B. J., Kraase, M., Logan, N., McMonagle, E. L., Samman, A. & Hosie, M. J. (2010). Modulation of the virus-receptor interaction by mutations in the V5 loop of feline immunodeficiency virus (FIV) following in vivo escape from neutralising antibody. *Retrovirology* **7**, 38.

Willett, B. J., McMonagle, E. L., Bonci, F., Pistello, M. & Hosie, M. J. (2006). Mapping the domains of CD134 as a functional receptor for feline immunodeficiency virus. *J Virol* **80**, 7744-7747.

Willett, B. J., Picard, L., Hosie, M. J., Turner, J. D., Adema, K. & Clapham, P. R. (1997). Shared usage of the chemokine receptor CXCR4 by the feline and human immunodeficiency viruses. *J Virol* **71**, 6407-6415.

Chapter 5

Influence of feline lymphoid tissue stromal cells on FIV infection and replication in PBMC

Chapter 5a

Feline lymphoid tissue reticular cell isolation and culture

Adapted from:

Roukaerts ID, Acar DD, Van Bockstael S, Desmarets LM and Nauwynck HJ, 2016. Manuscript in preparation.

Abstract

Feline mesenchymal stromal cells were successfully isolated from red bone marrow, thymus, lymph nodes and spleen, and immortalized with SV40 large T-Ag. Characterization showed that these cells express typical mesenchymal markers, vimentin and smooth muscle actin, and produce the extracellular matrix protein fibronectin. The production of CCL19, CCL21, CXCL12 and IL7, important for lymphoid organ function, was demonstrated at the mRNA level. These cells may be useful for *in vitro* proliferation of hematopoietic stem cells (HSC) and differentiation into functional immune cells for research or therapy and for *in vitro* modeling of immune responses against feline pathogens.

5.1. Introduction

Feline immunodeficiency virus (FIV) targets multiple cell types of the immune system, including monocyte/macrophages, and T- and B-lymphocytes (Brown *et al.*, 1991; Pedersen *et al.*, 1987). Infection and death of these cells, especially $CD4^+$ T-cells, ultimately lead to a profound dysregulation of the immune system. Furthermore, FIV can infect hematopoietic progenitor cells in the bone marrow, and cause involution and destruction of the thymus and lymph nodes (Beebe *et al.*, 1992; Huisman *et al.*, 2004). Together, these phenomena lead to the inability of the cat's immune system to respond to the invasion of pathogens, causing an acquired immunodeficiency syndrome (feline AIDS) (Callanan *et al.*, 1992; O'Neil *et al.*, 1996).

To study the effects of FIV infection in the lymphoid organs, stromal cells that are responsible for the structure and function of these organs should get full attention. The lymphoid organs can be divided into primary and secondary lymphoid organs. The bone marrow and thymus are the primary organs, they are responsible for the production and maturation of functional immune cells that are able to respond to foreign organism and substances to protect the body from harmful effects. In the secondary lymphoid organs, like the lymph nodes, spleen and mucosa associated lymphoid tissues (MALT); the adaptive immune response is orchestrated. Professional antigen presenting cells encounter T- and B-cells in a controlled environment, allowing the generation and stimulation of an effective adapted immune response against pathogens detected in the body.

Stromal cells shape the framework of tissues and produce extracellular matrix proteins in which the cells responsible for the function of the organ reside. In case of the lymphoid tissues these functional cells are the hematopoietic cells. The capillary network in the bone marrow ends in single walled sinuses with a discontinuous basement membrane. Reticular cells surround these sinuses and create a niche for hematopoiesis by producing reticular fibers, extracellular matrix, and growth factors (Nagasawa *et al.*, 2011). Mesenchymal stem cells (MSC) that reside in the bone marrow are believed to be the precursor of these reticular cells. In adults, hematopoietic activity is reduced, and the red bone marrow transforms into yellow bone marrow as the reticular cells differentiate into adipocytes (Nombela-Arrieta *et al.*, 2011). The thymus develops from an outgrowth of the endoderm originating from the third pharyngeal pouch of the embryo. The structural network of the thymus is composed of epithelial cells, divided into cortical and medullar thymic epithelial cells

(cTEC and mTEC, respectively). These cells are responsible for the guidance, selection and maturation of T-cells progenitors by expressing chemo- and cytokines, presenting self-antigens and interacting with the T-cell receptor (Derbinski *et al.*, 2005; Gotter *et al.*, 2004; Sanos *et al.*, 2011; Takahama, 2006). The development, growth and differentiation of the epithelial network in the thymus depends on the presence of mesenchymal cells, that originate from the embryonic neural crest cells and are defined by platelet derived growth factor receptor (PDGFR) (Itoi *et al.*, 2007; Jenkinson *et al.*, 2007; Odaka, 2009)). The secondary lymphoid organs, lymph nodes, spleen and MALT, all have a similar composition. T- and B-lymphocytes accumulate in T-cell zones and follicles, respectively. In the T-cell zone, a reticular fiber network is formed by reticular cells. B-cells gather in follicles populated with specialized reticular cells called follicular dendritic cells (Nairn & Helbert, 2006). Stromal cells in the lymph nodes of human and mice have already been described, and they can be differentiated based on the expression of podoplanin (gp38) and platelet/endothelial cell adhesion molecule 1 (PECAM1/CD31). Lymph node stromal cells comprise: $gp38^{-}$ $CD31^{+}$ blood endothelial cells (BEC), $gp38^{+}$ $CD31^{+}$ lymphatic endothelial cells (LEC), $gp38^{+/-}$ $CD31^{-}$ follicular dendritic cells (FDC), $gp38^{+}$ $CD31^{-}$ fibroblastic reticular cells (FRC), $gp38^{-}$ $CD31^{-}$ integrin $\alpha7^{+}$ pericytes (IAP), and a small proportion of undefined stromal cells (Chang & Turley, 2015; Seibert *et al.*, 1995; Zotes *et al.*, 2013). In the spleen FDC, FRC and BEC can also be found. In mice, the same markers can be applied as for the lymph nodes (Zotes *et al.*, 2013), while in humans additional markers are needed (Steiniger *et al.*, 2014).

In this report, stromal cells from feline primary and secondary organs were isolated, cultured and immortalized for further use. A first characterization was performed by means of immunofluorescent staining for general lineage cell markers and through chemokine and cytokine mRNA profiling.

5.2. Materials and Methods

5.2.1. Isolation and primary cell culture

In veterinary practices, cats are euthanized regularly for various reasons. The use of tissues from these animals helps to reduce the number of laboratory animals. Therefore, tissues from euthanized conventional cats were used in this study, after informed consent of the owners. This study was approved by the ethical committee of the Faculty of Veterinary Medicine, Ghent University (EC2012/043). Eight weeks old cats were sedated by intramuscular injection of 0.1 mg/kg dexmedetomidine

hydrochloride (Dexdomitor, Orion Corporation) and 0.1 mg/kg ketamine (Anesketin, Dechra). Subsequently, the cats were euthanized with an overdose of 20% sodium-pentobarital intracardially. Immediately after euthanasia, various lymphoid tissues were collected and kept on ice in PBS before further processing.

5.2.2. Red bone marrow

Both the left and right femur and humerus were removed and rinsed in PBS containing 100 U/ml penicillin and 0.1 mg/ml streptomycin. All following procedures were performed in a laminar flow cabinet. The bones were cleared of any tissue remaining on the bone, and placed in a sterile bacterial plate. The ends of the bones were clipped with scissors, and the marrow was flushed out by insertion of a 18G needle and 5 ml syringe. Flushing was performed with ice cold RPMI containing 2 % fetal calf serum, 10 U/ml heparin, 100 U/ml penicillin and 0.1 mg/ml streptomycin. Following flushing, the marrow was broken down into little pieces by repeatedly sucking the pieces through the needle into the syringe. All cells were collected and placed in 50 ml tube on ice for 15 minutes to allow bone marrow fat to solidify. Next, the tissue mixture was strained over a 100 μm cell strainer, and centrifuged at 300 xg for 10 minutes. Contaminating red blood cells were lysed by resuspending the cell pellet in 10 ml of red blood cell (RBC) lysis buffer. Cells were seeded on fibronectin (10 μg/cm2), gelatin (10 mg/ml), or in non-coated 24-well plates in DMEM supplemented with 10 % fetal bovine serum, 100 U/ml penicillin, 0.1 mg/ml streptomycin, 0.1 mg/ml gentamycin, 1 % non-essential amino acids 100 x, 2 mM sodium pyruvate (stromal cell medium). Cells were kept at 37°C in a humidified incubator with 5 % CO2.

5.2.3. Thymus and lymph nodes

The isolation of stromal cells from the thymus and lymph nodes was based on the protocol described by Fletcher and colleagues (Fletcher *et al.*, 2011). In young cats the thymus is a prominent organ in the chest. After excision, the attached blood vessels were removed. The tissue was minced with needles and washed to remove the loose thymocytes. Hereafter, the remaining tissue was incubated with 0.2 mg/ml collagenase IV in DMEM with continuous stirring for 30 minutes at 37 °C. The tissue was washed to collect lose cells. The residual pieces were incubated with 0.4 mg/ml collagenase IV for 30 minutes at 37 °C with regular agitation by pipetting. This step was repeated until all tissue was digested. The axillary, submandibular, and inguinal lymph nodes were collected, and kept in ice cold PBS. The complete lymph node was incubated for 20 minutes in an enzyme mix containing 0.2 mg/ml collagenase IV and

0.8 mg/ml dispase I in DMEM supplemented with 2 % fetal calf serum, 1.2 mM $CaCl_2$, 100 U/ml penicillin and 0.1 mg/ml streptomycin. Following this initial digest, the lymph nodes were aspirated to break the capsule. Large pieces were allowed to settle and supernatant was collected. The pieces of tissue were resuspended in the enzyme mixture and left to incubate for 10 minutes at 37 °C and mixed by pipetting every 5 minutes. This step was repeated until all tissue was digested. The cells isolated from thymus and lymph node were strained over a 100 μm cell strainer and centrifuged at 300 xg for 10 minutes. If cell pellets showed signs of contaminating RBC, a RBC lysis step was included. The isolated cells were seeded in stromal cell medium onto fibronectin (10 μg/cm2), gelatin (10 mg/ml), or non-coated 24-well plates.

5.2.4. Spleen

The spleen was excised, rinsed in PBS containing 100 U/ml penicillin and 0.1 mg/ml streptomycin and attached omentum was removed. The tissue was cut into small pieces (± 0.5 cm^3). To remove lose cells, the pieces were shaken vigorously at 4 °C in ice cold DMEM supplemented with 100 U/ml penicillin and 0.1 mg/ml streptomycin. This step was repeated twice, after which the pieces were broken down to ± 0.2 cm^2, and an additional shaking step was performed. The remaining tissue was digested with 0.5 mg/ml collagenase I and 0.5 mg/ml collagenase IV for 20 minutes at 37 °C. After replacement of the enzyme mixture, the tissue was digested for an additional 20 minutes at 37 °C with agitation by pipetting every 5 minutes. Because the spleen tissue seemed to be resistant to degradation with the collagenase mixture, after removal of lose cells, the remaining pieces of tissue were digested with DMEM containing 20 % trypsin for 40 min at 37 °C with regular agitation. The reaction was neutralized by the adding an excess of fetal calf serum. Cells detached by the collagenase and trypsin treatment were kept separately. The enzymatic washes were centrifuged at 300 xg for 10 min, and red blood cells were removed by incubation with RBC lysis buffer. Cells were strained over a 100 μm cell strainer, and washed with DMEM. The isolated cells were seeded in stromal cell medium on fibronectin (10 μg/cm2) or gelatin (10 mg/ml) coated 24-well plates, or in non-coated 24-well plates.

5.2.5. Immortalization

The primary cultures of the stromal cells (7 days after seeding) from various tissues were transduced with commercial recombinant lentiviruses (Gentaur) expressing the human telomerase reverse transcriptase (hTERT) or the simian vacuolating virus 40 large T antigen (SV40 T-Ag), or a combination of these two lentiviruses. After 30

minutes of inoculation with 200 µl virus suspension, complete culture medium was added, and the cells were incubated overnight with the virus/medium (1:1) inoculum. The next day, the inoculum was removed, and replaced by complete culture medium. When reaching 80 % confluency, cells were trypsinized (0.25 % trypsin with 0.02 % EDTA), and seeded into 25 cm^2 culture vessels. The clonal expansion of the cells was evaluated daily.

5.2.6. Immunofluorescent staining

To investigate the origin of the isolated cells, immunofluorescence staining with different cell markers was performed on early passage (p5-10) immortalized cells. For staining, cells were seeded on glass coverslips and allowed to reach 70 % confluence. Cells were fixed with 1 % paraformaldehyde in PBS containing Ca^{2+} and Mg^{2+} (rPBS) for 10 minutes at room temperature, followed by permeabilization with 0.1 % Triton X-100 for 2 minutes at room temperature. Staining was performed against vimentin (Lab Vision Corporatio), desmin (Dako), cytokeratin (Dako), smooth muscle actin (Dako), fibronectin (Biorad) and PECAM-1/CD31 (LifeSpan Biosciences). Primary antibodies were visualized with appropriate fluorescently labeled secondary antibodies, and counterstained with a Hoechst 33342 (Molecular probes) nuclear staining. Coverslips were mounted on microscopic slides with glycerin/PBS containing 2.5 % 1,4-diazabicyclo(2,2,2)octane (Janssens) and analyzed with a confocal laser scanning microscope (Leica TSC SPE system with Leica DM2500 CQS microcope).

5.2.7. Cytokine and chemokine mRNA RT-PCR

Early passage (p5-10) immortalized lymphoid stromal cells and feline venous endothelial cells (Olyslaegers *et al.*, 2013) were seeded in 25 cm^2 culture vessels and allowed to reach 70 % confluency. Cells were collected by trypsinization and mRNA was isolated with the RNeasy mini kit (Qiagen). To remove any contaminating DNA, all samples were incubated with DNase I (NEB) for 15 min at 37 °C. The enzyme was inactivated prior to PCR at 70 °C for 10 minutes. The RNA was used as a template in a one-step reverse transcriptase PCR for different cyto- and chemokines (Table 1). In brief, a 25 µl reaction mix contained 1 µg of sample RNA mixed with 10µl reaction buffer 5 x, 2 µl dNTP mix, specific forward and reverse primers (Table 1), RNase free water and 2 µl of QIAGEN OneStep RT-PCR Enzyme Mix. The reverse transcription took place at 50 °C for 30 min, followed by an initial activation of the DNA polymerase at 95 °C for 15 minutes. Next, samples were temperature cycled for 30 times, with denaturation at 94 °C for 1 min, annealing at the primer specific temperature for 30 s,

and extension at 72 °C for 1 min. After cycling any unfinished products were extended at 72 °C for 10 min. The PCR product was separated on a 1.5 % agarose gel in 0.5 x TAE buffer for 35 min at 100 mV, and bands were visualized with ethidium bromide solution (Sigma). The absence of DNA in the samples was controlled by regular PCR.

Table 1: Cytokine and chemokine mRNA RT-PCR primers presented in 5' to 3' orientation.

Gene	Forward primer	Reverse primer
GM-CSF	CGG GGC AGC CTC ACC A	GGC TCC CAG CAG TCA AAG
CCL19	GAT GCT GAA GAC TGC TGC	TCT GCA GTC TCC GGA TG
CCL21	GAC CCA AGG CAG TGA TG	CTC CTT TGT CCC TCT TAC AG
CXCL12 (SDF1)	CCG TGT GGC AGA TGG AAG GG	CTA TAA ATG CGG GTG TCT ACG
IL7	AAC AAG GAT CAG GGG AGG AAT	AAA GAA CCA GCC GCA GAG ACC
ICAM1b	GTG AGC CAG AGG TCT CAG	TTC CGC TGG CGG TTA T-AG

5.3. Results and discussion

5.3.1. Primary and immortalized stromal cell culture

5.3.1.1. Bone marrow

One day after isolation, the seeded cells were washed gently to avoid disturbance of the attached cells. Independent of the used cell culture surface, a lot of cells remained in suspension after 24 h. Pictures of the primary bone marrow culture can be found in Figure 1. Overall, the adherent cells could be divided into two groups based on their morphology; (1) cells resembling monocytes, and (2) large spindle-like cells. Adherence of spindle-like cells was best on fibronectin, followed by gelatin. Cell culture grade plastic showed the worst performance but allowed stretching of macrophage-like cells. The spindle-like cells on fibronectin started to form clusters on day 2 and showed proliferation on day 3. The macrophage-like cells started to form giant cells that contained multiple nuclei. The spindle-like cells formed bundles, forming growth cavities around the giant cells. The culture showed contact inhibition and cells ceased to grow and started dying once confluency was reached. Six days post-isolation, the cells seeded on fibronectin reached confluency and were split with 0.025% trypsin and versene solution. The spindle-like cells loosened readily with this treatment, while the giant cells remained firmly attached to the coating. In this way, a first separation of the different cell types could be made. However, in the first passage culture vessels, some remaining macrophage-like cells were observed.

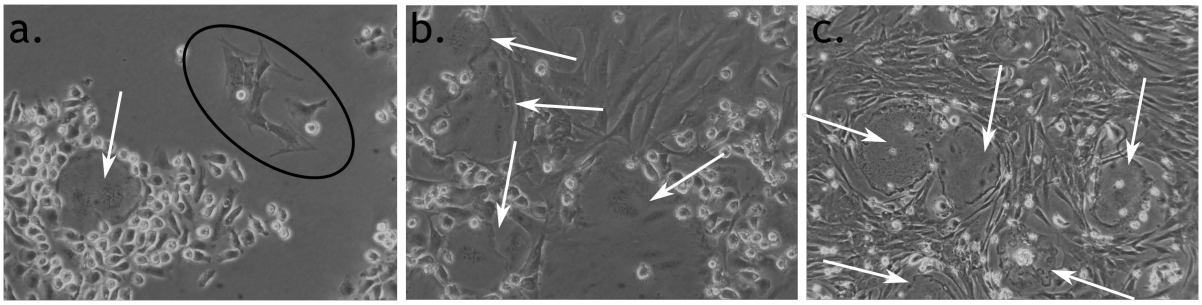

Figure 1: Primary bone marrow culture seeded on a fibronectin coated culture dish. (a.) Two days after isolation, non-adherent cells were washed away. The white arrow indicates a macrophage-like giant cell with multiple nuclei, surrounded by loosely adhering smaller cells. Firmly attached stretched out fibroblast-like cells are present in the black circle. 200 x magnification. (b.) On day 3, the clusters of fibroblastic cells started to expand and more giant cells appeared (white arrows). 200 x magnification. (c.) After 7 days in culture, the fibroblast-like cells filled the culture dish, showing contact inhibition and leaving spaces for the giant cells (white arrows). 100 x magnification.

Primary cells could be kept in culture for several passages. Cells cultured on cell culture plastic showed slower growth kinetics compared to cultures on fibronectin coated plates. On cell culture grade plastic, confluency could not be reached, and connected cell clusters were formed. On the other hand, cells seeded on fibronectin were able to form a monolayer that showed an organization and direction of cells in bundles and waves. However, in order to establish a stable cell line for further work, first passage cells were transduced using commercial lentiviruses that contained the SV40 T-Ag or hTERT gene, or a combination of both lentiviruses. Following transduction, only cells transduced with SV40 T-Ag or the hTERT/SV40 T-Ag combination could be maintained, with better survival and growth kinetics in the SV40 T-Ag only cells. Immortalized cells were morphologically similar to their primary counterparts, but cell lines lost contact inhibition, and reduced self-organization of the culture in bundles and waves during growth. In contrast to their primary counterparts, immortalized cells were able to form monolayers on uncoated culture surfaces.

5.3.1.2. Thymus

After washing away loose cells 24 h post-seeding, a small amount of cells had attached to the culture plates, but the majority stayed in suspension. It is not surprising that non-adherent cells were still present, since the seeded cell suspension probably still contained thymocytes, T-cell progenitor cells that were maturing in the thymus. T-cells do not adhere to cell culture plastic and adhere only loosely to fibronectin. There was not a large difference in cell attachment between fibronectin and gelatin coated plates, but the coated plates performed better than non-coated plates.

Progression of the primary culture is shown in Figure 2. Among the adhered cells, three cell types could be distinguished morphologically; polygonal cells, spindle-like cells and macrophage-like cells. Some thymocytes remained in the culture dishes after gentle washing. Cells collected from the 24 h washing steps were seeded in non-coated culture plates and incubated for an additional two days. After this re-seeding more spindle-like cells were recovered, but also smaller polygonal cells. It is possible that washing 24 h after seeding was too early, and the stromal cells needed more time to adhere. Another explanation could be a too high cell number in the well, inhibiting contact between cells and the culture surface. The simultaneous isolation of small polygonal cell and fibroblast-like cells from thymus was already reported by Rzhaninova and colleagues for the human fetal thymus (Rzhaninova *et al.*, 2005). Three days post-isolation, outgrowth could be seen of the spindle-like cell clusters in the fibronectin coated plates. Cells were split with a 0.025% trypsin and versene solution 7 days post-isolation. After passage, the groups of polygonal cells were not seen anymore, it is possible that individual polygonal cells were still present in the cultures.

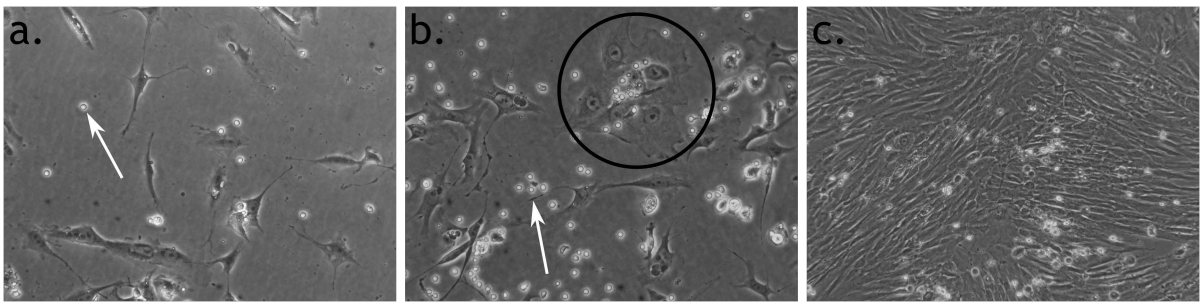

Figure 2: Primary thymus culture seeded on a fibronectin coated culture dish. (a.) Two days after isolation, non-adherent cells were washed away. Spindle-like cells were firmly attached and stretched out. Some thymocytes remained in the culture dish after washing (white arrow). 200 x magnification. (b.) On day 3, the fibroblastic cells started to expand, some cell clusters showed more polygonal cell bodies (black circle) compared to the more spindle like cells. There were still some thymocytes present (white arrow). 200 x magnification. (c.) After 7 days in culture, the spindle-like cells filled the culture dish, showed contact inhibition and an organized growth pattern. 100 x magnification.

Primary cells could be kept in culture for several passages, but cell growth was slow, independent of the culture substrate. In order to establish a stable cell line with better growth kinetics for future work, passage one cells were transduced using commercial lentiviruses that contained the SV40 T-Ag or hTERT gene, or a combination of both lentiviruses. As was noticed for the bone marrow stromal cell cultures, only thymus stromal cells transduced with the SV40 T-Ag and the SV40 T-Ag/hTERT combination survived. After immortalization, the growth rate was improved but still slow compared

to bone marrow stromal cells. Unlike immortalized bone marrow stromal cells, immortalized thymus stromal cells still needed fibronectin coating to be able to from a monolayer. On uncoated culture surfaces cells became large and stopped growing (Fig. 5). Rzhaninova and colleagues reported that basic fibroblastic growth factor (bFGF) was needed for effective growth of mesenchymal cells isolated from the human thymus (Rzhaninova *et al.*, 2005), although this growth factor is not required for bone marrow mesenchymal cells (Walsh *et al.*, 2000). Hence, addition of bFGF might improve growth of the feline thymus mesenchymal cells as well.

5.3.1.3. Lymph node

Similar to cells isolated from the thymus, only few cells attached to the culture surface after 24 h. After washing, the loose cells were seeded again into new non-coated culture plates and incubated for two more days. Once more, this strategy allowed a larger quantity of primary cells to be isolated. Gelatin and fibronectin achieved better results than cell-culture plastic. Two cell types were observed; the spindle-like cells, and macrophage-like cells (Fig. 3). On day two, the first expansion of spindle-like cells was seen in the gelatin coated wells. The macrophage-like cells stretched out and started to form giant cells. Once full confluency was reached, cell growth stopped due to contact inhibition.

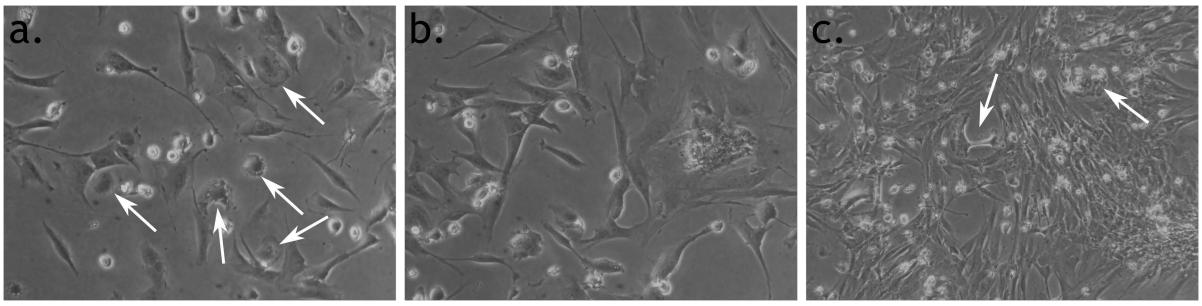

Figure 3: Primary lymph node culture seeded on a fibronectin coated culture dish. (a.) Two days after isolation, non-adherent cells were washed away. Spindle-like cells were firmly attached and stretched out. Large macrophage-like cells were present in the culture (white arrows). 200 x magnification. (b.) On day 3, the fibroblastic cells started to expand. 200 x magnification. (c.) After 7 days in culture, the spindle-like cells filled the culture dish, showed contact inhibition and an organized growth pattern, but left spaces for macrophages (white arrows). 100 x magnification.

The primary culture was split 7 days after seeding of the isolated cells with a 0.025% trypsin and versene solution. Similar to the bone marrow primary culture, spindle-like cells loosened easily, while the macrophage-like cells remained attached to the cell surface. Growth kinetics and patterns of the spindle-like cells from the lymph node were similar to those isolated from the bone marrow, and the primary cultures could be passaged several times without immortalization. Cells were only able to establish a

monolayer on fibronectin coated surfaces. On non-coated surfaces, cells formed an interconnected network of cell clusters that had the tendency to loosen due to tractive forces generated by the cells. In order to establish a stable cell line for future work, first passage lymph node stromal cells were transduced using commercial lentiviruses that contained the SV40 T-Ag or hTERT gene, or a combination of both lentiviruses. As was noticed for the bone marrow and thymus stromal cell cultures, only cells transduced with the SV40 T-Ag and the SV40 T-Ag/hTERT combination survived passaging. Growth of the immortalized cells on uncoated surfaces was possible but slow, and cells became large and stretched. Similar to immortalized thymus stromal cell cultures, immortalized cultures from the lymph nodes had better growth characteristics when seeded on fibronectin (Fig. 5).

5.3.1.4. Spleen

The tissue digested with collagenase or trypsin was seeded onto different culture plates, again containing the different surface coatings. One day after seeding, a lot of platelets and red blood cell-debris had attached to the culture surface. Most of the cells collected after collagenase digestion showed a macrophage-like morphology. Trypsin digestion, on the other hand, resulted in the collection of both macrophages and spindle-like cells. Like the stromal network in the lymph nodes, FRC in the spleen forme a network of reticular fibers and extracellular matrix. The FRC encapsulate these matrix proteins to from a conduit system. Apparently, in contrast to trypsin, the digestion with collagenase was not potent enough to detach the stromal cells from the extracellular matrix. The resident macrophages of the red pulp and cells of the white pulp, T- and B-cells, are not firmly attached to the extracellular matrix, but reside within the network shaped by the FRC and other stromal cells. On the fibronectin coated wells, outgrowth of fibroblastic cells from cell clusters was already seen one day post-isolation, but only for the trypsin digested tissue. Although some spindle-like cells could be seen on the other growth surfaces (gelatin and cell-culture plastic), they were less supportive for growth of the fibroblastic cells, and mainly contained macrophages. Two and three days after isolation, the platelets and debris were removed by actions of the macrophages, which also started to merge into giant cells (Fig. 4). As was seen in the primary bone marrow cultures, the spindle-like cells grew in bundles around the macrophages, leaving a niche. The growth kinetics of the isolated spindle-like cells was fast and subject to contact inhibition. Hence, on day 5 post-isolation, the fibroblastic cells growing on fibronectin were split with 0.025% trypsin and versene, and seeded in fibronectin coated wells. As already explained

before, only the spindle-like cells loosened during trypsin treatment. The stromal cells organized themselves in waves when seeded on fibronectin, and showed heavily decreased growth kinetics when seeded on cell culture plastic.

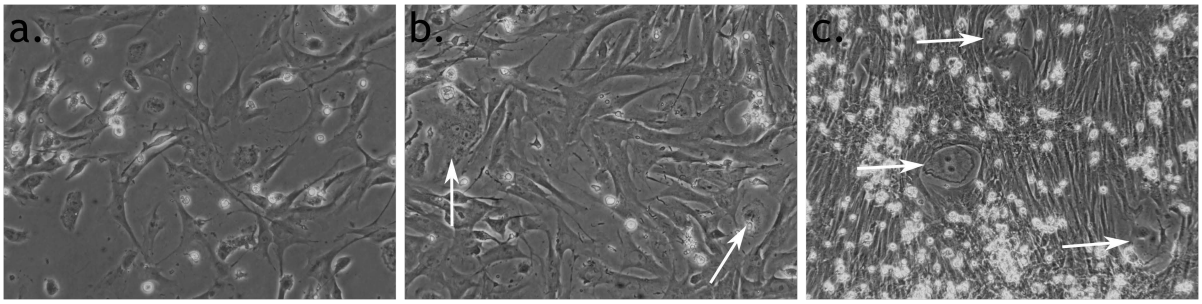

Figure 4: Primary spleen culture seeded on gelatin coated culture dish. (a.) Day 2 after isolation, non-adherent cells were washed away. Spindle-like cells were firmly attached and stretched out. 200 x magnification. (b.) On day 3, the fibroblastic cells started to expand. Large macrophage-like cells were present in the culture (white arrows). (c.) After 5 days in culture, the spindle-like cells filled the culture dish, showed contact inhibition and an organized growth pattern. The spindle-like cells grew around the macrophage-like cells (white arrows). 100 x magnification.

First passage spleen stromal cells were transduced using commercial lentiviruses that contained the SV40 T-Ag or hTERT gene, or a combination of both lentiviruses. As for all other lymphoid stromal cell lines, only cells transduced with SV40 T-Ag or the hTERT/SV40 T-Ag combination could be maintained, with better survival and growth kinetics in the SV40 T-Ag only cells. Immortalized cultures behaved similar to primary cells, with fast growth on fibronectin coating a reduced growth on uncoated plastic (Fig.5).

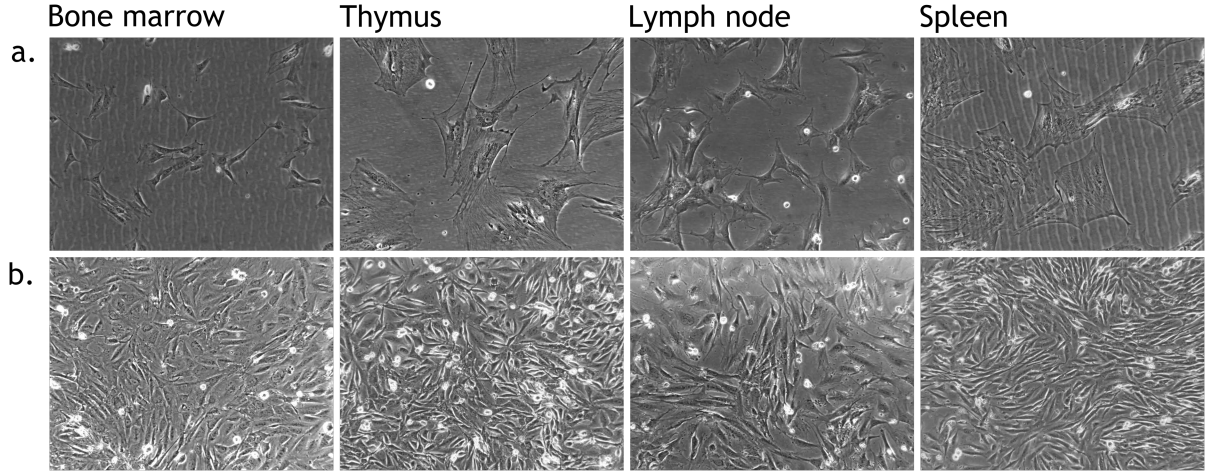

Figure 5: Immortalized lymphoid stromal cells cultures (a) on cell culture grade plastic and (b) on a fibronectin coating. (a) Passage 8 immortalized cell cultures seeded on cell culture plastic. (b) Passage 5 immortalized cell cultures seeded on a fibronectin coated culture surface, forming a monolayer. 100 x magnification

5.3.2. Characterization

5.3.2.1. Marker staining

The general structure of lymphoid organs is determined by a network of different stromal cells. Hematopoietic cells enter and exit the lymphoid organs via the blood and lymphoid vasculature, composed of specialized endothelial cells. Stromal cell cultures, both primary and immortalized, were analyzed for the expression of the epithelial cell marker, cytokeratin, and different mesenchymal markers, such as smooth muscle actin (SMA), vimentin, desmin and fibronectin. In humans and mice, cells in the secondary lymphoid organs are further characterized by the expression of podoplanin (gp38), a heavily glycosylated membrane protein; and platelet/endothelial cell adhesion molecule 1 (PECAM1/CD31). Unfortunately, no validated antibody is available to test podoplanin expression on feline cells. PECAM1 expression was tested with an antibody cross-reacting with feline cells. Results are summarized in Table 2.

Table 2: Presence of different cellular markers in stromal cells isolated from bone marrow, thymus, lymph nodes and spleen.

	Bone marrow	Thymus	Lymph node	Spleen
Cytokeratin	-	-/+	-	-
Vimentin	+	+	+	+
Desmin	-	-	-	-
Fibronectin	+	+	+	+
Smooth muscle actin	+	+	+	-
PECAM1	-	-	-	-

Immortalized stromal cell cultures from bone marrow, lymph node and spleen were consistently negative for cytokeratin expression (Fig. 6). Conversely, the stromal cell culture from the thymus showed smaller polygonal cells that were positive for cytokeratin expression (Fig. 6). These cells were already noticed morphologically via light microscopy. Therefore, it will be important to further clone the thymus stromal cell culture, in order to split the two different cell types.

Vimentin, an intermediate filament characteristic of mesenchymal cells, was uniformly expressed by stromal cells of all the isolated lymphoid tissues (Fig. 6). The expression of vimentin confirms the mesenchymal origin of the isolated cells. This means that some cells isolated from the thymus express both the epithelial cell marker cytokeratin as well as the mesenchymal marker vimentin. Dual expression of cytokeratin and vimentin has been reported before in thymus epithelial cell lines from mouse and rat (Colić, 1991; Ehmann *et al.*, 1986), and intestinal epithelial cell cultures (Desmarets *et al.*, 2013). Epithelial cells can express mesenchymal markers as a result of epithelial-mesenchymal transition (EMT) (Kalluri & Weinberg, 2009). EMT can be induced by

immortalization and culturing, but also occurs in the adult thymus. Current understanding of the fattening of the thymus indicates a role for EMT in the transition of thymus epithelial cell into fibroblasts that can commit to the adipocyte lineage (Dixit, 2010). Hence, the cytokeratin$^+$/vimentin$^+$ cells in the feline thymus cell cultures represent most likely TEC that are undergoing partial EMT, either induced by immortalization and culture, or as a result of fattening of the post-natal thymus.

None of the stromal cells isolated from the different lymphoid tissues showed expression of desmin, an intermediate filament found in muscle tissue (Fig. 6).

Stromal cells from all selected tissues produced and excreted fibronectin (Fig. 6). Fibronectin is an important extracellular matrix component produced by (myo)fibroblasts and epithelial cells. It contains several binding sites for other extracellular matrix proteins like collagen, especially with type III collagens, also known as reticulin, the constituent of reticular fibers (Engvall *et al.*, 1978). Apart from binding other matrix proteins, fibronectin also binds cell adhesion molecules, cytokines and growth factors. Furthermore, binding between the fibronectin receptor, integrin α5β1, and fibronectin induces cell signaling leading to actin cytoskeleton rearrangements, defining the orientation and migration of cells (Huttenlocher & Horwitz, 2011). Signaling induced by the fibronectin used to coat the culture vessels is most likely responsible for the organization of the mesenchymal cells in waves during culture as discussed above, and allowing for the formation of monolayers which was not seen on non-coated culture surfaces.

Smooth muscle actin, a contractile element found in myofibroblasts and smooth muscle tissue, was highly expressed in non-confluent stromal cell cultures of the various lymphoid tissues, except for the spleen (Fig. 6). However, upon reaching confluency, SMA expression was downregulated or absent. Stiffness of cell culture surfaces can induce the expression of SMA and the production of stress fibers in fibroblasts, and is related to the physiological pathway seen during tissue repair after injury (Hinz, 2010). The expression of SMA and the concomitant ability of cells to generate tractive forces can be responsible for loosening of cells seen in stromal cell cultures in non-coated cell culture plates. Coating wells with extracellular matrix proteins gives contracting cells something to firmly adhere to, avoiding loosening of cells. In the lymph nodes and spleen, the expression of fibronectin and SMA are characteristic for FRC (Aguzzi *et al.*, 2014; Malhotra *et al.*, 2012).

In the lymph node, contractility of the reticular network is regulated by interaction between podoplanin expressed on FRC and C-type lectin 2 (CLEC-2) on dentritic cells, and is important during lymph node activation following an inflammatory response (Chang & Turley, 2015). In the thymus, expression of SMA actin has been shown around vascular structures, and may represent pericytes, a multipotent mesenchymal cell type also found in the bone marrow (Bianco *et al.*, 2008; Odaka, 2009).

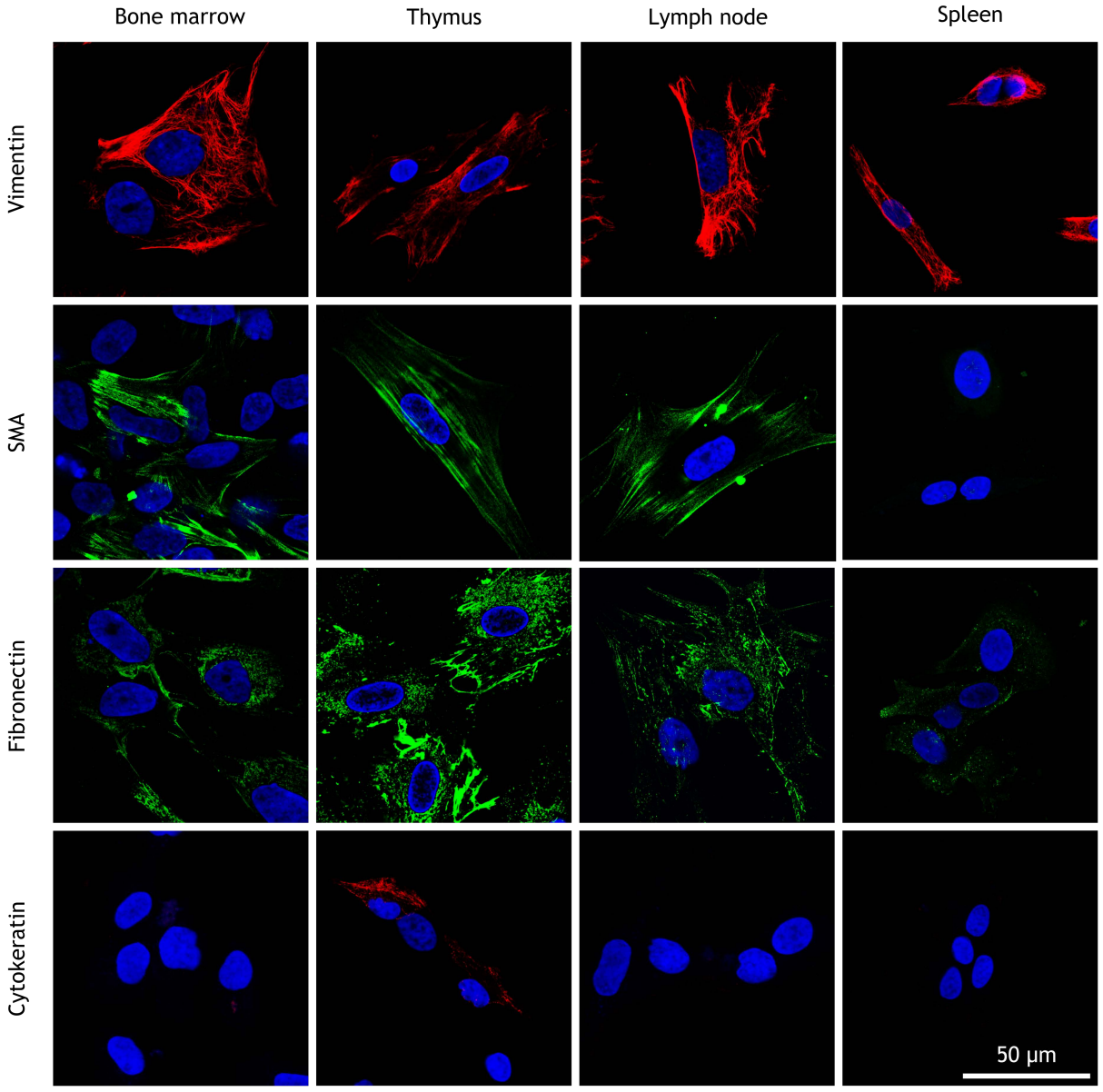

Figure 6: Expression of mesenchymal and endothelial cell markers by cells isolated from feline bone marrow, thymus, lymph node and spleen (red and green). Immunofluorescent staining was performed on non-confluent immortalized cells. Cell nuclei are counterstained with Hoechst (blue). Scale bar indicates 50µm.

5.3.2.2. mRNA profile

The mRNA expression of chemokines and cytokines important for the function of lymphoid tissues was assessed via RT-PCR of early passage immortalized stromal cells (Fig. 7). RT-PCR products were verified by sequencing.

CCL19 and CCL21 are chemokines produced in lymphoid tissues, with the former being the soluble form of the latter. CCL21 is immobilized on glycans present on cell surfaces or in the extracellular matrix. These chemokines are the ligands for CCR7, that is expressed on immune cells, and induce the chemotaxis of immune cells to the lymphoid organs (Chang & Turley, 2015). CCL19 mRNA was present in every lymphoid stromal cell culture, while CCL21 was not. It is known that CCL21 expression in lymphoid stromal cells is rapidly lost after *in vitro* culture. Expression can be restored by fluid flow over the cells, indicating that interstitial lymph flow in the organs is necessary for a complete differentiation and function of the reticular cells (Tomei *et al.*, 2009). In the thymus expression of CCL19 and CCL21 by mTEC guide immature T-cells back from the thymic cortex to the medulla during their selection and maturation process (Bunting *et al.*, 2011). It is possible that the detected CCL19 mRNA originates from the cytokeratin$^+$/vimentin$^+$ cells found in the feline thymus stromal cell culture. Endothelial cells can be induced to produce CCL19, and play a role in attracting lymphocytes during inflammation (Alt *et al.*, 2002; Yu *et al.*, 2015). The production of these chemokines mainly by FRC in the secondary lymphoid organs is important for the generation of the T-cell zone (Cyster, 2000; Koning & Mebius, 2012; Mebius & Kraal, 2005).

CXCL12, also known as stromal derived factor 1 (SDF1), is an important lymphocyte homing factor that binds to the receptor CXCR4, that also functions as the FIV secondary receptor (Joshi *et al.*, 2005). As can be seen in Figure 7, CXCL12 mRNA was present in all of the tested cell cultures. In the bone marrow CXCL12 is mainly produced by CXCL12-abdundant reticular cells (CAR cells), but also by other perivascular cells, endothelial cells and osteoblasts and is crucial to HSC maintenance and retention (Mercier *et al.*, 2012; Sugiyama *et al.*, 2006). Cortical thymus epithelial cells produce CXCL12 as a guide for the CXCR4-expressing T-cell progenitors to travel towards the cortex of the thymus during their maturation and selection (Plotkin *et al.*, 2003), and also provides survival signals (Bunting *et al.*, 2011). In the spleen CXCL12 signal is produced by stromal cells in the red pulp, marginal zone and white pulp by FRC, and is important for the migration of immune cells to their specific niche

(Hargreaves *et al.*, 2001; Umemoto *et al.*, 2012). The expression of CXCR4 on lymphocytes reassures recirculation of the lymphocytes from the blood through the lymph nodes, in which FRC are the main source of CXCL12 (Malhotra *et al.*, 2012).

Stromal cells from the bone marrow, thymus and spleen showed presence of IL7 mRNA, as well as the feline venous endothelial cells. In the bone marrow IL7 is produced by stromal cells, and determines B-cell lineage commitment (Kikuchi *et al.*, 2005), while in the thymus production of IL7 in TEC and mesenchymal cells induces survival and maturation of T-cells (Kang *et al.*, 1999). In the spleen IL7 aids in the organization of B-cells the marginal zone (Willems *et al.*, 2011).

Lymphocytes bind to endothelial cells and stromal cells through several adhesion molecules like intercellular adhesion molecule 1 (ICAM-1). ICAM-1 is constitutively expressed on endothelial cells and cell membrane expression of this molecule is increased during inflammation. It is an important factor for the extravasation and activation of blood leukocytes that enter tissues. Expression of ICAM-1 in the feline venous endothelial cells was previously shown by Olyslaegers and colleagues (Olyslaegers *et al.*, 2013). FRC and FDC in the secondary lymphoid organs share a common ancestor, the lymphoid tissue organizer cells (LTo cells) that express ICAM-1 among other adhesion factors to retain the hematopoietic cells at the place of lymph node development. Mature FRC and FDC retain the expression of adhesion molecules important for clustering and signal transduction in hemapoietic cells (Aguzzi *et al.*, 2014; Koning & Mebius, 2012).

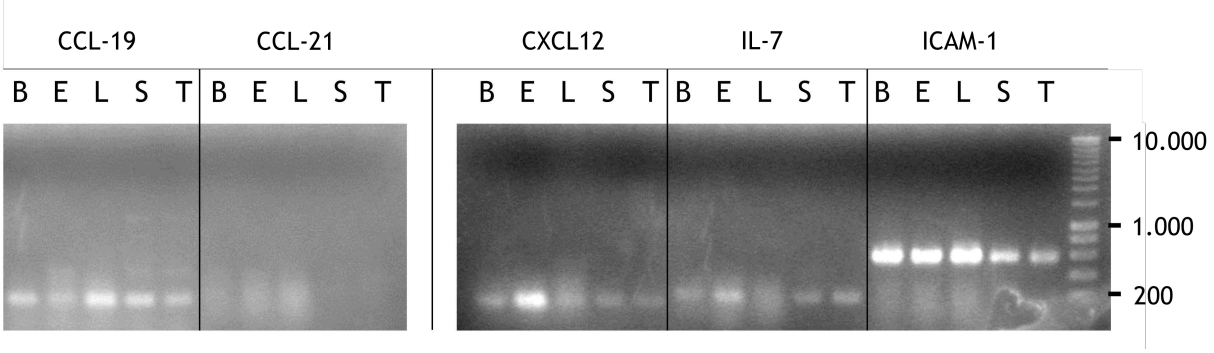

Figure 7: The mRNA expression of different cytokines and chemokines in immortalized lymphoid stromal cell cultures. Bone marrow (B), lymph node (L), spleen (S), thymus (T); and venous endothelial cells (E).

Although the cells isolated from the different lymphoid tissues express markers typical for mesenchymal stromal cells, and express mRNA of cytokines essential to lymphoid tissue function, further characterization will be needed. Furthermore, reciprocal interaction with hematopoietic cells is essential for differentiation of the mesenchymal

cells into fully functional lymphoid tissue stromal cells (Koning & Mebius, 2012; Kumar *et al.*, 2015). These interactions will enable us to validate the complete expression profile of the isolated and immortalized feline lymphoid tissue stromal cells.

5.4. Conclusion

Feline mesenchymal stromal cells were successfully isolated from bone marrow, thymus, lymph nodes and spleen. The cells were successfully immortalized with SV40 T-Ag only. Immortalization induced loss of contact inhibition during growth. Characterization showed that these cells express the typical mesenchymal markers and produced the extracellular matrix protein fibronectin. The cells produced various cytokines important for lymphoid organ function at the mRNA level.

Acknowledgements

We thank Ytse Noppe for her excellent technical support. IDMR was supported by the Institute for Promotion of Innovation through Science and Technology in Flanders (IWT-Vlaanderen). SVB was supported by the Special Research Fund of Ghent University.

References

Aguzzi, A., Kranich, J. & Krautler, N. J. (2014). Follicular dendritic cells: origin, phenotype, and function in health and disease. *Trends Immunol* **35**, 105-113.

Alt, C., Laschinger, M. & Engelhardt, B. (2002). Functional expression of the lymphoid chemokines CCL19 (ELC) and CCL 21 (SLC) at the blood-brain barrier suggests their involvement in G-protein-dependent lymphocyte recruitment into the central nervous system during experimental autoimmune encephalomyelitis. *Eur J Immunol* **32**, 2133-2144.

Beebe, A. M., Dua, N., Faith, T. G., Moore, P. F., Pedersen, N. C. & Dandekar, S. (1994). Primary stage of feline immunodeficiency virus infection: viral dissemination and cellular targets. *J Virol* **68**, 3080-3091.

Beebe, A. M., Gluckstern, T. G., George, J., Pedersen, N. C. & Dandekar, S. (1992). Detection of feline immunodeficiency virus infection in bone marrow of cats. *Vet Immunol Immunopathol* **35**, 37-49.

Bianco, P., Robey, P. G. & Simmons, P. J. (2008). Mesenchymal stem cells: revisiting history, concepts, and assays. *Cell Stem Cell* **2**, 313-319.

Brown, W. C., Bissey, L., Logan, K. S., Pedersen, N. C., Elder, J. H. & Collisson, E. W. (1991). Feline immunodeficiency virus infects both CD4+ and CD8+ T lymphocytes. *J Virol* **65**, 3359-3364.

Bunting, M. D., Comerford, I. & McColl, S. R. (2011). Finding their niche: chemokines directing cell migration in the thymus. *Immunol Cell Biol* **89**, 185-196.

Chang, J. E. & Turley, S. J. (2015). Stromal infrastructure of the lymph node and coordination of immunity. *Trends Immunol* **36**, 30-39.

Colić, M. (1991). Cultivation, characterization and modulation of rat thymic non-lymphoid cells in vitro. *Cytotechnology* **5**, 107-115.

Cyster, J. G. (2000). Leukocyte migration: scent of the T zone. *Curr Biol* **10**, R30-33.

Derbinski, J., Gäbler, J., Brors, B., Tierling, S., Jonnakuty, S., Hergenhahn, M., Peltonen, L., Walter, J. & Kyewski, B. (2005). Promiscuous gene expression in thymic epithelial cells is regulated at multiple levels. *J Exp Med* **202**, 33-45.

Desmarets, L. M., Theuns, S., Olyslaegers, D. A., Dedeurwaerder, A., Vermeulen, B. L., Roukaerts, I. D. & Nauwynck, H. J. (2013). Establishment of feline intestinal epithelial cell cultures for the propagation and study of feline enteric coronaviruses. *Vet Res* **44**, 71.

Dixit, V. D. (2010). Thymic fatness and approaches to enhance thymopoietic fitness in aging. *Curr Opin Immunol* **22**, 521-528.

Ehmann, U. K., Shiurba, R. A. & Peterson, W. D. (1986). Long-term proliferation of mouse thymic epithelial cells in culture. *In Vitro Cell Dev Biol* **22**, 738-748.

Engvall, E., Ruoslahti, E. & Miller, E. J. (1978). Affinity of fibronectin to collagens of different genetic types and to fibrinogen. *J Exp Med* **147**, 1584-1595.

Fletcher, A. L., Malhotra, D., Acton, S. E., Lukacs-Kornek, V., Bellemare-Pelletier, A., Curry, M., Armant, M. & Turley, S. J. (2011). Reproducible isolation of lymph node stromal cells reveals site-dependent differences in fibroblastic reticular cells. *Front Immunol* **2**, 35.

Gotter, J., Brors, B., Hergenhahn, M. & Kyewski, B. (2004). Medullary epithelial cells of the human thymus express a highly diverse selection of tissue-specific genes colocalized in chromosomal clusters. *J Exp Med* **199**, 155-166.

Hargreaves, D. C., Hyman, P. L., Lu, T. T., Ngo, V. N., Bidgol, A., Suzuki, G., Zou, Y. R., Littman, D. R. & Cyster, J. G. (2001). A coordinated change in chemokine responsiveness guides plasma cell movements. *J Exp Med* **194**, 45-56.

Hartmann, K. (2012). Clinical aspects of feline retroviruses: a review. *Viruses* **4**, 2684-2710.

Hinz, B. (2010). The myofibroblast: paradigm for a mechanically active cell. *J Biomech* **43**, 146-155.

Huttenlocher, A. & Horwitz, A. R. (2011). Integrins in cell migration. *Cold Spring Harb Perspect Biol* **3**, a005074.

Itoi, M., Tsukamoto, N., Yoshida, H. & Amagai, T. (2007). Mesenchymal cells are required for functional development of thymic epithelial cells. *Int Immunol* **19**, 953-964.

Jenkinson, W. E., Rossi, S. W., Parnell, S. M., Jenkinson, E. J. & Anderson, G. (2007). PDGFRalpha-expressing mesenchyme regulates thymus growth and the availability of intrathymic niches. *Blood* **109**, 954-960.

Kalluri, R. & Weinberg, R. A. (2009). The basics of epithelial-mesenchymal transition. *J Clin Invest* **119**, 1420-1428.

Kang, J., Coles, M. & Raulet, D. H. (1999). Defective development of gamma/delta T cells in interleukin 7 receptor-deficient mice is due to impaired expression of T cell receptor gamma genes. *J Exp Med* **190**, 973-982.

Kikuchi, K., Lai, A. Y., Hsu, C. L. & Kondo, M. (2005). IL-7 receptor signaling is necessary for stage transition in adult B cell development through up-regulation of EBF. *J Exp Med* **201**, 1197-1203.

Koning, J. J. & Mebius, R. E. (2012). Interdependence of stromal and immune cells for lymph node function. *Trends Immunol* **33**, 264-270.

Kumar, V., Dasoveanu, D. C., Chyou, S., Tzeng, T. C., Rozo, C., Liang, Y., Stohl, W., Fu, Y. X., Ruddle, N. H. & Lu, T. T. (2015). A dendritic-cell-stromal axis maintains immune responses in lymph nodes. *Immunity* **42**, 719-730.

Malhotra, D., Fletcher, A. L., Astarita, J., Lukacs-Kornek, V., Tayalia, P., Gonzalez, S. F., Elpek, K. G., Chang, S. K., Knoblich, K., Hemler, M. E., Brenner, M. B., Carroll, M. C., Mooney, D. J., Turley, S. J. & Consortium, I. G. P. (2012). Transcriptional profiling of stroma from inflamed and resting lymph nodes defines immunological hallmarks. *Nat Immunol* **13**, 499-510.

Malhotra, D., Fletcher, A. L. & Turley, S. J. (2013). Stromal and hematopoietic cells in secondary lymphoid organs: partners in immunity. *Immunol Rev* **251**, 160-176.

Mebius, R. E. & Kraal, G. (2005). Structure and function of the spleen. *Nat Rev Immunol* **5**, 606-616.

Mercier, F. E., Ragu, C. & Scadden, D. T. (2012). The bone marrow at the crossroads of blood and immunity. *Nat Rev Immunol* **12**, 49-60.

Nagasawa, T., Omatsu, Y. & Sugiyama, T. (2011). Control of hematopoietic stem cells by the bone marrow stromal niche: the role of reticular cells. *Trends Immunol* **32**, 315-320.

Nairn, R. & Helbert, M. (2006). *Immunology for medical students*: MOSBY.

Nombela-Arrieta, C., Ritz, J. & Silberstein, L. E. (2011). The elusive nature and function of mesenchymal stem cells. *Nat Rev Mol Cell Biol* **12**, 126-131.

Odaka, C. (2009). Localization of mesenchymal cells in adult mouse thymus: their abnormal distribution in mice with disorganization of thymic medullary epithelium. *J Histochem Cytochem* **57**, 373-382.

Olyslaegers, D. A., Desmarets, L. M., Dedeurwaerder, A., Dewerchin, H. L. & Nauwynck, H. J. (2013). Generation and characterization of feline arterial and venous endothelial cell lines for the study of the vascular endothelium. *BMC Vet Res* **9**, 170.

Pedersen, N. C., Ho, E. W., Brown, M. L. & Yamamoto, J. K. (1987). Isolation of a T-lymphotropic virus from domestic cats with an immunodeficiency-like syndrome. *Science* **235**, 790-793.

Pedersen, N. C., Yamamoto, J. K., Ishida, T. & Hansen, H. (1989). Feline immunodeficiency virus infection. *Vet Immunol Immunopathol* **21**, 111-129.

Plotkin, J., Prockop, S. E., Lepique, A. & Petrie, H. T. (2003). Critical role for CXCR4 signaling in progenitor localization and T cell differentiation in the postnatal thymus. *J Immunol* **171**, 4521-4527.

Rzhaninova, A. A., Gornostaeva, S. N. & Goldshtein, D. V. (2005). Isolation and phenotypical characterization of mesenchymal stem cells from human fetal thymus. *Bull Exp Biol Med* **139**, 134-140.

Sanos, S. L., Nowak, J., Fallet, M. & Bajenoff, M. (2011). Stromal cell networks regulate thymocyte migration and dendritic cell behavior in the thymus. *J Immunol* **186**, 2835-2841.

Steiniger, B. S., Wilhelmi, V., Seiler, A., Lampp, K. & Stachniss, V. (2014). Heterogeneity of stromal cells in the human splenic white pulp. Fibroblastic reticulum cells, follicular dendritic cells and a third superficial stromal cell type. *Immunology* **143**, 462-477.

Sugiyama, T., Kohara, H., Noda, M. & Nagasawa, T. (2006). Maintenance of the hematopoietic stem cell pool by CXCL12-CXCR4 chemokine signaling in bone marrow stromal cell niches. *Immunity* **25**, 977-988.

Takahama, Y. (2006). Journey through the thymus: stromal guides for T-cell development and selection. *Nat Rev Immunol* **6**, 127-135.

Tomei, A. A., Siegert, S., Britschgi, M. R., Luther, S. A. & Swartz, M. A. (2009). Fluid flow regulates stromal cell organization and CCL21 expression in a tissue-engineered lymph node microenvironment. *J Immunol* **183**, 4273-4283.

Umemoto, E., Otani, K., Ikeno, T., Verjan Garcia, N., Hayasaka, H., Bai, Z., Jang, M. H., Tanaka, T., Nagasawa, T., Ueda, K. & Miyasaka, M. (2012). Constitutive plasmacytoid dendritic

cell migration to the splenic white pulp is cooperatively regulated by CCR7- and CXCR4-mediated signaling. *J Immunol* **189**, 191-199.

Walsh, S., Jefferiss, C., Stewart, K., Jordan, G. R., Screen, J. & Beresford, J. N. (2000). Expression of the developmental markers STRO-1 and alkaline phosphatase in cultures of human marrow stromal cells: regulation by fibroblast growth factor (FGF)-2 and relationship to the expression of FGF receptors 1-4. *Bone* **27**, 185-195.

Willems, L., Li, S., Rutgeerts, O., Lenaerts, C., Waer, M. & Billiau, A. D. (2011). IL-7 is required for the development of the intrinsic function of marginal zone B cells and the marginal zone microenvironment. *J Immunol* **187**, 3587-3594.

Willett, B. J., Picard, L., Hosie, M. J., Turner, J. D., Adema, K. & Clapham, P. R. (1997). Shared usage of the chemokine receptor CXCR4 by the feline and human immunodeficiency viruses. *J Virol* **71**, 6407-6415.

Yu, H. R., Sung, M. L., Kuo, H. C., Lin, C. H. & Chen, C. N. (2015). Shear Stress Modulates Resistin-Induced CC Chemokine Ligand 19 Expression in Human Aortic Endothelial Cells. *J Cell Physiol* **230**, 2120-2127.

Zotes, T. M., Spada, R., Mulens, V., Pérez-Yagüe, S., Sorzano, C. O., Okkenhaug, K., Carrera, A. C. & Barber, D. F. (2013). PI3K p110δ is expressed by gp38(-)CD31(+) and gp38(+)CD31(+) spleen stromal cells and regulates their CCL19, CCL21, and LTβR mRNA levels. *PLoS One* **8**, e72960.

Chapter 5b

Effect of lymphoid tissue stromal cells on FIV infection and replication in PBMC

Adapted from:

Roukaerts IM, Van Bockstael S, Acar DD, Desmarets LM and Nauwynck HJ, 2016. Manuscript in preparation.

Abstract

Feline immunodeficiency virus (FIV) has a broad tropism among cells of the immune system, infecting monocytes/macrophages, and both T- and B-lymphocytes. Replication in these cells takes a toll on the immune system, eventually leading to an acquired immunodeficiency. Important changes occur in lymphoid tissue organization during the FIV disease course, and recently it was shown that while FIV replication is absent in blood circulating leukocytes, replication is active in the lymph nodes. Recently, we isolated and characterized feline mesenchymal stromal cells from different lymphoid tissues. It was investigated if these cells influenced the susceptibility of leukocytes for FIV infection and if they altered FIV replication in these cells. Co-culture with lymphoid mesenchymal stromal cells induced expression of the FIV receptors, CD134 and CXCR4, on PBMC. Activated endothelium and lymph node mesenchymal cells were able to elevate FIV infection (percentage of infected cells) in PBMC. Furthermore, lymphoid stromal cells from bone marrow and lymph node were able to enhance spread of FIV infection in PBMC cultures.

5.1. Introduction

Worldwide, up to 30% of the cat population is infected with the feline immunodeficiency virus (FIV) (Yamamoto *et al.*, 2007). This important pathogen is the feline homologue of the human immunodeficiency virus (HIV), and has a similar disease course. Following infection, flue-like symptoms may be observed for a short period of time. Hereafter, the disease goes silent, with a long asymptomatic phase that may last for many years. Eventually, the FIV infected cat will develop clinical signs of the acquired immunodeficiency, leading to secondary infections that are often the cause of death (O'Neil *et al.*, 1996). Like HIV, FIV infects cells of the immune system including cells of the myeloid lineage, T-lymphocytes, and B-lymphocytes (Brown *et al.*, 1991; Dow *et al.*, 1999; English *et al.*, 1993). FIV susceptible cells express the primary receptor CD134, an activation marker belonging to the tumor necrosis factor receptor superfamily, and the chemokine receptor CXCR4 (Pedersen *et al.*, 1987; Shimojima *et al.*, 2004). Under the influence of neutralizing antibodies, FIV may develop escape mutants with reduced need for CD134-binding to induce infection (Hartmann *et al.*, 2012).

Early in FIV infection, secondary lymphoid tissues show signs of a boosted immunity, with an increased influx of leukocytes around the high endothelial venules (HEV) and the development of numerous germinal centers (Bach *et al.*, 1994; Huisman *et al.*, 2004). Heavy FIV infection is observed in the thymus, causing disappearance of the cortical thymocytes, and concomitant involution of the thymic cortex (Huisman *et al.*, 2004; Orandle *et al.*, 1997). Active FIV replication in the thymus leads to the influx of immune cells that form follicles and germinal centers in the thymic medulla (Huisman *et al.*, 2004; Woo *et al.*, 1997). FIV infection also causes alterations in the bone marrow, an increased cellularity as a result of myeloid hyperplasia is detected, and hematopoietic precursor cells may also be infected (Beebe *et al.*, 1992; Huisman *et al.*, 2004; Shelton *et al.*, 1990). When the cat's body can no longer resupply immune cells that are depleted due to direct FIV replication and bystander apoptosis, an involution and depletion of the immune cells in the secondary lymphoid organs is seen (Rideout *et al.*, 1992). Furthermore, the functional organization of these organs by stromal cells is lost as well. T-cell numbers decline rapidly, while plasma viremia becomes detectable once again. At this stage, severe immunodeficiency causes rapid disease progression, leading to death by secondary infections.

The lymphoid tissue stromal cells shape the network in which hematopoietic cells reside. They create a microenvironment needed for proper function and organization of the different lymphoid tissues. Stromal cells produce extracellular matrix proteins, communicate with the hematopoietic cells through cytokine production and contact, and lay chemotactic tracks for compartmentalization of the different cell types in these tissues (Bunting *et al.*, 2011; Mebius & Kraal, 2005; Mercier *et al.*, 2012; Seibert *et al.*, 1995). Recently it was shown by Eckstrand and colleagues that FIV replication is silent in leukocytes circulating in blood, but active in leukocytes in the lymph nodes of FIV-infected cats during the asymptomatic phase (Eckstrand *et al.*, 2016). This raises the hypothesis that lymphoid organs may serve as a viral replication reservoir during FIV infection. The lymphoid micro-milieu may activate and/or support FIV replication in leukocytes. Previously, we have isolated, cultured and characterized lymphoid stromal cells from feline bone marrow, thymus, lymph nodes, and spleen (Roukaerts *et al.*, 2016). In the present study we investigated if stromal cells from these organs can influence the sensitivity of leukocytes for FIV infection, and if these cells influence FIV replication in FIV infected leukocytes.

5.2. Materials and Methods

5.2.1. Cells

Feline mesenchymal stromal cells from lymph node and bone marrow (Roukaerts et al., 2016), and feline endothelial cells from vena cava (Olyslaegers *et al.*, 2013) were maintained in DMEM supplemented with 10 % fetal bovine serum (FBS), 100 U/ml penicillin, 0.1 mg/ml streptomycin, 0.1 mg/ml gentamycin, 1 % non-essential amino acids 100 x, 2 mM sodium pyruvate.

Peripheral blood mononuclear cells (PBMC) were collected from fresh blood obtained by venipuncture of the jugular vein from 3 male neutered specific pathogen free cats (EC2015/79). PBMC were purified by density centrifugation on Ficoll Paque (GE Healthcare). PBMC cultures were established by stimulation for 3 days with 2.5 µg/ml concanavalin A (Sigma-Aldrich), after which 100 U/ml interleukin 2 (IL2) (Roche) was added for the duration of the culture. PBMC cultures were kept in lymphocyte medium containing RPMI (Gibco BRL), 10% FBS, 100 U/ml penicillin, 0.1 mg/ml streptomycin, 1% non-essential amino acids (100 x), and 2 mM sodium pyruvate.

5.2.2. Virus

Virus was grown by transfecting GFox cells with a plasmid containing the FIV-PPR provirus and allowing virus replication for 2 days. Stocks were titrated by end-point dilution on GFox cells. Virus material was obtained through the AIDS Reagent Program, Division of AIDS, NIAID, NIH: FIV-PPR from Dr. Elder JH (Phillips *et al.*, 1990).

5.2.3. Co-culture of venous endothelial cells or lymphoid mesenchymal cells with PBMC

Endothelial cells and mesenchymal cells were seeded at 25,000 cells/ml in 24-well plates in double. Freshly isolated PBMC were co-cultured with these cells at a density of 250,000 PBMC/ml 12h prior to FIV inoculation. PBMC that had attached to the endothelial cells or mesenchymal stromal cells were inoculated by adding 200 µl of $10^{3.28}$ TCID50/ml FIV inoculum for 1.5 h to the wells. PBMC that had not attached during co-culture or were inoculated prior to co-culture, were inoculated by spinoculation. Briefly, PBMC were collected by centrifugation and resuspended in virus inoculum containing $10^{3.28}$ TCID50/ml at a concentration of 1,000,000 cells/ml inoculum. The PBMC inoculum mixture was transferred to 6-well plates and spun at 1200 xg for 1h at 32°C. After centrifugation, the plates were incubated at 37°C for an additional 30 min. Following inoculation, all cells were washed, and co-culture was continued for 48h, samples were collected at indicated time points.

5.2.4. Immunofluorescence staining

5.2.4.1. Cell markers

The different cell types in the PBMC culture were stained with markers against CD3 (Nishimura *et al.*, 2004) for T-lymphocytes, CD21 (clone CA2.1D6, Biorad) for B-lymphocytes and CD13 (clone 25-2B, VMRD) for myeloid cells. Staining was performed either on glass inserts for cells that adhered during the first 24 h post inoculation, or in suspension just after isolation and of the population that remained in suspension during culture. Adherent cells were fixed with 1% paraformaldehyde and washed with phosphate buffer saline containing Mg^{2+} and Ca^{2+} (rPBS) and 300mM glycine. Next, the cell marker antibodies were diluted in rPBS with 10 % normal goat serum (NGS) and incubated with the cells for 1 h at 37°C. After washing, the primary antibodies were visualized with fluorescently labeled goat-anti-mouse polyclonal antibodies for 1 h at 37°C, and nuclei were counter-stained with Hoechst (Molecular

Probes). Cells in suspension were fixed in 1% paraformaldehyde and washed with regular PBS. They were incubated with the primary antibodies diluted in PBS with 10 % NGS at 37°C for 1 h with gentle shaking. Primary antibodies were labeled with matching fluorescent conjugated goat-anti-mouse polyclonal antibodies (Invitrogen), and nuclei were labeled with Hoechst. Following staining, the suspension cells were cytospined onto microscope slides for analysis by fluorescent microscopy.

5.2.4.2. FIV receptors

FIV receptor staining was performed on life cells at 0°C (on ice). Briefly, cells were incubated for 1.5 h in ice cold PBS containing 10 µg/ml anti-CXCR4 (IgG2a, clone 374606, R&D Systems) and 20 µg/ml anti-CD134 (IgG1, clone 7D6, AbD Serotec), with gentle shaking. After incubation with the primary antibody mix, cells were washed and fixed with 1% paraformaldehyde in PBS for 10 minutes at room temperature. The primary antibody mix was visualized with isotype specific goat anti-mouse secondary antibodies, GαM-IgG2a-AF488 and GαM-IgG1-AF594, respectively.

5.2.4.3. FIV infection staining

PBMC were stained for FIV infection after fixation with 1 % paraformaldehyde in PBS for 10 minutes at room temperature. Next, cells were spun onto silicon coated microscope slides and permeabilized with 0.5 % triton-X100 for 15 minutes at 37°C. The samples were incubated with 13.3 µg/ml anti-FIV Gag (PAK3-2C1, CMI) or 13.3 ug/ml anti-FIV Env (SU1-30, CMI) in PBS containing 10 % normal goat serum at 37°C for 1,5 h. The primary antibody was visualized with a goat anti-mouse IgG1-AF594 conjugated antibody. Samples were counterstained with Hoechst nucleus staining. All stainings were analyzed by confocal laser scanning microscopy (Leica TSC SPE system with Leica DM2500 CQS microcope). Pictures were taken with the Leica LAS X interface. Subsequent processing of the pictures was performed with the ImageJ software (NIH).

5.2.5. FIV *gag* qPCR

Supernatant from FIV infected cells was analyzed at various time point post infection for the amount of viral RNA using an FIV *gag* qPCR. A one step quantitative real-time RT-PCR with SYBR Green detection was performed with primers for the FIV capsid protein (forward primer *gag*-1356bp: AAC AAG CAG AAS CWA GAT T; reverse primer *gag*-1455bp: CGA GGA GAT TTA GCC TTT). Synthetic FIV standard RNA was produced *in vitro*, as follows. Viral RNA was isolated from FIV-PPR stock using the QIAamp Viral RNA Mini Kit (Qiagen). From this viral RNA, cDNA was made using the

SuperScript™ III First-Strand Synthesis System for RT-PCR (Invitrogen). For this reaction, 5 ng viral RNA was incubated with 2 µM reverse primer for FIV gag and 10 mM dNTP mix for 5 min at 65°C. After cooling on ice, an equal amount of cDNA synthese mix containing 10x RT buffer, 25 mM $MgCl_2$, 100 mM DTT, 40 U RNase OUT and 200 U Superscript II RT was added and incubated at 50°C for 50 min. The reaction was terminated by heating at 85°C for 5 min. RNA was cleared from the produced cDNA by incubation with RNase H for 20 min at 37°C. The produced cDNA was amplified with Heculase II polymerase (Agilent Technologies Inc.) in a reaction with the FIV gag forward primer extended with a T7-promotor and FIV gag reverse primer. The reaction was cycled with an initial denaturation at 98°C for 1 min, after which 30 cycles of 95°C for 20 s, 50°C for 20 s and 68°C for 1 min followed. A final extension took place for 4 min at 68°C. The 50 µl reaction mix contained 5x Herculase II buffer, 25 mM dNTP mix, 1.25 µl forward and reverse primer, 0.5 µl Herculase II polymerase, and 2 µl cDNA template. From this FIV gag cDNA, the synthetic FIV mRNA standard was transcribed. The cDNA was transcribed for 1 h at 37°C in a reaction mix containing 10x transcription buffer, 500 mM rNTP, and 20 U T7 RNA polymerase-Plus Enzyme Mix. The template cDNA was removed by incubation with 2 U DNAse for 15 min at 37°C. The DNAse was inactivated at 70°C for 10 min. The amount of synthetic FIV Gag RNA was determined by spectroscopic measurement with the Nanodrop 2000 system.

RNA was extracted from cell culture medium using the QIAamp Viral RNA Mini Kit (Qiagen). To 17 µl of One step Precision Master Mix (Primer Design), 3 µl of sample was added for a final reaction volume of 20 µl. The One step Precision Master Mix contains SYBR® Green and ROX for detection of amplification, and was cycled on a Step One Plus™ real-time PCR system (Applied Biosystems). Reverse transcription took place at 55°C for 10 min, followed by an inactivation of the reverse transcriptase and activation of the DNA polymerase at 98°C for 10 min. Next, amplification was allowed for 40 cycles of 10 s at 95°C and 1 min at 56°C, fluorescence was detected every cycle. A first-derivative melting curve analysis was performed by heating the reaction to 95 °C for 15 s, cooling to 60 °C for 1 min and reheating to 95°C at 0.3°C increments. The standard curve was set-up by a serial ten-fold dilution of the synthetic FIV Gag RNA (Efficiency: 104.4%, R^2:0.991).

5.3. Results

5.3.1. Influence of lymphoid mesenchymal cells on FIV susceptibility of PBMC

The PBMC fraction of the blood consists of monocytes and B- and T-lymphocytes; RBC, platelets and granulocytes (mast cells, neutrophiles and eosinophiles) are removed by density centrifugation. The amount of monocytes, B-cells and T-cells in the PBMC fraction was determined immediately after isolation for each cat (Figure 1a). Myeloid cells (monocytes and remaining granulocytes) were identified by the expression of aminopeptadase N (CD13), and represented 16 ± 3% of the PBMC. B-lymphocytes are characterized by the expression of complement receptor 2 (CD21), and corresponded to 12 ± 4 % of the isolated PBMC. T-lymphocytes can be recognized by expression of the T-cell receptor complex (CD3), with a total of 56 ± 10 %.

Immediately after isolation, PBMC did not express the FIV receptors CD134 and CXCR4 (Fig. 1b). Culturing PBMC *in vitro* is enough to trigger the recruitment of intracellular pools of CXCR4 to the plasma membrane (Troth *et al.*, 2008). Culturing cells for 24 h while allowing plastic adherence resulted in more than 85% of the PBMC expressing CXCR4, both on suspension cells and adhered cells (Fig. 1b). To stimulate *in vitro* proliferation and induce expression of the FIV receptors, PBMC are usually stimulated with concanavalin A (conA), a plant lectin that induces mitoses, for 3 days. This initial stimulation is followed by interleukin 2 (IL2), a cytokine important for T-lymphocyte survival, for duration of the culture. After stimulation with conA and IL2, the expression of CXCR4 declined, and stabilized at around 30% $CXCR4^+$ cells. Unlike CXCR4, CD134 was not yet expressed on PBMC 24 h post isolation (without stimulation), but was up-regulated to 16 ± 3% after 3 days of conA stimulation. Four days of IL-2 incubation further boosted CD134 expression, reaching maximum levels of 33 ± 4% (Fig. 1b). The mitogenic stimuli also altered the phenotype of the T-cells from small and round to cells with an increased size, extended cytoplasm, and the appearance of plasma membrane protrusions. When culturing PBMC in presence of conA and IL2, monocytes and B-lymphocytes were not maintained in the culture, with numbers declining steeply resulting in 5% B-cells. Monocytes are partially lost due to adherence to the culture plastic, less than 1% monocytes were found in PBMC cultures after 15 days of culture (Fig. 1a).

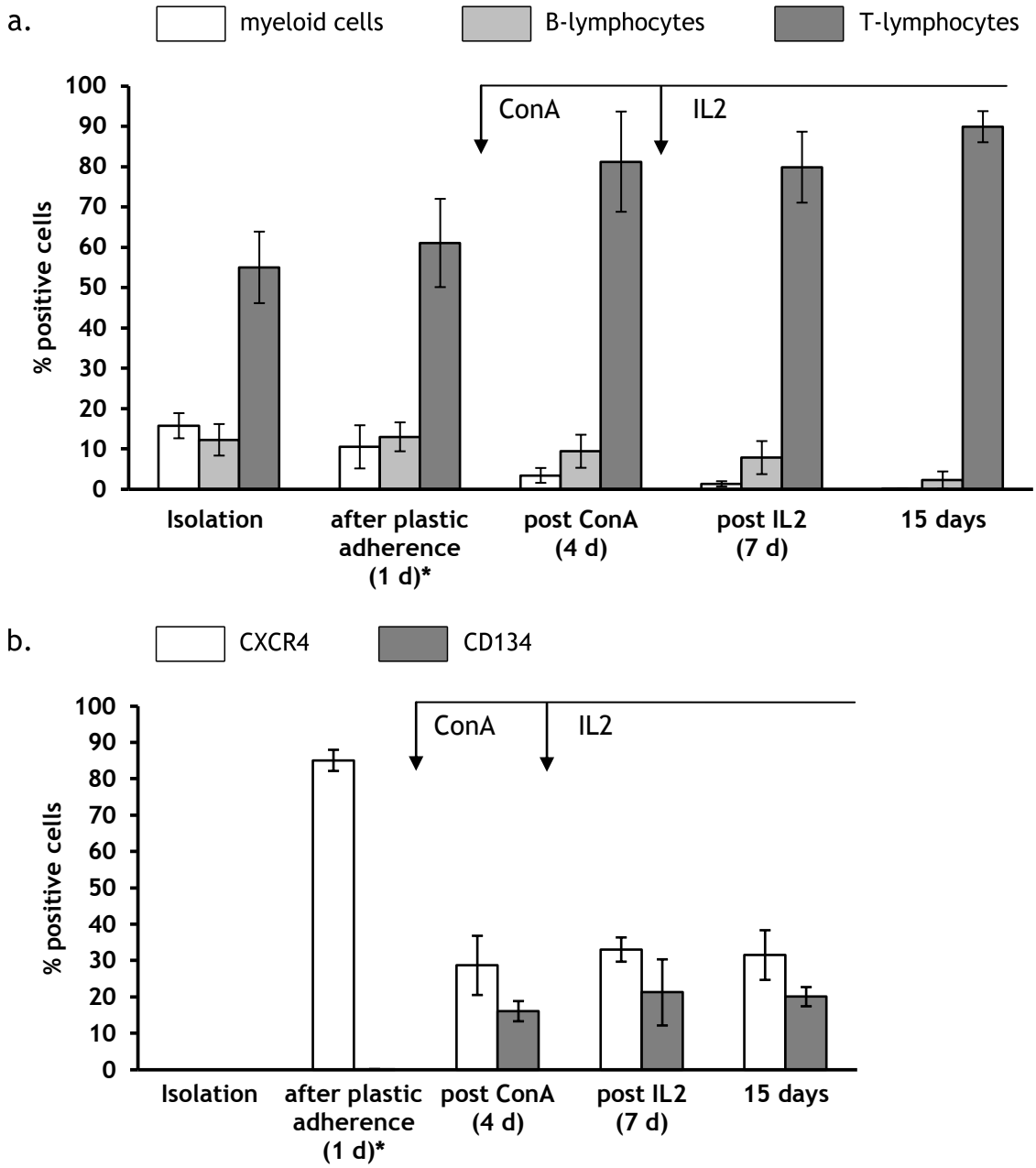

Figure 1: Change in cell-types present in the PBMC culture and expression of the FIV receptors CXCR4 and CD134 over time in presence of conA and IL2 stimulation. (a) PBMC cell-type composition; myeloid cells as detected with CD13 (white), B-lymphocytes as detected with CD21 (grey), T-lymphocytes as detected with CD3 (dark grey). (b) Expression of the FIV receptors CXCR4 (white) and CD134 (grey) in PBMC cultures under influence of conA and IL2 stimulation, initiated after plastic adherence. *Stained both on cells that have adhered to the culture plastic and cells that remained in suspension after 1 day of culture. Subsequent time points were stained on suspension cells only.

To be able to influence the susceptibility of feline PBMC for FIV, lymphoid mesenchymal stromal cells should be able to induce CD134 and CXCR4 expression. Feline endothelial cells are used as a control, representing the blood vessel wall, since no FIV replication is detected in blood. Freshly isolated cells were co-cultured for 12 h with venous endothelial cells to represent the blood vessel wall, and mesenchymal

stromal cells from bone marrow and lymph node. To simulate an inflammatory environment, the endothelial and mesenchymal cells were incubated with 1 ng/ml TNF-α for 12 h prior to co-culture with PBMC. Cell membrane expressed CXCR4 reached levels above 80% for all three cats with every cell type after the 12 h incubation period. Co-culture with the different cells also induced expression of CD134 on the PBMC, reaching 11-28% after 12 h. Freshly isolated PBMC and PBMC in culture for 24 h without stimulation (Fig. 1b), can be used as a baseline control for these results. No significant difference (kruskal-wallis test) was found between the different cell-types with or without TNF-α pre-incubation (Fig. 2). Also, no difference was found between venous endothelial cells and lymphoid mesenchymal cells.

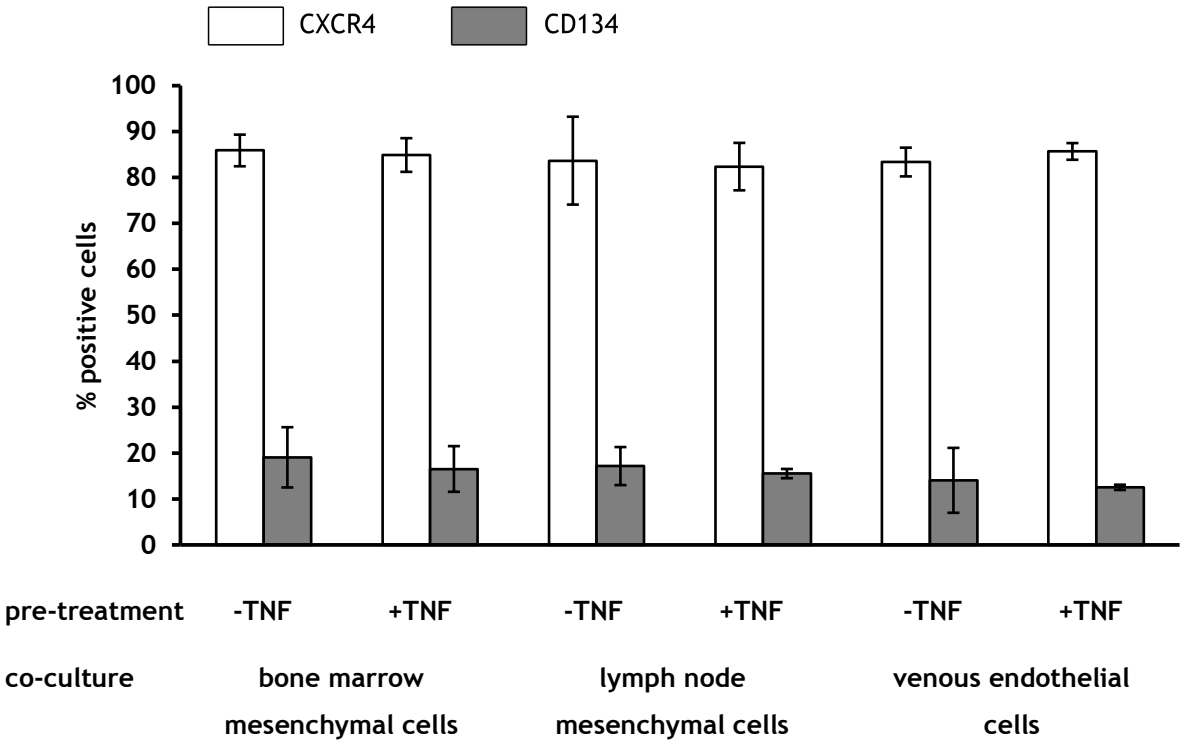

Figure 2: Expression of CXCR4 and CD134 on PBMC after a 12 h co-culture with lymphoid mesenchymal cells and endothelial cells. B: bone marrow mesenchymal cells, L: lymph node mesenchymal cells, E: venous endothelial cells. Cells were pre-treated with TNF-α for 12 h prior to PBMC co-culture (+) or untreated (-).

Since mesenchymal cells from lymphoid tissues and venous endothelial cells were able to induce the expression of the FIV receptors, it was tested if these cells could alter FIV sensitivity of PBMC. After a 12 h co-culture period, PBMC were inoculated with FIV, and further cultured together with venous endothelial cells or lymphoid mesenchymal cells. Samples were taken at 12, 36 and 48 h post inoculation, covering one replication cycle. After 12 h, viral proteins expression was barely detectable. Infection percentages remained low, but detectable at 36 (not shown) and 48 h (Fig. 3). No statistical

difference (kruskal-wallis test) was found between the FIV infection percentages in PBMC co-cultured with the different cell types. This lack of significance is partly due to the great variance in infection percentage between PBCM isolated from cat 1 and 2, and cat 3. Overall the infection percentage was much lower in cat 3 compared to the other cats, except for PBMC co-cultured with mesenchymal cells of the lymph nodes. Here FIV infection percentages increased in cat 3, but are lower compared to co-culture with bone marrow mesenchymal cells or endothelial cells for cat 1 and 2. Although not statistically different, FIV infection percentages in PBMC co-cultured with endothelial cells stimulated with TNF-α are higher for cat 1 and 2. Virion production was measured at the different time points by RT-qPCR, but did not reach levels higher than those measured at 0 h post inoculation, representing remaining inoculation virus (data not shown).

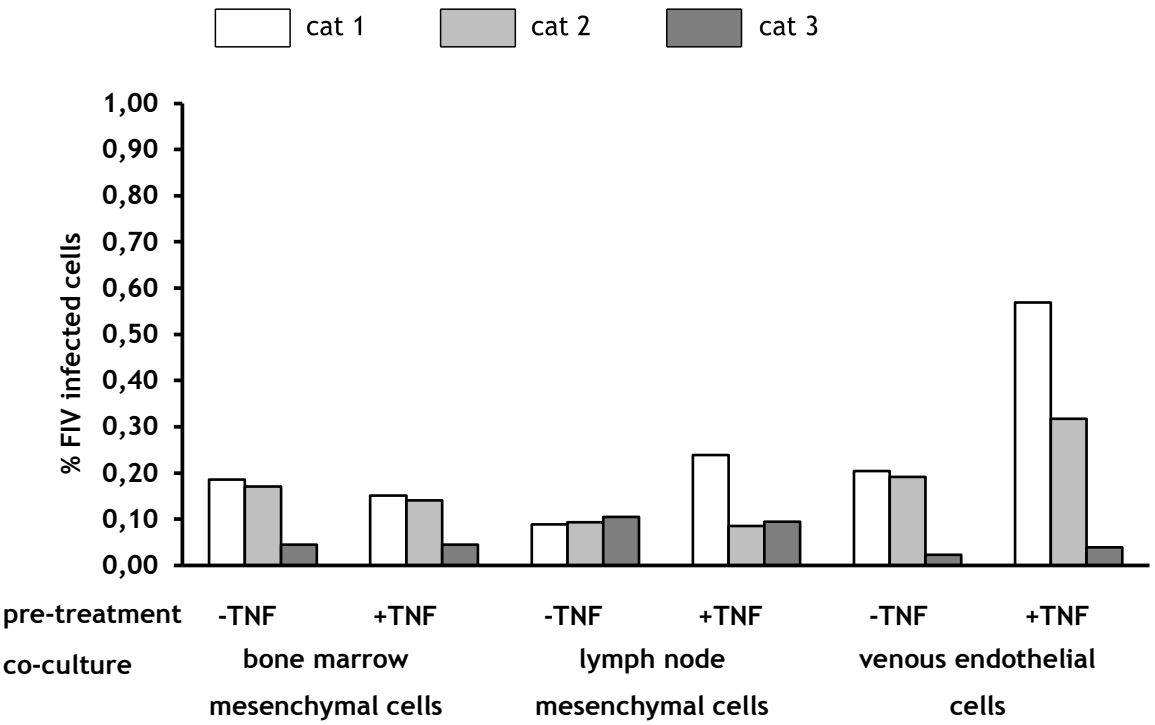

Figure 3: Percentage of FIV infected cells in PBMC co-cultured with lymphoid mesenchymal cells and venous endothelial cells for 48 h. Cells were pre-treated with TNF-α for 12 h prior to PBMC co-culture (+) or untreated (-). Results are presented for every cat; cat 1 (white), cat 2 (grey), cat 3 (dark grey).

5.3.2. Influence of lymphoid mesenchymal cells on FIV replication in FIV infected PBMC

Next, it was tested if the mesenchymal stromal cells could influence FIV replication in PBMC already infected with FIV. PBMC (cat 1) were artificially stimulated with conA and IL2, and inoculated with FIV immediately prior to co-culture with mesenchymal cells from bone marrow and lymph node. Lipopolysaccharide (LPS) was used as a

control for inflammatory conditions. Infection percentages were determined on one and four days post-inoculation. Already on day 1, infection percentages were much higher in PBMC stimulated with LPS or co-cultured with the lymphoid mesenchymal cells compared to control PBMC in regular lymphocyte medium. The effect was even more prominent on day 4 post inoculation.

The amount of virus in the cell culture medium was determined by RT-qPCR. After 4 days of co-culture, a one $\log_{10}$ increase was measured compared to day 1, but no difference was observed between the different culture conditions.

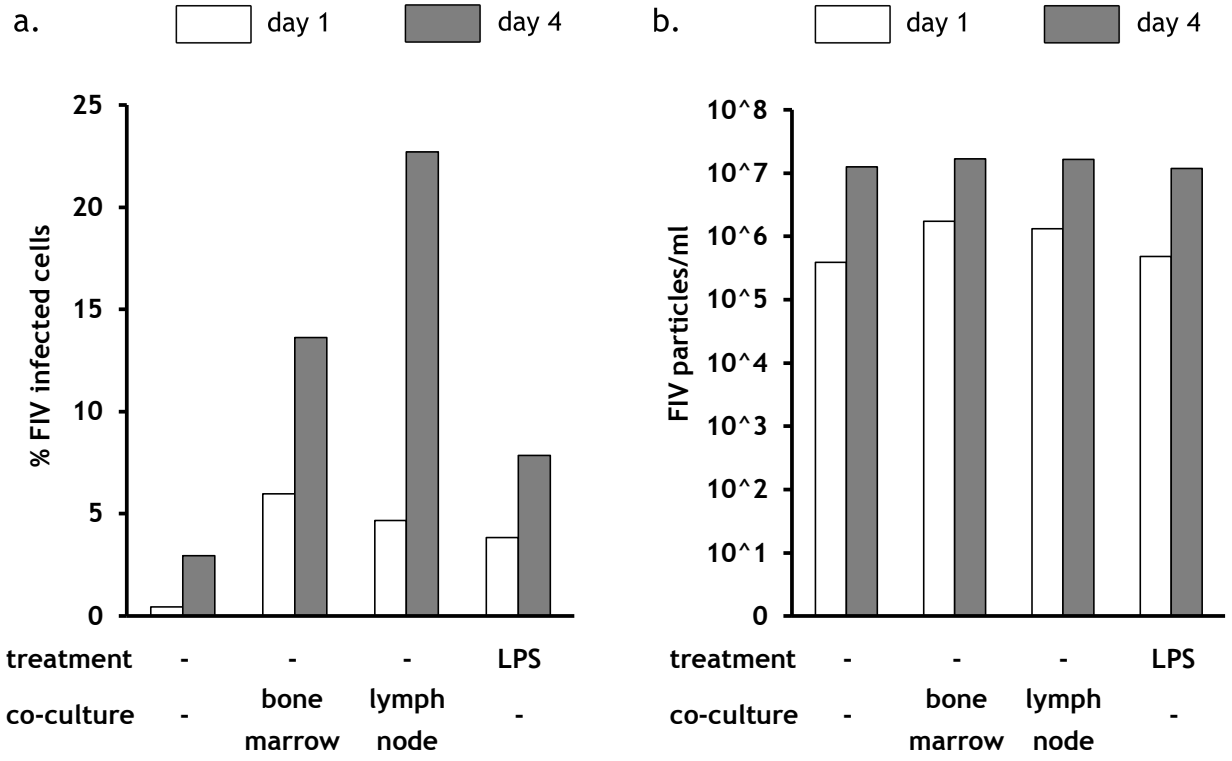

Figure 4: Percentage of FIV infected cells in PBMC inoculated with FIV prior to co-culture with lymphoid mesenchymal cells and the amount of virus particles shed in the medium. (a) Percentage of FIV infected cells in FIV inoculated PBMC co-cultured with bone marrow or lymph node mesenchymal stromal cells, or cultured in presence of LPS. IL2 stimulated inoculated PBMC were used as a control. Infection percentages were determined on day 1 (white) and day 4 (grey) post co-culture. (b) Amount of FIV virus particles in culture medium of FIV inoculated PBMC co-cultured with bone marrow or lymph node mesenchymal stromal cells, or cultured in presence of LPS. IL2 stimulated inoculated PBMC were used as a control. An FIV qPCR on the culture medium was performed on day 1 (white) and day 4 (grey) post co-culture.

5.4. Discussion

FIV affects the structure and function of both primary and secondary lymphoid organs in infected cats. Recently, active replication of FIV was found in the lymph nodes, while this is absent in blood. Therefore it was investigated whether lymphoid stromal

cells are able to influence the susceptibility of PBMC for FIV infection and if they could alter FIV replication in these cells.

The expression of the FIV receptors, CD134 and CXCR4, was absent on freshly isolated feline PBMC, and was up-regulated after artificial stimulation or co-culture with venous endothelial cells and mesenchymal stromal cells originating from bone marrow and lymph nodes. CD134 is up-regulated after initial stimulation of immune cells, and provides additional stimulation signaling securing prolonged proliferation, survival and expression of cytokines (Salek-Ardakani & Croft, 2006). Willett and colleagues described that CD134 expression is predominant on feline $CD4^+$ T-lymphocytes, but also occurs to a lesser extent on $CD8^+$ T-lymphocytes, B-cells and macrophages (Willett *et al.*, 2007). Expression of CD134 on macrophages can be up-regulated after LPS stimulation (Willett *et al.*, 2007). On naïve cells, induction of CD134 expression is slow, and onset may take from 12 h up to 5 days. Memory cells, on the other hand, can show expression as early as 1 h post activation (Croft, 2010). Our results also show that CD134 expression on PBMC is slow after artificial stimulation, and is dependent on activation signaling provided by conA and IL-2 stimulation. It has been shown before that IL2 can enhance and prolong CD134 expression (Croft, 2010). After co-culture with lymphoid mesenchymal cells and venous endothelial cells, comparable levels of CD134 were detected already after 12 h of co-culture. This shows that the co-culturing provides stimulation, either direct or indirect, that causes rapid CD134 expression. Surprisingly no difference was found between the blood vessel wall control (venous endothelial cells) and the lymphoid mesenchymal cells. Although these immortalized endothelial cells seem phenotypically unaltered, it is possible that they do produce different cytokines *in vitro* compared to the *in vivo* situation. Furthermore, it is likely that they are able to communicate with the PBMC that are added during co-culture. Although CXCR4 expression is absent on freshly isolated cells, culture of PBMC was enough to induce CXCR4 expression as has been shown before (Saleh *et al.*, 2007; Troth *et al.*, 2008). The increased expression of CXCR4 *ex vivo* might be due to the absence of its ligand stromal derived factor-1 (SDF1/CXCL12) that induces internalization of the receptor after binding. However, CXCR4 is down-regulated after mitogenic stimulation of PBMC with conA, as was shown here, or phytoheamaglutinin (Bermejo *et al.*, 1998). It can thus be concluded that lymphoid stromal cells are more potent inducers of CD134 expression on PBMC, while maintaining CXCR4 expression.

Because the lymphoid mesenchymal cells and endothelial cells were able to induce FIV receptor expression, their influence on FIV infection sensitivity of PBMC was tested. Although there were no statistical significant differences in FIV sensitivity of PBMC co-cultured with the different cell-types, some promising observations were made. One cat (cat 3) showed much lower infection percentages compared to the other two (cat 1 & 2). When looking at the composition of the PBMC population upon isolation, this cat has a lower proportion of T-cells and monocytes compared to the other cats. It is known for HIV that multiple host factors influence the susceptibility to the virus and the progression of the disease (Lama & Planelles, 2007). This probably holds true for cats as well. For instance, the long-term FIV infection study by the group of Murphy B recently demonstrated the existence of a long-term nonprogressor cat (Eckstrand *et al.*, 2016). Although overall infection percentages were low in PBMC of cat 3, upon co-cultured with mesenchymal cells of the lymph nodes, infection percentages matched those of the other cats. It has been shown that while CXCR4 expression is absent on freshly isolated feline PBMC, it is high on cells residing in lymphoid tissues (Troth *et al.*, 2008). The FIV isolate used for inoculation, FIV-PPR, uses both CD134 and CXCR4 to establish infection. However, it has been shown that in cells expressing high levels of CXCR4, the CD134 interaction becomes dispensable (de Parseval *et al.*, 2004). Thus, co-culture with mesenchymal cells from the lymph node might increase CXCR4 concentrations on the cell surface of PBMC, leading to higher FIV infection percentages.

An elevated FIV infection percentage in PBMC of cat 1 and 2 when co-cultured with TNF-α treated venous endothelial cells was observed. Stimulation of these endothelial cells with TNF-α induces the expression of several leukocyte adhesion factors (Olyslaegers *et al.*, 2013), allowing leukocytes to actively interact with these cells. Furthermore, TNF-α can induce the expression of CD134 ligand (CD134L/CD252) on the cell surface of vascular endothelial cells (Imura *et al.*, 1996), and thereby adhere activated leukocytes and induce CD134/CD134L signaling on both sides. CD134L exists as a membrane anchored and soluble form, and signaling through the cytoplasmic tail of membrane bound CD134L is believed to increase cytokine production in vascular endothelium (Kotani *et al.*, 2002). For HIV it was shown that stimulation of resting CD4+ T-cell with CCL19/21, a cytokine expressed by lymphoid tissues and activated endothelium to attract leukocytes (Chang & Turley, 2015; Yu *et al.*, 2015), can increase integration of the HIV provirus upon infection (Saleh *et al.*, 2007). Activation causes upregulation of both FIV receptors on lymphocytes and

macrophages, and increases signaling that actives transcription factors that can bind the FIV promoter region enhancing transcription of FIV mRNA (Busillo & Benovic, 2007; Croft, 2010; Sparger *et al.*, 1992). Activation of leukocytes via direct cellular interactions and indirectly through cytokines might create a favorable environment for FIV infection at inflammatory sites, but further research will be needed.

Results might suggest that FIV susceptibility and replication in PBMC of cat 1 and 2 relies on different processes compared to cat 3. Cat 1 and 2 showed increased FIV infection percentages in the activated endothelium environment, while cat 3 showed increased FIV infection in the CXCR4 inducing lymph node environment.

Preliminary results suggest that mesenchymal cells from bone marrow and lymph node can enhance FIV replication efficiency in infected PBMC (cat 1), at least for some cats. Co-culture of inoculated PBMC with mesenchymal stromal cells was even more potent in increasing the number of infected PBMC than an artificial stimulus with LPS. Further work, involving a greater number of cats and a more fine-tuned lymphoid tissue model, is needed to confirm these first results. This will allow us to confirm if and how lymphoid tissues sustain ongoing FIV replication, and which factors and processes are involved. Additionally, results from more cats could also shed some light on reasons for the differences in FIV progression between cats. Recent work showed active FIV replication in lymph nodes even in the asymptomatic phase of the FIV disease course (Eckstrand *et al.*, 2016). It will be interesting to investigate if mesenchymal stromal cells from lymphoid tissue are able to reactivate FIV replication in latently infected cells, and by doing so assure replenishing the FIV reservoir.

Acknowledgements

We thank Ytse Noppe for her excellent technical support. IDMR was supported by Agency for the Promotion of Innovation through Science and Technology in Flanders (IWT-Vlaanderen). SVB was supported by the Special Research Fund of Ghent University.

References

Aguzzi, A., Kranich, J. & Krautler, N. J. (2014). Follicular dendritic cells: origin, phenotype, and function in health and disease. *Trends Immunol* **35**, 105-113.

Alt, C., Laschinger, M. & Engelhardt, B. (2002). Functional expression of the lymphoid chemokines CCL19 (ELC) and CCL 21 (SLC) at the blood-brain barrier suggests their involvement in G-protein-dependent lymphocyte recruitment into the central nervous system during experimental autoimmune encephalomyelitis. *Eur J Immunol* **32**, 2133-2144.

Bach, J. M., Hurtrel, M., Chakrabarti, L., Ganiere, J. P., Montagnier, L. & Hurtrel, B. (1994). Early stages of feline immunodeficiency virus infection in lymph nodes and spleen. *AIDS Res Hum Retroviruses* **10**, 1731-1738.

Beebe, A. M., Gluckstern, T. G., George, J., Pedersen, N. C. & Dandekar, S. (1992). Detection of feline immunodeficiency virus infection in bone marrow of cats. *Vet Immunol Immunopathol* **35**, 37-49.

Bermejo, M., Martín-Serrano, J., Oberlin, E., Pedraza, M. A., Serrano, A., Santiago, B., Caruz, A., Loetscher, P., Baggiolini, M., Arenzana-Seisdedos, F. & Alcami, J. (1998). Activation of blood T lymphocytes down-regulates CXCR4 expression and interferes with propagation of X4 HIV strains. *Eur J Immunol* **28**, 3192-3204.

Bianco, P., Robey, P. G. & Simmons, P. J. (2008). Mesenchymal stem cells: revisiting history, concepts, and assays. *Cell Stem Cell* **2**, 313-319.

Brown, W. C., Bissey, L., Logan, K. S., Pedersen, N. C., Elder, J. H. & Collisson, E. W. (1991). Feline immunodeficiency virus infects both CD4+ and CD8+ T lymphocytes. *J Virol* **65**, 3359-3364.

Bunting, M. D., Comerford, I. & McColl, S. R. (2011). Finding their niche: chemokines directing cell migration in the thymus. *Immunol Cell Biol* **89**, 185-196.

Busillo, J. M. & Benovic, J. L. (2007). Regulation of CXCR4 signaling. *Biochim Biophys Acta* **1768**, 952-963.

Callanan, J. J., McCandlish, I. A., O'Neil, B., Lawrence, C. E., Rigby, M., Pacitti, A. M. & Jarrett, O. (1992). Lymphosarcoma in experimentally induced feline immunodeficiency virus infection [corrected]. *Vet Rec* **130**, 293-295.

Chang, J. E. & Turley, S. J. (2015). Stromal infrastructure of the lymph node and coordination of immunity. *Trends Immunol* **36**, 30-39.

Colić, M. (1991). Cultivation, characterization and modulation of rat thymic non-lymphoid cells in vitro. *Cytotechnology* **5**, 107-115.

Croft, M. (2010). Control of immunity by the TNFR-related molecule OX40 (CD134). *Annu Rev Immunol* **28**, 57-78.

Cyster, J. G. (2000). Leukocyte migration: scent of the T zone. *Curr Biol* **10**, R30-33.

de Parseval, A., Ngo, S., Sun, P. & Elder, J. H. (2004). Factors that increase the effective concentration of CXCR4 dictate feline immunodeficiency virus tropism and kinetics of replication. *J Virol* **78**, 9132-9143.

Derbinski, J., Gäbler, J., Brors, B., Tierling, S., Jonnakuty, S., Hergenhahn, M., Peltonen, L., Walter, J. & Kyewski, B. (2005). Promiscuous gene expression in thymic epithelial cells is regulated at multiple levels. *J Exp Med* **202**, 33-45.

Desmarets, L. M., Theuns, S., Olyslaegers, D. A., Dedeurwaerder, A., Vermeulen, B. L., Roukaerts, I. D. & Nauwynck, H. J. (2013). Establishment of feline intestinal epithelial cell cultures for the propagation and study of feline enteric coronaviruses. *Vet Res* **44**, 71.

Dixit, V. D. (2010). Thymic fatness and approaches to enhance thymopoietic fitness in aging. *Curr Opin Immunol* **22**, 521-528.

Dow, S. W., Mathiason, C. K. & Hoover, E. A. (1999). In vivo monocyte tropism of pathogenic feline immunodeficiency viruses. *J Virol* **73**, 6852-6861.

Eckstrand, C. D., Hillman, C., Smith, A. L., Sparger, E. E. & Murphy, B. G. (2016). Viral Reservoirs in Lymph Nodes of FIV-Infected Progressor and Long-Term Non-Progressor Cats during the Asymptomatic Phase. *PLoS One* **11**, e0146285.

Ehmann, U. K., Shiurba, R. A. & Peterson, W. D. (1986). Long-term proliferation of mouse thymic epithelial cells in culture. *In Vitro Cell Dev Biol* **22**, 738-748.

English, R. V., Johnson, C. M., Gebhard, D. H. & Tompkins, M. B. (1993). In vivo lymphocyte tropism of feline immunodeficiency virus. *J Virol* **67**, 5175-5186.

Engvall, E., Ruoslahti, E. & Miller, E. J. (1978). Affinity of fibronectin to collagens of different genetic types and to fibrinogen. *J Exp Med* **147**, 1584-1595.

Fletcher, A. L., Malhotra, D., Acton, S. E., Lukacs-Kornek, V., Bellemare-Pelletier, A., Curry, M., Armant, M. & Turley, S. J. (2011). Reproducible isolation of lymph node stromal cells reveals site-dependent differences in fibroblastic reticular cells. *Front Immunol* **2**, 35.

Gotter, J., Brors, B., Hergenhahn, M. & Kyewski, B. (2004). Medullary epithelial cells of the human thymus express a highly diverse selection of tissue-specific genes colocalized in chromosomal clusters. *J Exp Med* **199**, 155-166.

Hargreaves, D. C., Hyman, P. L., Lu, T. T., Ngo, V. N., Bidgol, A., Suzuki, G., Zou, Y. R., Littman, D. R. & Cyster, J. G. (2001). A coordinated change in chemokine responsiveness guides plasma cell movements. *J Exp Med* **194**, 45-56.

Hartmann, K., Stengel, C., Klein, D., Egberink, H. & Balzarini, J. (2012). Efficacy and adverse effects of the antiviral compound plerixafor in feline immunodeficiency virus-infected cats. *J Vet Intern Med* **26**, 483-490.

Hinz, B. (2010). The myofibroblast: paradigm for a mechanically active cell. *J Biomech* **43**, 146-155.

Huisman, W., Schrauwen, E. J., Pas, S. D., Karlas, J. A., Rimmelzwaan, G. F. & Osterhaus, A. D. (2004). Antibodies specific for hypervariable regions 3 to 5 of the feline immunodeficiency virus envelope glycoprotein are not solely responsible for vaccine-induced acceleration of challenge infection in cats. *J Gen Virol* **85**, 1833-1841.

Huttenlocher, A. & Horwitz, A. R. (2011). Integrins in cell migration. *Cold Spring Harb Perspect Biol* **3**, a005074.

Imura, A., Hori, T., Imada, K., Ishikawa, T., Tanaka, Y., Maeda, M., Imamura, S. & Uchiyama, T. (1996). The human OX40/gp34 system directly mediates adhesion of activated T cells to vascular endothelial cells. *J Exp Med* **183**, 2185-2195.

Itoi, M., Tsukamoto, N., Yoshida, H. & Amagai, T. (2007). Mesenchymal cells are required for functional development of thymic epithelial cells. *Int Immunol* **19**, 953-964.

Jenkinson, W. E., Rossi, S. W., Parnell, S. M., Jenkinson, E. J. & Anderson, G. (2007). PDGFRalpha-expressing mesenchyme regulates thymus growth and the availability of intrathymic niches. *Blood* **109**, 954-960.

Joshi, A., Garg, H., Tompkins, M. B. & Tompkins, W. A. (2005). Preferential feline immunodeficiency virus (FIV) infection of CD4+ CD25+ T-regulatory cells correlates both with surface expression of CXCR4 and activation of FIV long terminal repeat binding cellular transcriptional factors. *J Virol* **79**, 4965-4976.

Kalluri, R. & Weinberg, R. A. (2009). The basics of epithelial-mesenchymal transition. *J Clin Invest* **119**, 1420-1428.

Kang, J., Coles, M. & Raulet, D. H. (1999). Defective development of gamma/delta T cells in interleukin 7 receptor-deficient mice is due to impaired expression of T cell receptor gamma genes. *J Exp Med* **190**, 973-982.

Kikuchi, K., Lai, A. Y., Hsu, C. L. & Kondo, M. (2005). IL-7 receptor signaling is necessary for stage transition in adult B cell development through up-regulation of EBF. *J Exp Med* **201**, 1197-1203.

Koning, J. J. & Mebius, R. E. (2012). Interdependence of stromal and immune cells for lymph node function. *Trends Immunol* **33**, 264-270.

Kotani, A., Hori, T., Matsumura, Y. & Uchiyama, T. (2002). Signaling of gp34 (OX40 ligand) induces vascular endothelial cells to produce a CC chemokine RANTES/CCL5. *Immunol Lett* **84**, 1-7.

Kumar, V., Dasoveanu, D. C., Chyou, S., Tzeng, T. C., Rozo, C., Liang, Y., Stohl, W., Fu, Y. X., Ruddle, N. H. & Lu, T. T. (2015). A dendritic-cell-stromal axis maintains immune responses in lymph nodes. *Immunity* **42**, 719-730.

Lama, J. & Planelles, V. (2007). Host factors influencing susceptibility to HIV infection and AIDS progression. *Retrovirology* **4**, 52.

Malhotra, D., Fletcher, A. L., Astarita, J., Lukacs-Kornek, V., Tayalia, P., Gonzalez, S. F., Elpek, K. G., Chang, S. K., Knoblich, K., Hemler, M. E., Brenner, M. B., Carroll, M. C., Mooney, D. J., Turley, S. J. & Consortium, I. G. P. (2012). Transcriptional profiling of stroma from inflamed and resting lymph nodes defines immunological hallmarks. *Nat Immunol* **13**, 499-510.

Mebius, R. E. & Kraal, G. (2005). Structure and function of the spleen. *Nat Rev Immunol* **5**, 606-616.

Mercier, F. E., Ragu, C. & Scadden, D. T. (2012). The bone marrow at the crossroads of blood and immunity. *Nat Rev Immunol* **12**, 49-60.

Nagasawa, T., Omatsu, Y. & Sugiyama, T. (2011). Control of hematopoietic stem cells by the bone marrow stromal niche: the role of reticular cells. *Trends Immunol* **32**, 315-320.

Nairn, R. & Helbert, M. (2006). *Immunology for medical students*: MOSBY.

Nishimura, Y., Shimojima, M., Sato, E., Izumiya, Y., Tohya, Y., Mikami, T. & Miyazawa, T. (2004). Downmodulation of CD3epsilon expression in CD8alpha+beta- T cells of feline immunodeficiency virus-infected cats. *J Gen Virol* **85**, 2585-2589.

Nombela-Arrieta, C., Ritz, J. & Silberstein, L. E. (2011). The elusive nature and function of mesenchymal stem cells. *Nat Rev Mol Cell Biol* **12**, 126-131.

O'Neil, L. L., Burkhard, M. J. & Hoover, E. A. (1996). Frequent perinatal transmission of feline immunodeficiency virus by chronically infected cats. *J Virol* **70**, 2894-2901.

Odaka, C. (2009). Localization of mesenchymal cells in adult mouse thymus: their abnormal distribution in mice with disorganization of thymic medullary epithelium. *J Histochem Cytochem* **57**, 373-382.

Olyslaegers, D. A., Desmarets, L. M., Dedeurwaerder, A., Dewerchin, H. L. & Nauwynck, H. J. (2013). Generation and characterization of feline arterial and venous endothelial cell lines for the study of the vascular endothelium. *BMC Vet Res* **9**, 170.

Orandle, M. S., Papadi, G. P., Bubenik, L. J., Dailey, C. I. & Johnson, C. M. (1997). Selective thymocyte depletion and immunoglobulin coating in the thymus of cats infected with feline immunodeficiency virus. *AIDS Res Hum Retroviruses* **13**, 611-620.

Pedersen, N. C., Ho, E. W., Brown, M. L. & Yamamoto, J. K. (1987). Isolation of a T-lymphotropic virus from domestic cats with an immunodeficiency-like syndrome. *Science* **235**, 790-793.

Phillips, T. R., Talbott, R. L., Lamont, C., Muir, S., Lovelace, K. & Elder, J. H. (1990). Comparison of two host cell range variants of feline immunodeficiency virus. *J Virol* **64**, 4605-4613.

Plotkin, J., Prockop, S. E., Lepique, A. & Petrie, H. T. (2003). Critical role for CXCR4 signaling in progenitor localization and T cell differentiation in the postnatal thymus. *J Immunol* **171**, 4521-4527.

Rideout, B. A., Lowensteine, L. J., Hutson, C. A., Moore, P. F. & Pedersen, N. C. (1992). Characterization of morphologic changes and lymphocyte subset distribution in lymph nodes from cats with naturally acquired feline immunodeficiency virus infection. *Vet Pathol* **29**, 391-399.

Rzhaninova, A. A., Gornostaeva, S. N. & Goldshtein, D. V. (2005). Isolation and phenotypical characterization of mesenchymal stem cells from human fetal thymus. *Bull Exp Biol Med* **139**, 134-140.

Saleh, S., Solomon, A., Wightman, F., Xhilaga, M., Cameron, P. U. & Lewin, S. R. (2007). CCR7 ligands CCL19 and CCL21 increase permissiveness of resting memory CD4+ T cells to HIV-1 infection: a novel model of HIV-1 latency. *Blood* **110**, 4161-4164.

Salek-Ardakani, S. & Croft, M. (2006). Regulation of CD4 T cell memory by OX40 (CD134). *Vaccine* **24**, 872-883.

Sanos, S. L., Nowak, J., Fallet, M. & Bajenoff, M. (2011). Stromal cell networks regulate thymocyte migration and dendritic cell behavior in the thymus. *J Immunol* **186**, 2835-2841.

Seibert, S. A., Howell, C. Y., Hughes, M. K. & Hughes, A. L. (1995). Natural selection on the gag, pol, and env genes of human immunodeficiency virus 1 (HIV-1). *Mol Biol Evol* **12**, 803-813.

Shelton, G. H., Linenberger, M. L., Grant, C. K. & Abkowitz, J. L. (1990). Hematologic manifestations of feline immunodeficiency virus infection. *Blood* **76**, 1104-1109.

Shimojima, M., Miyazawa, T., Ikeda, Y., McMonagle, E. L., Haining, H., Akashi, H., Takeuchi, Y., Hosie, M. J. & Willett, B. J. (2004). Use of CD134 as a primary receptor by the feline immunodeficiency virus. *Science* **303**, 1192-1195.

Sparger, E. E., Shacklett, B. L., Renshaw-Gegg, L., Barry, P. A., Pedersen, N. C., Elder, J. H. & Luciw, P. A. (1992). Regulation of gene expression directed by the long terminal repeat of the feline immunodeficiency virus. *Virology* **187**, 165-177.

Steiniger, B. S., Wilhelmi, V., Seiler, A., Lampp, K. & Stachniss, V. (2014). Heterogeneity of stromal cells in the human splenic white pulp. Fibroblastic reticulum cells, follicular dendritic cells and a third superficial stromal cell type. *Immunology* **143**, 462-477.

Sugiyama, T., Kohara, H., Noda, M. & Nagasawa, T. (2006). Maintenance of the hematopoietic stem cell pool by CXCL12-CXCR4 chemokine signaling in bone marrow stromal cell niches. *Immunity* **25**, 977-988.

Takahama, Y. (2006). Journey through the thymus: stromal guides for T-cell development and selection. *Nat Rev Immunol* **6**, 127-135.

Tomei, A. A., Siegert, S., Britschgi, M. R., Luther, S. A. & Swartz, M. A. (2009). Fluid flow regulates stromal cell organization and CCL21 expression in a tissue-engineered lymph node microenvironment. *J Immunol* **183**, 4273-4283.

Troth, S. P., Dean, A. D. & Hoover, E. A. (2008). In vivo CXCR4 expression, lymphoid cell phenotype, and feline immunodeficiency virus infection. *Vet Immunol Immunopathol* **123**, 97-105.

Umemoto, E., Otani, K., Ikeno, T., Verjan Garcia, N., Hayasaka, H., Bai, Z., Jang, M. H., Tanaka, T., Nagasawa, T., Ueda, K. & Miyasaka, M. (2012). Constitutive plasmacytoid dendritic cell migration to the splenic white pulp is cooperatively regulated by CCR7- and CXCR4-mediated signaling. *J Immunol* **189**, 191-199.

Walsh, S., Jefferiss, C., Stewart, K., Jordan, G. R., Screen, J. & Beresford, J. N. (2000). Expression of the developmental markers STRO-1 and alkaline phosphatase in cultures of human marrow stromal cells: regulation by fibroblast growth factor (FGF)-2 and relationship to the expression of FGF receptors 1-4. *Bone* **27**, 185-195.

Willems, L., Li, S., Rutgeerts, O., Lenaerts, C., Waer, M. & Billiau, A. D. (2011). IL-7 is required for the development of the intrinsic function of marginal zone B cells and the marginal zone microenvironment. *J Immunol* **187**, 3587-3594.

Willett, B. J., McMonagle, E. L., Logan, N., Spiller, O. B., Schneider, P. & Hosie, M. J. (2007). Probing the interaction between feline immunodeficiency virus and CD134 by using the novel monoclonal antibody 7D6 and the CD134 (Ox40) ligand. *J Virol* **81**, 9665-9679.

Woo, J. C., Dean, G. A., Pedersen, N. C. & Moore, P. F. (1997). Immunopathologic changes in the thymus during the acute stage of experimentally induced feline immunodeficiency virus infection in juvenile cats. *J Virol* **71**, 8632-8641.

Yamamoto, J. K., Pu, R., Sato, E. & Hohdatsu, T. (2007). Feline immunodeficiency virus pathogenesis and development of a dual-subtype feline-immunodeficiency-virus vaccine. *AIDS* **21**, 547-563.

Yu, H. R., Sung, M. L., Kuo, H. C., Lin, C. H. & Chen, C. N. (2015). Shear Stress Modulates Resistin-Induced CC Chemokine Ligand 19 Expression in Human Aortic Endothelial Cells. *J Cell Physiol* **230**, 2120-2127.

Zotes, T. M., Spada, R., Mulens, V., Pérez-Yagüe, S., Sorzano, C. O., Okkenhaug, K., Carrera, A. C. & Barber, D. F. (2013). PI3K p110δ is expressed by gp38(-)CD31(+) and gp38(+)CD31(+) spleen stromal cells and regulates their CCL19, CCL21, and LTβR mRNA levels. *PLoS One* **8**, e72960.

Chapter 6

General discussion

Twenty years ago, the human immunodeficiency virus was discovered in patients that presented an acquired immunodeficiency resulting in the development of numerous secondary and opportunistic infections. Shortly after HIV, feline immunodeficiency virus (FIV) was discovered in cats with similar symptoms that were negative for feline leukemia virus infection (Pedersen *et al.*, 1987). Twenty years of feline retroviral research taught us a lot about the viral proteins, genome and the anti-FIV immune response, but nonetheless left major questions about the viral replication cycle and pathogenesis. There is no antiretroviral therapy commercially available for cats and a positive FIV diagnosis is often a death sentence. An FIV vaccine was developed, but efficacy of the vaccine is currently still a matter of debate. Therefore, the vaccine is not available in Europe and the use of this vaccine is not recommended.

This thesis aimed to shed some new light on open questions in the FIV pathogenesis: (1) how does FIV survive and cause a lifelong infection while the generated immune response is vigorous, and (2) how can the disease progress in the asymptomatic phase with no apparent viral replication. Before trying to answering these questions the strains that are circulating in Belgium and The Netherlands were genetically characterized.

6.1. Low genetic variability between FIV strains in Belgium and The Netherlands.

FIV is divided into five different clades (A to E), based on phylogenetic analyses of variable regions 3 to 5 in the *env* gene (Kakinuma *et al.*, 1995; Sodora *et al.*, 1994). Overall, a low genetic variability was found between *env* and *gag* gene fragments of FIV field strains collected in Belgium and The Netherlands (**Chapter 3**). Except for one unknown virus, all viruses (n= 36) belonged to clade A FIV viruses. Clade A and B are found worldwide and might be considered as the general subtypes, while other clades are only found in geographic isolated regions (Yamamoto *et al.*, 2007). For example, subtype E has been found only in South-America and subtype D only in Japan (Kakinuma *et al.*, 1995; Pecoraro *et al.*, 1996). In Europe, clades A and B are most prevalent, followed by some reports of clade C virus in Germany and a new subtype in Portugal (Duarte & Tavares, 2006; Hosie *et al.*, 1989; Steinrigl *et al.*, 2010). This could mean that FIV viruses change locally, and might be spread again to other parts of the world by movement of FIV infected animals. FIV is a lentivirus that infects members of the Felidae and Hyenidea, and each host

harbors their own FIV variants (Brown *et al.*, 1994; Carpenter *et al.*, 1996; Troyer *et al.*, 2005). One might speculate that virus variance can also arise from recombination with FIV strains from other species. While such cross-over infections have been reported in captivity, these infections are very rare in the wild and often restricted due to incompatibility of the virus and the host (Troyer *et al.*, 2008; VandeWoude *et al.*, 2010). The lack of genetic variation between strains collected in Belgium and The Netherlands (**Chapter 3**) most likely indicates a relatively recent introduction of the virus in the region.

While this locally low variability might be encouraging to consider vaccination to prevent infection, caution is needed. Numerous vaccination trails have reported enhancement of disease upon challenge, and this enhancement seems to be attributed to anti-FIV Env antibodies (Haseltine, 1991; Miyazawa *et al.*, 1991; Rigby *et al.*, 1993; Zhu *et al.*, 1996). In addition, the generation of broad-neutralizing antibodies against FIV by vaccination has been proven to be an unsuccessful strategy (Bęczkowski *et al.*, 2015). Presence of broad-neutralizing antibodies against FIV in naturally infected cats did not correlate to slower disease progression or improved health status (Westman *et al.*, 2016). This is not that surprising since we and others have shown that neutralization sensitive epitopes are inaccessible on the mature FIV Env protein expressed on PBMC (**chapter 4**) (Richardson *et al.*, 1996), as will be discussed below. Furthermore, it has been proposed that vaccination may create FIV responsive memory cells that are rapidly activated upon challenge. Activated memory cells have accelerated CD134 expression (FIV primary receptor) kinetics upon activation and can cause a rapid expansion of the FIV target cells (Lecollinet & Richardson, 2008).

6.2. Hide and seek: FIV proteins on top of the game

All viruses in the genus *Lentivirus* are able to infect monocytes/macrophages. Equine infectious anemia virus (EAIV), caprine arthritis and encephalitis virus (CAEV) and maedi-visna virus (MVV) mainly infect monocytes and macrophages, and attract lymphocytes to the site of virion replication (Cheevers & McGuire, 1985; Larruskain & Jugo, 2013; Sellon *et al.*, 1992). Human, simian, bovines and feline immunodeficiency viruses, have evolved further and do not only infect monocytes/macrophages and attract lymphocytes, but also infect these bystander lymphocytes (Barré-Sinoussi *et al.*, 1983; Daniel *et al.*, 1985; Pedersen *et al.*, 1987; Whetstone *et al.*, 1997). The viruses are often studied in *in vitro* culture systems

with cell-free virus, although it has been known for some time now that cell-free lentivirus is poorly efficient in infecting new cells compared to cell-to-cell spread (Carr *et al.*, 1999; Dimitrov *et al.*, 1993; Phillips, 1994). The term "cell-to-cell" spread encompasses two different strategies. First, virus can spread directly from one cell to another by cell fusion and the formation of syncytia. Secondly, it may also refer to the formation of a virological synapse, a transient tight contact between two cells, in which virus can safely cross from one cell to the other, without interception by the immune system. The formation of the virological synapse has already been described for a number of retroviruses, like human T-lymphotropic virus (HTLV), HIV, and murine leukemia virus (MLV) (Bangham, 2003; Jin *et al.*, 2009; Jolly *et al.*, 2004).

In **chapter 4** we showed that FIV infected PBMC show a high concentration of both Gag and Env proteins in restricted areas at the plasma membrane. After translation, Gag polyprotein is targeted towards the plasma membrane by myristoylation and a patch of basic residues in the matrix protein (Manrique *et al.*, 2001; Manrique *et al.*, 2004). Furthermore, the FIV Env protein has been shown to be palmitoylated, a protein modification that can target proteins to lipid rafts (González *et al.*, 2012). Recently, Brown and colleagues showed that depletion of PI(4,5)P2, a lipid that serves as a docking site for proteins, from the plasma membrane of FIV-infected CrFK cells inhibited production of FIV particles (Brown *et al.*, 2015). The remarkable accumulation of Env and Gag in restricted areas in the plasma membrane raises the hypothesis that FIV proteins are targeted to specific micro-domains in the plasma membrane of infected PBMC, and that this polarization may be indicative for the existence of active cell sites for virus budding, and/or be the prerequisite for the formation of virological synapses, similar to what is described for HIV and MLV (Fais *et al.*, 1995; Jolly *et al.*, 2004; Jolly *et al.*, 2011; Jouvenet *et al.*, 2006; Owens *et al.*, 1991; Perotti *et al.*, 1996). Unlike MLV, FIV was not able to induce a polarized expression of its viral proteins at cell contacts in CrFK or GFox, which are unpolarized cells (Jin *et al.*, 2011; Li *et al.*, 2013). It is therefore reasonable to believe that FIV, similar to HIV, can hijack the natural polarization of activated PBMC for its egress (Jolly *et al.*, 2011; Miranda *et al.*, 2002).

Virological synapses used by retroviruses that replicate in immune cells are related to, but distinct from immunological synapses (Fig. 1). The virological synapses described for HIV are initiated by contacts between the HIV envelope protein on the infected cell and the HIV receptors on the contact cell (Groot *et al.*, 2008; Jolly *et al.*, 2004). The immunological synapse, on the other hand, is initiated by contact between an MHC molecule loaded with antigen and the T-cell receptor complex. While the immunological synapse is strictly limited to an antigen presenting cell (APC) and T-cells, the virological synapse can also exist between T-cells. Both types of synapse are stabilized by adhesion molecule/integrin interactions. To create and maintain the interaction between cells and ensure proper activation, cytoskeleton dynamics are required. Upon formation of the immunological synapse, the MTOC is reorientated towards the contact site (important for directed vesicle transport) and actin polymerizes (formation of signaling platforms) (Billadeau *et al.*, 2007). At the virological synapse, the MTOC is reorientated towards the cell-cell contact area only in infected cells (Jolly, 2010). For HTLV, it has been shown that the viral transactivator protein Tax, an accessory protein, accumulates at the microtubule organizing center (MTOC), thereby sensitizing the cell for ICAM-1 induced MTOC polarization upon formation of the virological synapse.

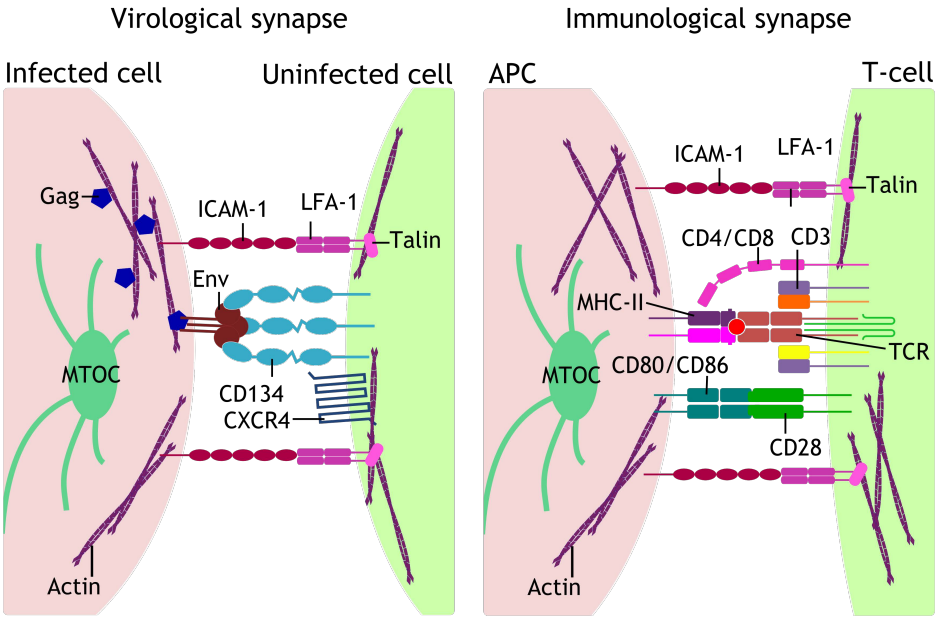

Figure 1: Composition of the virological synapse and the immunological synapse. The virological synapse (left) is initiated by interaction between the viral envelope protein and its receptors. The synapse is stabilized by interactions between adhesion molecules and integrins. The immunological synapse (right) is initiated by recognition of an antigen bound on a MHC-II molecule on an antigen presenting cell (APC) and the T-cell receptor (TCR) complex. Co-stimulatory signals are provided to the T-cell by interaction between CD80/CD86 and CD28. The synapse is stabilized by a ring of adhesion molecule-integrin interactions.

Several mechanisms of virus transmission at the virological synapse have been observed or hypothesized for other lentiviruses. For the interaction between an infected macrophage and uninfected T-cell, it is proposed that HIV particles are dumped into the synapse from an internal HIV compartment (Waki & Freed, 2010). Cell-free particles may also be released into the synapsic cleft and interact with their receptors on the uninfected cell. Another phenomenon is the virus transport across filopodia-like cell protrusions. These so called "tunneling nanotubes" (TNT), are shown to form between T-cells after close cell contact (Sowinski *et al.*, 2008), and are also induced by infected macrophages (Eugenin *et al.*, 2009), and transport virus to the uninfected cell. These nanotubes are not open-ended tunnels and do not allow membrane or cytoplasm exchange, the virus spread remains receptor dependent. These filopodial bridges have been shown for MLV and HIV (Lehmann *et al.*, 2005; Sherer *et al.*, 2007). Further research is needed to further elucidate if the observed polarization of FIV proteins leads to the formation of an active virological synapse between cells during FIV infection.

The expression of the envelope protein on the plasma membrane of an infected cell can be a major recognition antigen for the immune system, and may lead to cytolytic attacks from α-FIV cytotoxic T-cells or by the complement system. We have shown that FIV Env adopts a number of antigenically different conformations during its intracellular processing and trafficking. Furthermore, we have shown that upon cell surface expression of the mature trimeric Env protein, the protein was unrecognizable by Env-specific monoclonal antibodies (**Chapter 4**). Our results with the anti-V3 antibodies support the finding that the FIV secondary receptor (CXCR4) binding-epitope is located in a crypt that is only opened after interaction with the primary FIV receptor (CD134) (Egberink *et al.*, 1994; Pedersen *et al.*, 1987). Other regions (V2 and V4) on FIV Env remain hidden for other reasons, possibly as a result of steric occlusion or glycosylation, like has been shown for HIV and SIV Env (Chen *et al.*, 2002; Kwong *et al.*, 1998). This means that mature trimeric FIV Env expressed on the cell surface of infected cells, or incorporated in FIV virions might not by recognized by the mounted humoral antiviral response. This is in line with work by Richardson and colleagues who showed that B-cell epitopes are poorly recognized on mature Env, and do not contribute to virus neutralization (Richardson *et al.*, 1996). For HIV it was suggested that most of the anti-Env response is directed against the unprocessed Env protein and/or against disassembled Env that is released as cellular or viral

debris, and hence is not effective against the mature Env protein (Parren *et al.*, 1997).

A hypothetical model of the processing, trafficking and cell surface expression of the FIV Env protein, and of the viral protein polarization in PBMC, based on the results of **Chapter 4** is summarized in Figure 2, and discussed below. The envelope protein is translated in the rough ER as a polyprotein, in which the V3 loop has not yet adopted a closed conformation, and hence CXCR4-binding epitopes in the crypt are accessible (Fig. 2 (1)). After cleavage of TM and SU, and further adaptation of the sugar trees in the Golgi complex, the V2 and V4 loop acquire the right conformation, and can be recognized by their respective antibodies (Fig. 2 (2)). Processed Env is transported to the plasma membrane via vesicular transport, however, it remains to be investigated if Env is expressed on the plasma membrane continuously or if these vesicles are recruited after signaling and/or formation of the virological synapse (Fig. 2 (3)), like suggested for HIV (Jolly *et al.*, 2011; Miranda *et al.*, 2002). It is unclear if Gag associates with Env on the membrane of cytoplasmic vesicles and/or at the plasma membrane (Fig. 2 (4)). As described before, both proteins are modified in such a way that ensures association with lipid bilayers, and more specifically with lipid rafts (González *et al.*, 2012; Manrique *et al.*, 2001). Receptor interaction causes a series of conformational changes in FIV Env (Pedersen *et al.*, 1987). Antibodies that target SU in a post-receptor conformation generated positive staining at close cell contact, another indication for the existence of the FIV virological synapse. After secondary receptor binding, SU dissociates from TM, and the fusion peptide of TM can insert into the target cell (Gallo *et al.*, 2003; Hosie *et al.*, 2009), causing fusion of the membranes and release of viral capsid into the target cell. It is not known if the conformational changes in SU also cause liberation of SU from the FIV receptors. If SU remains bound to the receptors, complexes that stay behind on the cell surface after infection may be extruded from the cell surface, or get internalized for degradation to clear the newly infected cell from FIV antigens that may be recognized by the immune system. Cross-linking of CD134 by antibodies at 37°C causes formation and extrusion of CD134-antibody caps, while CXCR4 gets internalized (Roukaerts ID, unpublished results). Further research will show which strategy is used by FIV SU. Both phenomena have been described before in our lab for other viruses (Dewerchin *et al.*, 2014; Favoreel *et al.*, 1999; Favoreel *et al.*, 1997).

More information about the formation of the virological synapse might allow the development of new therapeutic strategies against synapse-inducing viruses. Not only viral proteins associated with the process might be targeted, but also cellular proteins involved in trafficking of the viral protein and stabilization of the synapse. Another strategy that may be proposed is the treatment with CD134-peptides that open the SU molecule and render it more susceptible to V3-loop neutralizing antibodies. However, if FIV makes use of the virological synapse for spread, CD134-peptides might not be able to reach most of the SU molecules during FIV infection of a new cell. This problem might be solved by developing small molecules that can target the Env protein and open up its structure. For this purpose, elucidation of the crystal structure of FIV Env will be vital.

Figure 2 (next page): Hypothetical model of the processing, trafficking and cell surface expression of the FIV Env protein, and the polarization of viral proteins in PBMC. (1) FIV Env (red) is translated by ribosomes that are associated with the ER. In the ER the leader sequence is still attached, and SU and TM are not separated. The CXCR4 receptor binding epitope on V3 (orange) is exposed. (2) After cleavage of the leader sequence the Env protein is transported towards the Golgi complex for further processing. the surface part (SU) and the transmembrane part (TM) are separated through cleavage by furin, but stay non-covalently associated. The SU protein takes shape and epitopes on the V2 and V4 loop take form. The TM protein is palmitoylated. The processing of Env generates a molecule that is protected from antibodies by a glycan shield. (3) It is unclear at the moment if the majority of Env is stored in secretory vesicles, or is continuously transported to the plasma membrane. Further research will be needed to elucidate if FIV Env (3a) is stored in secretory vesicles that get recruited after contact, or (3b) is present on the membrane and polarizes to the contact site upon interaction between the FIV infected (left) and uninfected cell (right). Trimerization of the Env protein, in vesicles or on the cell membrane may provide sterical hindrance for antibody binding. (4) FIV Gag is translated in the cytoplasm by free ribosomes. The matrix part is myristoylated and associated with lipids through a patch of basic residues. For FIV it has not been investigated if Gag associates with Env (4a) on intracellular membranes of vesicles, and/or (4b) at the plasma membrane. FIV Gag might be transported to the trailing edge of activated leukocytes by interaction between the capsid protein and the actin network. (5) FIV Env is expressed as a trimer on the cell surface of infected cells. Env interacts with its primary receptor CD134, which is also expressed as a trimer. Interaction with the primary receptor induces a conformational change that exposes the CXCR4-binding V3 crypt (orange). After binding to CXCR4 a secondary conformational change leads to the dissociation between SU and TM, and allows TM to insert its fusion peptide into the plasma membrane of the target cell. It is unsure if SU remains associated to the receptors or is shed in the extracellular space.

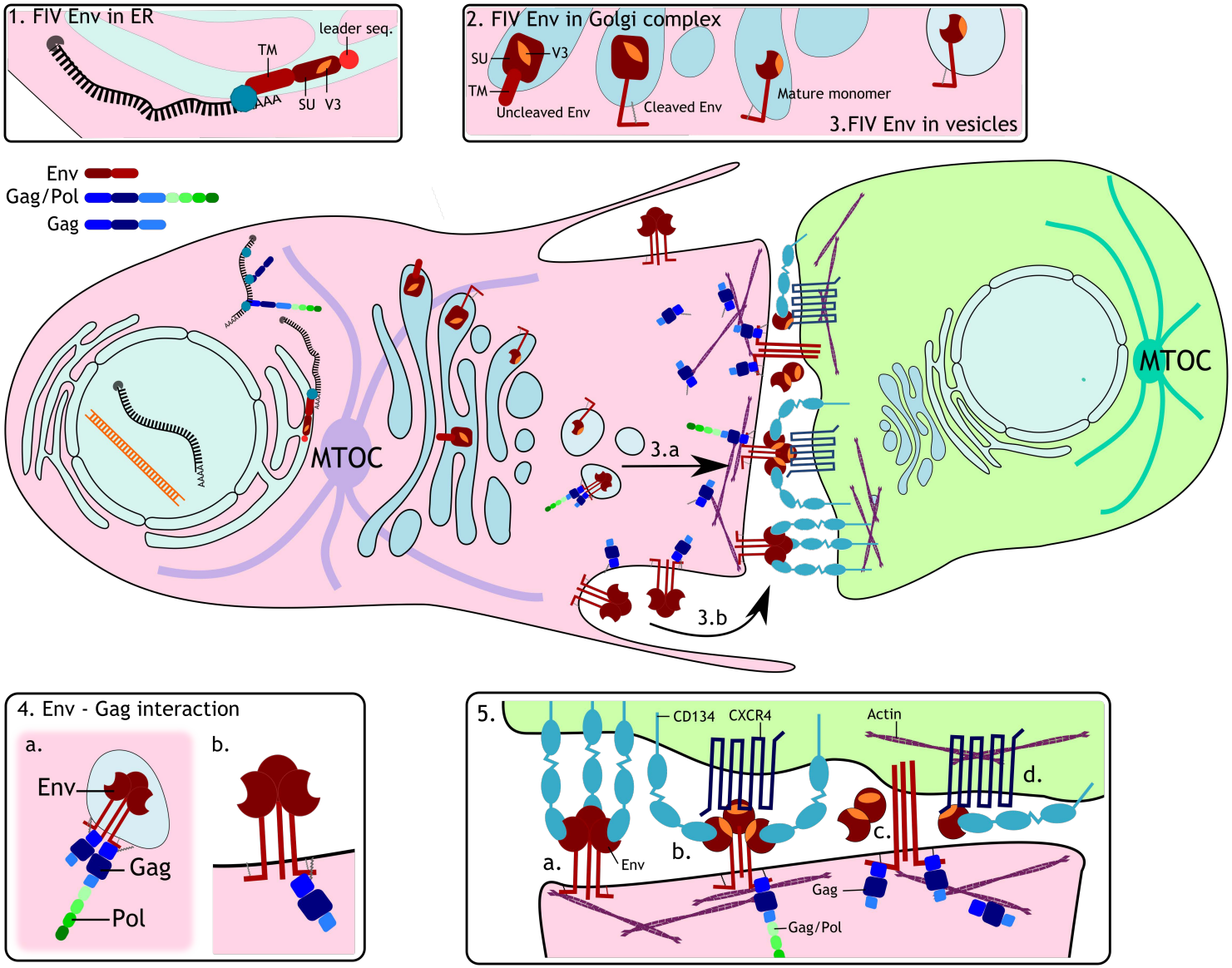
1. FIV Env in ER
leader seq.
TM
AAA
SU
V3
2. FIV Env in Golgi complex
SU
V3
TM
Uncleaved Env
Cleaved Env
Mature monomer
3.FIV Env in vesicles
Env
Gag/Pol
Gag
MTOC
3.a
3.b
MTOC
4. Env - Gag interaction
a.
b.
Env
Gag
Pol
5.
CD134
CXCR4
Actin
a.
Env
b.
c.
d.
Gag
Gag/Pol

6.3. FIV finds a sanctuary in the lymphoid tissues

Based on these results generated in Chapter 5 and results from others we propose a model for the early dissemination of FIV upon infection, and the progression of the disease during the asymptomatic phase (Fig. 3). Cats are infected by biting incidents, transferring the virus from the saliva of an infected cat into the wound of the bitten cat. The exact mechanism of primary infection is still not elucidated. Cell-free virus or cell-associated virus might infect resident macrophages or dendritic cells at the biting wound, or the virus might get drained directly to the lymph nodes. Our results might suggest that activated endothelial cells that line blood vessels at the site of inflammation elevate the susceptibility of leukocytes for FIV infection (**Chapter 5b**). Destruction of tissue and micro-organisms in the saliva of animals will induce an inflammatory response at the bite wound inflicted by the FIV positive cat. It can be speculated that in the presence of FIV susceptible leukocytes might induce a first replication round at the site of the bite wound, before FIV infected cells or dendritic cells loaded with virus move to the lymph nodes. For HIV it has been shown that phagocytosis of HIV infected T-lymphocytes can cause infection of macrophages (Baxter *et al.*, 2014). If this is true for FIV as well, phagocytosis of non-self infected cells that are present in the saliva might cause infection of the opsonizing macrophage.

From the draining lymph node, FIV is rapidly distributed to other lymphoid organs by infected leukocytes (Huisman *et al.*, 2004). After this acute phase, seroconversion will take place, and the infection is partially controlled leading to an asymptomatic phase with low to undetectable virus titers in the blood. Although virus titers are extremely low, and cats present no symptoms of disease, over the course of time a severe dysregulation of the immune system takes place, and eventually $CD4^+$ T-cell counts plummet (Lerner *et al.*, 1995; Ohno *et al.*, 1994; Shelton *et al.*, 1990). Recently, it was shown that viral mRNA, viral proteins and newly produced virus can be found in lymph nodes, whereas viral mRNA expression is absent in blood leukocytes (Eckstrand *et al.*, 2016). This was not only shown for FIV, but also for HIV infected humans, even when they are treated with highly active antiretroviral therapy (HAART) (Lorenzo-Redondo *et al.*, 2016; Pantaleo *et al.*, 1993a). It can thus be hypothesized that lymph nodes are preferential sites of lentiviral replication, and that while replication is blocked in blood leukocytes it can be activated once these cells enter lymph nodes.

In **chapter 5** we provided the first evidence that stromal mesenchymal cells from lymphoid tissues might increase susceptibility of naïve PBMC for FIV infection, and might enhance FIV replication and spread in already infected PBMC. For HIV it has been proposed that follicular dendritic cells (FDC), a specialized stromal mesenchymal cell type in the follicles of secondary lymphoid organs, can capture FIV particles, store them for several months and present them to leukocytes, causing infection of the latter (Burton *et al.*, 1997; Pantaleo *et al.*, 1993b). Maturation of monocytes into macrophages increases susceptibility of these cells for lentiviral infection and also activates replication in these cells (Dow *et al.*, 1999; Gendelman *et al.*, 1986; Narayan *et al.*, 1983; Rich *et al.*, 1992). Furthermore, for HIV it has been shown that FDC directly interact with infected monocytes/macrophages and activate HIV replication at the transcriptional level in these cells (Ohba *et al.*, 2009). The long terminal repeats (LTR) that enclose the FIV provirus in the genome of the infected cell contain a number of signaling sequences for the binding of transcription factors and enhancers. A number of these sites are conserved between FIV isolates, like the TATA-box, AP4, AP1 and ATF/CREB sites (Sparger *et al.*, 1992; Talbott *et al.*, 1989). Some viruses may also contain additional sites to bind transcription factors like NF-κB, NF-1, C/EBP and LBP-1 (Sparger *et al.*, 1992; Thompson *et al.*, 1994). Signaling induced by chemokines or other molecules produced by / or present on mesenchymal stromal cells in these organs may activate these transcription factors and lead to FIV transcription. For instance, signaling via chemokine receptors and activation via the T-cell receptor activate NF-κB. Besides transcriptional activation and storage of infectious particles, the densely packed leukocytes in the lymphoid tissues constantly interact with each other. Since leukocytes can also adhere to the stromal network, the mesenchymal stromal cells might stabilize or enhance these leukocyte interactions. In this way, these cells may also aid in the formation of the virological synapse between an FIV infected cell and a target cell, and increase cell-to-cell spread of FIV.

Infected cells will also travel to the bone marrow, possibly infected memory cells that home in the bone marrow (Alexaki & Wigdahl, 2008; Tokoyoda *et al.*, 2009). Myeloid precursor cells (i.e. myeloblasts) can become infected (Beebe *et al.*, 1992), giving rise to a persistent pool of latent provirus-carrying offspring. Monocytes may also become infected *de novo*, resulting in a non-productive infection until they become activated and differentiate. Provirus-containing monocytes that give

rise to tissue resident macrophages may cause local damage upon activation of FIV replication. This is for instance the cause of damage to the central nervous system in FIV infected cats (Hein *et al.*, 2005; Ryan *et al.*, 2005). FIV positive tissue macrophages may also drain to the lymph nodes after encountering other pathogens. Last but not least, pro-virus containing monocytes may recirculate to the lymph nodes, where they may become activated by antigens, pathogens or inflammatory signals, and pass the virus to T- and B-lymphocytes. Recent work at the University of Glasgow (Dr. Hosie M, unpublished) identified the existence of tissue compartment specific FIV variants, with differential use of the FIV receptors. More information on these variants and their circulation may lead to a better understanding of the FIV tissue reservoirs (Techakriengkrai *et al.*, 2014).

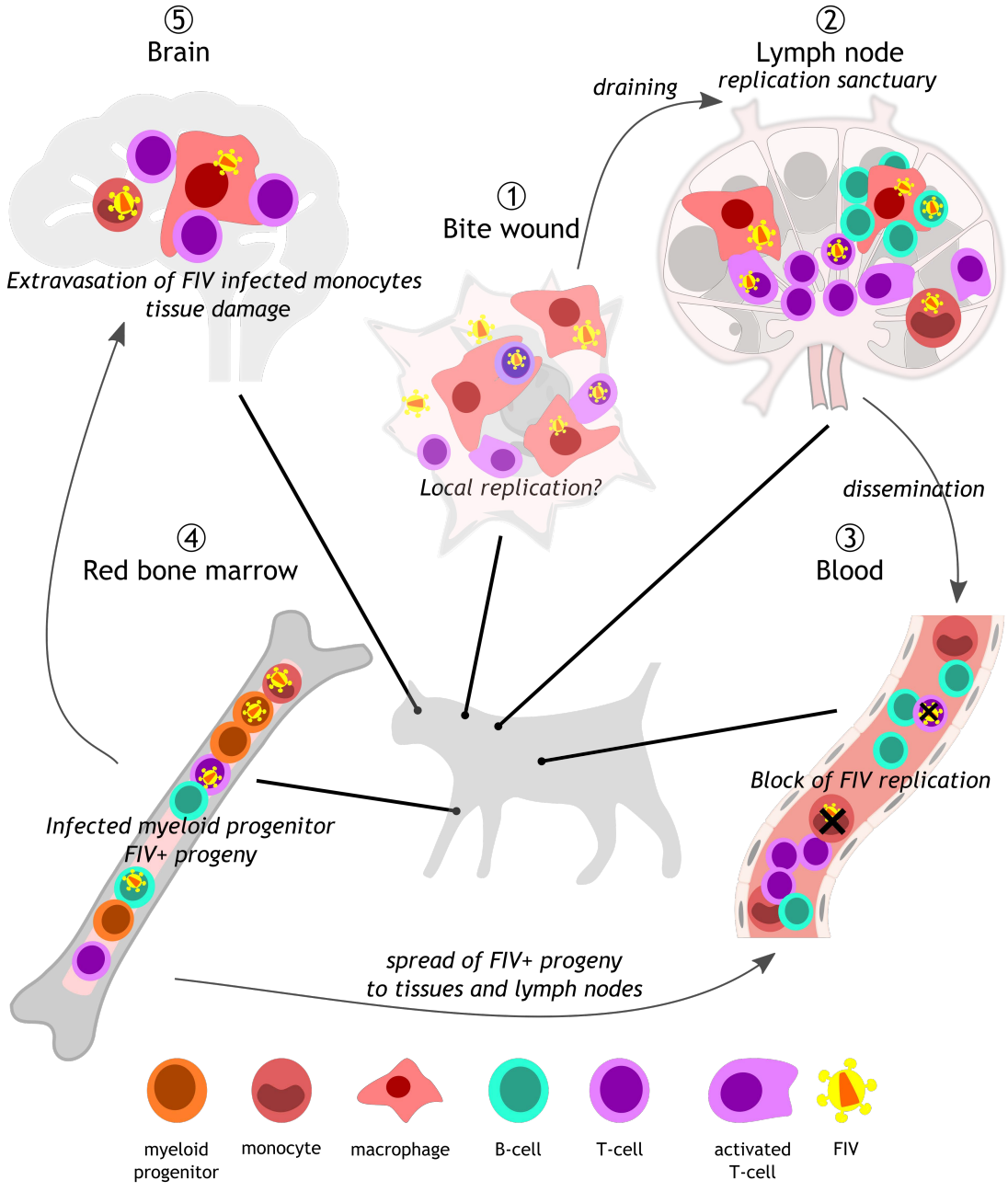

Figure 3: Hypothetical model for initial dissemination of FIV, and sites of ongoing FIV replication during the asymptomatic phase. (1) Cell-free or cell-associated FIV in saliva enters the cat at a bite wound inflicted during fights. Macrophages may become infected by phagocytosis of FIV^+ cells or by uptake of FIV virions. Activation of infiltrating leukocytes by the local blood vessel endothelium may increase FIV susceptibility of these cells. Activated leukocytes can support a local FIV replication round before draining to the lymph nodes. (2) During acute infection, FIV infected cells may spread from the draining lymph node and disseminate the virus to other lymphoid tissues, like the spleen, thymus and bone marrow. (3) While FIV replication is ongoing in the lymph nodes, no active replication can be detected in infected blood leukocytes during the asymptomatic phase. (4) FIV can infect myeloid progenitor cells in the red bone marrow, which will pass the integrated provirus to their progeny, creating FIV-carrying monocytes. These FIV^+ monocytes will spread once again across the cat, inducing replication when they mature into macrophages. (5) Extravasation of FIV^+ monocytes in the brain can cause inflammation because of FIV replication, leading to FIV induced damage.

Conclusions

- There is a low genetic variability of FIV in Belgium and The Netherlands and clade A is the most prevalent subtype, but caution is needed since new introductions and recombination can increase this variability (**Chapter 3**).
- FIV Env and Gag polarize towards specific sites at the plasma membrane in infected PBMC, which may indicate a preferred budding site or induction of the virological synapse. Cell-to-cell spread via the virological synapse can hide FIV from the immune system (**Chapter 4**).
- FIV Env adopts a closed conformation upon expression of the functional protein on the plasma membrane of infected cells, and may be protected from antibody binding by a glycan shield and steric hindrance. This way FIV infected cells and free FIV virions may evade the mounted anti-FIV response (**Chapter 4**).
- Mesenchymal stromal cells from lymph nodes and activated endothelium may increase susceptibility of PBMC for FIV infection (**Chapter 5b**).
- Lymph nodes and bone marrow mesenchymal stromal cells may augment FIV replication in PBMC. This may explain why the lymphoid organs are a FIV replication sanctuary during the asymptomatic phase of the FIV disease course (**Chapter 5b**).

References

Alexaki, A. & Wigdahl, B. (2008). HIV-1 infection of bone marrow hematopoietic progenitor cells and their role in trafficking and viral dissemination. *PLoS Pathog* **4**, e1000215.

Bangham, C. R. (2003). The immune control and cell-to-cell spread of human T-lymphotropic virus type 1. *J Gen Virol* **84**, 3177-3189.

Barré-Sinoussi, F., Chermann, J. C., Rey, F., Nugeyre, M. T., Chamaret, S., Gruest, J., Dauguet, C., Axler-Blin, C., Vézinet-Brun, F., Rouzioux, C., Rozenbaum, W. & Montagnier, L. (1983). Isolation of a T-lymphotropic retrovirus from a patient at risk for acquired immune deficiency syndrome (AIDS). *Science* **220**, 868-871.

Baxter, A. E., Russell, R. A., Duncan, C. J., Moore, M. D., Willberg, C. B., Pablos, J. L., Finzi, A., Kaufmann, D. E., Ochsenbauer, C., Kappes, J. C., Groot, F. & Sattentau, Q. J. (2014). Macrophage infection via selective capture of HIV-1-infected CD4+ T cells. *Cell Host Microbe* **16**, 711-721.

Beebe, A. M., Gluckstern, T. G., George, J., Pedersen, N. C. & Dandekar, S. (1992). Detection of feline immunodeficiency virus infection in bone marrow of cats. *Vet Immunol Immunopathol* **35**, 37-49.

Billadeau, D. D., Nolz, J. C. & Gomez, T. S. (2007). Regulation of T-cell activation by the cytoskeleton. *Nat Rev Immunol* **7**, 131-143.

Brown, E. W., Yuhki, N., Packer, C. & O'Brien, S. J. (1994). A lion lentivirus related to feline immunodeficiency virus: epidemiologic and phylogenetic aspects. *J Virol* **68**, 5953-5968.

Brown, L. A., Cox, C., Baptiste, J., Summers, H., Button, R., Bahlow, K., Spurrier, V., Kyser, J., Luttge, B. G., Kuo, L., Freed, E. O. & Summers, M. F. (2015). NMR structure of the myristylated feline immunodeficiency virus matrix protein. *Viruses* **7**, 2210-2229.

Burton, G. F., Masuda, A., Heath, S. L., Smith, B. A., Tew, J. G. & Szakal, A. K. (1997). Follicular dendritic cells (FDC) in retroviral infection: host/pathogen perspectives. *Immunol Rev* **156**, 185-197.

Bęczkowski, P. M., Harris, M., Techakriengkrai, N., Beatty, J. A., Willett, B. J. & Hosie, M. J. (2015). Neutralising antibody response in domestic cats immunised with a commercial feline immunodeficiency virus (FIV) vaccine. *Vaccine* **33**, 977-984.

Carpenter, M. A., Brown, E. W., Culver, M., Johnson, W. E., Pecon-Slattery, J., Brousset, D. & O'Brien, S. J. (1996). Genetic and phylogenetic divergence of feline immunodeficiency virus in the puma (Puma concolor). *J Virol* **70**, 6682-6693.

Carr, J. M., Hocking, H., Li, P. & Burrell, C. J. (1999). Rapid and efficient cell-to-cell transmission of human immunodeficiency virus infection from monocyte-derived macrophages to peripheral blood lymphocytes. *Virology* **265**, 319-329.

Cheevers, W. P. & McGuire, T. C. (1985). Equine infectious anemia virus: immunopathogenesis and persistence. *Rev Infect Dis* **7**, 83-88.

Chen, J. J., Huang, J. C., Shirtliff, M., Briscoe, E., Ali, S., Cesani, F., Paar, D. & Cloyd, M. W. (2002). CD4 lymphocytes in the blood of HIV(+) individuals migrate rapidly to lymph nodes and bone marrow: support for homing theory of CD4 cell depletion. *J Leukoc Biol* **72**, 271-278.

Daniel, M. D., Letvin, N. L., King, N. W., Kannagi, M., Sehgal, P. K., Hunt, R. D., Kanki, P. J., Essex, M. & Desrosiers, R. C. (1985). Isolation of T-cell tropic HTLV-III-like retrovirus from macaques. *Science* **228**, 1201-1204.

Dewerchin, H. L., Desmarets, L. M., Noppe, Y. & Nauwynck, H. J. (2014). Myosins 1 and 6, myosin light chain kinase, actin and microtubules cooperate during antibody-mediated internalisation and trafficking of membrane-expressed viral antigens in feline infectious peritonitis virus infected monocytes. *Vet Res* **45**, 17.

Dimitrov, D. S., Willey, R. L., Sato, H., Chang, L. J., Blumenthal, R. & Martin, M. A. (1993). Quantitation of human immunodeficiency virus type 1 infection kinetics. *J Virol* **67**, 2182-2190.

Dow, S. W., Mathiason, C. K. & Hoover, E. A. (1999). In vivo monocyte tropism of pathogenic feline immunodeficiency viruses. *J Virol* **73**, 6852-6861.

Duarte, A. & Tavares, L. (2006). Phylogenetic analysis of Portuguese Feline Immunodeficiency Virus sequences reveals high genetic diversity. *Vet Microbiol* **114**, 25-33.

Eckstrand, C. D., Hillman, C., Smith, A. L., Sparger, E. E. & Murphy, B. G. (2016). Viral Reservoirs in Lymph Nodes of FIV-Infected Progressor and Long-Term Non-Progressor Cats during the Asymptomatic Phase. *PLoS One* **11**, e0146285.

Egberink, H., Keldermans, L., Schuurman, N., Stam, J., Hesselink, W., van Vliet, A., Verschoor, E., Horzinek, M. & de Ronde, A. (1994). Monoclonal antibodies to immunodominant and neutralizing domains of the envelope surface protein of feline immunodeficiency virus. *J Gen Virol* **75 (Pt 4)**, 889-893.

Eugenin, E. A., Gaskill, P. J. & Berman, J. W. (2009). Tunneling nanotubes (TNT) are induced by HIV-infection of macrophages: a potential mechanism for intercellular HIV trafficking. *Cell Immunol* **254**, 142-148.

Fais, S., Capobianchi, M. R., Abbate, I., Castilletti, C., Gentile, M., Cordiali Fei, P., Ameglio, F. & Dianzani, F. (1995). Unidirectional budding of HIV-1 at the site of cell-to-cell contact is associated with co-polarization of intercellular adhesion molecules and HIV-1 viral matrix protein. *AIDS* **9**, 329-335.

Favoreel, H. W., Nauwynck, H. J., Halewyck, H. M., Van Oostveldt, P., Mettenleiter, T. C. & Pensaert, M. B. (1999). Antibody-induced endocytosis of viral glycoproteins and major histocompatibility complex class I on pseudorabies virus-infected monocytes. *J Gen Virol* **80 (Pt 5)**, 1283-1291.

Favoreel, H. W., Nauwynck, H. J., Van Oostveldt, P., Mettenleiter, T. C. & Pensaert, M. B. (1997). Antibody-induced and cytoskeleton-mediated redistribution and shedding of viral glycoproteins, expressed on pseudorabies virus-infected cells. *J Virol* **71**, 8254-8261.

Gallo, S. A., Finnegan, C. M., Viard, M., Raviv, Y., Dimitrov, A., Rawat, S. S., Puri, A., Durell, S. & Blumenthal, R. (2003). The HIV Env-mediated fusion reaction. *Biochim Biophys Acta* **1614**, 36-50.

Gendelman, H. E., Narayan, O., Kennedy-Stoskopf, S., Kennedy, P. G., Ghotbi, Z., Clements, J. E., Stanley, J. & Pezeshkpour, G. (1986). Tropism of sheep lentiviruses for monocytes: susceptibility to infection and virus gene expression increase during maturation of monocytes to macrophages. *J Virol* **58**, 67-74.

González, S. A., Paladino, M. G. & Affranchino, J. L. (2012). Palmitoylation of the feline immunodeficiency virus envelope glycoprotein and its effect on fusion activity and envelope incorporation into virions. *Virology* **428**, 1-10.

Groot, F., Welsch, S. & Sattentau, Q. J. (2008). Efficient HIV-1 transmission from macrophages to T cells across transient virological synapses. *Blood* **111**, 4660-4663.

Haseltine, W. A. (1991). Molecular biology of the human immunodeficiency virus type 1. *FASEB J* **5**, 2349-2360.

Hein, A., Martin, J. P. & Dörries, R. (2005). Early pathological changes in the central nervous system of acutely feline-immunodeficiency-virus-infected cats. *Virology* **343**, 162-170.

Hosie, M. J., Addie, D., Belak, S., Boucraut-Baralon, C., Egberink, H., Frymus, T., Gruffydd-Jones, T., Hartmann, K., Lloret, A., Lutz, H., Marsilio, F., Pennisi, M. G., Radford, A. D., Thiry, E., Truyen, U. & Horzinek, M. C. (2009). FELINE IMMUNODEFICIENCY ABCD guidelines on prevention and management. *Journal of Feline Medicine and Surgery* **11**, 575-584.

Hosie, M. J., Robertson, C. & Jarrett, O. (1989). Prevalence of feline leukaemia virus and antibodies to feline immunodeficiency virus in cats in the United Kingdom. *Vet Rec* **125**, 293-297.

Huisman, W., Schrauwen, E. J., Pas, S. D., Karlas, J. A., Rimmelzwaan, G. F. & Osterhaus, A. D. (2004). Antibodies specific for hypervariable regions 3 to 5 of the feline immunodeficiency virus envelope glycoprotein are not solely responsible for vaccine-induced acceleration of challenge infection in cats. *J Gen Virol* **85**, 1833-1841.

Jin, J., Li, F. & Mothes, W. (2011). Viral determinants of polarized assembly for the murine leukemia virus. *J Virol* **85**, 7672-7682.

Jin, J., Sherer, N. M., Heidecker, G., Derse, D. & Mothes, W. (2009). Assembly of the murine leukemia virus is directed towards sites of cell-cell contact. *PLoS Biol* **7**, e1000163.

Jolly, C. (2010). T cell polarization at the virological synapse. *Viruses* **2**, 1261-1278.

Jolly, C., Kashefi, K., Hollinshead, M. & Sattentau, Q. J. (2004). HIV-1 cell to cell transfer across an Env-induced, actin-dependent synapse. *J Exp Med* **199**, 283-293.

Jolly, C., Welsch, S., Michor, S. & Sattentau, Q. J. (2011). The regulated secretory pathway in CD4(+) T cells contributes to human immunodeficiency virus type-1 cell-to-cell spread at the virological synapse. *PLoS Pathog* **7**, e1002226.

Jouvenet, N., Neil, S. J., Bess, C., Johnson, M. C., Virgen, C. A., Simon, S. M. & Bieniasz, P. D. (2006). Plasma membrane is the site of productive HIV-1 particle assembly. *PLoS Biol* **4**, e435.

Kakinuma, S., Motokawa, K., Hohdatsu, T., Yamamoto, J. K., Koyama, H. & Hashimoto, H. (1995). Nucleotide sequence of feline immunodeficiency virus: classification of Japanese isolates into two subtypes which are distinct from non-Japanese subtypes. *J Virol* **69**, 3639-3646.

Kwong, P. D., Wyatt, R., Robinson, J., Sweet, R. W., Sodroski, J. & Hendrickson, W. A. (1998). Structure of an HIV gp120 envelope glycoprotein in complex with the CD4 receptor and a neutralizing human antibody. *Nature* **393**, 648-659.

Larruskain, A. & Jugo, B. M. (2013). Retroviral infections in sheep and goats: small ruminant lentiviruses and host interaction. *Viruses* **5**, 2043-2061.

Lecollinet, S. & Richardson, J. (2008). Vaccination against the feline immunodeficiency virus: the road not taken. *Comp Immunol Microbiol Infect Dis* **31**, 167-190.

Lehmann, M. J., Sherer, N. M., Marks, C. B., Pypaert, M. & Mothes, W. (2005). Actin- and myosin-driven movement of viruses along filopodia precedes their entry into cells. *J Cell Biol* **170**, 317-325.

Lerner, D. L., Wagaman, P. C., Phillips, T. R., Prospero-Garcia, O., Henriksen, S. J., Fox, H. S., Bloom, F. E. & Elder, J. H. (1995). Increased mutation frequency of feline immunodeficiency virus lacking functional deoxyuridine-triphosphatase. *Proc Natl Acad Sci U S A* **92**, 7480-7484.

Li, F., Jin, J., Herrmann, C. & Mothes, W. (2013). Basic residues in the matrix domain and multimerization target murine leukemia virus Gag to the virological synapse. *J Virol* **87**, 7113-7126.

Lorenzo-Redondo, R., Fryer, H. R., Bedford, T., Kim, E. Y., Archer, J., Kosakovsky Pond, S. L., Chung, Y. S., Penugonda, S., Chipman, J. G., Fletcher, C. V., Schacker, T. W., Malim, M. H., Rambaut, A., Haase, A. T., McLean, A. R. & Wolinsky, S. M. (2016). Persistent HIV-1 replication maintains the tissue reservoir during therapy. *Nature* **530**, 51-56.

Manrique, M. L., Celma, C. C., González, S. A. & Affranchino, J. L. (2001). Mutational analysis of the feline immunodeficiency virus matrix protein. *Virus Res* **76**, 103-113.

Manrique, M. L., González, S. A. & Affranchino, J. L. (2004). Functional relationship between the matrix proteins of feline and simian immunodeficiency viruses. *Virology* **329**, 157-167.

Miranda, L. R., Schaefer, B. C., Kupfer, A., Hu, Z. & Franzusoff, A. (2002). Cell surface expression of the HIV-1 envelope glycoproteins is directed from intracellular CTLA-4-containing regulated secretory granules. *Proc Natl Acad Sci U S A* **99**, 8031-8036.

Miyazawa, T., Fukasawa, M., Hasegawa, A., Maki, N., Ikuta, K., Takahashi, E., Hayami, M. & Mikami, T. (1991). Molecular cloning of a novel isolate of feline immunodeficiency virus biologically and genetically different from the original U.S. isolate. *J Virol* **65**, 1572-1577.

Narayan, O., Kennedy-Stoskopf, S., Sheffer, D., Griffin, D. E. & Clements, J. E. (1983). Activation of caprine arthritis-encephalitis virus expression during maturation of monocytes to macrophages. *Infect Immun* **41**, 67-73.

Ohba, K., Ryo, A., Dewan, M. Z., Nishi, M., Naito, T., Qi, X., Inagaki, Y., Nagashima, Y., Tanaka, Y., Okamoto, T., Terashima, K. & Yamamoto, N. (2009). Follicular dendritic cells activate HIV-1 replication in monocytes/macrophages through a juxtacrine mechanism mediated by P-selectin glycoprotein ligand 1. *J Immunol* **183**, 524-532.

Ohno, K., Okamoto, Y., Miyazawa, T., Mikami, T., Watari, T., Goitsuka, R., Tsujimoto, H. & Hasegawa, A. (1994). Induction of apoptosis in a T lymphoblastoid cell line infected with feline immunodeficiency virus. *Arch Virol* **135**, 153-158.

Owens, R. J., Dubay, J. W., Hunter, E. & Compans, R. W. (1991). Human immunodeficiency virus envelope protein determines the site of virus release in polarized epithelial cells. *Proc Natl Acad Sci U S A* **88**, 3987-3991.

Pantaleo, G., Graziosi, C., Demarest, J. F., Butini, L., Montroni, M., Fox, C. H., Orenstein, J. M., Kotler, D. P. & Fauci, A. S. (1993a). HIV infection is active and progressive in lymphoid tissue during the clinically latent stage of disease. *Nature* **362**, 355-358.

Pantaleo, G., Graziosi, C. & Fauci, A. S. (1993b). The role of lymphoid organs in the pathogenesis of HIV infection. *Semin Immunol* **5**, 157-163.

Parren, P. W., Burton, D. R. & Sattentau, Q. J. (1997). HIV-1 antibody--debris or virion? *Nat Med* **3**, 366-367.

Pecoraro, M. R., Tomonaga, K., Miyazawa, T., Kawaguchi, Y., Sugita, S., Tohya, Y., Kai, C., Etcheverrigaray, M. E. & Mikami, T. (1996). Genetic diversity of Argentine isolates of feline immunodeficiency virus. *J Gen Virol* **77 (Pt 9)**, 2031-2035.

Pedersen, N. C., Ho, E. W., Brown, M. L. & Yamamoto, J. K. (1987). Isolation of a T-lymphotropic virus from domestic cats with an immunodeficiency-like syndrome. *Science* **235**, 790-793.

Perotti, M. E., Tan, X. & Phillips, D. M. (1996). Directional budding of human immunodeficiency virus from monocytes. *J Virol* **70**, 5916-5921.

Phillips, D. M. (1994). The role of cell-to-cell transmission in HIV infection. *AIDS* **8**, 719-731.

Rich, E. A., Chen, I. S., Zack, J. A., Leonard, M. L. & O'Brien, W. A. (1992). Increased susceptibility of differentiated mononuclear phagocytes to productive infection with human immunodeficiency virus-1 (HIV-1). *J Clin Invest* **89**, 176-183.

Richardson, J., Fossati, I., Moraillon, A., Castelot, S., Sonigo, P. & Pancino, G. (1996). Neutralization sensitivity and accessibility of continuous B cell epitopes of the feline immunodeficiency virus envelope. *J Gen Virol* **77 (Pt 4)**, 759-771.

Rigby, M. A., Holmes, E. C., Pistello, M., Mackay, A., Brown, A. J. & Neil, J. C. (1993). Evolution of structural proteins of feline immunodeficiency virus: molecular epidemiology and evidence of selection for change. *J Gen Virol* **74 (Pt 3)**, 425-436.

Ryan, G., Grimes, T., Brankin, B., Mabruk, M. J., Hosie, M. J., Jarrett, O. & Callanan, J. J. (2005). Neuropathology associated with feline immunodeficiency virus infection highlights prominent lymphocyte trafficking through both the blood-brain and blood-choroid plexus barriers. *J Neurovirol* **11**, 337-345.

Sellon, D. C., Perry, S. T., Coggins, L. & Fuller, F. J. (1992). Wild-type equine infectious anemia virus replicates in vivo predominantly in tissue macrophages, not in peripheral blood monocytes. *J Virol* **66**, 5906-5913.

Shelton, G. H., Linenberger, M. L., Grant, C. K. & Abkowitz, J. L. (1990). Hematologic manifestations of feline immunodeficiency virus infection. *Blood* **76**, 1104-1109.

Sherer, N. M., Lehmann, M. J., Jimenez-Soto, L. F., Horensavitz, C., Pypaert, M. & Mothes, W. (2007). Retroviruses can establish filopodial bridges for efficient cell-to-cell transmission. *Nat Cell Biol* **9**, 310-315.

Sodora, D. L., Shpaer, E. G., Kitchell, B. E., Dow, S. W., Hoover, E. A. & Mullins, J. I. (1994). Identification of three feline immunodeficiency virus (FIV) env gene subtypes and comparison of the FIV and human immunodeficiency virus type 1 evolutionary patterns. *J Virol* **68**, 2230-2238.

Sowinski, S., Jolly, C., Berninghausen, O., Purbhoo, M. A., Chauveau, A., Köhler, K., Oddos, S., Eissmann, P., Brodsky, F. M., Hopkins, C., Onfelt, B., Sattentau, Q. & Davis, D. M. (2008). Membrane nanotubes physically connect T cells over long distances presenting a novel route for HIV-1 transmission. *Nat Cell Biol* **10**, 211-219.

Sparger, E. E., Shacklett, B. L., Renshaw-Gegg, L., Barry, P. A., Pedersen, N. C., Elder, J. H. & Luciw, P. A. (1992). Regulation of gene expression directed by the long terminal repeat of the feline immunodeficiency virus. *Virology* **187**, 165-177.

Steinrigl, A., Ertl, R., Langbein, I. & Klein, D. (2010). Phylogenetic analysis suggests independent introduction of feline immunodeficiency virus clades A and B to Central Europe and identifies diverse variants of clade B. *Vet Immunol Immunopathol* **134**, 82-89.

Talbott, R. L., Sparger, E. E., Lovelace, K. M., Fitch, W. M., Pedersen, N. C., Luciw, P. A. & Elder, J. H. (1989). Nucleotide sequence and genomic organization of feline immunodeficiency virus. *Proc Natl Acad Sci U S A* **86**, 5743-5747.

Techakriengkrai, N., Logan, N., Willett, B. & Hosie, M. (2014). Tissue compatmentalization in feline immunodeficiency virus infection. In *International feline retrovirus research symposium*. Niagara-on-the-lake, Canada.

Thompson, F. J., Elder, J. & Neil, J. C. (1994). Cis- and trans-regulation of feline immunodeficiency virus: identification of functional binding sites in the long terminal repeat. *J Gen Virol* **75 (Pt 3)**, 545-554.

Tokoyoda, K., Zehentmeier, S., Hegazy, A. N., Albrecht, I., Grün, J. R., Löhning, M. & Radbruch, A. (2009). Professional memory CD4+ T lymphocytes preferentially reside and rest in the bone marrow. *Immunity* **30**, 721-730.

Troyer, J. L., Pecon-Slattery, J., Roelke, M. E., Johnson, W., VandeWoude, S., Vazquez-Salat, N., Brown, M., Frank, L., Woodroffe, R., Winterbach, C., Winterbach, H., Hemson, G., Bush, M., Alexander, K. A., Revilla, E. & O'Brien, S. J. (2005). Seroprevalence and genomic divergence of circulating strains of feline immunodeficiency virus among Felidae and Hyaenidae species. *J Virol* **79**, 8282-8294.

Troyer, J. L., Vandewoude, S., Pecon-Slattery, J., McIntosh, C., Franklin, S., Antunes, A., Johnson, W. & O'Brien, S. J. (2008). FIV cross-species transmission: an evolutionary prospective. *Vet Immunol Immunopathol* **123**, 159-166.

VandeWoude, S., Troyer, J. & Poss, M. (2010). Restrictions to cross-species transmission of lentiviral infection gleaned from studies of FIV. *Vet Immunol Immunopathol* **134**, 25-32.

Waki, K. & Freed, E. O. (2010). Macrophages and Cell-Cell Spread of HIV-1. *Viruses* **2**, 1603-1620.

Westman, M. E., Malik, R., Hall, E., Harris, M. & Norris, J. M. (2016). The protective rate of the feline immunodeficiency virus vaccine: An Australian field study. *Vaccine* **34**, 4752-4758.

Whetstone, C. A., Suarez, D. L., Miller, J. M., Pesch, B. A. & Harp, J. A. (1997). Bovine lentivirus induces early transient B-cell proliferation in experimentally inoculated cattle and appears to be pantropic. *J Virol* **71**, 640-644.

Yamamoto, J. K., Pu, R., Sato, E. & Hohdatsu, T. (2007). Feline immunodeficiency virus pathogenesis and development of a dual-subtype feline-immunodeficiency-virus vaccine. *AIDS* **21**, 547-563.

Zhu, Y. Q., Remington, K. M. & North, T. W. (1996). Mutants of feline immunodeficiency virus resistant to 2',3'-dideoxy-2',3'-didehydrothymidine. *Antimicrob Agents Chemother* **40**, 1983-1987.

Chapter 7

Summary/Samenvatting

7.1. Summary

The feline immunodeficiency virus is the causing agent of feline aids, an incurable disease that eventually leads to death. The virus has been known for almost 20 years and a lot of progress has been made in understanding the replication cycle and disease progression. However, there is no treatment available for infected cats, they are treated symptomatically.

In **chapter 1** an in depth introduction is given on the FIV genome structure, proteins and replication cycle. The anti-viral response is discussed and the known countermeasures FIV employs to escape from this immune response. Because more and more evidence is indicating a central role for the lymphoid tissues in the FIV pathogenesis, the second part of the introduction focuses on the structure of the lymphoid tissues and how FIV infection affects these organs.

The aims of this work are explained in **chapter 2**.

When starting the current work on FIV in Belgium no information existed on the circulating strains in the area. An up-to-date overview of FIV field strains in Belgium and the Netherlands is presented in **Chapter 3**. Viruses from naturally infected FIV positive cats were genotyped and their similarity was tested. Since cats can be infected with more than one FIV strain due to low cross-protection, recombinant viruses belonging to more than one subtype exist. Therefore, collected strains were genotyped for two regions in the FIV genome (the *gag* and *env* gene). Phylogenetic trees were assembled for both genes together with reference strains from all over the world. Except for one, all viruses collected in Belgium and the Netherlands clustered together with known clade A FIV viruses. One sample originating from a cat living in the Amsterdam region in the Netherlands had a clade A *gag* gene, but the *env* gene could not be matched to any known FIV subtype. Recombination analysis was performed to find out if the *env* gene was the product of inter-gene recombination. This analysis showed that the *env* gene partially matched other clade A FIV *env* genes, and the other part resembled a sequence reported in a cat infected with FIV in Sri Lanka, and belonged to an unknown FIV subtype. Based on the strains found in Belgium, further work was conducted with a clade A FIV virusstrain called FIV-PPR.

Once FIV is contracted, it establishes a lifelong infection of its host and causes a severe immunodeficiency that eventually leads to death. The FIV envelope protein (Env) and Gag protein are major stimulators of the anti-FIV response. Although infected cats

develop a strong antiviral response, FIV is not cleared. In **Chapter 4** the expression of FIV Env and Gag, and the availability of different epitopes on these viral proteins during replication were investigated in commonly used feline cell lines and feline PBMC. Large differences were found between the cell lines and PBMC. One of the most remarkable observations was the total lack of recognition of epitopes on the FIV envelope proteins when expressed on the cell surface of PBMC, but not on the feline adherent cell lines. Testing of the studied epitopes against sera from naturally infected cats showed that all cats developed a strong response against the conserved FIV receptor binding site. However, since these epitopes were shielded on mature envelope protein they probably don't contribute to anti-FIV immunity. A second phenomenon was the polarization of both Gag and Env towards specific sites in the plasma membrane at the end of the FIV replication cycle in PBMC. Again, this was not observed in the feline cell lines. The polarization of viral protein may indicate a preferred composition of the plasma membrane for virion budding in this region, but may also be the perquisite to the formation of viral synapses between cells. In virological synapses virus transfer from cell-to-cell takes place hidden from the immune system.

Another aspect of the FIV pathogenesis is the absence of FIV replication in leukocytes circulating in blood while the disease is asymptomatic but nonetheless progressing. Recently, it was shown that FIV replication is active in lymphoid tissues during the asymptomatic phase. Stromal cells of the lymphoid tissues not only shape the matrix framework of the organ in which the hematopoietic cells reside, they also provide signaling essential for the correct functioning of the organ. **Chapter 5a** focused on the isolation, characterization and immortalization of feline stromal cells from primary lymphoid tissues (bone marrow and thymus) and secondary lymphoid tissues (lymph nodes and spleen). Characterization showed that these cells express typical mesenchymal markers, vimentin and smooth muscle actin, and produce the extracellular matrix protein fibronectin. Production of various cytokines important for lymphoid organ function was demonstrated on the mRNA level. These cells were used in **Chapter 5b** to study the influence of lymphoid organ stromal cells on the sensitivity of peripheral blood mononuclear cells for FIV infection. Lymphoid mesenchymal stromal cells were able to induce expression of the FIV receptors, CD134 and CXCR4, on PBMC. Activated endothelium and lymph node mesenchymal cells elevated FIV infection percentages in PBMC. Furthermore, lymphoid stromal cells

from bone marrow and lymph node enhanced spread of FIV infection in PBMC cultures.

In **Chapter 6** all results generated during this PhD are combined and placed in a broader perspective.

7.2. Samenvatting

Het feline immunodeficiëntie virus veroorzaakt aids in katten, een ongeneesbare ziekte die de dood tot gevolg heeft. Het virus werd 20 jaar geleden ontdekt niet veel na de ontdekking zijn menselijke tegenhanger het humaan immunodeficiëntie virus. In de loop der jaren werd er reeds veel vooruitgang geboekt in het begrijpen van de FIV replicatiecylus en de pathogenese veroorzaakt door het virus. Tot op heden is er voor katten echter nog geen behandeling beschikbaar en worden de geïnfecteerde dieren enkel symptomatisch behandeld.

In **Hoofdstuk 1** word een diepgaande inleiding gegeven omtrent de FIV genoom structuur, de virale proteïnen en de replicatiecyclus. Er wordt besproken hoe het immuunsysteem reageert op een FIV infectie en hoe het virus deze immuun respons weet te omzeilen. Omdat er steeds meer bewijzen zijn die een centrale rol voor de lymfoïde weefsels binnen de FIV pathogenese aangeven, wordt in een tweede deel de structuur van deze weefsels besproken, alsook hoe een FIV infectie deze organen aantast.

Het **tweede hoofdstuk** verduidelijkt de doelen die gesteld werden voor dit doctoraatsproefschrift.

Bij de aanvang van dit doctoraat was er geen informatie over de FIV veldstammen die circuleren in België en Nederland. Een actueel overzicht van de FIV stammen in België en Nederland wordt gegeven in **Hoofdstuk 3**. Uit het bloed van FIV positieve katten werd het virus geïsoleerd en er werd een genotypering uitgevoerd. De gelijkenis tussen al deze stammen werd bestudeerd. Omdat katten met meerdere FIV virussen tegelijkertijd kunnen worden geïnfecteerd, doordat er maar weinig kruisbescherming bestaat, geeft dit de kans aan FIV virussen om met elkaar te recombineren. Om die reden werden twee regio's uit het FIV genoom getypeerd, met name het *gag* en *env* gen. De resultaten van deze twee genen werden samen met referentie stammen van over de hele wereld fylogenetisch geanalyseerd. Alle stalen verzameld in België en Nederland buiten één behoorden tot de clade A FIV virussen. Eén kat afkomstig uit Amsterdam was besmet met een FIV virus waarvoor de sequentie het *env* gen niet kon

worden ondergebracht bij de gekende clades, terwijl de *gag* sequentie tot de clade A virussen behoorde. Een recombinatie analyse toonde aan dat het eerste deel van de *env* sequentie grote gelijkenis vertoonde met de clade A virussen, maar dat het tweede deel leek op de *env* sequentie van een kat die geïnfecteerd werd met FIV in Sri Lanka. Het is nog maar de tweede keer dat deze sequentie werd teruggevonden en ze behoort tot een ongekende FIV subgroep. Omdat FIV virussen van subtype A de meest voorkomende zijn in België werd verder werk ook uitgevoerd met een FIV virus van dit subtype, met name FIV-PPR.

Eens een kat geïnfecteerd is met FIV, zal ze levenslang drager zijn van dit virus. Het virus veroorzaakt net zoals bij de mens een verworven immunodeficiëntie die de dood tot gevolg heeft. Het FIV envelop en Gag eiwit zijn de belangrijkste mikpunten van de anti-FIV immuniteit. Hoewel een kat een sterke antivirale respons kent, wordt een FIV infectie niet opgeruimd. In **Hoofdstuk 4** wordt de expressie van de Env en Gag eiwitten tijden de FIV replicatie in feliene cellijnen en PBMC in detail bestudeerd. Er werden grote verschillen gevonden tussen de vaak gebruikte feliene cellijnen en PBMC. Een van de belangrijkste waarnemingen was het gebrek aan herkenning van specifieke epitopen op het envelop eiwit wanneer het op het celmembraan van PBMC zit. Dit was niet zo op de celmembranen van de cellijnen waar deze epitopen wel werden gebonden door antistoffen. Uit een analyse van de sera van natuurlijk geïnfecteerde FIV katten bleek dat katten een sterke immuun respons hebben tegen de geconserveerde FIV receptorbindingsplaats, maar omdat deze verborgen zit op het eiwit dragen antistoffen hiertegen wellicht niet bij aan de anti-FIV immuniteit. Een tweede fenomeen dat werd geobserveerd, was de polarisatie van zowel Gag als Env naar specifieke zones van het plasmamembraan aan het einde van de FIV replicatiecyclus. Deze polarisatie van virale eiwitten kunnen wijzen op de aanwezigheid van een specifieke samenstelling van het plasmamembraan die wordt verkozen voor virusvorming. Het kan ook een voorstadium zijn van een virussynaps die wordt gevormd tussen twee cellen. In zo een virussynaps kunnen virussen zich verspreiden van cel naar cel zonder gezien te worden door het immuunsysteem.

Wanneer een kat geïnfecteerd is met FIV worden er slechts zeer weinig leukocyten in het bloed teruggevonden die FIV eiwitten tot expressie brengen. De ziekte is asymptomatisch maar toch verslechtert de toestand van het immuunsysteem geleidelijk aan. Het werd recent aangetoond dat ook in de asymptomatische fase er actieve FIV replicatie kan worden teruggevonden in leukocyten die zich in de lymfoïde

weefsels bevinden. De stromale cellen die de lymfoïde weefsels vorm geven door de productie van extracellulaire matrix produceren ook signaalmoleculen essentieel voor de functie van deze weefsels. In **Hoofdstuk 5a** wordt beschreven hoe cellen van de primaire lymfoïde weefsels (beenmerg en thymus) en van de secundaire lymfoïde weefsels (lymfeknopen en milt) werden geïsoleerd, geïmmortaliseerd en gekarakteriseerd. Deze cellen brengen merkers die typisch zijn voor mesenchymale cellen tot expressie, zijnde vimentine, gladde spiercel actine en het extracellulaire matix eiwit fibronectine. De productie van cytokinen werd aangetoond op mRNA niveau. Deze mesenchymale cellen van de lymfoïde weefsels werden gebruikt in **Hoofdstuk 5b** om te bestuderen of zij een effect hebben op de gevoeligheid van PBMC voor FIV. Deze cellen konden PBMC stimuleren om de FIV receptoren CD134 en CXCR4 tot expressie te brengen. Aanwezigheid van geactiveerde vasculaire endotheelcellen en mesenchymale cellen van de lymfeknopen leidden tot een verhoogt FIV infectiepercentage in PBMC. Verder zorgde de aanwezigheid van mesenchymale cellen van de lymfeknopen en het beenmerg tot een betere verspreiding van FIV in een PBMC cultuur.

In **Hoofdstuk 6** worden alle resultaten die werden bekomen tijdens dit doctoraat samengevoegd en in een breder perspectief geplaatst.

Curriculum Vitae

Inge Roukaerts werd op 27 september 1987 geboren te Genk. In 2005 behaalde zij het getuigschrift middelbaar onderwijs aan het Sint-Jan Bergmanscollege te Genk in de richting Wetenschappen-Wiskunde. Ze studeerde verder aan de Vrije Universiteit Brussel en Universiteit Hasselt waar ze in 2010 het diploma Master in de Biomedische Wetenschappen (afstudeerrichting klinische moleculaire wetenschappen) met onderscheiding behaalde. In maart 2011 kreeg zij de kans het onderzoek naar het felien immunodeficiëntie virus op te starten in de vakgroep Virologie, Immunologie en Parasitologie aan de faculteit Diergeneeskunde van de Universiteit Gent onder begeleiding van Prof. Dr. Hans Nauwynck. In datzelfde jaar verwierf zij een doctoraatsbeurs van het Agentschap voor Innovatie door Wetenschap en Techniek Vlaanderen (IWT) om het onderzoek naar de immuno-evasieve strategieën van het felien immunodeficiëntie virus verder te zetten.

List of publications & conference abstracts

Publications in international peer reviewed journals (including submitted papers)

- **Roukaerts I**, Grant C, Theuns S, Christiaens I, Acar D, Van Bockstael S, Desmarets L, Nauwynck H. Differences in Env and Gag protein expression patterns and epitope availability in feline immunodeficiency virus infected PBMC compared to infected and transfected feline model cell lines. Vir Res. 2016 *accepted*.
- Acar D, Olyslaegers D, Dedeurwaerder A, **Roukaerts I**, Baetens W, Van Bockstael S, De Gryse G, Desmarets L, Nauwynck H. Upregulation of endothelial cell adhesion molecules characterizes veins close to granulomatous infiltrates in the renal cortex of cats with feline infectious peritonitis and is indirectly triggered by feline infectious peritonitis virus infected monocytes in vitro. Gen Virol. 2016 Aug 19. Epub ahead of print.
- Theuns S, Conceição-Neto N, Heylen E, Zeller M, **Roukaerts I**, Desmarets L, Van Ranst M, Nauwynck H, Matthijnssens J. Characterization of a genetically heterogeneous porcine rotavirus C, and other viruses present in the fecal virome of a non-diarrheic Belgian piglet. Infect Genet Evol. 2016 Sep 43:135-45.
- Theuns S, Vyt P, Desmarets L, **Roukaerts I**, Heylen E, Zeller M, Matthijnssens J, Nauwynck H. Presence and characterization of pig group A and C rotaviruses in feces of Belgian diarrheic suckling piglets. Virus Res. 2016 Feb 2;213:172-83.
- Desmarets L, Vermeulen B, Theuns S, Conceição-Neto N, Zeller M, **Roukaerts I**, Acar D, Olyslaegers D, Van Ranst M, Matthijnssens J, Nauwynck H. Experimental feline enteric coronavirus infection reveals an aberrant infection pattern and shedding of mutants with impaired infectivity in enterocyte cultures. Sci Rep. 2016 Jan 29;6: 20022.
- Theuns S, Vyt P, Desmarets L, **Roukaerts I**, Heylen E, Zeller M, Matthijnssens J, Nauwynck H. Presence and characterization of pig group A and C rotaviruses in feces of Belgian diarrheic suckling piglets. Virus Res. 2015 Dec 8;213:172-183.
- Reddy V, Theuns S, **Roukaerts I**, Zeller M, Matthijnssens J, Nauwynck H. Genetic Characterization of the Belgian Nephropathogenic Infectious Bronchitis Virus (NIBV) Reference Strain B1648. Viruses. 2015 Aug 7;7(8):4488-506.
- Theuns S, Conceição-Neto N, Christiaens I, Zeller M, Desmarets L, **Roukaerts I**, Acar D, Heylen E, Matthijnssens J, Nauwynck H. Complete genome sequence of a

porcine epidemic diarrhea virus from a novel outbreak in belgium, january 2015.Genome Announc. 2015 May 21;3(3).

- **Roukaerts I**, Theuns S, Taffin E, Daminet S, Nauwynck H. Phylogenetic analysis of feline immunodeficiency virus strains from naturally infected cats in Belgium and The Netherlands. Virus Res. 2015 Jan 22;196:30-6.
- Theuns S, Heylen E, Zeller M, **Roukaerts I**, Desmarets L, Van Ranst M, Nauwynck H, Matthijnssens J. Complete genome characterization of recent and ancient Belgian pig group A rotaviruses and assessment of their evolutionary relationship with human rotaviruses. J Virol. 2015 Jan 15;89(2):1043-57.
- Desmarets L, Theuns S, **Roukaerts I**, Acar D, Nauwynck H. Role of sialic acids in feline enteric coronavirus infections. J Gen Virol. 2014 Sep;95(Pt9):1911-8.
- Theuns S, Desmarets L, Heylen E, Zeller M, Dedeurwaerder A, **Roukaerts I**, Van Ranst M, Matthijnssens J, Nauwynck H. Porcine group A rotaviruses with heterogeneous VP7 and VP4 genotype combinations can be found together with enteric bacteria on Belgian swine farms. Vet Microbiol. 2014 Aug 6;172(1-2):23-34.
- Dedeurwaerder A, Olyslaegers D, Desmarets L, **Roukaerts I**, Theuns S, Nauwynck H. ORF7-encoded accessory protein 7a of feline infectious peritonitis virus as a counteragent against IFN-α-induced antiviral response. J Gen Virol. 2014 Feb;95(Pt 2):393-402.
- Desmarets L, Theuns S, Olyslaegers D, Dedeurwaerder A, Vermeulen B, **Roukaerts I**, Nauwynck H. Establishment of feline intestinal epithelial cell cultures for the propagation and study of feline enteric coronaviruses. Vet Res. 2013 Aug 21;44:71.

Abstracts at international conferences

- **Roukaerts I**, Van Bockstael S, Acar D, Desmarets L, Nauwynck H. Newly established lymphoid organ-derived mesenchymal cell cultures enhance FIV replication in lymphocytes. Joint Symposium of the International Society for Companion Animal Infectious Diseases and the International Feline Retrovirus Research Symposium 2016. Bristol, United Kingdom. ***(Poster)***
- Acar D, Olyslaegers D, Dedeurwaerder A, **Roukaerts I**, Baetens W, Van Bockstael S, De Gryse G, Desmarets L, Nauwynck H. Upregulation of endothelial adhesion molecules by the feline infectious peritonitis virus. Joint

Symposium of the International Society for Companion Animal Infectious Diseases and the International Feline Retrovirus Research Symposium 2016. Bristol, United Kingdom.

- Theuns S, Desmarets L, **Roukaerts I**, Christiaens I, Heylen E, Zeller M, Van Ranst M, Matthijnssens J, Nauwynck H. Successive subclinical group A and C rotavirus infections in piglets after weaning on a closed Belgian pig farm. 3rd Belgian Society for Virology meeting, 2015, Brussels, Belgium.
- Desmarets L, Vermeulen B, Theuns S, Conceição-Neto N, Zeller M, **Roukaerts I**, Acar D, Olyslaegers D, Van Ranst M, Matthijnssens J and Nauwynck H. Experimental feline enteric coronavirus infection reveals an aberrant infection pattern and shedding of mutational variants with impaired enterocyte tropism. 3rd Belgian Society for Virology meeting, 2015, Brussels, Belgium.
- Theuns S, Conceição-Neto N, Heylen E, Zeller M, **Roukaerts I**, Desmarets L, Van Ranst M, Nauwynck HJ, Matthijnssens J. The fecal virome of a Belgian non-diarrheic piglet contains group A and C rotaviruses, and an astro- and enterovirus. Twelfth International Double-Stranded RNA Virus Symposium 2015, Goa, India.
- Theuns S, Desmarets L, **Roukaerts I**, Christiaens I, Heylen E, Zeller M, Van Ranst M, Matthijnssens J, Nauwynck HJ. Successive subclinical rotavirus A and C infec4ons in pigs a7er weaning on a closed Belgian pig farm. Twelfth International Double-Stranded RNA Virus Symposium 2015, Goa, India.
- **Roukaerts I**, Grant C, Desmarets L, Theuns S, Christiaens I, Acar D, Nauwynck H. Staining and expression kinetics of the feline immunodeficiency virus envelope glycoprotein. Xth Conference of the European Society of Veterinary Virology 2015, Montpelier, France. ***(oral presentation)***
- Desmarets L, Theuns S, Conceição-Neto N, **Roukaerts I**, Acar D , Matthijnssens J, Nauwynck H. Clinical, virological, and immunological parameters during experimental feline enteric coronavirus infection. Xth Conference of the European Society of Veterinary Virology 2015, Montpelier, France.
- Theuns S, Heylen E, Zeller M, **Roukaerts I**, Desmarets L, Van Ranst M, Nauwynck H, Matthijnssens J. Complete genome characterization of recent and ancient Belgian pig group A rotaviruses and assessment of their

evolutionary relationship with human rotaviruses. Xth Conference of the European Society of Veterinary Virology 2015, Montpelier, France.

- Christiaens I, Conceição-Neto N, Theuns S, Zeller M, Desmarets L, **Roukaerts I**, Heylen E, Matthijnssens J, Nauwynck H. Genetic characterization of porcine epidemic diarrhea virus strains isolated from novel outbreaks in the European Union, Belgium. Xth Conference of the European Society of Veterinary Virology 2015, Montpelier, France.
- Theuns S, Vyt P, Desmarets L, **Roukaerts I**, Heylen E, Zeller M, Van Ranst M, Matthijnssens J, Nauwynck H. Rotavirus A and C infections in Belgian Diarrheic suckling pigs. Xth Conference of the European Society of Veterinary Virology 2015, Montpelier, France.
- Theuns S, Heylen E, Zeller M, **Roukaerts I**, Desmarets L, Van Ranst M, Nauwynck H, Matthijnssens J. Complete genome characterization of recent and ancient Belgian pig group A rotaviruses and assessment of their evolutionary relationship with human rotaviruses. 6th European Rotavirus Biology Meeting, 2015, Dijon, France.
- Theuns S, Vyt P, Desmarts L, **Roukaerts I**, Heylen E, Zeller M, Van Ranst M, Matthijnssens J, Nauwynck H. Circulation of pig group A and C rotaviruses in Belgian diarrheic suckling piglets and its impact on veterinary diagnostical analyses. 6th European Rotavirus Biology Meeting, 2015, Dijon, France.
- **Roukaerts I**, Theuns S, Taffin E, Daminet S, Nauwynck H. Phylogenetic analysis of FIV strains from naturally infected cats in Belgium and The Netherlands. 2nd Belgian Society for Virology meeting, 2014, Brussels, Belgium.
- Theuns S, Heylen E, Zeller M, **Roukaerts I**, Desmarets L, Van Ranst M, Nauwynck H, Matthijnssens J. Complete genome characterization of recent and ancient Belgian pig group A rotaviruses and assessment of their evolutionary relationship with human rotaviruses. 2nd Belgian Society for Virology meeting, 2014, Brussels, Belgium.
- **Roukaerts I**, Theuns S, Taffin E, Daminet S, Nauwynck H. Phylogenetic analysis of FIV strains from naturally infected cats in Belgium and the Netherlands. 12th International Feline Retrovirus Research Symposium 2014, Niagara-on-the-lake, Canada. ***(oral presentation)***

- Desmarets L, Theuns S, **Roukaerts I**, Acar D, Nauwynck H. Role of sialic acids in feline enteric coronaviruses infections. XIIIth International Nidovirus Symposium, 2014, Salamanca, Spain.
- Desmarets L, Theuns S, Olyslaegers D, Dedeurwaerder A, Vermeulen B, **Roukaerts I**, Nauwynck H. Establishment of feline intestinal epithelial cell cultures for the propagation and study of feline enteric coronaviruses. XIIIth International Nidovirus Symposium, 2014, Salamanca, Spain.
- Dedeurwaerder A, Acar D, Olyslaegers D, Desmarets L, **Roukaerts I**, Theuns S, Nauwynck HJ. ORF7-encoded accessory protein 7a of feline infectious peritonitis virus as a counteragent against interferon-alpha induced antiviral response. XIIIth International Nidovirus Symposium, 2014, Salamanca, Spain.
- Theuns S, Desmarets L, Heylen E, Zeller M, Dedeurwaerder A, **Roukaerts I**, Van Ranst M, Matthijnssens J, Nauwynck HJ. Unraveling the role of porcine group A rotaviruses in the pathogenesis of piglet diarrhea and their evolutionary relationship with human rotaviruses. 11th International Rotavirus Symposium, 2014, New Delhi, India.
- **Roukaerts I**, Olyslaegers D, Desmarets L, Theuns S, Dedeurwaerder A, Nauwynck H. Feline peripheral blood mononuclear cell cultivation: cell population evolution, FIV receptor expression & FIV replication. 1st Belgian Society for Virology meeting, 2013, Brussels, Belgium.
- Desmarets L, Theuns S, Olyslaegers D, Dedeurwaerder A, Vermeulen B, **Roukaerts I**, Nauwynck H. Establishment of feline intestinal epithelial cell cultures for the propagation and study of feline enteric coronaviruses. 1st Belgian Society for Virology meeting, 2013, Brussels, Belgium.
- Dedeurwaerder A, Olyslaegers D, Desmarets L, **Roukaerts I**, Theuns S, Nauwynck H. The ORF7-encoded accessory protein 7a of feline infectious peritonitis virus as a counteragent against interferon-alpha induced antiviral response. 1st Belgian Society for Virology meeting, 2013, Brussels, Belgium.

Dankwoord / Acknowledgements

Alle technische details en bevindingen die te maken hadden met dit proefschrift zijn geschreven, rest alleen nog het dankwoord. Iedereen die mij een beetje kent weet dat ik geen dichterlijk of literair talent ben. Toch zal ik hier nog een woordje richten aan iedereen die een bijdrage heeft geleverd aan het voltooien van dit werk.

Geen kansen, geen doctoraat. Ongeveer 6 jaar geleden reageerde ik op een vacature binnen de FIP-groep van het labo virologie. Het moet zijn dat jullie (Hans en Hannah) toch iets in mij zagen want nog geen 10 dagen later was ik aan de slag. Hannah, bedankt voor de intense begeleiding van het IWT project en de vele uren oefening voor de verdediging! Zonder jouw jarenlange ervaring in het virologisch onderzoek was dat nooit gelukt. Ook zette je me op de rails in het onderzoek met protocols en praktische tips. Hans, jij nam het promotorschap van mijn doctoraat op je. Ik wil je bedanken voor je niet aflatend enthousiasme, met daarbij horend een onuitputtelijke bron aan nieuwe (niet altijd even conventionele) hypothesen en zienswijzen. Verder moet het ook gezegd dat je gave om bij tegenslag een goede “peptalk” te geven zoals een echte top-coach behoort zeker een steun was! Ik denk dat je wel kan zeggen dat “dat meisje uit Limburg” met heel wat meer levenswetenschap je labo verlaat.

Finding the right reagents for our FIV research was not an easy task. Luckily, some guy in the States was willing to send me some antibody samples. Chris Grant, if it wasn’t for you, much of my research would simply not exist! Thank you for your excitement when I sent you the first microscopy pictures, and your interest and support along the way! I will never forget!

Aan de leden van de examenjury een dankjewel voor de tijd die ze genomen hebben om mijn werk grondig door te nemen en de opmerkingen die dit werk merkelijk hebben verbeterd.

Ik kwam binnen in een labo waar twee “top-tjoolders” druk in de weer waren met darmen allerlei. Het ene idee was al zotter als het andere :D. Lowiese-ken en Bassie, die darmen hebben voor jullie beiden tot een super doctoraat en ook een mooie post-doc carrière geleid. Ik zal die eerste zotte jaren dat we samen in het labo zaten nooit vergeten! De vrijdagfilmkes, de telkamer, de goed gezekerde gasfles, kattenvangen, kaka-score lijsten, llama’s, zijprojecten allerhande, vroege ochtend experimenten, opkuisacties, koffietassen, meer kaka en darmen, ozewiezewoze, banaan stickertjes, ikea-shopping, en zo kan ik nog even doorgaan… Alle gekheid op een stokje, Lowiese

een hele dikke merci voor de vele hypothesen en experiment besprekingen, en voor het nalezen, verbeteren, meer nalezen en meer verbeteren, en nog meer nalezen van al mijn gekribbel. Nu nog ozewiezewoze uit mijn hoofd krijgen :p. Bassie, naast serieuze zaken kon ik bij jou ook terecht om eens goed te zagen of onnozel te doen, of nog beter om onze fantasie de vrije loop te laten. Een welgemeende dank je wel en… *never let your inner child die* ;), BAZINGA!!

Naast deze tjoolders liepen er nog enkele figuren rond op "het eerste verdiep" die ik zeker moet bedanken. Ben, wanneer Hannah mij niet kon helpen werd ik aan jou overgeleverd want jij wist hoe lymfocyten moesten worden behandeld. Van jou leerde ik een hoop technieken die onmisbaar zouden blijken tijdens mijn doctoraat. Dominique en Annelike, toen ik binnen kwam op het labo waren jullie voor mij de geroutineerde doctoraatsstudenten. Van jullie expertise en doorzettingsvermogen (want het ging niet altijd van een leien dakje) daar konden wij nog iets van leren!! Allebei merikes voor de fijne babbels, FIP-meetingen, protocols, enz… en om ons af en toe eens een hart onder de riem te steken!

Isaura, eerst zagen we elkaar vooral aan de bushalte, maar na een tijdje kwamen we elkaar meer tegen in het (moleculair) labo en uiteindelijk verhuisde je zelfs naar "het eerste verdiep". Als mede-biomedische tussen die vele dierenartsen kon ik met jou al eens brainstormen over welke strategie het beste was op moleculair vlak. Ik vond het altijd fijn om ons kritisch oog op allerhande zaken te laten schijnen, met onverbloemde meningen. Maar onder die ruwe bolster, misschien toch ook een blanke pit, jij was altijd daar met steun of een bemoedigend woord wanneer nodig, waarvoor waarlijk dank! Zoals dat gaat in een labo komt er altijd maar vers bloed binnen wanneer anderen verdere horizonten opzoeken. Zo kwam er één binnen die in de eerste week al op de werkbank zat om de hele FIP-hypothese uit te tekenen. Delphine, dierenarts eerste klas, jij bracht een frisse wind in het labo. Af en toe op je gezicht gaan, daar trek jij je niets van aan. Je maakte ook onmiddellijk aanspraak op een plaats in team onverbloemd ;). Raak nooit die wilde haren kwijt, de onderzoeks- en academische wereld kunnen dat goed gebruiken!! In mijn laatste jaar verraste Hans me met een student, die zowaar het hele jaar zou blijven! Dankzij een gelukkig toeval, zoals dat wel vaker gaat in het onderzoek, hadden we plots toch een project voor jou. Sebastiaan, Sebas, Bockie, Ryan, ondertussen heb je al vele namen, maar eigenlijk blijf je gewoon mijn duckling. Jou nieuwsgierigheid en verwondering brachten ook bij mij de zin en plezier om onderzoek te doen terug, iets wat je (geloof mij) wel kan

gebruiken in die laatste loodjes van een doctoraat!! Ik vond het heel plezierig om voor jou de deuren van de “niet zo suffe ;)” onderzoekswereld (en dan vooral de FACS blijkbaar) te openen!! Nu op naar nieuwe horizonten en nog meer flowcytometrie, het ga je goed ;). p.s. hoe zit het nu eigenlijk met die dans-moves op Little Apple… Gaetan, Wendy, Eleni en Kasper, jullie vervolledigen de nieuwe charge in de bureau(s). Gaetan, we adopteerden jou uit de kelder als onze eigenste Shrimpie. Allemaal nieuw die garnalen toestanden, we overlaadden je dan ook met de meest uiteenlopende vragen. Nu hoef je niet meer alleen rond te zwerven naar god weet waar om gekke experimenten te doen, want nu ben je een team met Kasper. Ik wens jullie het allerbest, en als ik een scampi (aka een gamba zonder kop) eet, zal ik altijd even aan jullie denken. Met Lowiese *soon on the move*, werd er versterking voor het FIP-team gezocht. Een gekke biologe uit het Brusselse vervulde de eer. Wendy, ik er zeker van dat je samen met Delphine de eer van het FIP onderzoek in Gent hoog kunt houden. Eleni, “*a woman’s touch*” dat kon de georganiseerde chaos van Bassie wel gebruiken. Daar mocht er ene zijn pollekes kussen met jou komst om al die biggen op te volgen en te helpen met extracties en qPCR’s. TingTing, you are another asset of the Rota group. In the beginning a bit shy, but now on the road to success. I hope you and your husband will have some more beautiful years in Belgium, with two nice PhD’s in the end! Every once in a while I will listen to some Chinese pop music to remember you ;).

Ytse, dat zootje ongeregeld dat ik hierboven het beschreven wandelt voortdurend in en uit “jouw labo” en zet ook soms (lees: vaak) de boel op stelten. Gelukkig hebben we daar een kordate West-Vlaamse om alles een beetje in de gaten te houden. Een hele dikke merci voor de vele fantastische kleuringen en andere experimenten die ik met een gerust hart aan je kon toevertrouwen!! Wat zouden we daar toch zonder jou doen!

FIP-ers en aanverwanten…het was een genoegen!!!

Het mag gezegd dat het labo staat of valt met de kwaliteit van de technische crew. Wel nu mogen wij van geluk spreken dat we kunnen rekenen op een fantastisch team laboranten. Carine, Lieve, Nele, Melanie en Chantal, dankjewel voor al de adviezen, antwoorden en experimentele ondersteuning, alsook de leuke babbels tussendoor!! Op een faculteit diergeneeskunde zijn ook altijd veel dieren aanwezig dus wat zouden we zijn zonder professionele verzorging. Een dikke merci aan Zeger en Magda voor het onderhoud v an het labo, de stallen en de dieren.

Buiten het labo was er natuurlijk ook nood aan verstrooiing en eveneens een vangnet, want zo een doctoraat, dat krijg je niet zomaar cadeau. Aan mijn familie en in het bijzonder oma en opa, een dikke merci omdat jullie altijd nieuwsgierig waren naar wat ik daar in het verre Gent allemaal uitspookte. Mama en papa dankjewel voor de kansen die geleid hebben tot het aanvangen en voltooien van dit proefschrift, voor de niet aflatende steun wanneer het even moeilijker ging en voor de grote tuin waar ik altijd mijn zinnen kon verzetten. Ik kan dat niet in woorden uitdrukken hoezeer jullie mij geholpen hebben. Mijn lieve kleine broerke Arnout, die jeneverkes op de kerstmarkt na het afleggen van de IWT-verdediging, dat was een moment dat me altijd zal bijblijven. Met jou kon ik het al eens hebben over het wel en wee van de doctoraatsstudent of de aanpak van een artikel bespreken. Bedankt voor het relaxte tegengewicht voor mijn soms overspannen ziel :).

Chris, waar te beginnen… :), ik hoef je hier niet te vertellen wat we allemaal hebben meegemaakt, want je was er altijd bij, je volgde me zelfs tot in Gent en weer terug! Niemand heeft alles van zo nabij meegemaakt als jij, maar er is ook niemand die nu zo veel in mijn vreugde kan delen!

Inge

To infinity… and beyond!!!